UNIVERSITY OF UTAH
RESEARCH INSTITUTE
EARTH SCIENCE LAB

SUBJ
MNG
PAB

processes as applied to the most varied conditions, and new methods of determination was c mentally. It was shown that the error is not gr 10%.

A theoretical analysis was made, and the error due to the

Sov. Non-Fe
1977 v. 5 N 5

UDC 546.19+541.8-165

Precipitation of arsenic by calcium phosphate

Yu O Grigor'ev, N G Tyurin and N N Pustovalov (Urals Polytechnical Institute. Department of the Metallurgy of Light Metals)

It is known that the use of phosphate ions during the liming of arsenic-containing effluents makes it possible to achieve a high degree of purification of the solutions from arsenic and from a series of other toxic substances[1-3]. Suggestions about a mechanism of coprecipitation of arsenic with calcium phosphate have been put forward in a number of papers[4,5]. On the basis of the isostructural characteristics of the PO_4^{3-} and AsO_4^{3-} ions and also of their tendency towards isomorphism the authors consider that the high purification of solutions from arsenic takes place as a result of the formation of solid solutions in the PO_4^{3-} - AsO_4^{3-} - calcium system, in which arsenate and phosphate ions substitute each other. A molar ratio $PO_4^{3-}: AsO_4^{3-} \geq 1.5:1$ in the solution is a sufficient condition for the formation of such compounds[5].

However, investigations[6] have shown that the mechanism of the precipitation of arsenic in the Ca^{2+} - PO_4^{3-} - AsO_4^{3-} - H_2O system is much more complex than follows from the solid solution concept. Special investigations were undertaken in order to determine the effect of various factors and to investigate the mechanism of the precipitation of arsenic in this system. In the work we used solutions of pentavalent arsenic, prepared by the usual methods. Calcium phosphate was precipitated from solutions of calcium nitrate and sodium phosphate with sodium hydroxide. The experiments on the precipitation of arsenic were carried out under static conditions. The precipitation time was sufficient for the attainment of a state close to equilibrium. The solubility of the precipitates, which hardly contained any excess $Ca(OH)_2$, was investigated in closed flasks with periodic stirring over 96h. The analysis of the component was realised by published methods[7,8].

It was established (fig.1) that phosphorus is precipitated initially from the Ca^{2+} - PO_4^{3-} - AsO_4^{3-} - H_2O system at pH 12.2 together with calcium. With an excess of phosphorus in the system the arsenic is not held by the precipitate which forms, irrespective of its mass. With a Ca/P ratio of 1.6 or more in the solution (fig.1) the arsenic begins to be precipitated strongly, and with an excess of calcium in relation to phosphate ions it passes almost completely into the precipitate. It is interesting to note that in the absence of phosphate ions the arsenic is precipitated from the system even with small concentrations of calcium hydroxide, but in this case complete precipitation of the arsenic is not observed.

Analysis of the precipitate showed that with a Ca:P ratio of <1.7 the precipitate does not contain arsenate ions. In this case the solution contains phosphate and arsenate ions. With a higher ratio the precipitate contains arsenic, but the mother solution does not contain phosphate and, under optium conditions, arsenate ions.

A series of authors[9,10], investigating the CaO-P_2O_5-H_2O system at various pH values, established that compounds of the $Ca_3(HPO_4)_2$ type are formed in an acidic medium. In the reaction of such a compound with water or with alkaline solutions and also at pH>11 a poorly soluble compound with the composition $Ca_y(PO_4)_x(OH)_y$ is formed. The numerical values of the coefficients in this compound differ, but they are characterised by a constant Ca/P ratio of 5/3. This ratio is characteristic of a wide range of compounds (hydroxylapatites). Numerous investigations have shown that hydroxylapatite is the least soluble of all the calcium phosphate compounds. The solubility product of hydroxylapatite with the composition $Ca_{10}(PO_4)_6(OH)_2$ Lp

is $10^{-120.13}$[11].

The freshly deposited precipitates can contain an excess of sorbed calcium or phosphate ions, which enter into the structure of the hydroxylapatite. Precipitates formed with a calcium-phosphorus ratio of <1.68 in the solution (fig.1) are characterised by a reduced Ca/P molar ratio of 1.0-1.68, i.e., contain [according to [12]] an excess of adsorbed phosphate ions, which occupy the sites of the hydroxylapatite structure. Such precipitates do not sorb arsenic from the solution. With a Ca/P ratio of >1.68 the precipitate becomes sorption active. In this case the arsenic is precipitated strongly from the system both on the precipitates which have formed and during their formation.

To determine the mechanism of the sorption of arsenic by the hydroxylapatite precipitates the latter were brought into contact with the arsenic solutions. After being held for 120-150h the filtrates were analysed for calcium, phosphorus, arsenic, and hydroxide ions. The experimental data are given in the table. From the data in the table it follows that the arsenic, being sorbed by the precipitate, does not displace the phosphate ions in the solution. An increase in the pH of the medium, due to the passage of hydroxide ions into the precipitate, is observed in the solution. During contact between the freshly formed precipitate and aqueous solutions not containing arsenate ions ageing of the precipitate occurs, and this accompanied by the transfer of acid phosphates into the medium and by acidification of the solutions. During the sorption of one mole of arsenic into the solution, with allowance for the acidification process, an average of 2.7 mole of hydroxide ion is desorbed.

During the joint coprecipitation of arsenic the degree of sorption is somewhat higher than on the previously formed precipitate, and this can be atrributed to a change in the structure of the precipitate during the ageing process. It should be noted that arsenic is readily displaced from the freshly formed precipitates by phosphate ions.

The IR spectra of the hydroxylapatite precipitates are given in fig.2. In the IR spectra there are infrared absorption bands in the region of the deformation vibrations (500-600 cm^{-1}) and stretching vibrations (800-1200 cm^{-1}) of the phosphate and arsenate ions[13]. In the spectrum of the hydroxylapatite precipitate there is one broad band at 1000-1200 cm^{-1} with a maximum at 1140 cm^{-1}, corresponding to the PO_4^{3-} ion. In the spectrum of the arsenic-containing precipitate the maximum of this band is shifted into the more long-wave region, and a maximum appears at 870 cm^{-1}, characteristic of arsenate ions. The stretching vibrations of the OH^- group of the hydroxylapatite precipitate (3600 cm^{-1}) are poorly defined, but after the sorption of the arsenic this line becomes flatter; this is also due to the presence of water in the structure of the molecules, which are evidently present in nonequilibrium energy states and secure an absorption band in the region of 3100-3600 cm^{-1} in the IR spectra.

The thermograms and derivatograms of samples of hydroxylapatite have a form identical with that of hydroxylapatite containing arsenic and contain one endothermic effect at $800^\circ C$, whereas calcium arsenate is characterised by three endothermic effects at 155, 520, and $820^\circ C$, accompanied by the corresponding changes on the thermogravimetric curve (fig.3). On the thermogravimetric curve the hydroxylapatite precipitates give two steps. Adsorption-bound water is removed in the range of $75-300^\circ C$, and water of crystal-

lisation is removed after 800°C with further disintegration of the hydroxylapatite structure[14]).

The freshly formed arsenic-containing precipitate based on hydroxylapatite is amorphous to Xrays. During ageing in the mother solution it crystallises and acquires the hydroxylapatite structure. The structure of calcium arsenate is absent in the precipitate, and the lines on the Debye pattern are shifted towards greater interplanar separations.

On the basis of the investigations it is possible to propose the following mechanism for the coprecipitation of arsenic from the $Ca^{2+}-PO_4^{2-}-AsO_4^{2-}-H_2O$ system. Initially an amorphous matrix of hydroxylapatite with a Ca/P ratio of 1.0-1.68 is formed in the system, where the sites of the hydroxyl groups are occupied by phosphate ions. This precipitate does not sorb arsenic from the solution (fig.1). With increase in the concentration of calcium in the precipitate a rearrangement of the compound occurs on account of the reaction of sorbed phosphate ions with calcium ions. The Ca/P ratio increases and reaches a value of 5/3. Here, in the matrix of the hexagonal hydroxylapatite lattice which forms the sites of the hydroxyl groups are occupied by arsenic anions, as shown by balancing tests (table). In this case a decrease in the intensity of the stretching vibrations for the hydroxyl groups is observed and an absorption band in the region of 870 cm^{-1}, characteristic of the arsenate ion, appears in the IR spectrum (fig.2). The absorption maximum corresponding to the phosphate ion (1140 cm^{-1}) is shifted towards the more long-wave region ($\Delta\nu = 65$ cm^{-1}), and this is evidently due to the deformation of the PO_4^{2-} ion during the formation of the arsenic-containing structure. According to the thermographic and derivatographic analyses, the compound which forms corresponds to the hydroxylapatite precipitate. With further increase in the amount of calcium in the solution it is sorbed by the hydroxylapatite precipitate on account of the formation of hydrogen bonds with water molecules or of their substitution[12]). The arsenic reacts with the adsorbed calcium and is absorbed by the precipitate. After being held in the mother solution the precipitate crystallises and forms the hexagonal hydroxylapatite lattice with somewhat increased interplanar separations as a result of entry of hydrolysed arsenic anions into the structure.
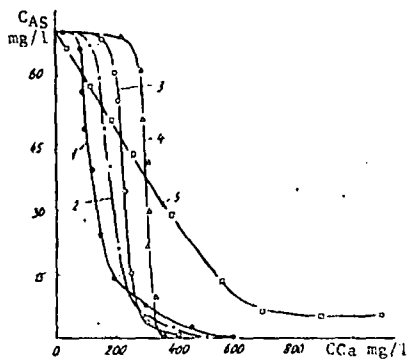
Fig.1 The effect of the concentration of calcium on the concentration of arsenic in the $Ca^{2+}-PO_4^{3-}-AsO_4^{3-}-H_2O$ system with various phosphoric acid concentrations, mg/l; 1 - 90; 2 - 180; 3 - 270; 4 - 360; 5 - 0. pH = 12.2; arsenic (V) concentration 70 mg/l; contact time 72 h; t = 20-22°C.
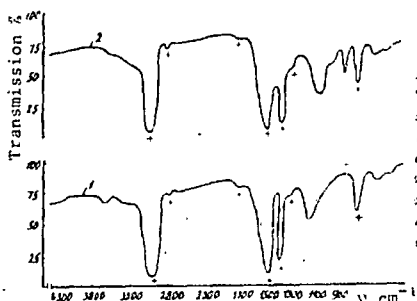
Fig.2
The infrared absorption spectra of hydroxylapatite precipitates without arsenic (1) and with arsenic (2). The + signs indicate the absorption bands of the dispersion medium.

The absorption of arsenic by the hydroxylapatite precipitate. pH$_{in}$ = 12.0, calcium concentration in precipitate 0.26 g/l, Ca/P = 1.8, temperature 25°C

Initial concentration of arsenic (V), mg/l	Equilibrium concentration of component mg/l			pH	OH (mole)/As (mole)
	Arsenic	Calcium	Phosphate ion		
0	0	1	0.5	11.85	-
250	107.5	H₂O	0.1	12.1	2.72
300	150	H₂O	0.2	12.0	2.81
400	250	H₂O	0.15	12.2	2.7
500	340.25	H₂O	0.1	12.0	2.51
600	430	H₂O	H₂O	12.05	2.63
700	520.5	H₂O	H₂O	12.07	2.68
800	620.7	H₂O	H₂O	12.08	2.75
1000	821	H₂O	H₂O	12.1	2.85
				Mean	2.7

During the coprecipitation of arsenic with the hydroxylapatite precipitate an average of 2.7 moles of hydroxide ion passes into solution for one arsenic anion. In the general case the coprecipitation of arsenic with calcium phosphate can be described by the following equation:

$$3Ca_{10+x}(PO_4)_6(OH)_{2(1+x)} + 2AsC_4^{3-} \rightleftharpoons$$

$$[Ca_{10+x}(PO_4)_6]_3 (AsO_4)_2 (OH)_{8x} + 6OH^- \qquad (1)$$
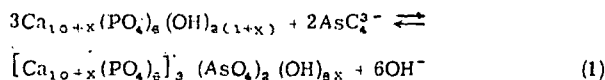
Thus, solid solutions are formed in the OH(H$_2$O)-AsO$_4$-apatite system. Subsequently, secondary rearrangement processes are not ruled out (particularly with change in the external conditions) during the ageing of the precipitate in contact with the mother solution and with increase in the crystallinity of the structure. The anomalous behaviour of arsenic under the conditions of the formation of the hydroxylapatite structure is similar to the problem of the formation of the structure of carbonate-apatites[12]).
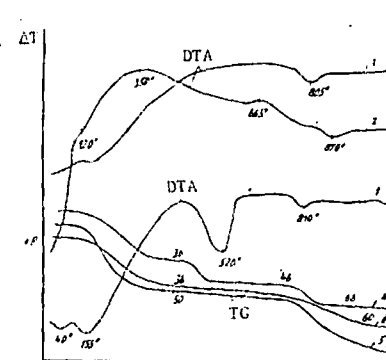
Fig.3
The thermograms and derivatograms of the precipitates. Heating rate 10 deg C/min. DTA: 1 - calcium arsenate; 2 - hydroxylapatite without arsenic; 3 - with arsenic. TG: 4 - calcium arsenate; 5 - hydroxylapatite without arsenic; 6 - with arsenic. The figures on curves 4-6 correspond to the decrease in the weight of the sample (mg).

Altogether, in spite of the detailed mechanism of the formation of compounds in the hydroxylapatite group, a decrease in the solubility as a function of the degree of crystallinity is common to them. Investigations into the solubility of arsenic-containing precipitates based on hydroxylapatite showed that the solubility of the precipitates with respect to arsenic decreases with increase in the length of contact in the mother solution (fig.4). The Xray amorphous precipitates have a solubility of 1.5-2.0 mg/l, which is 20-25 times lower than the solubility of calcium arsenate, equal to 32 mg/l or more. An increase in the calcium content of the solution to 200-300 mg/l reduces the solubility of the precipitate in arsenic by more than three times. Precipitates held in the mother solution for more than thirty days in a neutral medium have a solubility of 0.1-0.15 mg/l even with 100-200 mg/l of calcium. The pH range in which the precipitate has a solubility meeting the hygiene standards is extended with increase in the degree of crystallinity of the precipitate. Thus, precipitates which have been held for more than 30 days can be stored in the simplest settling ponds with a weakly alkaline reaction (pH > 7.5) at an equilibrium calcium concentration of 5-10 mg-eq/l.
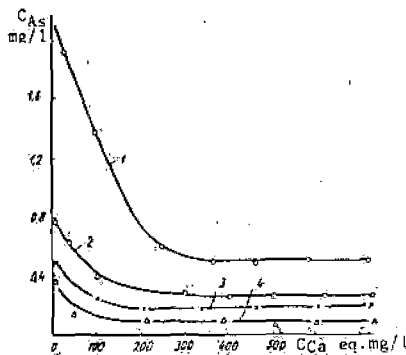
Fig. 4
The solubility of arsenic-containing precipitates based on hydroxylapatite as a function of the concentration of calcium in the solution and of the ageing time, pH = 7-7.5; amount of precipitate 500 mg/l; contact time 96 h; temperature 20-22°C. Holding time of precipitate in mother solution, days: 1 - 1; 2 - 12; 3 - 24; 4 - 35;

The salt composition of the water during the precipitation of the arsenic determines not only the effectiveness of the precipitation but also the solubility of the compounds which form. Thus, anions are capable of competing with the arsenic during the sorption on the hydroxylapatite precipitate. According to their effect on the precipitation of arsenic, the anions can be arranged in the following order:

$$CO_3^{2-} - SO_4^{2-} > Cl^- - NO_3^-$$
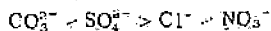
i.e., the precipitation of the arsenic becomes worse with increase in this series. It is most difficult to precipitate arsenic from carbonate waters by this method, whereas the presence of even small amounts of fluorine in the system considerably improves the precipitation of arsenic and reduces the solubility of the precipitate. In the general case it is possible to purify water with a salt content of not more than 5 g/l effectively by precipitation of the arsenic in the form of poorly soluble compounds based on hydroxylapatite. The results from the investigations were brought into use during the introduction of the method for the purification of effluents from the slime accumulator at one of the copper-smelting combines of the Urals.

Conclusions

1. A compound of the hydroxylapatite type, corresponding

to the composition $Ca_5(PO_4)_3OH$ and distinguished by low solubility, is formed initially in the $Ca^{2+} - PO_4^{3-} - AsO_4^{3-} - H_2O$ system.

2. Arsenic is precipitated as a result of substitution of hydroxyl groups by arsenic anions with the formation of a compound of the hydroxylapatite type, which changes into a crystalline form with time.

3. The proposed mechanism was confirmed by data on the solubility of arsenic-containing precipitates having a hydroxylapatite structure by the IR spectra and by Xray, thermographic, and derivatographic methods of analysis.

References

1) A V Nikolaev et alia: Izv. SO Akad. Nauk SSSR, Ser. Khim. Nauk 1970, 3, (7), 115.
2) V P Porubaev et alia: Tr. in-ta Kazmekhanobra Sb. 1972, 10, 110.
3) Yu O Grigor'ev et alia: Proceedings of Scientific-technical conference on "Methods for the high purification of effluents". Sverdlovsk 1975.
4) A V Nikolaev et alia: Izv. SO Akad. Nauk SSSR Ser. Khim. Nauk 1972, 5, (12), 121.
5) A V Nikolaev et alia: Izv. SO Akad. Nauk SSSR, Ser. Khim. Nauk 1974, 6, 12, 30.
6) B I Shramban et alia: Khimicheskaya Promyshlennost' 1974, (5), 396.
7) A K Babko et alia: Photometric analysis. Methods for the determination of non-metals. Khimiya, Moscow 1974.
8) Yu Yu Lur'e et alia: Chemical analysis of industrial effluents. Khimiya, Moscow 1974.
9) A V Kazakov: Tr. In-ta Udobrenii i insektofungitsidov 1973, 139.
10) A V Valyashko et alia: Geokhimiya 1968, (1), 26.
11) H M Pootare et alia: J. Colloid. Sci., 1962, 17, (3).
12) U A Dir et alia: Rock-forming minerals. Mir, Moscow 1966, 5.
13) M V Akhmanova: Uspekhi Khimii 1959, 27, (3), 312.
14) H A Schleede et alia: Elektrochemie 1932, 38, 633.
15) B P Nikol'skikh (editor): Chemists Handbook, Khimiya, Leningrad 1964, 2.

UDC 669.213.6+622.765.06

Extraction of noble metals from the tailings from the sorption cyaniding of ores

A S Romanov, N V Svistunov and V F Nechetalenko (North-Caucasian Mining-Metallurgical Institute - Department of the Metallurgy of Noble, Rare and Light Metals)

The sorption cyaniding of gold ores is finding wider and wider use particularly in the treatment of clay and ocherous ores. While possessing a series of advantages over the normal cyanide process, it also has disadvantages characteristic of the latter; stubborn gold (combined with sulphides and tellurides, coated by films insoluble in cyanide) is lost in the cyaniding tailings. The same applies to silver to an even greater degree. Methods which make it possible to extract the stubborn forms of noble metals from the tailings from sorption cyaniding by flotation of the gold and silver containing materials, in particular, are therefore of interest.

Examples of the flotation of the tailings from direct cyaniding have been described in the literature[1-3]. The need for such a combination of processes arises when the ore contains gold tellurides and also other valuable minerals (lead, bismuth, etc.), the loss of which with the cyaniding tailings is undesirable.

Gold tellurides are readily floated in a lime-cyanide medium[3], but other sulphide minerals are greatly depressed in the cyaniding process and must be activated before flotation. Washing out the depressers (lime and cyanide) with water is not always sufficiently effective. Acid treatment of the cyaniding tailings is therefore sometimes practiced[3]. Pyrite is activated in a soda medium by copper

sulphate and sodium sulphide. An essential condition for the flotation of copper sulphides from the cyaniding tailings is considered to be the absence of free cyanide in the liquid phase of the pulp.

Ore distinguished by the presence of silver and gold tellurides and also by a substantial content of silver, bismuth, lead, copper and antimony in the sulphide part are processed at one of the gold-extracting plants of Central Asia. The treatment of these ores by the sorption method secures high extraction of gold but leads to complete loss of valuable sulphides and also a considerable amount of the silver. Since washing out of the cyanide and lime from the sorption tailings before flotation is completely excluded under the conditions of ions-exchange technology, it seemed of interest to study the conditions for the extraction of noble metals and valuable sulphide minerals from the tailings by flotation.

Experiments were carried out under laboratory conditions on two samples of ore, the composition of which is given in table 1. The sulphide part of these ores was largely represented by pyrite, chalcopyrite, grey copper ores, bismuthite and tellurobismuthites. Samples of the ores weighing 1kg were ground in rod mills with a liquid-solid ratio of 1:1 to 75% of the -0.08mm class with a rod

181

PATTERNS OF ARSENIC DEPOSITION FROM SULFURIC ACID SOLUTIONS ON TITANIUM HYDROXIDE

UDC 669.778

M. Z. Ugorets and S. N. Novik

The object of this paper was to reveal some of the patterns of arsenic deposition from sulfuric acid solutions on titanium hydroxide.

Titanium hydroxide powder (composition $TiO_2 \cdot 1.9 \ H_2O$) produced by neutralization of

Fig. 1. Kinetic curves for arsenic deposition from sulfuric acid solutions at:
1 - 60°C; 2 - 75°C.

sulfate solution was placed in a sulfuric acid solution containing ~ 6 g/liter As (V) and processed in a thermostatically controlled cell with a mixer. Equilibrium was usually reached in 10 hours.

The statistical method of experiment planning was used to study the effect of temperature, the sulfuric acid concentration, the Ti:As ratio, and the mixing speed upon the extent of arsenic deposition from solution. The main parameters were varied within the following limits: temperature 15-75°C, acidity 50-250 g/liter H_2SO_4, Ti:As = 1:1.5, and mixing speed of 100--700 rpm.

The kinetic curves (Fig. 1) can be satisfactorily described by the equation:

$$\Gamma = K\tau^n, \qquad (1)$$

where Γ is the extent of arsenic deposition calculated relative to the maximum for the given conditions and τ - is the duration of the experiment, min.

An analysis of particular relationships of maximum extent of arsenic deposition to the studied parameters showed that the magnitudes of K and n in Equation (1) do not alter according to the acid concentration, the Ti:As ratio or the mixing rate are equal to about 30 and 0.22, respectively. However, they are substantially dependent upon temperature (Fig. 2). In our opinion, the nature of the changes in coefficients K and n indicates that the importance of physical deposition of arsenic acid decreases with a rise in temperature, but the importance of its chemical reaction with titanium hydroxide increases. The absolute magnitude of n indicates that the process is controlled by reagent diffusion through the solid reaction product layer.

Research on deposition of arsenic from industrial solution from copper electrorefining (9.6 g/liter As, 157 g/liter H_2SO_4, and 46 g/liter Cu) was conducted with titanium hydroxide (63.2% TiO_2), also produced by neutralization of sulfate solution. Fig. 3 shows the kinetic curves. With an increase in temperature, the time to achieve maximum arsenic deposition is reduced and the composition of the solid phase approximates $3 \ TiO_2 \cdot As_2O_5 \cdot 3H_2O$.

The obtained results were used as the basis for the method of removing arsenic and antimony from electrolyte which has been tested and adopted at the Balkhash Mining and Metallurgical Combine.
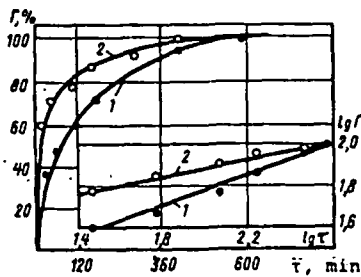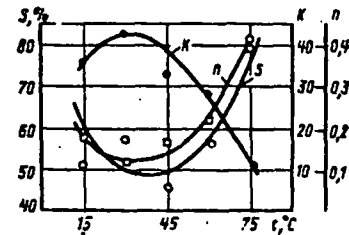

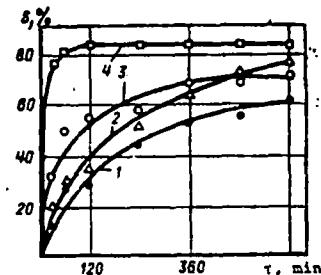Fig. 2. Relationship of maximum degree of arsenic deposition S and coefficients K and n to temperature.

Fig. 3. Kinetic curves for arsenic deposition from industrial electrolyte (Ti:As = 1) at:
1 - 30°C; 2 - 45°C; 3 - 60°C; 4 - 75°C.

compounds copper ions are obtained in the solution and arsenic and antimony trioxides are obtained in the solid form.

From comparison of the Pourbaix diagrams for the Cu_3As-H_2O and Cu_3Sb-H_2O systems it is seen that the region of potentials corresponding to the best technological requirements is considerably wider for copper antimonide than for copper arsenide. Moreover, the stability region of Cu_3As. (The width of the zone corresponding to stable existence amounts to 1.4 V for copper arsenide and 0.9V for copper antimonide). This indicates that the oxidation of copper antimonide takes place more readily than the oxidation of copper arsenide over the whole range of pH. All this shows that during oxidative leaching of speiss copper arsenide is present under more drastic conditions, and for uniform dissolution of the speiss the process must therefore be carried out under the most favourable conditions for the oxidation of copper arsenide. Thus, the analysis of the Pourbaix diagrams for the Cu-H_2O, Cu_3As-H_2O, and Cu_3Sb-H_2O systems made it possible to determine the most favourable conditions in technological respects for the oxidation of copper-lead speiss and the principal phase transformations during oxidation, and to solve the problem of the stability of one or the other state of the system. Copper ions and arsenic antimony trioxides are thermodynamically stable in acidic solutions at potentials of 0.45-0.5V. The difference in the states of aggregation makes it possible to separate these speiss oxidation products easily.

References

1) E I Ponomareva et alia: Extraction of arsenic from speiss. Tr. IMiO Akad. Nauk KazSSR, Alma-Ata, 1959,1.
2) N I Mikhailov et alia: Metallurgical and chemical industry of Kazakhstan, 1961,1,5,6.
3) Author's Certificate No.165306, 10 July 1963.
4) F L Stillwell: Ref. Chem. Abstrs. 1952,46, (14), 6565.
5) F M Loskutov: Metallurgy of lead. Metallurgizdat, Moscow 1965.
6) K D Gerlak et alia: Autoclave leaching of speiss. Collection: Hydrometallurgy. Metallurgiya, Moscow 1971.
7) S V Khryashchev et alia: Collection: Metallurgy and concentration. Alma-Ata 1965.
8) M Pourbaix: Atlas d'Euilibres Electrochimiques, Paris 1963.
9) E Peters: The physical chemistry of hydrometallurgy New York 1973.
10) V G Ageenkov et alia: Metallurgical calculations. Metallurgizdat, Moscow 1962.
11) V M Latimer: Oxidation states of the elements and their potentials in aqueous solutions. IL, Moscow 195\.
12) M Kh Karapet'yants and M L Karapet'yants: Fundamental thermodynamic constants of inorganic and organic materials. Khimiya, Moscow 1968.

Principles of the autoclave desiliconising of high-silicon sulphide concentrates

V G Shkodin, D N Abishev, E A Buketov, V P Malyshev and N S Bekturganov (Chemical-Metallurgical Institute, Academy of Sciences of the Kazakh SSR)

The treatment of high-silicon sulphide materials (e. g. the copper concentrates of the Dzhezkazgan or Udokansk deposits) by the traditional method of smelting the matte possesses a number of disadvantages associated with the pyrometallurgical process of separation of the silica (the high yield of slags, the reduced throughput, the high consumption of fluxes, etc.). Thus, according to data from the DGMK the output of waste slags amounts to 2.1-2.3 ton per ton of copper, and the losses of copper with the slags are not less than 1%. Preliminary selective separation of silicon dioxide, which makes it possible not only to remove the gangue materials but also to concentrate the valuable components, is therefore more useful. Such a process can be realised by alkaline autoclave leaching, since the sulphides of heavy nonferrous metals are practically insoluble in alkalis without access to an oxidising agent[1].

The investigations were carried out by rational experimental design[2-4] in stainless-steel autoclaves with the Dzhezkazgan copper concentrate, containing, wt.%: 32.02Cu, 4.78Fe, 2.30Pb, 1.27Zn, 11.70S_{tot}, 30.20SiO_2, 5.10Al_2O_3, 1.75CaO 0.67MgO, and 1.46Na_2O. In the experimental ranges of temperature (t) 120-200°C, process times (τ) 45-225 min, initial solution concentrations (N) 100-300 g/l Na_2O, and liquid-solid ratios in the initial pulp (r) 3-7 the partial dependences of the extraction of silica into the solution on the factors investigated was found:

$$\alpha_t = 0.6t - 60.43;$$

$$\alpha_t = 0.15\tau + 14.93;$$

$$\alpha_N = 0.0343N + 28.32;$$

$$\alpha_r = 4.89 (r - 3)^{1.3} + 29.9$$

From the data presented it follows that the process temperature has the greatest effect on the extraction of silica into solution under the experimental conditions. (The degree of leaching increases by almost six times with increase in the temperature from 120 to 200°C). The kinetics of the process are evidently determined mainly by the chemical event of

dissolution of silica in alkali, and this does not contradict known data on the leaching of silica from Krivorozh'e iron concentrates[6]. The initial alkalinity and liquid-solid ratio of the pulp affect the process considerably less, and this is due to the fact that saturation of the solutions with silica does not occur. On the basis of the data obtained we formulated the following generalised many-factor equation:

$$\alpha = \frac{(0.6t - 60.43)(0.15\tau + 14.93)(0.0343N + 28.32)}{35.18^3 [4.89 (r - 3)^{1/3} + 29.9]^{-1}}$$

from analysis of which we determined the leaching conditions: temperature, 160°C; length of autoclave treatment, 100 min; initial sodium hydroxide concentration, 160 g/l; liquid-solid ratio 4:1.
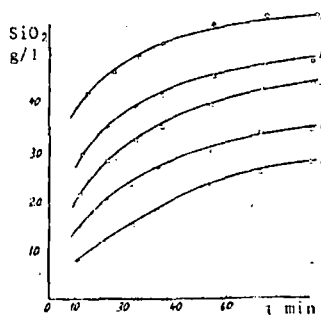
The kinetics of the leaching of silica with sodium hydroxide solution. 1 – 142°C; 2 – 150°C; 3 – 160°C; 4 – 170°C; 5 – 180°C.

During investigation of the kinetic characteristics of the leaching of silica from the same concentrates (fig); the experiments were carried out in a three-litre autoclave designed by the Gipronikel' Institute without a diffuser or turbine at a sodium hydroxide concentration of 160 g/l at 140-180°C) it was established that the activation energy of the process does not depend on the concentration of dissolved silica in the range of 20-50 g/l and amounts to 20.8 ± 1.4 kcal/mole. This value agrees well with the results obtained by Kurin and Stas'[6]. The concentration of copper, lead, and iron remains practically unchanged with time and does not exceed 0.005 g/l. The concentration of zinc and sulphur in the solution decreases with increase

50

The distribution of the metals during the autoclave leaching of copper concentrates
(1 - metal content, % g/l; 2 - distribution, %)

Name	Amount g, ml	Silica		Copper		Lead		Iron		Zinc		Sulphur		Aluminium	
		1	2	1	2	1	2	1	2	1	2	1	2	1	2
Loaded:															
1. Copper concentrate	300	30.2	100.0	32.0	100.0	2.3	100.0	4.8	100.0	1.3	100.0	11.7	100.0	2.7	100.0
2. Alkaline solution	1050	-	-	-	-	-	-	-	-	-	-	-	-	-	-
Total		100.0		100.0		100.0		100.0		100.0		100.0		100.0	
Obtained:															
1. Silicate solution	895	52.2	51.6	0.003	-	tr.	-	0.002	0.1	0.014	0.3	0.3	0.8	0.23	2.5
2. Wash water	3610	1.7	7.0	0.002	-	0.002	0.1	0.003	0.9	tr.	-	n/an.	-	0.01	0.5
3. Cake	223.2	15.2	37.5	42.7	99.3	3.1	101.0	6.5	101.0	1.6	92.4	15.2	96.7	3.4	92.5
Total		96.1		99.3		101.1		102.0		92.7		97.5		95.5	
Losses + discrepancy		+3.9		+0.7		-1.1		-2.0		+7.3		+2.5		+4.5	
Overall Total		100.0		100.0		100.0		100.0		100.0		100.0		100.0	

in the concentration of silica. This is due either to the salting out action of silicon dioxide or to the occurrence of secondary chemical reactions. Zinc evidently does not pass into solution in the form of sincates, since according to data given by Kuznetsov et alia[6] the presence of dissolved silica prevents the decomposition of sodium zincates even in supersaturated solutions. The passage of sulphur into solution(up to 0.3-0.4 g/l) is probably due to the presence of a small amount of pyrite in the initial concentrate[7] and to its dissolution[8]. Balancing tests were conducted in the autoclave under the optimum conditions. From the table it follows that the silica here passes into solution fairly selectively, and its residual content in the cake amounts to 15.2%. (With twofold leaching under these conditions it is possible to reduce the silica content in the cake to 6-8%). The content of copper and other components after leaching increased accordingly by 1.33 times. During treatment of such a desiliconised product at the DGMK by the existing technology hardly any addition of limestone to the electro-smelting charge was required. (At the present time 0.6-0.7 ton is used per ton of copper). On this account the output of waste slags can be reduced by more than half. Thus, a matte containing 59.38% of Cu and a slag containing 0.51%Cu were obtained from the smelting of desiliconised concentrate containing 14.5% SiO$_2$ with the addition of 15% of pyrite in a large-scale electric furnace. The output of slag amounted to about 36% or 0.84 ton per ton of copper. Since the solutions after leaching contain hardly any heavy nonferrous metals, their regeneration by known methods (e.g., by caustification with lime[9]) does not present major difficulties. By tests it was shown that silica is deposited almost completely at a temperature of 60-70°C with a molar CaO:SiO$_2$ consumption rate of 1.5-3.0 in 1.5-2.0 h; with an initial silica content of up to 50 g/l the residual concentration of silica amounts to not more than 0.15 g/l. Owing to its high degree of dispersion the calcium hydrosilicate deposit formed during caustification is a unique raw material for the production of building materials such as white high-alite cement[10]). In addition we established that rhenium passes from the concentrate into the solution to the extent of 55-65% under the conditions of autoclave desiliconising. The rhenium is not precipitated during regeneration of the silicate alkali on account of the comparatively high solubility of calcium perrhenate, and with repeated

use of the solutions it accumulates in them and can be extracted by known methods, e.g., by sorption. Here the unleached rhenium can be extracted by the appropriate technique.

During large-scale trials in a closed cycle it was shown that, with counterflow decantation for washing the alkali from the solid products, the overall consumption of sodium hydroxide for desiliconising amounts to 0.3 m³. Thus, although autoclave desiliconising is a supplementary preparatory operation to the existing pyrometallurgical treatment, its realisation nevertheless predetermines a quality improvement in the production of copper, a sharp improvement in the radical utilisation of raw material, an improvement in the working conditions, and improvement in the sanitary conditions of the water-air basin. The autoclave desiliconising process makes it possible to prepare a high-silica copper raw material for treatment by the most modern pyrometallurgical schemes for the production of copper and may find practical use, primarily, in the treatment of Dzhezkazgan and Udokansk ores.

References

1) R P Rafal'skii: Hydrothermal equilibria and processes in mineral formation. Atomizdat, Moscow 1973.
2) M M Protod'yakonov et alia: Method of rational experimental design. Nauka, Moscow 1970.
3) M M Protod'yakonov: Method of rational experimental design. Moscow 1961.
4) M M Protod'yakonov: Compilation of mining norms and their utilisation, Moscow-Leningrad-Novosibirsk, Gos. Nauchno-Tekhn. Gornoe Izd., 1932.
5) N P Kurin et alia: Zh. Prikl. Khim., 1975, **48**, (5), 1014.
6) S I Kuznetsov et alia: Izv. Vuz. Tsvetnaya Metallurgiya 1975, (1), 132.
7) T A Satpaeva: Collection: The Great Dzhezkazgan Geology and metallogeny. Alma-Ata 1961, p.165.
8) T A Nepokrytykh et alia: Izv. Vuz. Tsvetnaya Metallurgiya 1974, (4), 68.
9) I Z Pevzner et alia: Desiliconising of aluminate solutions. Metallurgiya, Moscow 1974.
10) A S Saduakasov et alia: Method for the production of cement clinker. Author's Certificate No.523063, 30 June 1976.
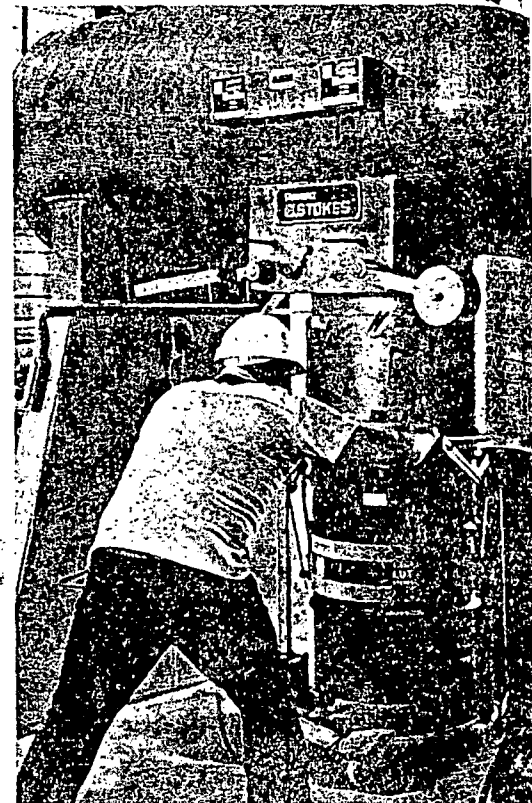
Reduction of molten copper and lead oxides with methane

J A Montil'o and V M Lopatin (Unipromed')

Published data on the reduction of nonferrous metal oxides are extremely limited. The question of the reducing power

U₃O₈ PROCESS AVOIDS SULPHATES AND CHLORIDES

UNIVERSITY OF UTAH
RESEARCH INSTITUTE
EARTH SCIENCE LAB.

A special adapter developed by IEC allows an operator to wheel a 55-gal drum under the dryer outlet and raise it tightly against the discharge opening to receive a load of dried yellowcake. When the barrel is full, the discharge valve is closed and the barrel is lowered and wheeled to a weighing station.

A yellowcake precipitation process developed by Intercontinental Energy Corp. (IEC) for its Zamzow in-situ uranium-leaching operations in Live Oak County, Tex., uses neither sulphates nor chlorides in extraction and precipitation. The process thereby avoids formation of uranium salts that require high-temperature calciners. IEC uses a solution of ammonium carbonate and hydrogen peroxide for leaching and live steam to sparge the pregnant eluate, driving off ammonia and carbon dioxide and precipitating yellowcake. A rotary vacuum dryer, the first to be used in such an application, accepts a yellowcake slurry containing 30% solids and produces a dry product ready for packaging.

Plant manager Kim Harden notes that the process does not require pollution control devices, such as stack filters and scrubbers, that must be installed for calciners. Utility costs for the vacuum drying system are quite low, and system components are packaged on skids that are positioned easily on concrete floors and relocated quickly to a new job site. The vacuum drying system was supplied by the Stokes Div. of Pennwalt Corp.

At Zamzow, IEC circulates leach solution through ore zones about 175 ft below ground. The solution oxidizes the uranium minerals to a form amenable to leaching by ammonium carbonate. Chemistry of the solution is controlled to prevent significant precipitation of calcium carbonate in the system. At any given time, 80 to 100 injection wells and 40 to 50 production wells are usually in operation to provide leach liquor for the plant. The wells are cased with PVC and are equipped with 3-hp to 5-hp stainless steel down-hole pumps that generate an average leachant flow of 1,050 gpm to three uranium recovery circuits. With minor exceptions, construction and completion of the wells follows conventional practices of the water well industry.

The well field operates in a balanced condition that confines leachants to the ore zones between injection and production wells. Water in a series of 4-in.-dia monitor wells surrounding the orebody is sampled biweekly to determine if any leachant is escaping from the well field.

Uranium-bearing leachant is pumped to a surface plant equipped with three parallel ion exchange circuits, each of which includes a 10,000-gal fiberglass surge tank, a 60-hp circulation pump, a series of filters to remove particulate matter, and three 7 x 8-ft down-flow resin ion exchange columns. After uranium has been extracted in the ion exchange circuits, the leachant is pumped back to the well field by 15-hp injection pumps.

When an ion exchange column becomes loaded to capacity, it is isolated from the circuit, and a solution of ammonium carbonate is used to strip the uranium from the ion exchange resin. The resulting pregnant eluate then advances to one of three 4,000-gal stainless steel tanks.

The eluate is sparged with live steam, driving off ammonia and carbon dioxide and precipitating the uranium. Offgasses are recovered, and the resulting uranium slurry is pumped to a 5,000-gal fiberglass storage tank for settling and decanting. After decantation, the slurry is pumped to the vacuum dryer.

A reverse-osmosis water treatment plant provides plant makeup water and water for the boilers. Leachants and elution solutions are prepared on the site by injecting anhydrous ammonia and carbon dioxide into water in a modified 4,000-gal stainless steel fertilizer mixer.

The rotary vacuum dryer in use at Zamzow is one of a line of Stokes units that have found a variety of applications, including installations to dry slurries of powdered metal, pharmaceuticals, herbicides, and pesticides. The near-zero

118

Vacuum drying system at Zamzow mine
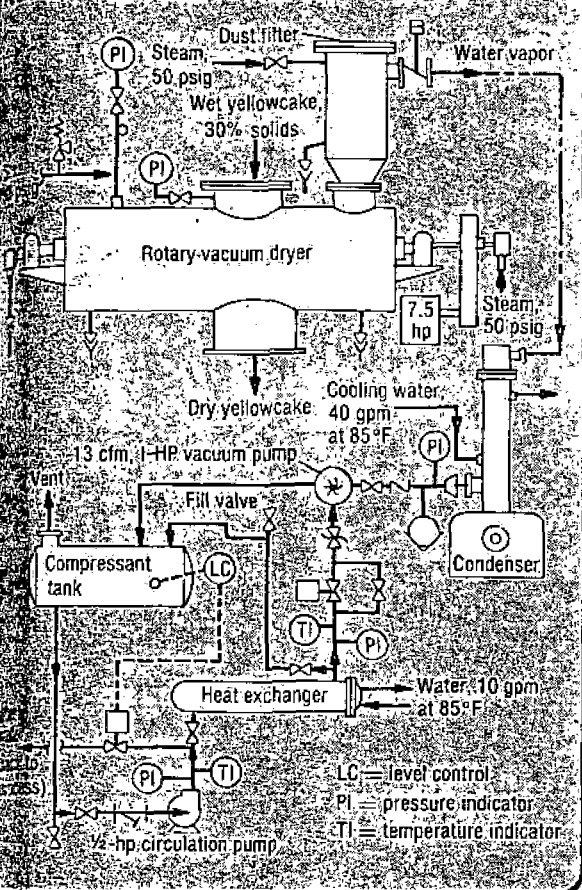
pollution characteristics of the system were very attractive to IEC. Because the system operates under vacuum, a leak results in air being drawn into the system, rather than contaminants being released to the atmosphere. The units are available in sizes ranging from 15 in. to 5 ft ID and from 20 in. to 30 ft internal length.

The dryer at Zamzow has an inside diameter of 3 ft and an internal length of 10 ft, providing a total volume of 70 cu ft and a capacity of 1,500 lb per day of yellowcake. It is heated by means of steam jacketing along the cylindrical container and steam inside the shaft and arms of the helical agitator. Heat transfer is aided not only by the continuous mixing action of the rotating agitator but also by spring-loaded scraper blades that prevent buildup of dried yellowcake on the inside heating surfaces.

Approximate utility requirements to process a 4,000-lb load of yellowcake slurry at 30% solids include: 250 lb per hr of steam at 50 psig, 40 gpm of condenser cooling water at 85°F, and electricity to drive a 10-hp motor.

Dried yellowcake discharges directly into 55-gal drums; the discharge valve port is fitted with a dust-tight shroud. An inverted, bag-type dust filter flange-mounted on top of the dryer prevents dust from getting into the vacuum systems. The bags are shaken mechanically at regular intervals, and dust is returned to the dryer.

Water vapor from the dryer is condensed in a vertical tube-type condenser, and the water that is recovered returns to the circuit, another significant pollution-control feature of the system. (See flowsheet.)

Zamzow, which is designed to produce 300,000 lb per year of U_3O_8, is the second in-situ leaching uranium mine developed by IEC in Texas, the first being located at Pawnee. Pacific Gas and Electric, which has contracted for the entire output of the Zamzow mine, received its first shipment of yellowcake on Aug. 1, 1978. ■
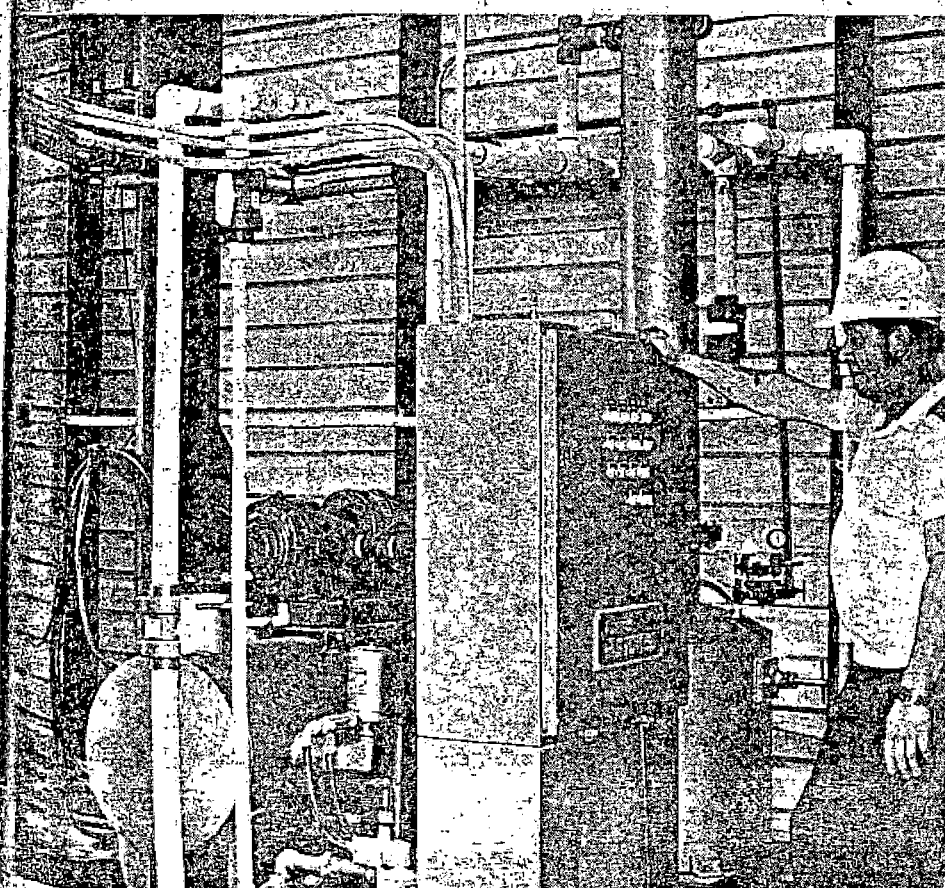
Dryer control panel includes motor starter, selector switches, pilot lights, and control power transformer. Vertical condenser column is at the operator's right hand. Compressant tank and vacuum pump are located behind the control panel.

SUBJ
MNG
PBSB

1976 v.12 N 2

PURIFICATION OF BISMUTH SOLUTIONS BY SOLVENT EXTRACTION WITH DI(2-ETHYLHEXYL) PHOSPHORIC ACID[1]

Yu. M. Yukhin, I. S. Levin, S. M. Barakov, A. P. Korzhov, and S. I. Kayukov

In the production of bismuth reagents, solutions containing bismuth are usually purified by hydrolytic precipitation [1]. In the existing precipitation-filtration scheme for the separation of bismuth from impurities, the commercial metal is dissolved in nitric acid and the bismuth is purified by gradual precipitation of basic bismuth nitrate with a mixture of $(NH_4)_2CO_3$ and NH_4OH over a period of 35 hr with strict temperature regulation ($22 \pm 2°C$). The disadvantages of this technique are that it is not always possible to obtain products of the necessary purity (especially in terms of lead), and the long duration of the process.

The object of the present investigation was to develop a solvent-extraction scheme for the removal of impurities from nitric acid solutions of bismuth with subsequent production of basic bismuth nitrate and oxide.

Solutions of salts of quaternary ammonium bases have been suggested as extractants for bismuth [2]. We studied tributyl phosphate (TBP), alkylphosphoric (di- and mono-) acids (APA), and caprylic and di(2-ethylhexyl)dithiophosphoric acids as extractants. The relationship between the bismuth distribution ratios and the nitric acid concentration in the aqueous phases when the extractants enumerated above are used is shown in Fig. 1, from which it is apparent that when di- and mono-2EHPA and caprylic acid are used as extractants the bismuth distribution ratios (D) fall sharply when the nitric acid concentration in the aqueous phase increases; this is usual when these extractants are used in the solvent extraction of metals, and is due to the cation-exchange mechanism of extraction. The distribution ratios pass through a peak when tributyl phosphate is used as the extractant. It is apparent from the data given that APAs are most effective in extracting bismuth. Thus D_{Bi} is much higher when bismuth is extracted from 0.25-0.5N HNO_3 solutions even with a 0.4N solution of APA in octane than when concentrated (6N) caprylic acid or concentrated TBP (3.67N) are used as extractants.
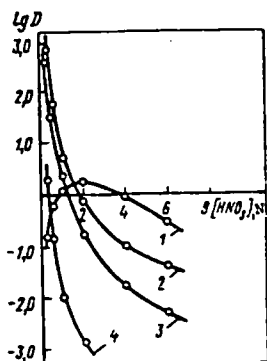

Fig. 1. Extraction of bismuth (III) from nitric acid solutions of 1 g/liter Bi: 1 - 3.76N TBP; 2 - 0.4N M2EHPA; 3 - 0.4N D2EHPA; 2,3 - diluent octane; 4 - 6.3N caprylic acid.

In spite of the fact that it is very effective in extracting Bi from a variety of solutions, di(2-ethylhexyl)dithiophosphoric acid is not suitable here, because HNO_3 breaks it down. We chose D2EHPA as the extractant for further investigations.

The principal impurities in industrial solutions obtained by dissolving commercial bismuth in nitric acid are Pb, Zn, Cu, and Ag. It is apparent from the data given (Fig. 2) that the metal distribution ratios fall sharply when the nitric acid concentration increases. It should be noted that the distribution ratios β of the Bi-Me pair, where Me is Pb, Zn, Cu, Ag, etc. respectively, also fall when the nitric acid concentration in the aqueous phase increases.

Bismuth is extracted by D2EHPA from nitric acid solutions according to the following equation [3]:

$$Bi_a^{3+} + 2,5 (H_2R_2)_0 = BiR_3 \cdot 2HR_0 + 3H_a^+$$

with constant

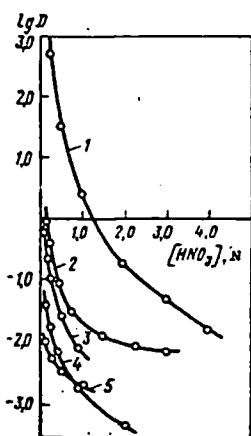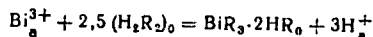$$K = \frac{D \cdot [H^+]_a^3 \cdot \Phi}{[H_2R_2]_0^{2.5}} .$$

Fig. 2. Extraction of Bi, Pb, Zn, Cu, and Ag with D2EHPA from nitric acid solutions of 1 g/liter Me; 0.4N D2EHPA (diluent octane): 1 - Bi; 2 - Pb; 3 - Zn; 4 -

As a rule, bivalent metals are extracted by D2EHPA according to the equation

$$Me_a^{2+} + 2 (H_2R_2)_0 \rightleftharpoons MeR_2 \cdot 2HR_0 + 2H_a^+$$
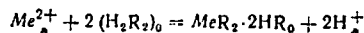
with constant

$$K_1 = \frac{D \cdot [H^+]_a^2 \cdot \Phi_1}{[H_2R_2]_0^2} .$$

where Φ is the complexing function, which takes account of metal complexing with nitrate ions. Accordingly

$$\beta = \frac{D_{Bl}}{D_{Me^{2+}}} = \frac{K \cdot [H_2 R_2]_0^{0.5} \cdot \Phi_1}{K_1 \cdot [H] \cdot \Phi} .$$

and consequently it is necessary to increase the concentration (1 g/liter Me; 0.4N D2EHPA, diluent octane) and to reduce the aqueous phase pH in order to reach the highest distribution ratios. This is confirmed by the following data:

[HNO$_3$] N	$\beta_{Bi/Pb}$	$\beta_{Bi/Zn}$	$\beta_{Bi/Cu}$	$\beta_{Bi/Ag}$
0.1	$2.4 \cdot 10^3$	$2.8 \cdot 10^3$	$5.3 \cdot 10^4$	$2.0 \cdot 10^3$
0.2	$5.0 \cdot 10^3$	$6.9 \cdot 10^3$	$1.3 \cdot 10^5$	$2.8 \cdot 10^3$
0.4	$8.9 \cdot 10^3$	$1.8 \cdot 10^3$	$1.2 \cdot 10^4$	$2.0 \cdot 10^4$
0.7	$3.3 \cdot 10^3$	$8.6 \cdot 10^3$	$3.8 \cdot 10^3$	$4.0 \cdot 10^3$
1.0	$1.1 \cdot 10^3$	$3.6 \cdot 10^3$	$1.8 \cdot 10^3$	$1.2 \cdot 10^3$
1.5	$4.3 \cdot 10$	—	$6.4 \cdot 10^3$	$3.6 \cdot 10^3$
2.0	$2.1 \cdot 10$	—	$4.0 \cdot 10^3$	—
3.0	9.1	—	—	—

Bismuth can be separated from the associated metals in solvent extraction from nitric acid solutions. In addition, when bismuth alkyl phosphate is extracted on a background of substantial Bi concentrations in the aqueous phase the probability of extraction of impurities decreases, because the extraction constant for bismuth with D2EHPA is much greater than for the impurities and bismuth displaces them from the organic phase; this helps to give an additional increase in the distribution ratios.

In extraction of bismuth with D2EHPA the nature of the organic diluent has a significant effect upon the distribution ratios. The use of saturated hydrocarbons as diluents has the least depressant effect upon D_{Bi}. The logarithm of the bismuth extraction constant is 3.40 under conditions uncomplicated by complexing in the aqueous phase when octane is used as the diluent. In extraction from nitric acid solutions with ionic strength $\mu = 1$ (NaNO$_3$) the logarithm of the bismuth extraction constant lgK' for octane is 2.30, i.e., where [NO$_3^-$] = 1 g-ion/liter, $\Phi = 12$.

Laboratory investigations have made it possible to plan a purification scheme for nitric acid solutions of bismuth in which bismuth is extracted with 1.0-1.5N solution of D2EHPA in kerosene from 0.8-1N HNO$_3$ and reextracted with 4-6N HNO$_3$.

Pilot tests on purification of bismuth solutions were carried out in a 14-stage extractor (Fig. 3; cell volume 20 liters) using the following scheme: six stages (1-6) for extraction, two (7,8) for washing the bismuth-bearing organic phase with 1N HNO$_3$, and two (13,14) for washing the circulating extractant with water.

The solutions were fed to the extractors from header tanks (15-20) through metering devices (25-30). The solutions were adjusted if necessary in storage tanks and repumped to the header tanks. The tests were conducted under continuous conditions with a closed extractant circuit.

Industrial bismuth solutions produced by dissolving commercial bismuth containing (wt.%) > 98 Bi, 1.5 Pb, 0.01 Sb, 0.02 Cu, 0.005 Fe, 0.15 Ag, 0.001 As, 0.01 Mg, and 0.02 Zn in nitric acid ([Bi] ~ 350 g/liter) were purified by solvent extraction. The extractant used was a 1.2N solution of commercial D2EHPA (concentration of principal substance 60-80%)* in lamp kerosene, containing 6 vol. % tributyl phosphate for better separation. The latter is a surface-active addition and does not significantly reduce D_{Bi} under the conditions selected. The initial solution obtained by dissolving commercial bismuth in nitric acid was diluted about 4 times with 0.8N HNO$_3$ at the extractor input.

Extraction was carried out in 6 stages with an aqueous (A) to organic (O) phase ratio of 1 : 1.6. The aqueous phase (initial solution and dilution solution) was fed to the 6th stage, the extractant to the 1st stage. Bismuth was not detected in the raffinate leaving the 1st stage ([Bi] < 0.02 g/liter). Five stages are sufficient to achieve the necessary degree of bismuth extraction. A reduction in the O : A ratio is undesirable because the organic phase becomes saturated with bismuth, more viscous, and less mobile, i.e., saturated bismuth alkyl phosphate BiR$_3$ forms in the organic phase instead of extraction of the solvated complex BiR$_3 \cdot$2HR.

The extract was washed to remove impurities with 1N HNO$_3$ at a ratio of extract to acid of 1.6 : 1, to obtain more complete separation of bismuth from impurities prior to reextraction of the bismuth with nitric acid. The wash solution was fed to the 8th stage. On leaving the 7th stage the solution contained 1.1 g/liter bismuth and was recirculated.[2]

The bismuth was reextracted in four stages, the A : O flow ratio being 1 : 2.8. The reextractant, 4.6N HNO$_3$, was fed to the 12th stage. Reextraction is practically complete in three stages. The reextractant contained 100-110 g/liter Bi and the following impurities, %:

---

* It is desirable that the M2EHPA concentration in the commercial D2EHPA should be minimal, to avoid formation of a monoalkyl phosphate precipitate.

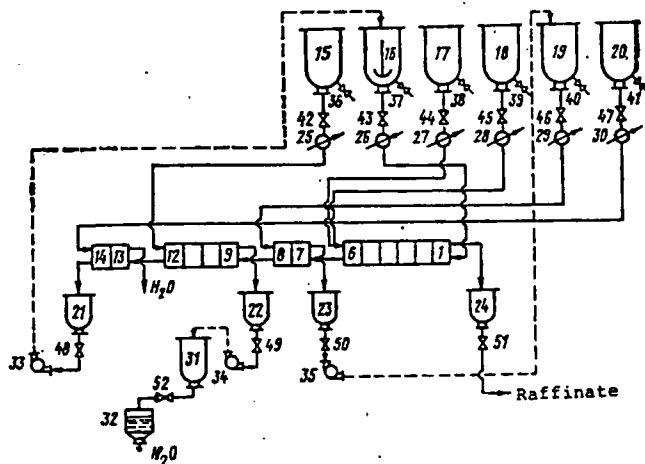[2] It is proposed in future to exclude washing of the extract with acid.

Fig. 3. Diagram of solvent-extraction installation: 1-14 - mixer-settlers; 15-20 - header tanks: 15 for reextractant, 16 for extractant, 17 for dilution solution, 18 for initial solution, 19 for wash solution, 20 for water; 21-24 - storage tanks: 21 for extractant, 22 for reextract, 23 for wash solution, 24 for raffinate; 25-30 - metering devices; 31 - reactor for precipitation of basic nitrate; 32 - Nutsch filter; 33-35 - pumps; 36-52 - valves.

Metal	1	2	3	4	5
Fe	0.0005	Undet.	0.001	Undet	0.0005
Cu	0.0001	0.0001	0.0001	Undet	0.0001
Pb	0.003	0.002	0.003	0.002	0.002
Mg	<0.001	<0.001	<0.001	<0.001	<0.001
Ca	<0.001	<0.001	<0.001	<0.001	<0.001
Na	0.0001	0.0002	0.0001	0.0001	0.0001

After reextraction of the bismuth, the extractant was fed to the 13th stage, washed with water, collected in vessel 21, and transferred by pump 33 to header tank 16.

The basic bismuth nitrate $BiONO_3 \cdot H_2O$ was precipitated from the reextract with aqueous ammonia solution. When the reextract is neutralized to pH 3 practically all the bismuth passes into the precipitate. The basic bismuth nitrate was washed with dilute HNO_3 solution (pH 2-3) and dried. The product was classifiable as analytical grade according to GOST 10217-62. Bismuth oxide Bi_2O_3 was produced by calcining the basic nitrate at 670°C. Bismuth oxide is a lemon-yellow powder containing > 99.7% Bi_2O_3 and chemically pure in grade according to GOST 10216-62.

REFERENCES

1. A. I. Busev, The Analytical Chemistry of Bismuth, Moscow, Izd-vo Akad. Nauk SSSR, 1953, 381 pages, illustrated.
2. S. T. Takezhanov, K. Z. Kuanysheva, A. M. Kunaev, et al., Vestnik Akad. Nauk Kazakh. SSR, 1973, No. 8, 59-64.
3. I. S. Levin, Yu. M. Yukhin, and I. A. Vorsina, Izv. Sibirsk. Otdel. Akad. Nauk SSSR, Seriya Khim. Nauk, 1970, No. 2, Issue 1, 61-68.

Spencer R. Titley

Porphyry Copper

Circumstantial evidence suggests that porphyry-related deposits, currently the world's principal source of copper, may have formed as by-products of volcanic activity

Copper runs the modern world, but most of us overlook, or are not aware of, the vital role it plays in bringing technological developments into our everyday lives. In North America, for example, a family of four may have more than thirty copper-wound electric motors in their home. Such motors are components of clocks, record and tape players, kitchen appliances, heating and cooling systems, vacuum cleaners, generators, and even electricity meters. Without copper, our ability to use electricity would be severely limited. Moreover, copper has such distinctive electrical, chemical, and mechanical properties that no other metal is completely adequate as a substitute. As a result of rising standards of living and growing expectations, more than 8 million tons of copper are mined each year. Where does it come from?

In much of the world, copper comes from two sources: recycling of scrap and used copper and mining of new copper from ore deposits. About 80% of the approximately 2 million tons of

Spencer R. Titley is Professor in the Department of Geosciences at the University of Arizona. He received the degree of Geological Engineer from the Colorado School of Mines and the Ph.D. from the University of Arizona. He has worked in industry in both mining operations and mineral exploration. He has carried out geologic investigations of ore deposits in the US, Canada, Central and South America, and the western and southwestern Pacific. His research has ranged from the details of mineralization to regional studies of ore deposits and has been concerned with many different types of deposits. His recent research has focused largely on porphyry deposits of the American southwest and their relationship to geologic events. Address: Department of Geosciences, University of Arizona, Tucson, AZ 85721.

copper consumed annually in the United States is new copper, while the remainder comes from recycling (~20%). During the 1970s, production from these two sources was very close to consumption.

Sources of copper

Any sample of rock, soil, or water, if carefully analyzed, will be found to contain copper. But in ordinary rocks, the amounts are so small (~0.006%), and the cost of recovery is so high, that we cannot consider them as sources of this valuable metal. Instead, we must look to the special, localized, all-too-rare concentrations of copper-rich rocks that we call copper ore deposits.

Such concentrations of copper may be produced by several different natural processes, the most important of which involves the circulation of hot saline waters, termed hydrothermal solutions, through the earth's crust. These solutions collect, transport, and precipitate copper, most commonly in the form of the minerals chalcopyrite ($CuFeS_2$), bornite (Cu_5FeS_4), and chalcocite (Cu_2S). The copper content of rocks that contain these minerals ranges from ~0.1% by weight to more than 10%.

A deposit of copper ore, which may consist of many other minerals besides copper minerals, most of them worthless, may also contain anywhere from a few thousand to more than a billion tons of metal-bearing rock. The ore deposit can take various forms, ranging from clearly demarcated tabular veins to large, irregular masses of rock within which copper minerals are more or less uniformly distributed. Although well-defined veins of rich copper ore are what

prospectors dream of, it is the large, low-grade masses of uniformly permeated rock that actually provide us with most of our copper. Of the several different kinds of large, low-grade deposits, by far the most important is that found in porphyritic igneous rocks, the porphyry copper deposit. Porphyry copper deposits account for almost half the new copper mined worldwide and nearly 95% of that mined in the United States.

Although the term *porphyry copper* has specific connotations for most geologists and copper miners, it turns out to be somewhat ambiguous when we try to define it. *Porphyry* refers to a kind of igneous rock, of variable composition, in which large, well-formed crystals are set in a matrix of fine-grained crystals or glass (Fig. 1). The large crystals, called phenocrysts, are believed to have been formed by the slow cooling and crystallization of deeply buried magma or silicate melt. The porphyritic texture develops when partly crystallized magma, consisting of phenocrysts and magma that is still liquid, is suddenly transported upward into an environment of rapid cooling, where the remaining liquid is quenched, thereby forming glass or a mass of tiny crystals in which the phenocrysts become suspended. The upward movement may take place in one or several stages, and events occurring during the rapid cooling process initiate the flow of hydrothermal solutions that leads to the deposition of copper. It is this association with porphyry that gives porphyry copper deposits their name.

While such deposits bear a spatial relationship to the porphyry responsible for their formation, the mineralized rock is not necessarily confined

within the boundaries of the porphyritic igneous rock. It may be located partly, or even solely, in the older rocks surrounding the igneous body, its distribution being strongly controlled by the paths along which the hydrothermal solutions flowed. The copper minerals are contained within a mass of finely shattered rock (Fig. 2), the fragments of which commonly have dimensions in the range of 1 to 20 cm, and are largely, but not entirely, confined to the fractures in the rock.

Rocks within the zone of mineralization have all undergone alteration—profound changes in composition caused by the circulation of large volumes of hydrothermal solutions through the broken rock. Because of differences in both rock composition and the degree of fracturing, there are wide variations in the alteration processes, the kinds and amounts of minerals in the ores, and the shapes and sizes of the deposits.

How porphyry deposits form

The rapid ascent and sudden cooling of partly crystallized magma required for the formation of porphyry have important consequences for the evolution of porphyry copper systems. When confined under high pressures—equivalent to a column of 16 km of overlying rock, for example—porphyry-forming magma can dissolve up to about 10% by weight of water. When crystals of anhydrous minerals, such as feldspar ($KAlSi_3O_8$), form in the melt, the water content of the remaining liquid melt increases. The ability of a magma to dissolve water, however, diminishes as the confining pressure decreases, and for pressures less than the pressure exerted by 4 km of overlying rock, it diminishes very rapidly (Burnham and Jahns 1962), as Figure 3 shows. Thus, a saturated magma that is rising rapidly must rid itself of much of its water. We still do not know if porphyry-forming magma bodies were initially saturated with water, but the presence in the rocks of water-bearing minerals, such as mica, means that some water is always present. It is equally apparent that at some stage in their cooling history, porphyries may become saturated and suddenly release dissolved water. The effects of such an abrupt release depend on many factors, one of which
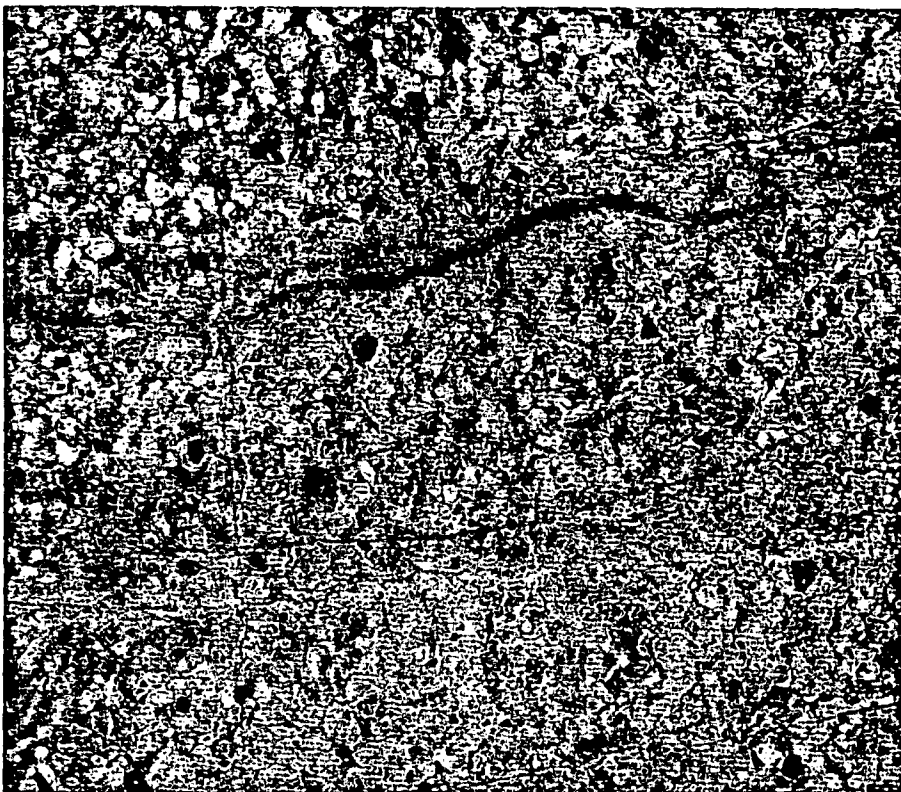
Figure 1. This porphyry from Silver Bell, Arizona, shown to size, has a typical texture of large crystals of feldspar (*light color*) and mica (*black*) set in a matrix of smaller crystals of silicate minerals. Hydrothermal solutions move through fractures that develop as magma cools, thereby forming various alteration products, the specific kind depending on the temperature. One of these is the copper-bearing mineral chalcopyrite ($CuFeS_2$), which here occupies the crack. The vein with the wide, diffuse halo is one along which feldspar has reacted with quartz to form sericite. (All photos are by the author.)

Figure 2. In this breccia (magnified ~1.5 times) from the copper deposit at Sierrita, Arizona, the angular rock fragments are cemented by the copper mineral chalcopyrite. The light, vertical lines are thin, quartz-filled cracks that formed after the breccia hardened.

is the chemical composition of the magma.

Compared with most igneous rocks, the porphyritic rocks with which copper deposits are associated are enriched in silica (SiO_2). When magma cools and is crystallized, the residual liquid magma becomes increasingly enriched in silica, which tends to polymerize, thereby producing a more viscous magma (Burnham 1967). Water is retained until its vapor pressure exceeds both the strength of the melt and the pressure of the overlying rocks. It may then be released suddenly, causing the crystallized parts of the porphyry to shatter. Stresses in the crystallized magma and the surrounding rocks, due to thermal effects of the hot magma, may also cause cracking of the porphyry. Both processes are believed to be responsible for the large volumes of fractured rock that host copper deposits.

The depth of emplacement of the porphyry rocks can only be inferred. In many locations, geological considerations suggest that the depths to the tops of the porphyry bodies at the time of their formation were at most a few kilometers. In the American southwest, for example, some porphyries are thought to have cooled within 2 km of the surface (Titley 1972). At Mt. Fubilan, in New Guinea, a porphyry copper deposit that formed only about a million years ago is now exposed at the surface (Bamford 1972), which means that even if the rate of erosion of the overlying rocks was rapid, the deposit was probably never covered by more than 2 km of rock. At depths of 2 km or less beneath the earth's surface, porphyry magma retains less than 2% by weight of dissolved water.

Following shallow emplacement and fracturing of the rock within and around them, porphyry bodies become large, high-temperature thermal engines, which start to circulate water. The temperature of the water ranges from the temperature at the earth's surface—about 25°C—to that of the hot, shattered porphyry body—about 650°C. The origins of the water whose circulation forms the ore deposit and of the copper and other metals that combine with sulfur to form the ore minerals have been the subjects of research and extensive discussion by many generations of
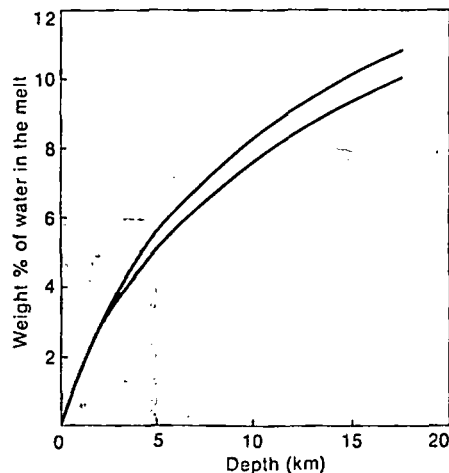

Figure 3. The solubility of water in magma depends in part on the pressure exerted by the overlying rocks. This dependence is steepest at shallow depths but tapers off lower down. It also depends on the chemical composition of the magma. The shallower curve is for magma with the composition of albite ($NaAlSi_3O_8$), the steeper for magma rich in silica, alumina, and potash. The curve for most porphyry magma probably lies somewhere near the curve for albite magma. The colored area shows the probable range in the water content of porphyry magma and in the depth at which copper deposits are most likely to be found. The sudden release of water as magma rises rapidly to the surface is believed to contribute to the extensive fracturing of copper-bearing rocks. (After Burnham 1967.)
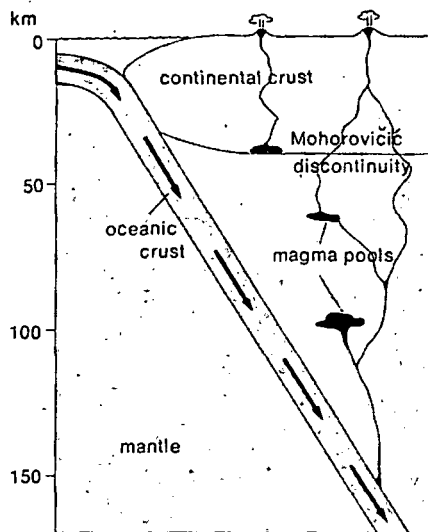

Figure 4. The angle at which oceanic crust moves beneath continental crust depends on the rate at which the two blocks of crust converge. When the rate is slow, the oceanic crust descends steeply, and the rise in temperature with depth and the friction resulting from the motion are believed to cause melting of the down-going slab at depths of ~150 km or below. The bodies of magma that give rise to porphyry copper deposits may derive from melting of oceanic crust at this depth or from melting of rocks higher in the mantle and at the base of the crust. Such bodies may ultimately find their way to the surface through zones of weakness, or faults, caused by the complex forces involved in the subduction process.

geologists. An understanding of how copper deposits evolved is important not only scientifically but also economically.

In the late nineteenth and early twentieth centuries, the debate was polarized between those who ascribed to the water a meteoric (surface-derived) origin and saw the metals and sulfur as originating in the rocks of the shallow crust and those who viewed the metals, sulfur, and water as all derived entirely from magma. Research during the past two decades, based on the relative abundances of the stable isotopes of oxygen and hydrogen (summarized by Taylor 1974), indicates that the source of water varies from one deposit to another. Such isotope studies have shown that within the central, hotter, less fractured parts of a porphyry system, the water is predominantly of magmatic origin, presumably derived from the parent porphyry. In the more fractured parts, usually around the periphery of the fractured rock, on the other hand, some of the water is of meteoric origin. Because the water in porphyry ore deposits does not come from a single source, it seems likely that the copper and associated metals, as well as the sulfur, may also derive from more than one source. The rocks of the shallow crust in which the porphyry intrusions are embedded and through which the hydrothermal solutions circulate constitute one possible source, the porphyry intrusion itself another.

The first minerals formed by crystallization of magma tend to be anhydrous minerals, such as calcium feldspars ($CaAl_2Si_2O_8$) and pyroxene ($CaMgSi_2O_6$), which contain no water of crystallization. At later times during cooling, water and other volatiles, such as carbon dioxide, that had become concentrated in the magma are released; the solution carries various ions, such as phosphate, arsenate, and halide ions, that cannot be incorporated readily in the silicate and oxide minerals that are crystallizing in the magma. The escaping solution also contains sulfur and metals, such as copper, lead, zinc, and molybdenum, which form ore deposits.

In seeking the origins of the metals and sulfur, consideration must be given to the parent material of the porphyry melts. According to the

theory of plate tectonics, oceanic crust is thrust beneath continental crust around the edge of the Pacific Basin (Fig. 4). When the subducted crust reaches depths of about 150 km below the surface, melting begins, and parent material for magma bodies is generated. Judging by their chemistry, the distinctive types of rocks associated with some porphyry copper deposits seem to derive from the melting of the various kinds of basalt that make up the oceanic crust. In other cases, the rock chemistry is indicative of a complex melting process that involves not only oceanic crust but mantle and deep continental crust as well.

Figure 5. Most porphyry copper deposits are located either along the rim of the Pacific or in a band extending from the Middle East through the south of the Soviet Union. (After Titley and Beane 1981.)

Porphyry melts derived solely from the basalts of the ocean floor have certain characteristics that are important in the generation of porphyry copper deposits. The copper content of such basalts is greater than the average value for the crust as a whole (0.006–0.009%) and for some types of basalt is as much as 0.025%. Thus, the parent material of the porphyry is already somewhat enriched—its copper content is 0.0087%, and its molybdenum and gold contents are 0.00015% and 0.0000004%, respectively, according to Turekian and Wedepohl (1961)—and most of the copper may be freed when the basalt partially melts to form the porphyry magma.

We cannot be completely confident that the magmatic emplacement and cooling processes outlined above are wholly responsible for forming porphyry deposits, because we cannot view the dimension of depth from the earth's surface. Since the copper minerals occupy fractures in the porphyry, they must postdate the time at which the rock was sufficiently brittle to fracture. This means that the progenitors of the water, sulfur, and metals must be either deeper or laterally displaced.

The uncertainty leads to an alternate viewpoint, that the source of the metals may lie within the mass of porphyry located at the same level. Since all silicate minerals contain trace amounts of metals, which are locked into their structures by isomorphous substitution—for example, copper in mica—it is possible that the metals in porphyry deposits may have been leached from the minerals by the hydrothermal solutions and then transported by the circulating fluid and deposited in fractures in the porphyry. Such an origin, by leaching and redeposition, is difficult to establish, however, because the large volumes of rock that have been altered and the overwhelming evidence for the transfer of material within circulation systems make precise determinations of the chemical compositions of the rocks before mineralization unfeasible.

Although we are unsure of where the water in such systems comes from and how the hydrothermal solutions collect the metals and sulfur that are found in the ore deposits, we think we understand how the solutions react with the rocks through which they pass. The moving volume of fluid, with all its dissolved components, changes composition as it seeks equilibrium with the different minerals along its path under changing conditions of temperature and pressure. Successive volumes of fluid flowing along the same path thus encounter slightly different mineralogies owing to past chemical reactions between the rocks and the solutions.

Complicated reactions involving large numbers of components and phases have been, and continue to be, the
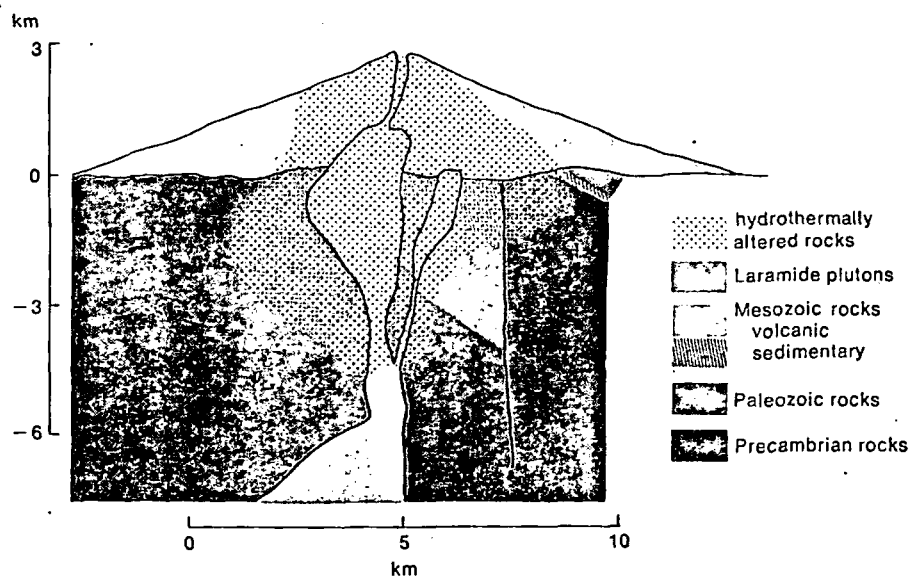

Figure 6. In the American southwest, erosion has largely stripped away the volcanic structures that once covered the porphyry copper deposits shown here in an idealized and generalized cross section. The deposits formed in a subvolcanic environment between 72 and 55 million years ago.

Figure 7. In the El Tiro area at Silver Bell, Arizona, a cluster of porphyry intrusions lies in the center of a large volume of altered rock. The distinctive characteristic of this rock is its high content of pyrite (Fe_2S), which was deposited in small amounts by hydrothermal solutions moving through the rocks. Individual porphyry intrusions within the area (*gray*) have given rise to concentrations of minerals containing copper (0.30%, *dark color;* 0.10–0.29%, *light color*) and molybdenum (25 ppm, *in areas enclosed by colored lines*), which are either centered on the porphyries or located near their boundaries. This porphyry copper deposit, formed about 60 million years ago, has been subject to erosion, which has removed the higher parts of the original hydrothermal system; thus, what we now see is a deeper level of that system. (Adapted from Graybeal, in press.)

object of research (Helgeson 1969, 1970). The reactions that form the silicate alteration minerals and the sulfides are pH-dependent and are affected by the concentrations of alkali and metals in the solutions (Meyer and Hemley 1967). Alteration of the feldspar orthoclase by a hydrothermal solution to produce sericite (mica) and quartz is such a reaction:

$$3KAlSi_3O_8 + 2H^+ \rightleftharpoons$$
feldspar

$$KAl_3Si_3O_{10}(OH)_2 + 2K^+ + 6SiO_2$$
sericite quartz

Increasing the acidity of the solution drives this reaction toward equilibrium with sericite. By studying many similar chemical reactions and by knowing the degree of chemical mass transfer in porphyry copper systems, we are making progress toward a better understanding of the processes that gave rise to such systems.

A volcanic origin?

From the foregoing discussion, it is apparent that porphyry copper deposits came into being as a result of special geological conditions. Much evidence has now been accumulated that leads us to suspect that the deposits were formed as by-products of volcanic activity where deep-seated magma bodies had suitable compositions and properties and where crustal characteristics permitted those bodies to rise rapidly to shallower levels. The evidence is indirect, and hence inconclusive, however, because the volcanic structures that may once have existed above the deposits would have been topographically and compositionally unstable and thus would have been removed rapidly by weathering, and because a large percentage of known deposits are now exposed as a result of millions or tens of millions of years of erosion.

Nevertheless, a volcanic origin for many porphyry copper deposits is consistent with the following facts. First, by far the greatest number of deposits are of Mesozoic age or younger—less than about 230 million years old—and are located in either the "ring of fire," the belt of volcanoes and volcanic rocks that encircles the Pacific Ocean, or the "Tethyan" belt, the east–west band of volcanic rocks and mountains that extends throughout the southern Soviet Union and into the Middle East (Fig. 5). The association of the deposits with volcanic rocks and the style of occurrence are much the same in both regions. Moreover, both these parts of the world are currently the sites of much earthquake activity and volcanism, which are believed to be manifestations of the same sorts of events as are known to have occurred in or near these regions ever since about 230 million years ago.

Second, although most of the rocks that existed at the time the ore was formed have been removed by erosion, there are a few deposits where remnants of volcanic rocks about the same age as the porphyries (up to 200 million years old) are found, and where porphyries containing copper deposits are present as intrusions in the volcanic rocks (Fig. 6). This coincidence of porphyries and volcanic rocks in both time and space is strong evidence for a volcanic origin for the deposits.

Third, the theory of the origin of porphyritic textures described previously involves two stages of cooling: an early stage, during which crystals of silicate minerals started to form, and a late stage, in which the residual magma was quenched to form a fine-grained matrix. The late stage of cooling was thought to be the result of magma rising rapidly to the cooler environment of the shallow crust. According to the volcanic genesis theory, the porphyry intrusions, which have compositions similar to those of many volcanic rocks, formed when magma rose rapidly toward the earth's surface through the core of a volcano.

Fourth, a large percentage of porphyry copper deposits contain bodies of breccia—angular fragments of rock, which, in some instances, are cemented with fine crystalline volcanic-like rock or with rock "flour" derived from the mutual abrasion of porphyry fragments (Fig. 2). Such bodies are commonly irregular, essentially vertical columns, or "pipes," with round or elliptical cross sections; less commonly, they assume a tabular form, such as that of a vertical sheet, or "dike." The transportation and pulverization of rocks in breccias, as well as the geometry of the breccia bodies, suggest that there may have been an opening to the surface at the time that they formed. Moreover, breccias that look like these are present in active volcanic systems, where openings clearly exist.

Fifth, the distribution of deposits in well-explored regions of the Pacific rim shows tendencies toward clustering, as in southwest North America, where clusters occur in areas about 30 km by 30 km (Fig. 7), and toward formation along lines on the earth's surface, as in the Andes. Volcanoes show similar tendencies to cluster or form along lines. This similarity in distribution of volcanic centers and porphyry ore deposits is not in itself compelling evidence for an associa-

Figure 8. The different colors in the southern wall of the open-pit copper mine at Santa Rita, New Mexico, are the result of oxidation of copper and iron sulfide minerals dispersed in the rock. Rocks from which copper has been leached and in which iron oxides remain are red; those containing iron sulfides that have been, and are still being, oxidized are yellow; and recently exposed, secondarily enriched copper ore is gray.

tion, but taken together with the other pieces of evidence, it strengthens the case.

The inferred link between circum-Pacific volcanism and the formation of porphyry ore deposits is extremely important, because it establishes a rational basis for searching for such deposits. Moreover, the high success rate—the discovery of more than a hundred new deposits—over the past two decades of searching premised in part on the assumption that the theory is correct attests in some measure to its validity.

Copper mining

The discussion so far has been concerned with the geological features, origin, and distribution of porphyry mineral deposits. The conversion of a mineral deposit to an ore deposit—that is, to an economically viable body of minerals—depends on both the state of mining and metallurgical technology and the interplay of many economic and sociopolitical factors. Porphyry copper deposits are

sources of other important metals, such as molybdenum and gold, which only rarely occur in sufficient concentrations to justify mining in the absence of other valuable metals. Even when these other metals are present, porphyry copper ores are of low intrinsic worth; the content of copper ranges from 0.2% to 0.8% by weight, that of molybdenum is commonly about 0.01%, and that of gold varies from 0.00001% to 0.00008% in some porphyry deposits. Because these percentages are so small, large quantities of material must be mined and processed cheaply if a profitable, continuing mining operation is to be sustained. Present-day production from porphyry copper deposits is variable and depends on many factors, including the prices of copper and the other metals found with it and the actual amount of copper in the rock of a particular ore deposit. Many operations produce 50,000 tons of ore per day from open-pit mines, and a few produce comparable amounts from underground mines, where the rock is blasted and extracted under controlled conditions.

The earliest attempt at mining low-grade deposits on a large scale was made at Bingham Canyon, Utah, in 1904 by Daniel Jackling, with the financial backing of Charles McNeil and Spencer Penrose. The same methods, albeit with more than seventy years' worth of technological improvements, are being applied today, on a scale that Jackling and his colleagues may never have imagined, to the mining of large deposits containing as little as 0.4% of copper.

Certain geological features of porphyry copper deposits contribute to their amenability to the bulk-materials-processing methods in use today. Thus, although such deposits are parts of large, diffuse mineralized systems, the high-grade portions—that is, the ore deposits—are smaller and more localized. Mining can thus be concentrated in relatively small areas and progress downward, rather than sideways. Furthermore, the closely spaced fractures of the rock in which the copper minerals are localized are lines of weakness. The rocks therefore fragment easily when

blasted: indeed, a million tons or more of ore may be broken by one blast of explosives. On such a scale, copper and associated metals tend to be uniformly distributed through the broken rock, which means that although some selective mining may be necessary to remove rock that does not contain valuable metals, in general, the entire rock mass can be profitably mined. The distribution of silicate alteration minerals, most commonly clay or fine-grained types of mica, is also fairly uniform, which permits establishment of fixed metallurgical recovery circuits.

Furthermore, chemical reactions involving rainwater and the atmosphere can, under certain favorable combinations of climatic and geographic conditions, produce a thin, but rich, zone of secondarily enriched copper ore near the top of a low-grade ore deposit (Fig. 8). Since many of the deposits are themselves located in areas of elevated topography, generally as a result of accidents of erosion and uplift in the American southwest, mining of such zones is helped, rather than hindered, by gravity. Even though these enriched blankets are usually of comparatively small tonnage, their high copper content has permitted rapid amortization of the large amount of capital invested in exploiting them. Because the process responsible for secondary enrichment also produces iron oxides, whose red coloration stands out, thereby making them obvious targets for exploration, we presume that most such secondarily enriched deposits have been discovered. A few continue to be found—and they are certainly worth seeking—but their number is diminishing, and the search for copper is now directed toward the discovery of higher-grade primary ores, which are much more difficult to find.

Although there are well over 150 porphyry copper mines and potential mines around the Pacific Basin and perhaps more than 50 in the Tethyan belt, the search for new deposits has continued at the same fast pace for the past 20 years or so. Even in regions such as southwestern North America and western Canada, where large numbers of deposits have been found, the intensity of the search remains undiminished. Continuing demand and projected increases in copper consumption provide the economic incentive for the expensive

search for porphyry copper deposits. Large amounts of potential copper ore certainly exist in other kinds of deposits, such as those formed by processes of sedimentation, but these occur most abundantly in countries of southern and central Africa, where political and economic factors have mitigated against extensive exploitation during the past two decades and the future for mining is uncertain. Thus, notwithstanding the existence of exploitable deposits formed in other ways, porphyry-related deposits seem destined to remain the premier source of the world's copper supply.

References

Bamford, R. W. 1972. The Mount Fubilan (Ok Tedi) porphyry copper deposits, Territory of Papua and New Guinea. Econ. Geol. 67: 1019–33.

Burnham, C. W. 1967. Hydrothermal fluids at the magmatic stage. In Geochemistry of Hydrothermal Ore Deposits, ed. H. L. Barnes, pp. 34–76. Holt, Rinehart, and Winston.

Burnham, C. W., and R. H. Jahns. 1962. A method for determining the solubility of water in silicate melts. Am. J. Sci. 260: 721–45.

Coney, P. J. 1980. Overview of Mesozoic-Cenozoic cordilleran plate tectonics. Geol. Soc. Am. Memo. 152:33–50.

Graybeal, F. T. In press. Geology of the El Tiro

area, Silver Bell mining district, Arizona. In Advances in Geology of the Porphyry Copper Deposits, Southwestern North America, ed. S. R. Titley, ch. 24. Univ. Arizona Press.

Helgeson, H. C. 1969. Thermodynamics of hydrothermal systems at elevated temperatures and pressures. Am. J. Sci. 267:729–804.

——— 1970. A chemical and thermodynamic model of ore deposition in hydrothermal systems. Mineral. Soc. Am., Spec. Paper 3:155–86.

Meyer, C., and J. J. Hemley. 1967. Wall rock alteration. In Geochemistry of Hydrothermal Ore Deposits, ed. H. L. Barnes, pp. 166–235. Holt, Rinehart, and Winston.

Norton, D., and J. E. Knight. 1977. Transport phenomena in hydrothermal systems; cooling plutons. Am. J. Sci. 277:937–81.

Sillitoe, R. H. 1972. A plate-tectonic model for the origin of porphyry copper deposits. Econ. Geol. 67:184–97.

Taylor, H. P., Jr. 1974. The application of oxygen and hydrogen isotope studies to problems of hydrothermal alteration and ore deposition. Econ. Geol. 69:843–83.

Titley, S. R. 1972. Pre-ore environment of southwestern North American porphyry copper deposits. In Proc. 24th Int. Geol. Congr., Sect. 4, ed. J. E. Gill, pp. 252–60. Ottawa: Geological Survey of Canada.

Titley, S. R., and R. E. Beane. 1981. Porphyry copper deposits. In Economic Geology: Seventy-Fifth Anniversary Volume, 1905–1980, pp. 214–69. El Paso: Economic Geology Publication Company.

Turekian, K. K., and K. H. Wedepohl. 1961. Distribution of the elements in some major units of the earth's crust. Geol. Soc. Am. Bull. 72:175–92.

"You call *this* cold? When I was a boy, in the Ice Age . . . "

Permeability of Crystalline and Argillaceous Rocks

W. F. BRACE*

SUBJ
MNG
PCAR

Readily available laboratory, in situ, and inferred values of permeability, k, of crystalline and argillaceous rocks have been compared. For crystalline rocks, in situ k ranged from about 1 μd (10^{-14} cm^2) to 100 md; for argillaceous rocks it was about 0.01 to 1 μd. No systematic decrease of k with depth was evident; over some interval at nearly every well, k was 1 to 100 md; these highly conductive intervals were as deep as 2–3 km. In situ permeability has been inferred from earthquake precursors, anomalous pore pressure, leakage from aquifers or other large-scale phenomena. Where crystalline rocks are involved, k was about 0.1 to 10 md, and thus about the same as the more permeable zones in wells; this is close to the permeability of many sandstones and is about 10^5 times greater than laboratory measurements for intact crystalline rocks. For argillaceous rocks, laboratory, in situ, and inferred values all agreed within about a factor of 10. Laboratory study of artificial fractures suggest that in situ values for crystalline rocks are high because of natural fractures; fractures may be sealed or absent in shale.

Based on observed variation in wells, k at particular sites in crystalline rock is not predictable within a factor of 10^5. For crystalline rocks, laboratory values provide little more than the minimum in situ k; for argillaceous rocks they may provide a good estimate of in situ k. Because of the great sensitivity of k to the effective stress, measurement or estimation of k must be tailored to the particular stress state of the application.

If, as tentatively suggested by in situ and inferred values of k, average crustal k is about 10 md, pore pressure much greater than hydrostatic seems ruled out in terrains of outcropping crystalline rocks. Apart from hot pluton environments, anomalously high pore pressures seem to require everywhere a thick blanket of clay-rich rocks, as originally suggested for sedimentary basins.

INTRODUCTION

Fluid flow in deeply buried rocks has long been a subject of interest to petroleum engineers, hydrologists, mining engineers, and economic geologists. Recently others have joined this group, particularly from fields related to energy resources. Fluid flow in rocks plays a central role in geothermal energy recovery [1], radioactive waste isolation [2], stimulation of tight gas sands [3], *in situ* coal gasification [3], and pumped energy storage in aquifers [3]. Outside of energy-related fields, fluid flow in rocks figures in recent studies of fault and earthquake mechanics [4, 5], in the heat balance near plate margins [6, 57, 51], and in magma crystallization [7].

Steady fluid flow in rocks is determined by pressure gradient, and by a single rock parameter, permeability. For most of the applications above, depths in the earth of a few 100 m to a few kilometers are relevant, and some volume of rock, perhaps a few 100 m in dimension, is involved. The central question addressed in all the specialities noted above, is, what is rock-mass permeability at an arbitrary location? Can permeability be predicted even approximately, or is a direct measurement necessary? Must permeability be measured directly in the rock-mass, or can it be inferred from other geophysical parameters, or from laboratory measurement on small rock samples?

In the present paper these questions are addressed. Our approach is to compare published *in situ* measurements which give rock-mass permeability with values obtained for laboratory samples and with values inferred from certain large-scale geologic phenomena. Even though *in situ* data are very limited, comparison of these three sets of permeability measures provide par-

* Department of Earth and Planetary Sciences, Massachusetts Institute of Technology, Cambridge, MA 02139, U.S.A.

tial answers to these questions, and, additionally, suggest where effort should be focussed to improve our understanding of rock mass permeability.

Very little in this paper is not already well known to most hydrogeologists. However, other specialists in the geosciences are now concerned with permeability, and it is really to them that this paper is directed. Hopefully it will not only be a useful review but will also provide a framework for discussion of the many new measurements of permeability now planned or in progress.

This paper is primarily concerned with measured values of permeability, not with measurement techniques, or with the implication of the values reported. We have rather uncritically assumed that reported values are correct to about an order of magnitude.

Definition, units of permeability

Like electrical or thermal conductivity, permeability is a second rank tensor connecting a flux with a gradient:

$$q_i = -K_{ij} \frac{\partial P}{\partial X_j} \qquad (1)$$

where q_i is volume flow per unit time, $\partial P/\partial X_j$ is pressure gradient, and K_{ij} are constants. This is an empiri-

cal relationship, known as Darcy's law, and is mathematically equivalent to Ohm's law or Fick's first law. Experiments show that even in scalar form, where K_{ij} becomes simply K, both fluid and medium characteristics are involved. We will wish to focus solely on medium properties so that an alternative form of (1) is used:

$$q_i = -\frac{k_{ij}}{\mu} \frac{\partial P}{\partial X_j},$$

$$\text{or,} \quad q = -\frac{k}{\mu} \frac{\partial P}{\partial X} \quad \text{in scalar form,} \qquad (2)$$

where μ is fluid viscosity, with dimensions FTL^{-2}, and k is *permeability*, with dimension L^2. k Depends solely on characteristics of the medium. This paper is concerned with the magnitude of k for rocks. Although k varies with direction in rocks [51, 76], principal values of k_{ij} are rarely available; we will therefore have to treat it as a scalar.

The units and even the dimensions of k are a source of endless confusion. We have tried to clarify this in Appendix 1 where some of the different units are compared. We will use the darcy, both for historical reasons and because the permeability of most rocks falls within
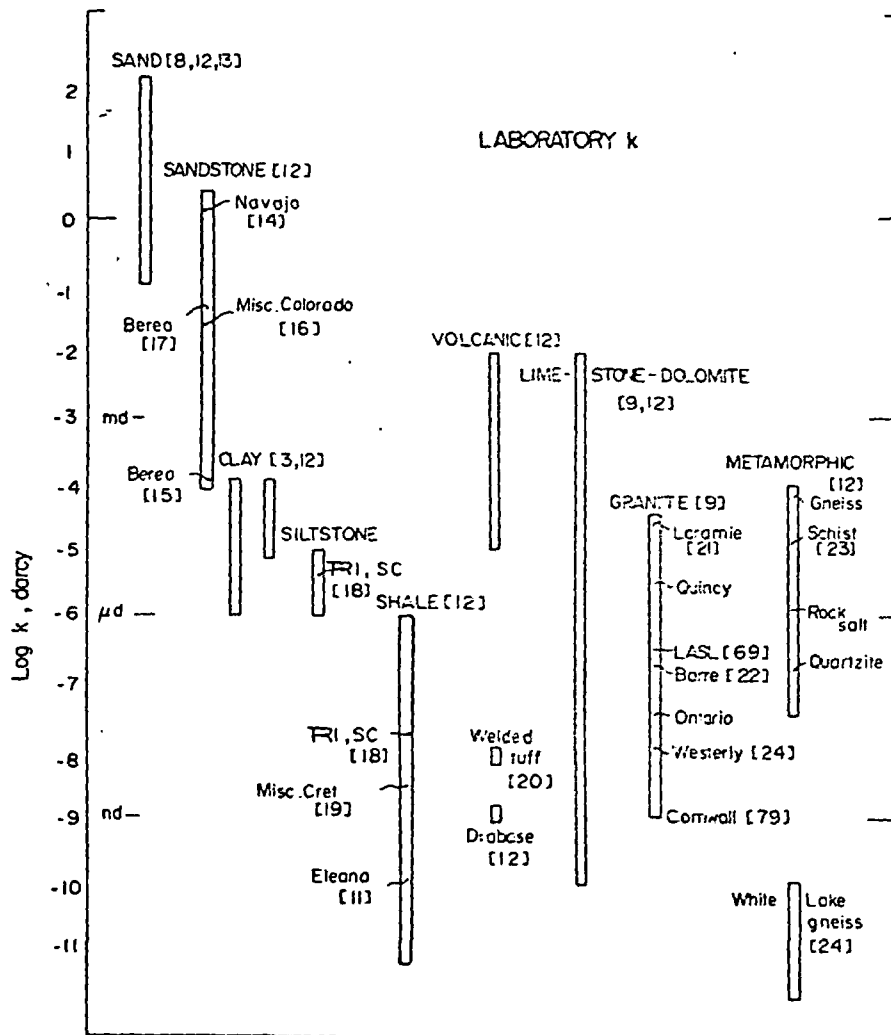
Fig. 1. Laboratory measurement of permeability of intact specimens. Boxes show range of measured values. Bracketed numbers are references. Pressure was hydrostatic and less than 10 MPa and temperature about 25°C.
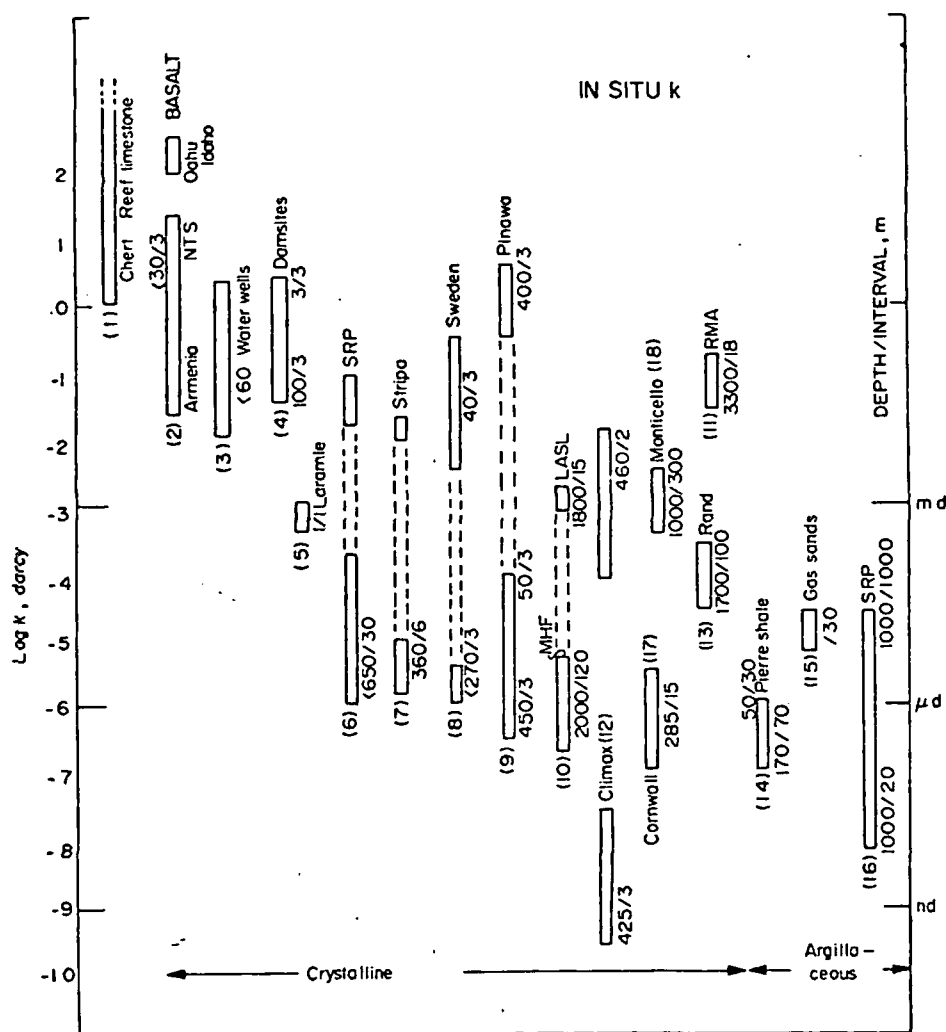
Fig. 2. *In situ* measurements of permeability. Numbers in parentheses refer to accompanying notes. Depth and interval length given in meters where known. Locality names are explained in notes.

1. Fractured chert in shale [27]; fractured limestone [28]; coralline reef limestone [29].

2. Armenian basalt [30]; Nevada Test Site basalt [31, 32]; Oahu, Idaho basalts [29].

3. Calculated from observed flow rates from water wells up to 60 m deep in fractured metamorphic rocks of northern Colorado [33].

4. Pumping tests at 38 damsites in crystalline rocks in western United States [34].

5. Pumping test in a surface outcrop of granite near Laramie, Wyoming [21].

6. Pumping and swabbing tests in crystalline basement rocks at the Savannah River Plant near Aiken, South Carolina [23, 35]. 1 μd was the detection limit.

7. Pumping test in the Stripa mine, Sweden [36, 82].

8. Over 500 pumping tests at 5 sites in granites and gneiss, Sweden [37].

9. Pumping and drill stem tests in the Lac du Bonnet batholith, near Pinawa, Manitoba [38]. 0.5 μd was the detection limit.

10. Drill stem tests at 5 depths in geothermal test hole No. 2, in granodiorite, near Los Alamos, New Mexico (LASL) [39]. MHF refers to a measurement made of water loss into the sides of the hydrofracture [40].

11. The Rocky Mountain Arsenal (RMA) well near Denver, during injection into 18 m of open hole in crystalline rocks. Values shown here calculated from an average transmissibility of 5000 md-ft/cp [41] or 5 darcy-ft [42] using interval of 70 ft and viscosity of 1 cp.

12. Two values from nearby sites in the Climax granitic stock; the high value came from both pressure decay and constant pressure tests [43] and the low value from constant pressure tests using air [44]. The upper values came from a region which may have been affected by the Piledriver nuclear explosion; permeability was probably enhanced by the damage.

13. Based on average water inflow into a tunnel in quartzite [45].

14. Packer tests made in several drill holes in the thick sections of the Pierre shale [46].

15. Pumping tests in Rulison and Gasbuggy sites (gas sands) [47].

16. From Triassic siltstone and mudstone near Aiken, South Carolina [18].

17. The range of a number of measurements using injection and pulse methods in the Carnmenellis granite, Cornwall, England [79]. Values for laboratory samples given in Fig. 1.

18. Packer tests at Monticello Reservoir, South Carolina [78].

that range of values in darcies covered by the familiar decimal prefixes. Thus, most values of k we well discuss range from a nanodarcy (10^{-21} m^2) to a darcy. The darcy (10^{-8} cm^2) is conveniently expressed in SI units using

$$1 \text{ darcy} = 1 \, (\mu m)^2 = 10^{-12} \text{ m}^2.$$

OBSERVATIONS

Laboratory measurements

Laboratory measurements have been made on samples 2.5–15 cm in minimum dimension. The samples were intact unless otherwise noted. Two techniques are used, depending on the anticipated permeability. Above about a microdarcy a steady-state measurement is made, in which volume of fluid is measured per unit time for fixed pressure gradient. This is a traditional method of soil and rock mechanics [8, 9]. For rocks with permeability less than about a microdarcy, the transient method is more convenient [10]. In this method, the decay of a pressure pulse suddenly applied to one end of the sample is observed. Thus, only pressure and time need to be measured; this method readily

adapts itself to high pressure measurement. Recent refinements in the transient method [11, 24] have lowered the detection level to around 10^{-12} darcy.

All readily available laboratory measurements for rocks are summarized in Fig. 1, together with typical values for soil, for comparison. The bars for each rock or soil type reflect the range of values reported. Some well-known rocks and field sites are identified alongside the bars. For all the measurements in Fig. 1, stress was approximately hydrostatic.

A number of aspects of laboratory permeability (Fig. 1) are worth noting:

(i) Some ten orders of magnitude separate the least from the most permeable rocks. Since it is not clear that our present detection limit coincides with the minimum permeability of rocks, this range could be even wider.

(ii) The widest variability among the rock types is observed for the carbonates and volcanics. This might have been predicted just on petrologic grounds (compare coquina and lithographic limestone, for example!).

(iii) However, permeability does not necessarily correlate with porosity. This is a fact well-known in soil mechanics [8, 72]; some clay is considerably more
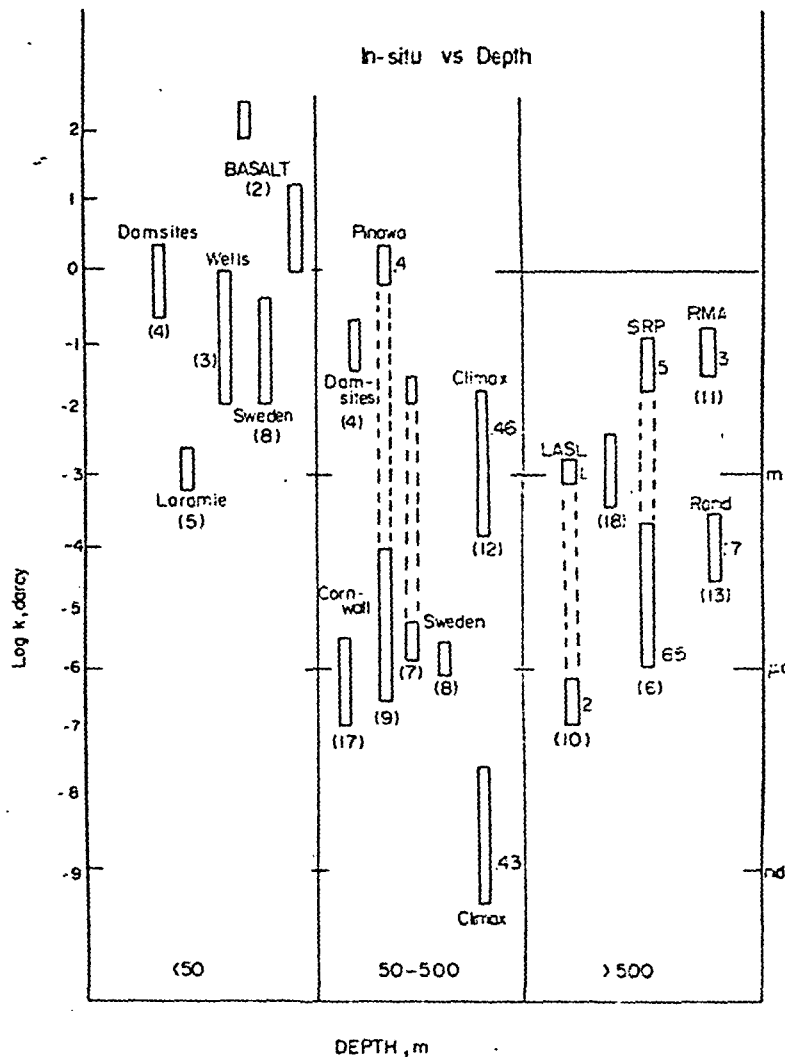
Fig. 3. *In situ* measurements of k for crystalline rocks from Fig. 2 arranged according to depth. Several depths are given in kilometers.

porous than sand; yet the relative permeabilities are reversed (Fig. 1). Also, typical crystalline rocks have an interconnected porosity of 0.01 or less [25] and yet their permeability is equivalent to shale which rarely has a porosity less than 0.10 [26].

(iv) If we assume that the term 'crystalline rocks' applies to the rocks grouped in Fig. 1 under 'granite' and 'metamorphic', then for crystalline rock, k of intact specimens is approximately equivalent to that of clay and shale.

In situ *measurements*

In situ measurements (Fig. 2) refer to values obtained, typically in drill holes, for rock, undisturbed and in place. There is a variety of methods [80, 81], all of which give an averaged value for some *interval*—the *interval* being the length of exposed rock along the drill hole where the test is performed. *In situ* methods usually take one of three forms:

(a) Flow of water lost across some interval is measured for a fixed constant pressure, the so-called packer or constant head injection test [for example, 43].

(b) Recovery of pressure or head is observed in a vertical drill hole after addition or removal of a known fluid volume, the so-called slug or pulse test [for example, 23].

(c) Flow of water or chemical tracers is measured between two or more holes while pressure drop is held constant [35].

The above methods yield quantities like 'coefficient of transmissibility', 'hydraulic conductivity', or, in some cases, permeability as defined here. Conversion to permeability has been made here using the factors given in the Appendix; special problems which have arisen in conversion are indicated in the Notes accompanying Fig. 2. As noted above, we have taken published or verbally communicated values to be correct and have made no attempt to assign probable errors to the field measurements.

In situ measurements of k (Fig. 2) are again grouped roughly according to rock type. Crystalline igneous and metamorphic rocks gave the values across the middle of the figure; a few important oil-producing rocks are given at the far-left, for contrast. Measurements in clay-rich rocks are given on the right side of Fig. 2. Approximate depths and the interval are given where known.

The range of *in situ* values of permeability is even greater than the range of laboratory values, spanning some twelve orders of magnitude. Four to six orders of magnitude variation is typical at a particular site, such as the LASL well or the SRP wells, or at the Climax granite (Fig. 2). For crystalline rocks in general, *in situ* k evidently ranges from about 1 μd to 100 md. The argillaceous rocks such as shales, siltstones and shaley sandstones are generally less permeable than the crystalline rocks by one or two orders of magnitude.

It is instructive to examine *in situ* permeability of crystalline rocks as a function of depth. Because data

are still very limited, only three depth zones have been chosen (Fig. 3), the surface to 50 m, 50–500 m, and below 500 m. Several features are evident:

(i) Permeability varies by over 4-orders of magnitude at a particular site, within the same depth interval.

(ii) There is a hint of decrease of permeability with depth but, as also pointed out by Maini & Hocking [49], hardly enough to justify the exponential law suggested [37, 48]. Compare particularly the values from depths greater than 500 m; no systematic variation with depth is evident.

(iii) At nearly every site some portion of the rock sampled by the drill holes has a permeability of 1–100 md. This relatively permeable zone may be as deep as 1.8 km (LASL) or 3.3 km (RMA). Similar zones were noted in a survey of 25 Canadian mines to 1.7 km [70].

Inferred permeability

Rock-mass permeability has been inferred a number of ways; the two principal methods require (a) measurements of fracture spacing and aperture of conducting fractures, or (b) observations of time and distance which relate phenomena thought to be controlled by hydraulic diffusion. The other methods used are indicated in the Notes accompanying Fig. 4.

Water flow in fractured rock may occur principally through joints, faults and other planar fractures [4]. Assuming plane parallel sets of such fractures, then rock-mass permeability can be calculated from

$$k = w^3/12S \qquad (3)$$

where w is fracture aperture and S fracture spacing [4, 34].

Flow of fluids through rocks, like chemical diffusion or heat flow, is governed in the transient regime by

$$t \sim L^2/a \qquad (4)$$

where t and L refer to time and distance, respectively, of a moving front of pressure, and a is hydraulic diffusivity. Here

$$a = k/\eta\mu\beta \qquad (5)$$

where k is permeability, η is porosity, μ is viscosity and β is compressibility of the fluid. Given some phenomenon thought to be due to transient flow, t and L can be found; one example is an earthquake believed due to pumping of fluid at a nearby well [5], t Would be the time between pumping and the earthquake, and L the distance between well and epicenter. k Can then be obtained from equation (5) if porosity of the rocks and μ and β of the fluid are known.

Permeabilities inferred in various ways are collected in Fig. 4; additional explanation of the methods used is given in the Notes which accompany the figure.

One rather remarkable feature of Fig. 4 is the close agreement of many of the values, between about 0.1 and 10^2 md. Not surprisingly the values obtained for joints were much higher. Perhaps the apertures, w, had become widened by surface processes like weathering
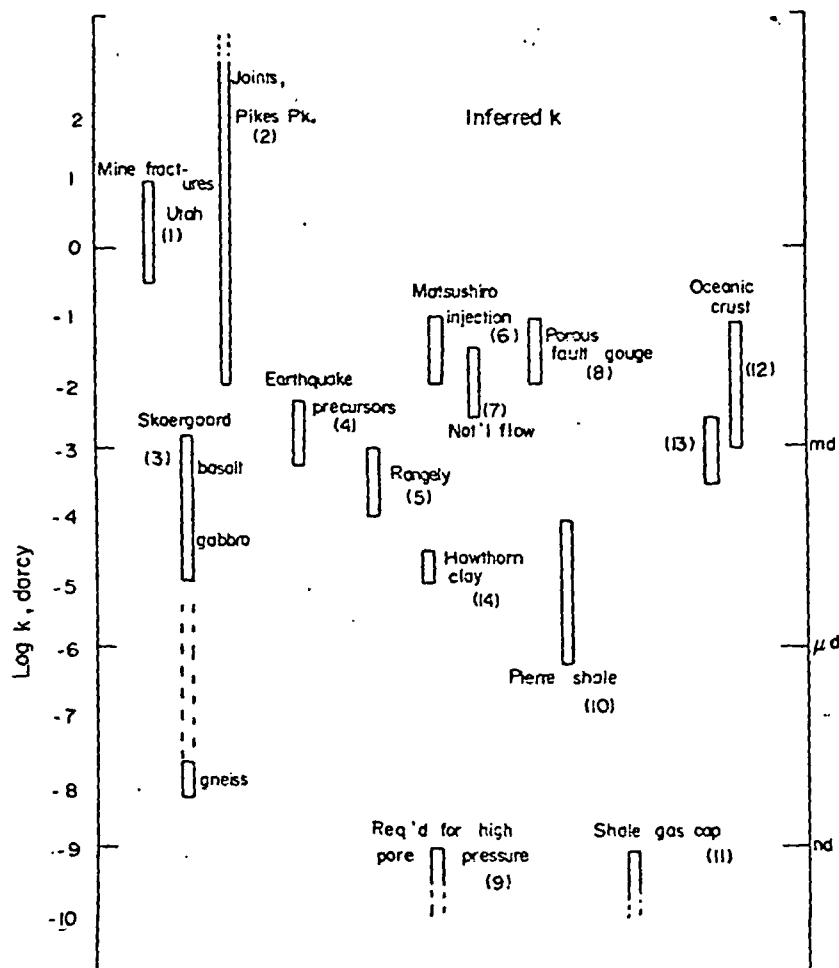
Fig. 4. Permeability *in situ* inferred from various large-scale phenomena. Numbers in parentheses refer to accompanying notes, which explain the calculation of *k*.

1. From observed fracture spacing and aperture in and around Mayflower Mine, Park City, Utah. *k* determined from equation (3) [50].

2. From measured fracture spacing and aperture at about 60 stations in the Pike's Peak granite, near Manitou Springs, Colorado [51].

3. Based on application of transport theory to the hydrothermal system associated with crystallization of the Skaergaard intrusion, Greenland [7]. The principal input to the models was variation of ^{18}O and exchange reactions between hydrothermal fluids and various rocks in the system. The estimates are shown for basalt host rocks (surface to about 7 km), intrusive gabbro (4–8 km) and intruded gneiss (7–10 km).

4. Based on precursor time vs length of aftershock zone for a wide variety of earthquakes [52, 53]. The slope of this relation, 10^4–10^5 cm^2/sec, gives a in equation (5). We used a porosity of 0.001, μ of 0.01 poise, and β of 0.2 mb^{-1} (0.002 GPa^{-1}) to calculate *k*.

5. Based on a personal communication of J. Healy quoted in [53] who observed pressure changes 0.25 mi from the well two hours after injection. The same porosity, viscosity and compressibility were used as in 4.

6. Ohtake [5] related a sequence of earthquakes at Matsushiro, Japan, with water injection at a well; the time lag was 5–10 days and the distance 5–15 km, giving a of 10^4 cm^2 sec.

7. Ground water discharge was also observed at Matsushiro [54] some time after an earthquake. The authors calculated the bulk permeability to be 10 md, assuming a porosity of 0.01 and viscosity of 10^{-3} poise.

8. Based on a different formulation than equation 5, for coupled deformation-diffusion in a porous fluid-filled medium thought to model the creeping zone of the San Andreas fault.

9. Upper bound estimate based on the permeability which would be required to cause pore pressure to attain lithostatic pressure within 10^6 yr [5]. The estimate is based on a fixed source of pore pressure at depth.

10. Based on observed water loss from the Dakota sandstone into the overlying Pierre shale [46], which is about 200 m thick.

11. An upper bound estimate based on the sealing properties of argillaceous rocks above oil and gas reservoirs in Siberia [56]. The calculated hydraulic diffusivity is less than 10^{-3} cm^2/sec. We used porosity of 0.01 and the properties of water to obtain the value of *k* shown.

12. Based on convection theory for porous media and observed heat flow for the Indian Ocean [6].

13. This upper bound estimate is based on reduction of heat flow due to assumed downward flow of cold ocean water in the top 5 km of oceanic crust in the Famous and Galapagos areas [57].

14. Based on an analysis of chloride contamination and water loss through a 60 m thick clay confining layer above an aquifer at Brunswick, Georgia [77].

or stress relaxation. The values of k for the mine fractures could have been complicated by aqueous solution reactions; apertures might have been widened or even reduced by reactions with the wall rock. In any event, these effects would strongly influence k, becasue of its third-power dependence on w [equation (3)].

Many of the inferred permeabilities gathered in Fig. 4 represent values averaged over distances of kilometers (Skaergaard, Matsushiro, oceanic crust, for example). The volumes of rock represented are therefore much larger than samples either in a laboratory measurement or in a typical in situ test. Careful comparison of these three data sets for particular sites may provide a better future understanding of the scale effect on permeability [75].

COMPARISON OF LABORATORY, IN SITU AND INFERRED PERMEABILITIES

We first compare observations from the SRP (Savannah River Project), and then turn to a general comparison of the three sets of values given in Figs 1, 3, and 4. SRP was chosen rather than other sites for which laboratory and in situ values are available (LASL, Laramie, for example) because of the larger number of measurements available.

For SRP, laboratory and in situ measurements from the same wells can be compared (Fig. 5). For the Triassic siltstones and mudstones, laboratory measurements are within about an order of magnitude of values in

situ; for the crystalline basement rocks certain intervals show about the same agreement, but k of the conducting zone is about 10^3 greater than laboratory values.

General comparison of laboratory, in situ and inferred values of k (Figs 1, 3, 4) suggest several important conclusions:

(i) For crystalline rocks most inferred values are about the same as the more permeable zones in situ; average k is 1–10 md. This suggests that pumping tests in wells may sample a volume of rock which is representative of much larger crustal volumes. For the Pierre shale (Figs 2 and 4) the same rock-mass is involved; inferred k is within an order of magnitude of k from in situ tests [46].

(ii) The average k for crystalline rocks noted above of 1–10 md is about 10^3 greater than laboratory measurements for crystalline rocks, and corresponds to that of many sandstones.

(iii) For rocks of appreciable clay content, laboratory and in situ values usually agree within about a factor of 10. Some intervals in wells also agree even for crystalline rocks (the SRP in Fig. 5, for example).

DISCUSSION

Fracture permeability

The marked difference between laboratory and in situ k of crystalline rocks noted above is usually explained by fractures [4, 23, 33, 49]. Joints, faults, and other planar
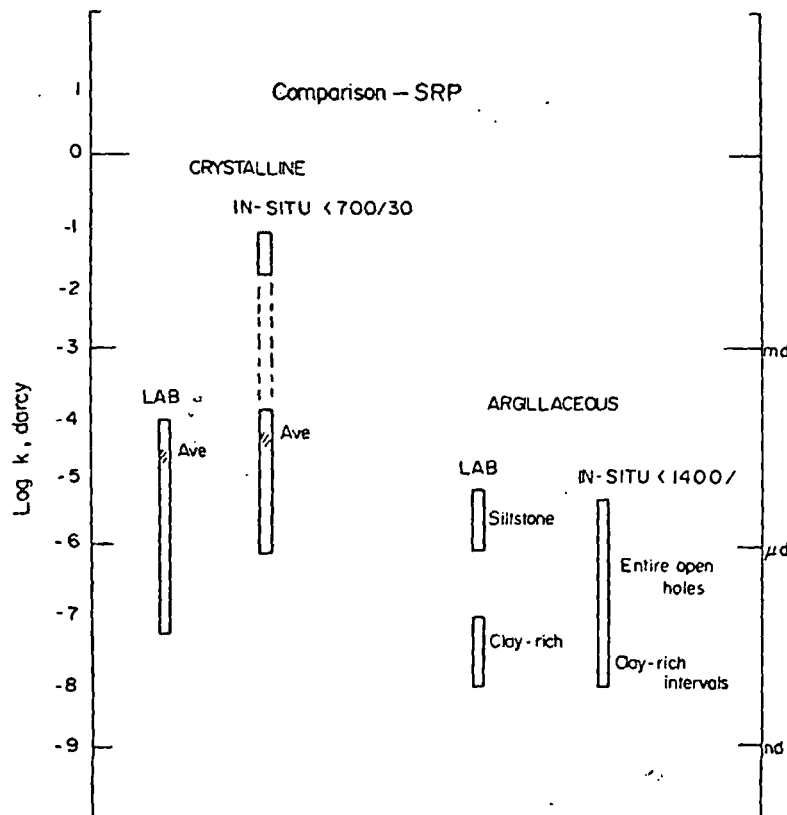
Fig. 5. Comparison of in situ and laboratory measurements for the same intervals at the Savannah River Plant; measurements for the crystalline rocks are given in [18] and argillaceous rocks in [23]. Numbers for the in situ values are depth and interval in meters.
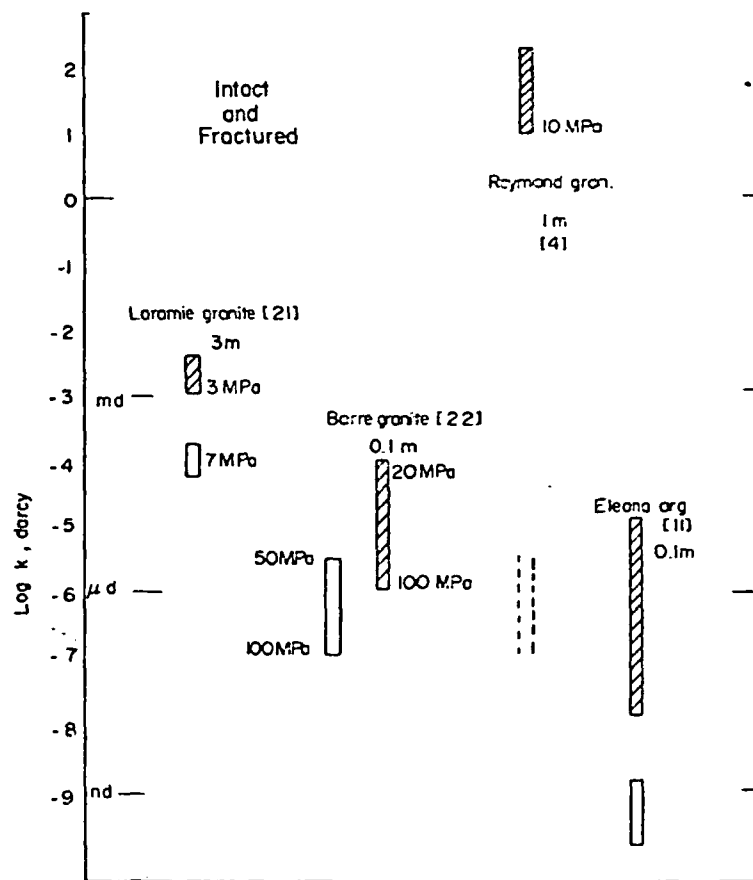
Fig. 6. Comparison of intact and fractured rocks. Cross-hatched boxes give k parallel with the single fracture or sawcut. k of intact Raymond granodiorite is not known: typical granite from Fig. 1 is shown by the dotted lines. The bracketed numbers are references.

discontinuities in a rock mass are usually not sampled for laboratory measurement and yet they may represent flow paths many times more significant than those in the intact laboratory sample. A simple demonstration of this is given by several laboratory or field experiments (Fig. 6). k was measured in an intact sample and compared with that of a sample containing a natural joint (Laramie granite [21]) or a sawcut (the other three rocks in Fig. 6). k was measured in the direction of the fracture plane and was several orders of magnitude greater than intact k.

This result is generally more characteristic of crystalline rocks than certain sandstones and shales. For example, the SRP and Pierre shales show close agreement between in situ and laboratory (Figs 1, 2, and 5). Field permeability measurements in a jointed sandstone near Rangely Co. showed that little if any flow of water followed the joints [58]. A similar conclusion was reached after hydrologic study of the Navajo sandstone [14, 59]. Thus, fractures may play a minor hydrologic role for certain argillaceous rocks and sandstone: the reasons are probably different. k of intact sandstone is already in the millidarcy range; fractures add little [60]. For shale with a high clay content, fractures probably seal at modest depths owing to plasticity. The Eleana argillite (Fig. 6) is nearly half lithic fragments and thus may not behave like typical shale.

Prediction of permeability

How predictable is rock-mass permeability, even at

those shallow depths where most measurements have been made? The in situ measurements vary widely, both from site to site and at a single well. About the only safe generalization for crystalline rocks is that there are regions at most sites where k is around 1 μd; but most sites also have permeable zones with k of up to 100 md.

Unfortunately these values range too widely to be of much practical use. Many additional measurements are needed, at various depths, and in a wide variety of geologic situations. Perhaps clearer trends will then emerge.

For crystalline rocks, laboratory k may provide a good measure of the minimum in situ k. It may also provide a value of rock-mass k at depths or in situations where fractures close or become sealed. Unfortunately these depths are not in general known.

In situ measurements are costly and time-consuming and some study is being made of techniques which might yield k indirectly [61 for example]. Based on current understanding of flow through porous media, such techniques, unless strictly empirical, have to yield two parameters, interconnected porosity and pore dimension [34, 60, 62]. Although porosity can be obtained from electrical resistivity and certain other rock properties, pore dimension, in situ, remains the missing element. Thus, at present, k of rock masses cannot be obtained indirectly. There would seem to be no way to obtain in situ k other than by direct measurement in drill holes. As we note below, such measurements must be made at relevant effective pressures.

Turning to other than crystalline rocks, laboratory measurements may be of use for argillaceous rocks and sandstone, based on the tentative agreement we noted above with *in situ* values. However, this agreement needs to be extensively tested, particularly for argillaceous rocks, since so few *in situ* values are yet available.

The effects of stress on permeability have been widely recognized [4,60], particularly for fractured rock; changes in normal stress of a few MPa can change k by a factor of 5. This has an important bearing on measurement of k. If k is desired for a particular application (earthquake control, waste isolation, water supply, for example) then the particular effective stress state for this application must be known and, further, k must be measured at this effective stress. k measured in some other way may bear little relation to the relevant k. For example k measured in pumping tests by injection will not be the same as measured by fluid withdrawal [63]. Measurement or estimation of k must be tailored to the application.

Crustal permeability and anomalous pore pressure

With so few measurements, discussion of an average permeability of crustal rocks is so speculative as to be hardly worthwhile. Nevertheless the surprisingly high values of k given by both *in situ* and inferred methods seem sufficiently close to warrant some comment. There are important implications of high crustal k.

In situ measurements reach 2–3 km (Fig. 2). The volumes of rock for which k has been inferred (Fig. 4) extend deeper. The earthquakes discussed emanate from as deep as 5–7 km; the oceanic crust mentioned involves rock to 5 km and the Skaergaard rocks to 10 km. Thus, we may regard the eath's crust as having been sampled to 10 km. Below this, little is known. There is mounting evidence that lower crustal rocks are electrically so conductive that a water-filled pore space seems required [64], although some laboratory studies argue differently [65]. In any event, even if porosity at, say, 20 km were known, k cannot be inferred without knowledge of pore dimensions [60,62]. Eventually, at still greater depths, temperature will reach a level sufficient to induce plastic flow of the rocks. 500°C is suggested by recent studies of granite [66], although the Skaergaard rocks retained their conductivity to 1000°C [7]. Plastic flow will probably impair the connectivity of pore space, to judge from experiments with calcite rocks [67], and rock salt [73], and, as we might infer from the measurements of permeability of argillaceous rocks reported above. When this occurs, k probably drops to levels equivalent to transport by grain boundary diffusion; we estimated this to be about 1 nd [10].

If we consider crustal rock to 10 km, *in situ* and inferred k range from 0.1 to 10 md, assuming that the more permeable zones found in wells dominate the general flow. This range is close to that of sandstone. If this proves to be general, there are a number of important implications, both for energy resources and for tectonics. Both the 'hot, dry rock' concept [1] and waste disposal in crystalline rocks [2] depend on imper-

meable rocks near the structure in question. Although it is not yet clear how impermeable rocks must be, 10 md may be too high. The Los-Alamos hot, dry rock pilot program is operational for rocks with k of 0.1–1 μd. Evidently the more permeable zones at LASL (Fig. 2) have been successfully avoided, and this may be the general solution for design of waste isolation sites as well. Clearly the spacing and flow characteristics of such zones will have to be carefully mapped along with the hydraulic gradient in and around candidate sites.

Anomalously high pore pressure has been observed in many areas of recent sedimentation [26] and it has been postulated in deeper rocks as well; high pore pressure may have great tectonic significance. It is thought to play an important role in overthrusting [26] and seismicity [5], for example; it would keep crustal stresses at levels commensurate with values calculated from heat flow and earthquake stress drops [68].

Bredehoeft & Hanshaw [55] analyzed the hydrologic characteristics of rocks containing high pore pressure and concluded that maintenance of high pore pressure depends critically on permeability. One result has already been given in Fig. 4; rocks of nanodarcy permeability are required to maintain pore pressure at observed levels for geologically significant times. For the sedimentary rocks they discussed, thick shale layers were indicated. Based on the results presented here, we can now extend this to crystalline rocks.

If crustal rocks have millidarcy permeability, as suggested by the handful of present measurements, then pore pressure much greater than hydrostatic would seem virtually ruled out in regions where crystalline rocks extend to the surface. They might still prevail in hot pluton environments [74], or perhaps at depths below 10 km. Otherwise high pore pressure would be limited, in the same way proposed in the Bredehoeft-Hanshaw study, to regions with a thick argillaceous cover.

REFERENCES

1. McGretchin T. Hot dry rock geothermal energy: status of exploration and assessment. *ERDA Rpt. 77-74*, 206 pp. (June, 1977).
2. Bredehoeft J. D., England A. W., Stewart D. B., Trask N. J. & Winograd I. J. Geologic disposal of high-level radioactive wastes—earth-science perspectives. *U.S. Geol. Surv. Circ.* 779, 15 pp. (1978).
3. Green S. J. Rock-mechanics limitations to energy resource recovery and development. *Draft copy of Panel Review. U.S. Natl. Commun. for Rock Mechanics*, NRC (July 21, 1977).
4. Witherspoon P. A. & Gale J. E. Mechanical and hydraulic properties of rocks related to induced seismicity. *Engng Geol.* 11, 23–55 (1977).

5. Ohtake M. Seismic activity induced by water injection at Matsushiro, Japan. *J. Phys. Earth* 22, 163–176 (1974).

6. Anderson R. N., Langseth M. G. & Sclater J. G. The mechanisms of heat transfer through the floor of the Indian Ocean. *J. geophys. Res.* 82, 3391 (1977).

7. Norton D. & Taylor H. P. Jr. Quantitative simulation of the hydrothermal systems of crystallizing magmas on the basis of transport theory and oxygen isotope data: an analysis of the Skaergaard intrusion. *J. Petrol.* 20, 421–486 (1979).

8. Scott R. F. *Principles of Soil Mechanics*. Addison-Wesley, Reading, MA (1963).

9. Ohle E. L. The influence of permeability on ore distribution in limestone and dolomite. *Econ. Geol.* 46, 667–706 (1951).

10. Brace W. F., Walsh J. B. & Frangos W. T. Permeability of granite under high pressure. *J. geophys. Res.* 73, 2225–2236 (1968).

11. Lin W. Measuring the permeability of Eleana Argillite from Area 17, Nevada Test Site, using the transient method. *Lawrence Livermore Lab. Rept. UCRL-52604* (December 11, 1978).

12. De Wiest R. *Geohydrology*, 336 pp. Wiley, New York (1965).

13. Zoback M. D. & Byerlee J. D. Effect of high-pressure deformation on permeability of Ottawa sand. *Am. Ass. Petrol. Geol. Bull.* 60(9), 1531–1542 (1976).

14. Nelson R. A. An experimental study of fracture permeability in porous rock. *Proc. Sym. on Percolation Theory in Fissured Rock, ISRM Paper 2A6*. Stuttgart, Germany (1972).

15. Zoback M. D. & Byerlee J. D. Permeability and effective stress. *Am. Ass. Petrol. Geol. Bull.* 59(1), 154–158 (1975).

16. Jobin D. A. Relation of the transmissive character of the sedimentary rocks of the Colorado Plateau to the distribution of uranium deposits. *U.S. Geol. Surv. Bull.* 1124 151 pp. (1962).

17. Johnston D. H., Toksoz M. N. & Timur A. Attenuation of seismic waves in dry and saturated rocks, Part II. Theoretical models and mechanisms. *Geophysics* 44(4), 691–711 (1979).

18. Marine I. W. Geohydrology of buried triassic basic at Savannah River Plant, South Carolina. *Am. Ass. Petrol. Geol. Bull.* 58, 1825–1837 (1974).

19. Young A., Low P. F. & McClatchie A. S. Permeability studies of argillaceous rocks. *J. geophys. Res.* 69(20), 4237 (1964).

20. Winograd I. J. Hydrogeology of ash flow tuff: a preliminary statement. *Water Resour. Res.* 1, 994–1006 (1971).

21. Pratt H. P., Black A., Brace W. F. & Swolfs H. Elastic and transport properties of an *in situ* jointed granite. *Int. J. Rock Mech. Min. Sci. & Geomech. Abstr.* 14, 35–45 (1977).

22. Kranz R. L., Frankel A. D., Engelder T. & Scholz C. H. The permeability of whole and jointed Barre granite. *Int. J. Rock Mech. Min. Sci. & Geomech. Abstr.* 16, 225–234 (1979).

23. Marine I. W. The permeability of fractured crystalline rock at the Savannah River plant near Aiken, South Carolina. *U.S. Geol. Surv. Prof. Paper 575-B*, B203–B211 (1967).

24. Heard H. C., Trimmer D., Duba A. & Bonner B. Permeability of generic repository rocks at simulated *in situ* conditions. *Lawrence Livermore Lab. Rept. UCRL-82609*, 12 pp. (April 23, 1979).

25. Brace W. F. Dilatancy-related electrical resistivity changes in rocks. *PAGEOPH* 113, 207–217 (1975).

26. Rubey W. W. & Hubbert M. K. Role of fluid pressure in mechanics of overthrust faulting. *Geol. Soc. Am. Bull.* 70, 175 (1959).

27. Regan L. J. Fractured shale reservoirs in California. *Am. Ass. Petrol. Geol. Bull.* 37, 201–216 (1953).

28. Daniel E. J. Fractured reservoirs of Middle East. *Am. Ass. Petrol. Geol. Bull.* 38, 774–815 (1954).

29. De Wiest R. J. M. (Ed.) *Flow Through Porous Media*. Academic Press, New York (1969).

30. Ter-Stepanian G. & Arakelian A. A case of deformation of lavas spread over pre-Pleistocene landslides. *Proc. 1st Congr. Int. Soc. Rock. Mech., Lisbon*, Vol. 1 (1966).

31. Banks D. C. *In situ* measurements of permeability in basalt. *Proc. Symp. on Percolation Theory in Fissured Rock, ISRM Paper T1-A*. Stuttgart, Germany (1972).

32. Lutton R. J. & Girucky F. E. Geological and engineering properties Project Sulky. *PNE-720, U.S. Army Eng. Waterways Exper. Station*, Vicksburg, Miss., 136 pp. (1966).

33. Snow D. T. Hydraulic characteristics of fractured metamorphic rocks of Front Range and implications to the Rocky Mountain Arsenal Well. *Colo. Sch. Mines. Q.* 63(1), 167–199 (1968).

34. Snow D. T. Rock fracture spacings, openings and porosities. *J. Soil. Mech. Fdns Div., Am. Soc. civ. Engrs* 94, 73–91 (1968).

35. Marine I. W. Hydraulic correlation of fracture zones in buried crystalline rock at the Savannah River Plant near Aiken, S.C. *U.S. Geol. Surv. Prof. Paper 550-D*, 223–227 (1966).

36. Lundstrom L. & Stille H. Large-scale permeability test of the granite in the Stripa mine and thermal conductivity test. *Lawrence Berkeley Lab. Tech. Rept. No. LBL-7052*, 33 pp. (July, 1978).

37. Carlsson A. & Olsson T. Variations of hydraulic conductivity in some Swedish rock types. *Rockstore 1977 (Stockholm)* 2, 85–91 (1977).

38. Davison C. C., Grisak G. E. & Williams D. W. Field permeability and hydraulic potential measurements in crystalline rock and solute transport through finely fractured media. *Proc. Workshop on Low Flow Permeability Measurements in Largely Impermeable Rocks. OECD*, Paris March 19–21 (1979, in press).

39. West F. G., Kintzinger P. R. & Purtymun W. D. Hydrologic testing geothermal test hole No. 2. *Los Alamos Informal Rept. LA-6717-MS. ERDA Contr. W-7405-ENG. 36.* 8 pp. (1975).

40. Delisle G. Determination of permeability of granitic rocks in GT-2 from hydraulic fracturing data. *Los Alamos Informal Rept LA-6169-MS.* 5 pp. (December, 1975).

41. van Poollen H. K. & Hoover D. B. Waste disposal and earthquakes at the Rocky Mountain Arsenal. *J. Petrol. Technol.* 22, 983 (1970).

42. Picket G. R. Properties of Rocky Mountain Arsenal disposal reservoir and their relation to Derby earthquakes. *Colo. Sch. Mines Q.* 63, 73–102 (1968).

43. McMullen E. T. & Pasternak A. D. Field measurements of fracture permeability in granodiorite. *Univ. of Calif. Livermore Rad. Lab. Rept. UCID 15653.* 23 pp. (1970).

44. Ballou L. Field permeability measurements. *Waste Isolation Projects: FY 1978, UCRL-50050. Lawrence Livermore Lab.* (Edited by L. D. Ramspott) 31 pp. (Jan. 12, 1979).

45. Cook N. G. W. Hydrogeology of tunnels and mines. *Symp. on Recent Trends in Hydrogeology.* Berkeley, February 8–9, 1979: *Geol. Soc. Am. Bull.* in press (1979).

46. Bredehoeft J. D. An analysis of the Dakota aquifer system in South Dakota. *Symp. on Recent Trends in Hydrogeology.* Berkeley, February 8–9, 1979. *Geol. Soc. Am. Bull.*, in press (1979).

47. Thomas R. D. & Ward D. C. Effect of overburden pressure and water saturation on gas permeability of tight sandstone cores. *J. Petrol. Technol. Paper No. SPE 3634* (1971).

48. Rice J. R. & Simons D. A. The stabilization of spreading shear faults by coupled deformation–diffusion effects in fluid-infiltrated porous materials. *J. geophys. Res.* 81, 4322–5334 (1976).

49. Maini T. & Hocking G. An examination of the feasibility of hydrologic isolation of a high level waste repository in crystalline rock. *Geol. Soc. Am. Bull.* in press (1979).

50. Villas R. N. & Norton D. Irreversible mass transfer between circulating hydrothermal fluids and the Mayflower Stock. *Econ. Geol.* 72, 1471–1504 (1977).

51. Bianchi L. & Snow D. T. Permeability of crystalline rock interpreted from measured orientations and apertures of fractures. *Arn. Arid Zone* (Jodhpur, India), 8(2), 231–245 (September, 1969).

52. Scholz C. H., Sykes L. R. & Aggarwal Y. P. Earthquake prediction: a physical basis. *Science* 181, 803–810 (1973).

53. Anderson D. L. & Whitcomb J. H. The dilatancy–diffusion model of earthquake prediction. *Proc. Conf. on Tectonic Problems of the San Andreas Fault System. Stanford Univ. Publ., Geol. Sci., Vol. XIII,* 417–425 (September, 1973).

54. Mizutani H. & Ishido T. A new interpretation of magnetic field variation associated with the Matsushiro earthquakes. *J. Geomagn. Geoelect., Kyoto* 28, 179–188 (1976).

55. Bredehoeft J. D. & Hanshaw B. B. On the maintenance of anomalous fluid pressure. *Geol. Soc. Am. Bull.* 79, 1097–1106 (1968).

56. Nesterov L. I. & Ushatinskii I. N. Sealing properties of the argillaceous rocks above oil and gas pools in the mesozoic deposits of the West Siberian lowland. *Sov. Geol. No.* 5, 51–63 (1971).

57. Fehn U. & Cathles L. M. Hydrothermal convection at slow-spreading mid-ocean ridges. *Tectonophysics.* in press (1979).

58. Swolfs H. S., Brechtel C. E., Brace W. F. & Pratt H. R. Mechanical properties of a jointed sandstone. *Tectonophysics*, in press (1979).

59. Nelson R. A. & Handin J. Experimental study of fracture permeability in porous rock. *Am. Ass. Petrol. Geol. Bull.* 61, 227–236 (1977).

60. Brace W. F. A note on permeability changes in geologic materials due to stress. *PAGEOPH* 116, 627–633 (1978).

61. Nelson P. Advances in borehole geophysics for hydrogeology. *Symp. on Recent Trends in Hydrogeology*, Berkeley, Feb. 8–9, 1979. *Geol. Soc. Am. Bull.* in press.

62. Brace W. F. Permeability from resistivity and pore shape. *J. geophys. Res.* 82, 3343–3349 (1977).

63. Iwai K. Fundamental studies of fluid flow through a single fracture. Ph.D. thesis, Univ. Calif., Berkeley, 208 pp. (1976).

64. Nekut A., Connerney J. E. P. & Kuckes A. F. Deep crustal electrical conductivity: evidence for water in the lower crust. *Geophys. Res. Lett.* 4(6), 239–242 (1977).

65. Housley R. M. & Oliver J. R. Electrical characteristics of igneous Precambrian basement rocks of Central North America. In *The Earth's Crust, Geophys. Monograph 20* (Edited by J. G. Heacock) pp. 181–195. Am. Geophys. Union. Washington (1977).

66. Tullis J. & Yund R. A. Experimental deformation of dry Westerly granite. *J. geophys. Res.* 82, 5705–5718 (1977).

67. Brace W. F. Pore pressure in geophysics. *Geophys. Monograph 16*, pp. 265–273. Am. Geophys. Union, Washington (1972).

68. Stesky R. M. & Brace W. F. Estimation of frictional stress on the San Andreas fault from laboratory measurements. *Proc. Conf. on Tectonic Problems of the San Andreas Fault System, Stanford Univ., June 20–23, 1973. Stanford Univ. Publ., Geol. Sci., Vol XIII.* pp. 206–214 (1973).

69. Potter J. M. Experimental permeability studies at elevated temperature and pressure of granitic rocks. *Los Alamos Sci. Lab. Thesis LA-7224-T*, 101 pp. (May, 1978).

70. Raven K. G. & Gale J. E. Subsurface containment of solid radioactive waste: A study of the surface and subsurface structural groundwater conditions at selected underground mines and excavations. *Div. of Energy & Mines Res., ERM/GSC-RW Int. Rep. No. 1/77*, Ottawa, 105 pp. (1977).

71. Davis E. E. & Lister C. R. B. Heat flow measured over the Juan de Fuca Ridge: Evidence for widespread hydrothermal circulation in a highly heat transportive crust. *J. geophys. Res.* 82(30), 4845–4860 (1977).

72. Scheidegger A. E. *Physics of Flow Through Porous Media*, 3rd edn.. Univ. Toronto. Oxford Univ. Press, London, 313 pp. (1974).

73. Sutherland S. J. & Cave S. P. Gas permeability of SENM rock salt. *Int. J. Rock Mech. Min. Sci. & Geomech. Abstr.* in press (1979).

74. Knapp R. B. & Knight J. E. Differential thermal expansion of pore fluids: fracture propagation and microearthquake production in hot pluton environments. *J. geophys. Res.* 82, 2515–2522 (1977).

75. Witherspoon P. A., Amick C. H., Gale J. E. & Iwai K. Observations of a potential size effect in experimental determination of the hydraulic properties of factures. *Tech. Info. Rept. No. 17, Lawrence Livermore Laboratory, LBL-8571*, 15 pp. (1979).
Berkeley

76. Gale J. E. & Witherspoon P. A. An approach to the fracture hydrology at Stripa: Preliminary results. *Tech. Info. Rept. No. 15, Lawrence Livermore Laboratory, LBL-7079*. 26 pp. (1979).

77. Bredehoeft J. D. & Pinder G. T. Mass transport in flowing groundwater. *Water Resour. Res.* 9, 194–210 (1973).

78. Zoback M. D. *In situ* measurement of parameters relevant to earthquake occurrence. *Geol. Soc. Am. Abstr. with Programs* 11, 547 (1979).

79. Batchelor A. S. Permeability enhancement studies in Southwest England. *1st Ann. Rept., Camborne School of Mines Cornwall*, 70 pp. (1978).

80. Wilson C. R., Doe T. W., Long J. C. S. & Witherspoon P. A. Permeability characterization of nearly impermeable rock masses for nuclear waste repository siting. *OECD Sympos. on Well Testing in Low Permeability Rock*, Paris, March 1979 (1979).

81. Louis C. Suggested methods for determining hydraulic parameters and characteristics of rock masses. *Commission on Standardization of Lab. and Field Tests, Category II, Part 6. Int. Soc. Rock Mech.*, Orleans (1977).

82. Witherspoon P. A., Nelson P., Doe T., Thorpe R., Paulsson B., Gale J. & Forster C. Rock mass characterization for storage of nuclear waste in granite. *Tech. Inf. Rept. No. 18, Lawrence Berkeley Lab. Rept. 8570*, 31 pp. (February, 1979).

APPENDIX

Usage here and [7, 26, 31, 34, for example]:
Permeability, k, has dimensions L^2. The unit is 1 darcy.

$$1 \text{ darcy (d)} \simeq 10^{-8} \text{ cm}^2 \simeq 10^{-11} \text{ ft}^2$$

Widely used in soil and rock mechanics, and hydrology [8, 18, 37, 46, 49, for example]:
Coefficient of permeability, which is equivalent to *hydraulic conductivity*, with dimensions, LT^{-1}. For water under standard conditions

$$1 \text{ darcy} \simeq 10^{-3} \text{ cm/sec} = 10^{-5} \text{ m/s}$$

$$1 \text{ Meintzer} = 1 \text{ gallon/day/ft}^2 \simeq 1/20 \text{ darcy}.$$

When transient flow is involved it is customary to discuss:
Hydraulic diffusivity, a, with dimensions $L^2 T^{-1}$. This is converted to permeability, *k*, if porosity, η, viscosity, μ, and compressibility, β, are known:

$$a = k/\mu\eta\beta.$$

The Precipitation of Copper from Aqueous Solutions by Hydrogen Reduction

E. PETERS* and E. A. VON HAHN†

INTRODUCTION

The first appearance of the metallic state in a metallurgical extraction process has always exerted a peculiar fascination on the metallurgist, and this is no less true when the metal precipitates or deposits from an aqueous leach liquor than it is for a process in which the metal first appears as a pool in the bottom of a furnace. Actually, the hydrometallurgist, when he is examining the fundamental aspects of his reaction, is primarily involved in kinetics and mechanisms, while the pyrometallurgist is more concerned with knowing the thermodynamics of the system and only rarely becomes involved in the kinetics of processes other than those of mass and heat transfer.

Recent advances in hydrometallurgy[1] include the application of pressure to permit the use of gaseous or volatile reagents such as hydrogen or ammonia, and to allow the use of temperatures considerably in excess of the normal boiling point.

Commercial applications of hydrogen-displacement reactions now involve the precipitation of copper, nickel and cobalt as metal powders.[1-6] Other metals, such as silver, mercury, the platinum metals, etc., have also been precipitated with hydrogen and the reactions have been studied extensively in some cases.[7-9] However, these are of no immediate commercial interest.

In general, the hydrogen-displacement reactions are divided into two main groups: those that occur homogeneously, as copper, silver, mercury, etc.; and those that proceed only by heterogeneous mechanisms, such as nickel and cobalt. The latter require seeding with a

* Associate Professor of Metallurgy, The University of British Columbia, Vancouver 8, B.C.
† Eldorado Mining and Refining Company, Ottawa, Canada.

nucleating powder,[4] and the reaction rate is proportional to the surface area of powder added. In the homogeneous cases no seeding appears to be necessary, nor does the addition of powder at the beginning of reduction affect the kinetics. Platinum metals usually are displaced simultaneously by homogeneous and heterogeneous mechanisms,[10,11] the former initiating the reaction and the latter accounting for most of the rate after it is well under way.

The distinction between homogeneous and heterogeneous hydrogen displacement of metals may not have been apparent to Ipatieff,[12] whose investigations of these reactions are the earliest recorded. Although his early work did not prove conclusively that the copper reduction was homogeneous, his later researches on hydrogenation of organic substrates showed that finely divided nickel was a useful catalyst for a wide variety of reactions, while metallic copper was very much less useful. The homogeneous nature of the copper-reduction reaction was probably suspected first by Halpern, who with his co-workers first showed the homogeneous precipitation of Cu_2O from cupric acetate solutions[13] and later the reduction of substrates such as dichromate by hydrogen in the presence of a variety of cupric salts.[14-16] With this work it became apparent that cupric ions and various cupric complexes in aqueous solutions functioned as homogeneous catalysts in the hydrogen reduction of any oxidizing substrate thermodynamically more easily reduced than divalent copper. It was also apparent that the precipitation of metallic copper must proceed by the same mechanism, unless heterogeneous processes play a role as well.

MECHANISM OF THE COPPER-CATALYZED HYDROGEN-REDUCTION REACTIONS

The mechanism for hydrogen reduction of copper or oxidizing substrates in aqueous solutions is given by the following equations:[17]

$$Cu^{++} + H_2 \underset{k_{-1}}{\overset{k_1}{\rightleftharpoons}} CuH^+ + H^+ \tag{1}$$

$$CuH^+ + Cu^{++} \overset{k_2}{\longrightarrow} 2Cu^+ + H^+ \tag{2}$$

$$2Cu^+ \overset{fast}{\rightleftharpoons} Cu^{++} + Cu^\circ \quad \text{or} \tag{3a}$$

$$2Cu^+ + O_x \rightarrow 2Cu^{++} + \text{Products} \tag{3b}$$
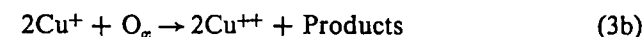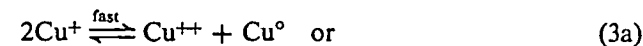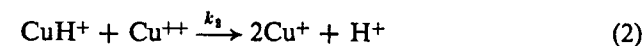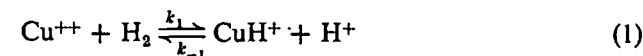
where O_x = Oxidant.

This mechanism is strictly applicable for solutions in which Cu^{++} is uncomplexed, except perhaps with water molecules, as in perchlorate solutions. The rate law for this mechanism, as derived by the steady-state approximation, is given by[17]

$$R = \frac{k_1[Cu^{++}]^2[H_2]}{\frac{k_{-1}}{k_2}[H^+] + [Cu^{++}]} \tag{4}$$

with k_1 having a value of 9.5×10^{-5} M^{-1} sec^{-1} and $\frac{k_{-1}}{k_2}$ a value of 0.26 from dichromate reduction rate measurements at 110°C. The activation energy for k_1 was found to be about 26 kcals per mole.[16]

Macgregor and Halpern[18] subsequently studied the copper precipitation itself at temperatures between 150°C and 175°C. The reduction rate curves were not analyzed, and only initial rates were used to check out the above mechanism (Equations 1, 2, and 3a) which yielded a value of 7.5×10^{-3} M^{-1} sec^{-1} for k_1 and a value of $\frac{k_{-1}}{k_2}$ of 1.3 at 160°C. The value for k_1 is very close to that extrapolated from the Arrhenius plot of the dichromate work.[15] It was therefore apparent that initial copper reduction rates and the catalytic reduction of dichromate yielded the same values under the same conditions, and the mechanism seemed confirmed.

However, two anomalies appeared to exist in the published literature that suggested this mechanism to be in error. McDuffie and co-workers[19] were not able to obtain an acid dependence in the hydrogen-oxygen recombination reaction at 250°C such as would be expected if the above mechanism were extrapolated to this temperature with oxygen replacing dichromate. Also, Potter[20] reported a mechanism in which the activity of the cuprous ions with hydrogen is larger than the activity of cupric ions. In addition to these considerations, the mechanism as described was not consistent with the shape of the complete reduction curves described by Macgregor and Halpern.[18] These curves showed that the reduction reaction slowed down with time to a much greater extent than was required by equation (4).

To resolve these difficulties, the authors studied[21] the dichromate reaction again, this time in the 160°-200°C range where the copper reduction rates had been studied, using lower copper and higher dichromate levels to bring the rates into the measurable range. The results of this study showed that a dichromate dependence appeared

under these conditions that indicated a direct attack of the oxidant on CuH^+, the reactive intermediate. The former mechanism still applied, with the addition of a supplementary reaction to account for the dichromate dependence, i.e.

$$CuH^+ + Cr^{VI} \xrightarrow{k_3} Cu^{++} + \text{Products} \tag{2a}$$
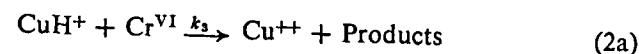
The resulting rate law becomes

$$R = \frac{k_1[Cu^{++}][H_2]\left\{\frac{k_2}{k_{-1}}[Cu^{++}] + \frac{k_3}{k_{-1}}[Cr^{VI}]\right\}}{[H^+] + \frac{k_2}{k_{-1}}[Cu^{++}] + \frac{k_3}{k_{-1}}[Cr^{VI}]} \tag{5}$$

The values obtained for k_1, $\frac{k_2}{k_{-1}}$, and $\frac{k_3}{k_{-1}}$ were 5.4×10^{-3} M^{-1} sec^{-1}, 2.7 and 42 respectively at 160°C.

It is apparent that the acid dependence would fall off for cases where $\frac{k_3}{k_{-1}}[Cr^{VI}] > [H^+]$; if the oxygen dependence were similar to that of dichromate, this would account for the anomaly described by McDuffie et al.[19]

The value for $\frac{k_2}{k_{-1}}$ in this work corresponds to a value of 0.37 at 160°C for its reciprocal $\frac{k_{-1}}{k_2}$, which was measured in earlier studies and which yielded a value of 0.26 at 110°C[17] from dichromate reduction rates and 1.3 at 160°C[18] from copper precipitation studies. The value obtained in the dichromate work also seems to be nearly temperature-independent, and therefore the high value obtained by Macgregor and Halpern[18] represents an additional anomaly that must be resolved for the complete and accurate understanding of this system.

The results of the dichromate work now appear to contain conclusive evidence for the validity of the mechanism including equation (2a) and of the rate law given in expression (5) for all copper-catalyzed reactions in which an oxidant exists that is capable of preventing the appearance of the cuprous state. This is not adequate, however, to the metallurgist who wishes to precipitate copper from solution. In such cases the cuprous state appears, at least transiently, and a knowledge of its properties and catalytic powers (if any) is essential to the complete understanding of the mechanism of reduction and to the determination

of the correct rate law. The role of Cu^I is of particular significance in the mechanism proposed by Dunning and Potter and may also account for the discrepancy in the values of $\frac{k_{-1}}{k_2}$ described above. Hence it has become essential to determine the cuprous concentrations of solutions under reduction conditions, and to determine, if possible, the dependence of the reaction on this important species. Since this work has not been reported elsewhere, a complete description of the experiments, their analysis and conclusions follows.

EXPERIMENTAL

The experimental apparatus used in these studies consisted essentially of a high-pressure autoclave* (capable of working pressures to 1000 psig at 300°C) fitted with a motor-driven stirrer, a thermal well, a sampling system, and external gas-burner heaters. Temperature control was provided to an accuracy of ±0.3°C at temperatures up to 200°C with either a Leeds and Northrop Micromax controller-recorder or a Thermistemp temperature controller manufactured by Yellow Springs Instrument Company. The autoclaves were of stainless steel but for most experiments titanium linings and internal parts were used for their superior corrosion resistance to perchloric acid solutions. The titanium linings were closely fitted to permit good thermal contact and were extended to the gasket seat to prevent transport of material to the annular shaped crevice between the lining and the main body of the vessel.

The sampling arrangement was specially designed to permit high temperature determination of Cu^I, since the uncomplexed cuprous ion is known to disproportionate rapidly on cooling. The arrangement is shown schematically in Fig. 1 and relies on a pressurized sample-bottle container as a receiver and a pressurized "burette" from which a titration solution is forced to join the sample through a "T" in the sample line before it flows into the sample bottle. The sample line was heated up to the "T" junction, and pressures were adjusted in the "burette" and sample receiver to allow acceptable flow rates. Sample volumes were determined by difference using volumetric flasks as sample bottles: these were filled with distilled water from a burette at

* Two autoclaves were used. One was a one-gallon vessel manufactured by Autoclave Engineers Inc., and the other a two-liter vessel manufactured by Parr Instrument Company.

room temperature after being removed from the container. Excess dichromate was determined spectrophotometrically when it was used as the titration reagent.

The above procedure was used to determine the cuprous content of the solution, and dichromate was the most common titrating reagent, since it seemed to oxidize cuprous stoichiometrically. The method
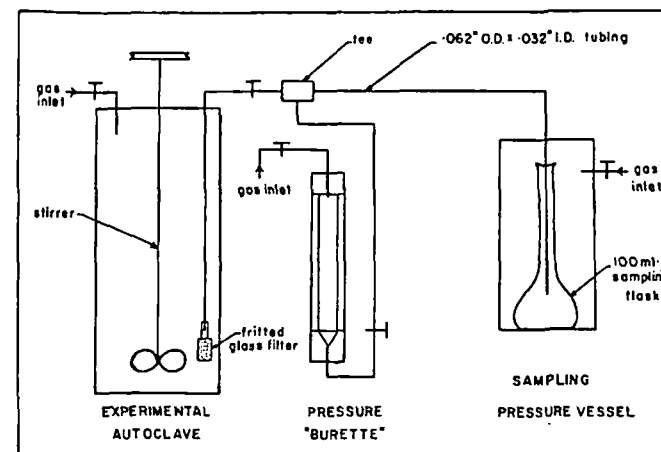
Fig. 1. Schematic diagram of experimental apparatus with pressure sampling system.

was checked by permitting the sample to disproportionate and determining metallic copper in the sample, and also by using NH_4CNS, KI or NaBr as a reagent which precipitates cuprous as insoluble cuprous thiocyanate, iodide or bromide. In these cases the precipitate was collected and analyzed for total copper. Good agreement was obtained by these methods, but the dichromate method yielded the lowest scatter in the results and was the most convenient.

Other determinations that were made include total copper by the electrolytic method, chloride ion by the Volhard method, and hydrogen ion (on disproportionated samples only) by titrating with sodium tetraborate solution.

The usual procedure followed in the kinetic experiments was to heat the solution of selected copper content to temperature, add hydrogen after good temperature control commenced, and sample by means of the above arrangement at selected time intervals. Some equilibrium experiments were also performed, to determine accurately the disproportionation constant of cuprous ions.

RESULTS AND DISCUSSION

Kinetic experiments were conducted under a variety of initial conditions ranging from 0.01 to 0.10M Cu(ClO$_4$)$_2$, 0.01 to 0.10M HClO$_4$, and 160° to 200°C. Typical rate plots are shown in Fig. 2 and indicate that the cuprous content of the solution rises to a maximum value, at which point it begins to fall, due to disproportionation to metallic copper and cupric. When the initial cupric content falls below 0.03M,
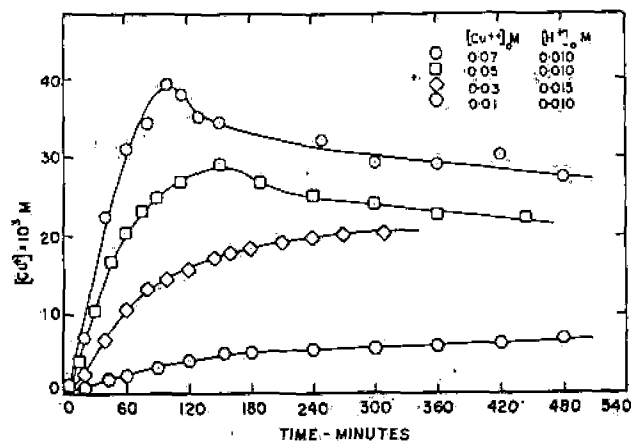
Fig. 2. Typical rate plots of [Cu$^+$] vs. time with and without disproportionation at experimental conditions; temperature 160°C, H$_2$–10 atm.

the cuprous level does not reach a maximum value and no evidence of disproportionation appears before cooling. However, metallic copper is present in all untreated samples that are cooled under hydrogen or helium because in such cases the disproportionation occurs on cooling.

Analytical results on samples after a significant amount of reaction has occurred reveal a copper-to-acid stoichiometry consistent with the overall equations

$$H_2 + 2\,Cu^{++} \longrightarrow 2\,Cu^+ + 2\,H^+ \tag{6}$$

and

$$H_2 + Cu^{++} \longrightarrow Cu° + 2\,H^+ \tag{7}$$
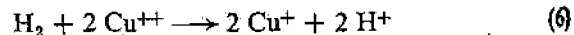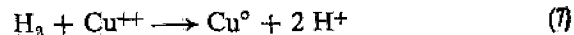
Only equation (6) applies to conditions before disproportionation (to the peaks of the curves in Fig. 2), while both equations apply to conditions after disproportionation begins.

Disproportionation Kinetics and Equilibria

It is evident from equation (3a) that the disproportionation reaction is responsible for the appearance of metallic copper. This emphasizes the need for determining the extent to which the disproportionation reaction affects the precipitation rates. Separate experiments were therefore conducted at 160°C to determine the disproportionation constant under equilibrium conditions. A cupric perchlorate solution was equilibrated with about 2100 cm^2 of copper foil cut into small squares, using an atmosphere of pure helium. Samples were withdrawn in the usual way and several additions of perchloric acid were made during the experiment. The disproportionation equation (3a), i.e.

$$2\,Cu^+ \rightleftharpoons Cu^{++} + Cu° \tag{3a}$$
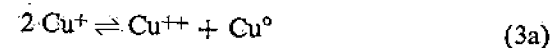
indicates that the reaction is pH independent, but if a significant amount

TABLE I

Values of the Equilibrium Constant K for the Cu$^+$—Cu^{++}—Cu° Equilibrium at 160°C and Varying H$^+$.

HClO$_4$, M	$K = \dfrac{[Cu^{++}]}{[Cu^+]^2}\ M^{-1}$
0.007	44.3 ± 3.1
0.035	26.1 ± 2.0
0.083	25.5 ± 2.0

of the cupric is hydrolyzed to Cu(OH)$^+$, an apparent pH-dependence of the resulting constant due to the associated equilibrium

$$2\,Cu^+ + H_2O \rightleftharpoons Cu[OH]^+ + Cu° + H^+ \tag{8}$$
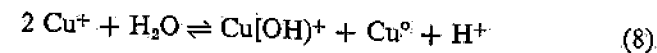
will appear. The results of this experiment are given in Table I and indicate that, above 0.03M [H$^+$], hydrolysis is not significant. The resulting disproportionation constant at 160°C for equation (3a) is:

$$\frac{[Cu^{++}]}{[Cu^+]_2} = 26 \pm 2\ M^{-1} \tag{9}$$

When this constant is used to calculate the equilibrium [Cu$^+$] concentrations corresponding to the determined [Cu^{++}] concentrations in a

kinetic experiment, good agreement with the determined cuprous concentrations is obtained, as shown in Fig. 3. There appears to be a small amount of supersaturation at the maximum in the experimental curve, indicating that nucleation of metallic copper may be a little slow in this region. The amount of supersaturation shown could also be within experimental limits of precision, since very small nuclei of metallic
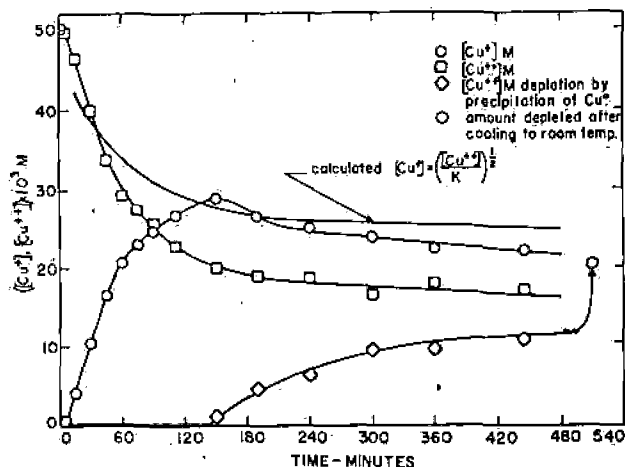

Fig. 3. Experimental rate plots of [Cu+], [Cu++] and Cu° vs. time; together with a [Cu+] curve calculated as a function of [Cu++] and $K = 26$ M^{-1}; temperature 160°C, H$_2$–10 atm., [HClO$_4$]$_0$–0.01M.

copper could pass through the sample filter and be determined as cuprous through oxidation by dichromate.

Nucleation rates for the disproportionation reaction have been measured by Courtney[22] at room temperature. The method used involved measuring the time of appearance of a Tyndall effect in a solution of cuprous ammonium sulphate that was rapidly acidified to destroy the stable cuprous amine complex ions. A tenth-power dependence on cuprous concentration for the reciprocal of this time was interpreted as evidence that the critical nucleus contained 5 copper atoms. The same nucleation mechanism probably applies in the case of hydrogen reduction but apparently never becomes rate-determining, except perhaps transiently at the onset of copper precipitation.

The value of 26 ± 2 M^{-1} at 160°C for the disproportionation constant Equation 9 is significantly lower than would be expected from

extrapolation of room temperature data, using published thermodynamic properties of Cu^{++}, Cu$^+$ and Cu°.[23] This would indicate that the thermodynamic properties, especially the entropies, of the aquo ions have second-order variations with temperature not evident in the room-temperature values. The change in the properties of water is primarily responsible for this, and very little has been done either experimentally or theoretically to show accurately the variation of thermodynamic properties from room temperature to high temperature (above 100°C) in ionic aqueous solutions. The method of C. M. Criss[24] for estimating entropies of ions at elevated temperature by the use of empirical equations derived from correlation diagrams may be used to advantage in this case.

The Integrated Rate Curve

It is possible to integrate the rate law expressed by equation (4) i.e.

$$\frac{-d[H_2]}{dt} = \frac{k_1[Cu^{++}]^2[H_2]}{\frac{k_{-1}}{k_2}[H^+] + [Cu^{++}]} \tag{4}$$

for experimental conditions, using values of k_1 and $\dfrac{k_{-1}}{k_2}$ obtained from the dichromate work. To perform this integration, the rate must be defined in terms of [Cu^{++}] or [Cu$^+$] and the values of [Cu^{++}] and [H$^+$] must be expressed in the same variable as the rate. For example, if the rate is expressed in cuprous, we have the equation:

$$\frac{-d[H_2]}{dt} = +\frac{1}{2}\frac{d[Cu^+]}{dt} \tag{10}$$

while [Cu^{++}] = [Cu^{++}]$_0$ − [Cu$^+$] before disproportionation and [Cu^{++}] = K[Cu$^+$]^2 after disproportionation begins. At the same time, [H$^+$] = [H$^+$]$_0$ + 2[Cu^{++}]$_0$ − [Cu$^+$] − 2[Cu^{++}]. The resulting rate law before disproportionation, can be expressed:

$$\frac{d[Cu^+]}{dt} = \frac{2k_1\{[Cu^{++}]_0 - [Cu^+]\}^2[H_2]}{\frac{k_{-1}}{k_2}\{[H^+]_0 + [Cu^+]\} + \{[Cu^{++}]_0 - [Cu^+]\}} \tag{11}$$

while after disproportionation begins, the equation has the form:

$$-\frac{d[Cu^{++}]}{dt} =$$

$$\left(\frac{k_1[Cu^{++}]^2[H_2]}{\left[\left(\frac{k_{-1}}{k_2}\right)\left\{[H^+]_0 + 2[Cu^{++}]_0 - 2[Cu^{++}] - \left(\frac{[Cu^{++}]}{K}\right)^{1/2}\right\} + [Cu^{++}]\right]} \right)$$

$$\times \left(\frac{1}{\left[1 + \frac{1}{4K^{1/2}[Cu^{++}]^{1/2}}\right]} \right) \quad (12)$$

The integrated forms associated with these are:

$$t = \frac{k_{-1}}{2k_2k_1[H_2]}\left\{\frac{[H^+]_0 + [Cu^{++}]_0}{[Cu^{++}]_0 + [Cu^+]} - \frac{[H^+]_0}{[Cu^{++}]_0} - 1\right\}$$

$$+ \frac{\left(\frac{k_{-1}}{k_2} - 1\right)}{2k_1[H_2]} \times 2.3 \log\left(\frac{[Cu^{++}]_0 - [Cu^+]}{[Cu^{++}]_0}\right) \quad (13)$$

before disproportionation and

$$t = \left(\frac{1}{x} - \frac{1}{x_0}\right)\frac{k_{-1}\left(Q - \frac{1}{4K}\right)}{k_1k_2[H_2]} + \left[2.3 \log\left(\frac{x_0}{x}\right)\right]\frac{1 - \left(\frac{2k_{-1}}{k_2}\right)}{k_1[H_2]}$$

$$+ \left(\frac{1}{x^{1/2}} - \frac{1}{x_0^{1/2}}\right)\frac{\left(\frac{1}{2} - \frac{3k_{-1}}{k_2}\right)}{k_1K^{1/2}[H_2]} + \left(\frac{1}{x^{3/2}} - \frac{1}{x_0^{3/2}}\right)\frac{k_{-1}Q}{6k_1k_2K^{1/2}[H_2]} \quad (14)$$

where $x = [Cu^{++}]$

$x_0 = [Cu^{++}]_0$

$Q = [H^+]_0 + 2[Cu^{++}]_0$

after disproportionation begins.

The above equations assume that there are no interfering side reactions that consume hydrogen by the copper-activation route, but do not reduce either cupric or cuprous. During experimental runs, however, chloride ions make their appearance due to decomposition

of perchlorate and the stoichiometry* in terms of equivalent cuprous oxidized indicates that this is particularily serious, i.e.

$$ClO_4^- + 8\,Cu^+ + 8\,H^+ \rightarrow Cl^- + 4\,H_2O + 8\,Cu^{++} \quad (15)$$
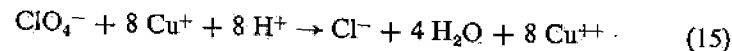
The effect of this is shown in Fig. 4 on comparing the theoretical curve A with the experimental curve shown. The corrected curve B in
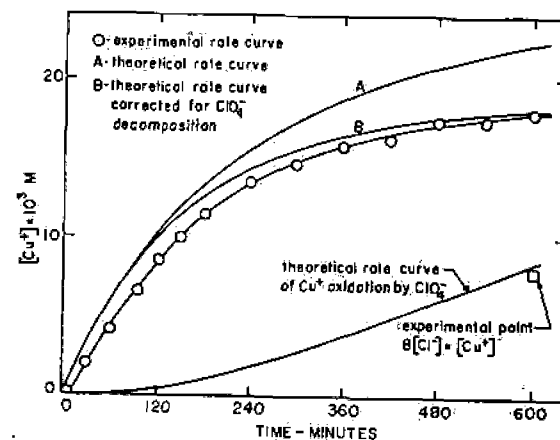
Fig. 4. Comparison of experimental and theoretical rate curves. Temperature 160°C, H_2–10 atm., $[Cu^{++}]_0 = 0.03M$, $[HClO_4]_0 = 0.01M$.

this same figure is the integrated form based on the rate law

$$\frac{1}{2}\frac{d[Cu^+]}{dt} = \frac{k_1[Cu^{++}]^2[H_2]}{\left(\frac{k_{-1}}{k_2}\right)[H^+] + [Cu^{++}]} - 4k_{Cl}[Cu^+][H^+][ClO_4^-] \quad (16)$$

where k_{Cl} is the third order rate constant for perchlorate reduction by Cu^+.†

---

* Direct attack of Cu^+ on ClO_4^- is not implied but also not excluded. Experiments performed without copper salt additions to the solution failed to produce measurable amounts of Cl^-, indicating that the presence of copper, probably as Cu^+, is responsible for perchlorate decomposition.

† This reaction is assumed to be of the form $\frac{d[Cl^-]}{dt} = k_{Cl}[Cu^+][H^+][ClO_4^-]$. The value of k_{Cl} was estimated by a graphical integration of this equation to the time when $[Cl^-]$ was measured, and was found to be $k_{Cl} = (2.07 \times 10^{-4} \pm 7\%)\,M^{-2}\,sec^{-1}$.

Kinetic Studies in the Perchlorate System

The above comparison already indicates that, when perchlorate decomposition is taken into account, Equation 4 is a relatively good approximation of the reduction rate, and this contains no dependence of the rate on any cuprous species. However, the effect of the presence of cuprous ions was also examined through comparison of differential
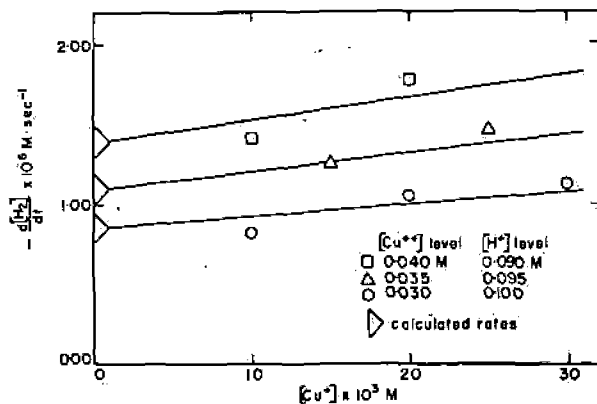

Fig. 5. Dependence of rate on [Cu⁺] in perchlorate solutions.*
Temperature 160°C, H₂–10 atm.

rate measurements made in several experiments in which the [H⁺] and [Cu⁺⁺] were unchanged at different values of cuprous. These rates are plotted as a function of Cu⁺ in Fig. 5 and show that with increasing Cu⁺ concentration the rate is increased measurably (20 to 30% at the highest cuprous values).

The cuprous contribution to the rate was not observed by Macgregor and Halpern, probably because they also neglected ClO_4^- decomposition which affects the rate even more extensively. The observation of this effect in this study is consistent with Dunning and Potter's observations of such a reaction in sulphate solutions, although the effect observed in perchlorate solutions is very much smaller.

Since the rate measurements are subject to appreciable uncertainties, it is not possible to evaluate completely the cuprous-dependent reaction

* Intercepts calculated with equation (4) ($k_1 = (5.40 \pm 0.7) \times 10^{-3} M$ sec⁻¹, $\frac{k_{-1}}{k_2} = 0.37$, from reference 21).

into a complete rate-law term that would allow corrections to be made on all rate measurements. Therefore, in subsequent analyses of rate measurements in perchlorate solutions, this contribution to the reaction rate has been ignored.

Equation (16) can be rearranged to the form

$$\frac{[Cu^{++}]}{\frac{1}{2}\frac{d[Cu^+]}{dt} + 4k_{Cl}[Cu^+][H^+][ClO_4^-]} = \frac{\left(\frac{k_{-1}}{k_2}\right)[H^+]}{k_1[Cu^{++}][H_2]} + \frac{1}{k_1[H_2]} \quad (17)$$

Since
$$\frac{1}{2}\frac{d[Cu^+]}{dt} + 4k_{Cl}[Cu^+][H^+][ClO_4^-] = \frac{-d[H_2]}{dt}$$

the function

$$\frac{[Cu^{++}]}{\frac{1}{2}\frac{d[Cu^+]}{dt} + 4k_{Cl}[Cu^+][H^+][ClO_4^-]}$$

can be plotted against $\frac{1}{[Cu^{++}]}$ and should yield a straight line of intercept $\frac{1}{k_1[H_2]}$ and slope $\frac{\left(\frac{k_{-1}}{k_2}\right)[H^+]}{k_1[H_2]}$. Plots of this form are shown in Fig. 6.

The average value of k_1 obtained from the intercepts is $6.7 \pm 20\% \times 10^{-3}$ M⁻¹ sec⁻¹. The slopes are also almost constant and from them a value of $\left(\frac{k_{-1}}{k_2}\right)$ of $0.51 \pm 20\%$ can be estimated. Plots can also be made of $\frac{1}{\frac{1}{2}\frac{d[Cu^+]}{dt} + 4k_{Cl}[Cu^+][H^+][ClO_4^-]}$ vs [H⁺] at constant [Cu⁺⁺] to confirm the hydrogen-ion dependence of equation (16). These are shown in Fig. 7. k_1 calculated from the intercepts of these plots has an average value of $8.5 \pm 30\% \times 10^{-3}$ M⁻¹ sec⁻¹ and $\left(\frac{k_{-1}}{k_2}\right)$ is $0.83 \pm 35\%$.

These values of k_1 (Table II) are in good agreement with those obtained by Macgregor and Halpern[18] from initial reduction rates and are somewhat larger than the value obtained in the dichromate reduction work.[21] Since the Cu⁺ contribution to the reaction rate was ignored in the copper-reduction studies the apparently higher values of k_1 and the
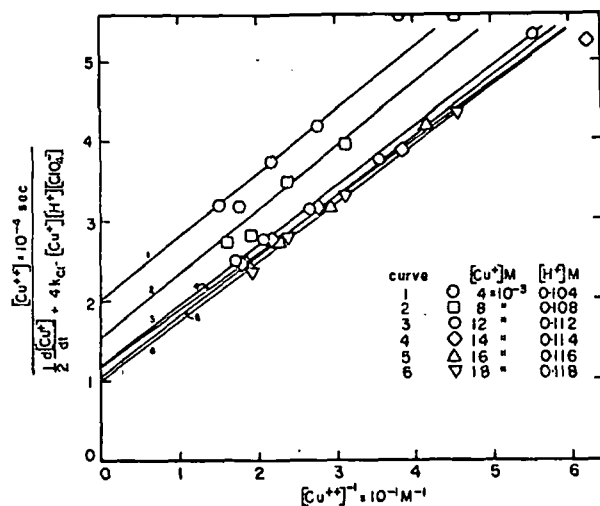
Fig. 6. Plot of [Cu++] (Rate Function)⁻¹ vs. [Cu++]⁻¹ at constant [H+] and [Cu+] levels. Temperature 160°C, H_2–10 atm., $[HClO_4]_0 = 0.10M$.
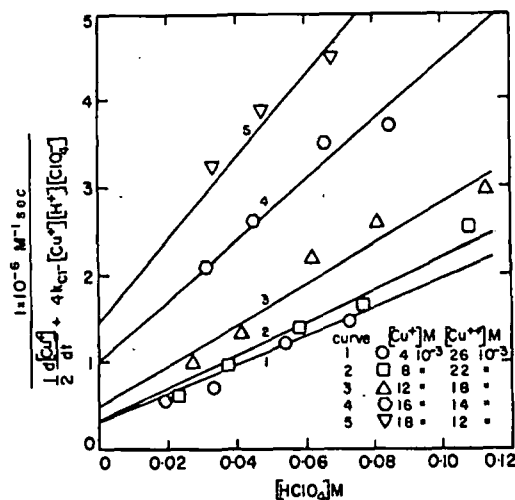
Fig. 7. Plot of (Rate Function)⁻¹ vs. [HClO₄] at constant [Cu++] and [Cu+] levels. Temperature 160°C, H_2–10 atm., initial Cu++–0.03M.

TABLE II

Values of k_1 and $\dfrac{k_{-1}}{k_2}$ from Various References and Figures 6 and 7.

Temperature °C	k_1 M⁻¹ sec⁻¹	$\dfrac{k_{-1}}{k_2}$	Reference or Figure
160	4.8 × 10⁻³*	—	15
160	7.5 × 10⁻³ ± 15%	1.3	18
160	5.4 × 10⁻³ ± 15%	0.37 ± 30%	21
160	6.7 × 10⁻³ ± 20%	0.51 ± 20%	Fig. 6
160	8.5 × 10⁻³ ± 30%	0.83 ± 35%	Fig. 7

* By extrapolation from Arrhenius plot.

rather different values of $\dfrac{k_{-1}}{k_2}$ in this work are not surprising. The values of $\dfrac{k_{-1}}{k_2}$ are considerably lower in this work than the value of Macgregor and Halpern and reasonably consistent with the dichromate value. Much higher values would be found in the present work if the perchlorate decomposition were ignored. Perchlorate decomposition probably does not take place during dichromate reduction because of the high oxidizing potential of the dichromate-containing system. Also, the values of $\dfrac{k_{-1}}{k_2}$ in the present work would be lower and agree more closely with the dichromate value if the contribution to the rate due to Cu+ activity were taken into account.

Reactions in the Presence of Metallic Copper

After the onset of disproportionation, metallic copper is always present in the system during further reduction. A number of experiments were performed in which copper was added initially, and in these the disproportionation equilibrium reversed on heating to yield cuprous ions through copper dissolution. Analyses of the resulting rate curves were reasonably consistent with the rates expected from Equation 4, and therefore it must be concluded that the presence of metallic copper does not introduce a heterogeneous supplementary reaction, nor does it interfere with the homogeneous mechanism in any way, at least in perchlorate solutions.
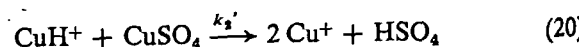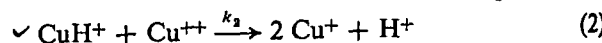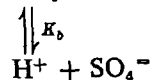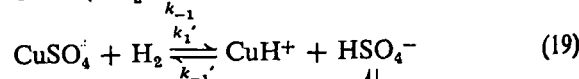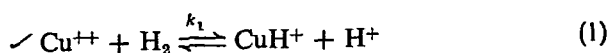
This observation is not consistent with the evidence presented by

Evans et al.[2] that the rate of reduction in sulphate solutions is dependent on particle size of precipitated metal, with finer powder being associated with faster rates. In their studies, particle size control was achieved with organic dispersants such as ammonium polyacrylate, and it is possible that the rate effects observed are the results of homogeneous effects of these dispersants, and are not associated with the heterogeneous results of the same additions.

Reaction Rates in Sulphate Solutions

The sulphate system is more interesting than the perchlorate system from a practical point of view, and that is undoubtedly why it has received so much attention from previous investigators. Much of the practical work, such as was done by Evans et al.,[2] was actually with a complex, partially-hydrolyzed slurry of ammonium sulphate and the kinetics could not be examined in detail. A detailed kinetic study was made by Dunning and Potter.[20] By following the cupric species spectrophotometrically they observed an increasing reaction rate with time, and attributed the dominant part of the reduction to a first-order autocatalysis by Cu[I]. Macgregor and Halpern[18] also made a study of the Cu[II] reduction in the sulphate system, but the initial rates were too fast to permit a kinetic evaluation of their results.

Generally speaking, the dominant effect of sulphate should be an enhancement of rate due to complexing, since the activity of the copper sulphate complex is about six times that of the cupric ion, for catalytic reduction of dichromate.[16] In addition the buffering effect of sulphate through formation of bisulphate ion should also increase reduction rates of copper sulphate solutions by lowering the hydrogen ion effect. The following set of equations indicates all possible reactions one might expect for the direct reduction of cupric sulphate.

$$Cu^{++} + SO_4^{=} \overset{K_a}{\rightleftharpoons} CuSO_4 \qquad (18)$$

$$Cu^{++} + H_2 \underset{k_{-1}}{\overset{k_1}{\rightleftharpoons}} CuH^+ + H^+ \qquad (1)$$

$$CuSO_4 + H_2 \underset{k_{-1}'}{\overset{k_1'}{\rightleftharpoons}} CuH^+ + HSO_4^- \qquad (19)$$

$$\Big\updownarrow K_b$$

$$H^+ + SO_4^{=}$$

$$CuH^+ + Cu^{++} \overset{k_2}{\longrightarrow} 2 Cu^+ + H^+ \qquad (2)$$

$$CuH^+ + CuSO_4 \overset{k_2'}{\longrightarrow} 2 Cu^+ + HSO_4 \qquad (20)$$

These equations yield a rate law corresponding to the following equation

$$-\frac{d[H_2]}{dt} = \frac{k_1[Cu^{II}]^2[H_2] \left\{ \dfrac{1 + \dfrac{k_1'}{k_1} K_a[SO_4^-]}{1 + K_a[SO_4^-]} \right\} \left\{ \dfrac{1 + \dfrac{k_2'}{k_2} K_a[SO_4^-]}{1 + K_a[SO_4^-]} \right\}}{\dfrac{k_{-1}}{k_2}[H^+]\left\{1 + \dfrac{k_{-1}'}{k_{-1}K_b}[SO_4^-]\right\} + [Cu^{II}]\left\{ \dfrac{1 + \dfrac{k_2'}{k_2} K_a[SO_4^-]}{1 + K_a[SO_4^-]} \right\}}$$

$$(21)$$

which is the rate law for perchlorate solutions.

This equation reduces to Equation 4 at sufficiently low values of [SO_4^-]. In pure sulphate solutions, however, the value of $SO_4^=$ can never get significantly lower than a limiting value determined by the second ionization constant of sulphuric acid, and so departures from the perchlorate rate law might be expected even in the most favourable cases where the solutions are strongly acid. Under these conditions the relationship can be substituted;

$$[SO_4^-] = \frac{K_b[HSO_4^-]}{[H^+]} \qquad (22)$$

and HSO_4^- is the dominant anion in the system.

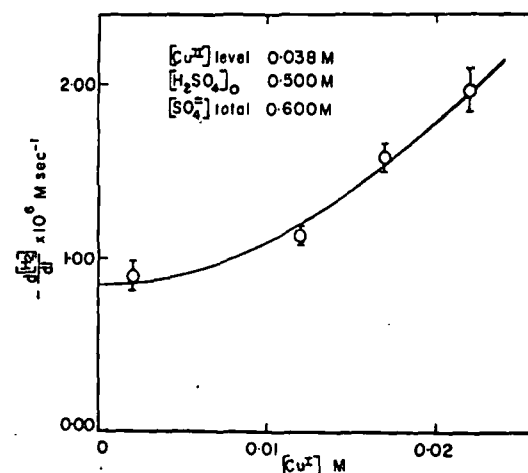Fig. 8. Dependence of reaction rate on [Cu[I]] in sulphate solutions at constant [Cu[II]]. Temperature 160°C, H₂–10 atm.

In the hope of substantiating the form of equation (21) a series of experiments was conducted with sulphate solutions, using the same experimental and analytical procedure as in the previous perchlorate experiment. The results of these experiments lead to two independent effects of the sulphate system:

1. A dependence of the reaction rate on the cuprous state is observed, and the magnitude of this effect is considerably larger than in perchlorate solutions. The cuprous dependence is apparent in Fig. 8 which suggests that this contribution to the reaction rate is second-order in Cu^I.

2. When the cuprous contribution to the reaction rate is deducted, the residual rate is still considerably faster than that calculated from the perchlorate rate law (Equation 4). As predicted, the rate was slowest in the most acidic solutions. The results are presented in Table III.

At higher pH values where $[SO_4^=]$ would be the predominant sulphate species, Equation (21) should reduce to

$$\frac{-d[H_2]}{dt} = k_1'[Cu^{II}][H_2] \tag{23}$$

and it should be possible to obtain a value for k_1' and thus $\frac{k_1'}{k_1}$. From dichromate reduction experiments at 110°C the value of $\frac{k_1'}{k_1}$ was found to be about 6, but the value could be significantly higher at 160°C. Experiments leading to these values have not been completed.

Equation 21 also suggests that values for $\frac{k_{-1}'}{k_{-1}}$, $\frac{k_2'}{k_2}$, and K_a (or K_aK_b) might be obtained by appropriate rate measurements and appropriate calculations with simultaneous equations of this form. Actually it appears unlikely that sufficiently accurate rate data can be obtained by the method used here.

To interpret the rate data completely, the rate law of the cuprous-dependent component must be determined. The complete rate law observed by Dunning and Potter was interpreted as a first-order cuprous-dependent reaction, but these workers used much stronger solutions than those described here, and no direct comparison can be made with the present work. Further experimental work is necessary before the dependence of the Cu^I-dependent rate term on other variables

TABLE III

Rate Measurements Observed in the Sulphate System and Calculated from Equation (4).
160°C, 10 atm H_2

$[Cu^{II}]$ M	$\frac{-d[H_2]}{dt}$ M sec^{-1} Measured	$\frac{-d[H_2]}{dt}$ M sec^{-1} Corrected*	$\frac{-d[H_2]}{dt}$ M sec^{-1} Calculated†	$\frac{\text{Corrected rate}}{\text{Calculated rate}}$
0.030	(a) 0.73 × 10⁻⁶	0.50 × 10⁻⁶	0.32 × 10⁻⁶	1.56
0.040	(a) 1.11	0.87	0.55	1.58
0.035	(a) 1.21	0.68	0.43	1.58
0.045	(a) 1.35	1.11	0.68	1.63
0.050	(a) 1.64	1.40	0.82	1.71
0.020	(b) 2.52	1.46	0.58	2.52
0.025	(b) 4.26	1.86	0.80	2.33
0.025	(b) 2.16	1.89	0.87	2.17
0.030	(b) 4.08	3.02	1.10	2.75

(a) Initial Conditions: $0.50M$ H_2SO_4; $0.10M$ $CuSO_4$ + Na_2SO_4 (or $ZnSO_4$)

Resulting $\frac{[HSO_4^-]}{[H^+]} \simeq 1.5$

(b) Initial Conditions: $0.10M$ H_2SO_4; $0.04 M$ $CuSO_4$ + Na_2SO_4.

Resulting $\frac{[HSO_4^-]}{[H^+]} \simeq 2.3$

* Corrected by deducting Cu^I effect observed in Figure 8, assuming second-order dependence on Cu^I.

† Calculated from Perchlorate Rate Law (Equation (4)) and assuming $[H^+] \simeq 2[H_2SO_4] - \{H_2SO_4 + CuSO_4 + Na_2SO_4\}$.

such as Cu^{++} and H^+ can be elucidated and only then can the kinetics be exploited to indicate possible mechanisms.

Reaction Rates in Other Systems that Complex Cu^{II}

The dichromate reduction rates have been measured in systems containing acetate,[14] propionate, butyrate, glycinate, chloride, and ethylenediamine complex ions of divalent copper.[16] Generally speaking, the dichromate rate measurements yield k_1 values for each system that may be assumed to apply equally well to metal reduction. This was, in a sense, confirmed by earlier work of Halpern and Dakers[13] who reduced cupric acetate solutions, although cuprous oxide rather than metallic copper was the reduction product in that case.

The reduction product may, in fact, be Cu_2O if the pH is appropriate and monovalent copper is not extensively complexed. Support for this is given by a pH-potential diagram for the $Cu-H_2O$ system shown in Fig. 9. This diagram shows that Cu_2O is the favored reduction product for pH's between 5 and 14, at room temperature. At elevated temperatures this diagram undoubtedly shifts somewhat and Cu_2O may form under more acid conditions.
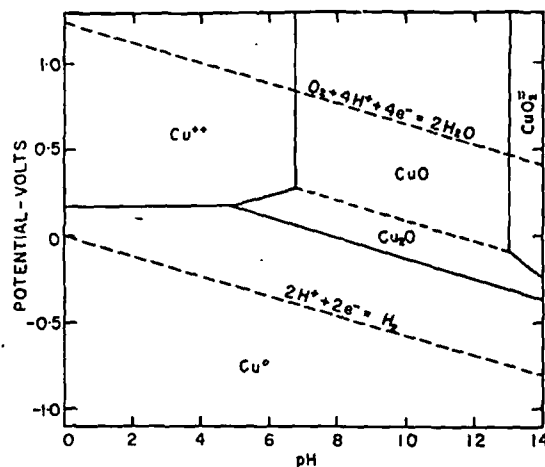

Fig. 9. pH-potential diagram for the system $Cu^{++}-H_2O$ at 25°C. [Taken from: J. Halpern, *J. Metals* 9, 280 (1957), *Trans. A.I.M.E.* 209, 280 (1957).]

A favorite leaching system for copper is ammonia, and industrial studies have been made of the hydrogen reduction of copper in ammonia-ammonium sulphate liquors.[2] These studies started with slurries of basic copper sulphate, and since no data on the amount of dissolved copper present are given, the data cannot be resolved into a simple rate law. Generally speaking, the reactions are much slower than those experienced[18] or predicted above for acid sulphate solutions.

Although it is probable that most of the rate decrease in the ammonia case described above is due to a low dissolved-copper content, it is also possible that a lower primary rate would occur in the first step of reaction, as it does with ethylenediamine and glycine complexes in the dichromate reduction work. Also Cu^I is complexed strongly by ammonia, and this will inhibit the disproportionation reaction until cupric levels are very low and Cu^I is the dominant copper species in solution. Since the reaction rate is dependent on both cupric and cuprous levels,

the rate of reduction beyond the cuprous state in such cases may depend much more on the Cu^I-dependent mechanism than in systems where Cu^I is not complexed.

SUMMARY AND CONCLUSIONS

The most interesting features of the reaction by which copper is displaced from aqueous solutions by hydrogen are the kinetics and mechanisms. Kinetic studies show that the mechanism of copper precipitation and that of reduction of oxidizing substrates in copper-containing solutions are closely related, in that they both involve a homogeneous reaction between H_2 and a Cu^{II} species to yield an intermediate hydride, CuH^+. This mechanism has been proposed previously in the reported literature, which has been reviewed. New data have been presented to show that the mechanism is reasonably consistent for measurements in the perchlorate system when interfering side reactions are taken into account, although a Cu^+-dependent reaction appears to contribute significantly, but not extensively, to the reaction rate. In sulphate solutions a similar rate law applies, but the cuprous-dependent contribution is considerably enhanced over that observed in the perchlorate system. Reactions in aqueous systems containing other complexing agents are discussed, and reaction rates for copper precipitation in these are predicted on the basis of their known properties, neglecting possible Cu^I-dependent contributions. Good rate measurements to confirm the form of the rate laws and determine the rate constants and the form of the Cu^I-dependent reactions remain to be made in these solutions.

Acknowledgement

References

1. F. A. Forward, *Mining Congress Journal*, April, 1957.
2. D. J. I. Evans, S. Romanchuck, and V. N. Mackiw, *C.I.M.M. Bull* 54, 530 (1961).

3. F. A. Forward, *Trans. C.I.M.M.* LIV, 363 (1953).
4. V. N. Mackiw, W. C. Lin, and W. Kunda, *J. Metals* 9, 786 (1957).
5. W. Kunda, J. P. Warner, and V. N. Mackiw, *Trans. C.I.M.M.* LXV, 21 (1962).
6. I. M. Kaneko and M. E. Wadsworth, *J. Phys. Chem.* 60, 457 (1956).
7. A. H. Webster and J. Halpern, *J. Phys. Chem.* 60, 280 (1956).
8. G. J. Korinek and J. Halpern, *J. Phys. Chem.* 60, 285 (1956).
9. R. T. Wimber and M. E. Wadsworth, *Trans. A.I.M.E.* 221, 1141 (1961).
10. V. V. Ipatieff, Jr., and V. G. Tronev, *Compt. rend. acad. sci. U.R.S.S.* 1, 624 (1935).
11. J. Halpern, J. F. Harrod, and P. E. Potter, *Can. J. Chem.* 37, 1446 (1959).
12. V. N. Ipatieff and W. Werchowski, *Ber.* 42, 2078 (1909).
13. J. Halpern and R. G. Dakers, *J. Chem. Phys.* 22, 1272 (1954).
14. E. Peters and J. Halpern, *Can. J. Chem.* 33, 356 (1955).
15. E. Peters and J. Halpern, *J. Phys. Chem.* 59, 793 (1955).
16. E. Peters and J. Halpern, *Can. J. Chem.* 34, 554 (1956).
17. J. Halpern, E. R. Macgregor, and E. Peters, *J. Phys. Chem.* 60, 1455 (1956).
18. E. R. Macgregor and J. Halpern, *Trans. A.I.M.E.* 212, 244 (1958).
19. H. F. McDuffie, E. L. Compere, H. H. Stone, L. F. Woo, and C. H. Secoy, *J. Phys. Chem.* 62, 1030 (1958).
20. W. J. Dunning and P. E. Potter, *Proc. Chem. Soc.* 244 (1960).
21. E. A. von Hahn and E. Peters, *Can. J. Chem.* 39, 162 (1961).
22. W. G. Courtney, *J. Phys. Chem.* 60, 1461 (1956).
23. W. M. Latimer, "Oxidation Potentials," 2d ed. Prentice-Hall, Inc., 1952, p. 185.
24. C. M. Criss, "Thermodynamic Properties of High Temperature Aqueous Solutions," Purdue University, Ph.D. Thesis 1961, University Microfilms, Inc., Ann Arbor, Michigan.

Recovery and Separation of Selenium and Tellurium by Pressure Leaching of Copper Refinery Slime

B. H. MORRISON

Technical Superintendent
Canadian Copper Refiners Limited, Montreal East, Quebec.

INTRODUCTION

Copper smelters treat concentrates of widely varying analyses and it is natural that the slime produced from the electrolytic refining of such anodes should have an equally broad range of composition. This diversity is illustrated in Table I,[1] which lists the approximate limits of concentration of the major elements in slime being treated at various copper refineries.

Hennig and Pawlek,[2] in a recent study of the constitution of copper refinery slime divided its components into three products:

TABLE I

Range of Composition of Slime
from Various Copper Refineries

	Per cent
Copper	3–35
Selenium	0.6–18
Tellurium	0.5–8
Arsenic	0.3–10
Antimony	0.1–16
Bismuth	Trace–1
Lead	0.3–15
Nickel	0.1–45
Iron	0.1–2
Sulphur	2.0–7
Insol.	0.3–16
Silver	6–30
Gold	0.05–1.7

227

Permeability Changes During the Flow of Water Through Westerly Granite at Temperatures of 100°–400°C

R. Summers, K. Winkler, and J. Byerlee

U.S. Geological Survey, Menlo Park, California 94025

Changes in permeability have been studied during the flow of water through granite for periods of time up to 17 days at temperatures of 100°, 200°, 300°, and 400°C with a constant confining pressure of 500 bars, differential stresses of 0–3500 bars, inlet pore pressure of 275 bars, and outlet pressure of 1 bar. In all cases the initial permeability at elevated temperatures was found to be higher by 1–2 orders of magnitude than the permeability at room temperature, perhaps because of thermal cracking. The high initial permeability did not persist with time and in nearly all cases decreased significantly during the first ½ day of water flow. Dissolution of plagioclase and quartz was concentrated near the inlet, where the pore pressure was highest. Precipitation occurred throughout the samples because of oversaturation as the pore pressure dropped, causing significant reduction in permeability. The final permeability after 10 days was less at 300°C than at lower temperatures, and measurable flow stopped in most of the 400°C samples.

INTRODUCTION

Natural geothermal steam is currently being harnessed for energy in several places throughout the world. Unfortunately, these natural steam sources occur only in limited areas. There are, however, many more places where hot, dry rock is accessible. Current proposals for producing energy from these dry geothermal sources suggest that energy can be extracted by drilling into the hot igneous rocks, injecting water to produce a large hydraulic fracture, and circulating water through the fracture [*Smith et al.*, 1975; *Kruger*, 1975]. The fracture would provide a large heat transfer area from which steam or hot water could be drawn off through a recovery well.

A viable plan for circulating water through a fracture system in the hot rock is fundamental to carrying out this geothermal energy extraction plan. It is important to know how permeability in large and small fracture systems will change with time. Measurements of the permeability of intact samples of Westerly granite at room temperature have been made by *Brace et al.* [1968], and changes in permeability due to dilatant cracking in Westerly granite have been investigated by *Zoback and Byerlee* [1975].

M. L. Batzle and G. Simmons (unpublished manuscript, 1975) speculated that in natural hydrothermal systems, fracturing would tend to increase the permeability and deposition of secondary minerals would tend to decrease it, but to date, there are no data in the published literature that would allow us to determine whether the permeability of rock would decrease or increase with time as water circulated through the hot rock.

In this paper we report the results of some experiments designed to study how the permeability of initially intact samples of granite changes with time as water is pumped through the rock at temperatures up to 400°C.

EXPERIMENTAL PROCEDURE

The samples used were Westerly granite cylinders 1.59 cm in diameter and 3.81 cm in length (Figure 1). They were placed under a confining pressure (P_c) of 500 ± 5 bars and subjected to an axial differential stress (σ_D) of 0–3500 ± 15 bars. The inlet pore pressure was 275^{+0}_{-25} bars, and the outlet pore pressure 1 bar. The nominal values given for the experimental temperatures are correct within 5% for the top and bottom

ends of the samples. Temperatures at the centers of the samples are higher than those at the ends by 5°, 7°, 9°, and 13°C for 100°, 200°, 300°, and 400°C, respectively. All samples except one were solid cylinders. The remaining sample (run at 300°C and 0-bar σ_D) had a saw-cut joint along the length of the cylinder. All samples were enclosed in an inner gold sleeve (1.59-mm wall) and sealed in a copper jacket (0.25-mm wall).

The mass flow rate of water into the sample was measured on the basis of the input pumping rate. The mass flow rate (dm/dt) is proportional to the permeability (k), where

$$k = dm/dt \, C_1 \tag{1}$$

and

$$C_1 = \frac{1}{A} \nu \left(\frac{dp}{dx}\right)^{-1} \tag{2}$$

Equation (2) was rearranged to the form

$$C_1 = \frac{L}{A} \left(\int_{P_0}^{P_1} \frac{dp}{dx}\right)^{-1} \tag{3}$$

which allows us to deal with the variable viscosity over the length of the sample. The constant C_1 was calculated by using a Fortran computer program. The kinematic viscosity (ν) of water as a function of temperature and pressure was entered in the program in tabular form from steam tables [*Keenan et al.*, 1969]. The integral in (3) was evaluated by the trapezoidal method by using the inlet and outlet pressures as limits.

In an attempt to keep the calculations simple we assumed uniform permeability throughout the sample. Since we know, however, that the permeability was not uniform, this simplifying assumption introduced a significant error into our estimates. In all experiments the effective pressure varied from 224 bars at the top of the sample to 500 bars at the bottom. This effective pressure gradient was sufficient to cause the permeability at the top of the sample to be about twice that at the bottom [*Brace et al.*, 1968]. In addition, temperature gradients in the samples produced small local variations in permeability. Thus the calculation of permeability at the beginning of each experiment has an uncertainty of about 50%. Since the alteration of minerals during each experiment is not uniform throughout the sample, permeability should become less uniform with time. Because of the remarkable decrease in flow rate observed in all experiments this means that the
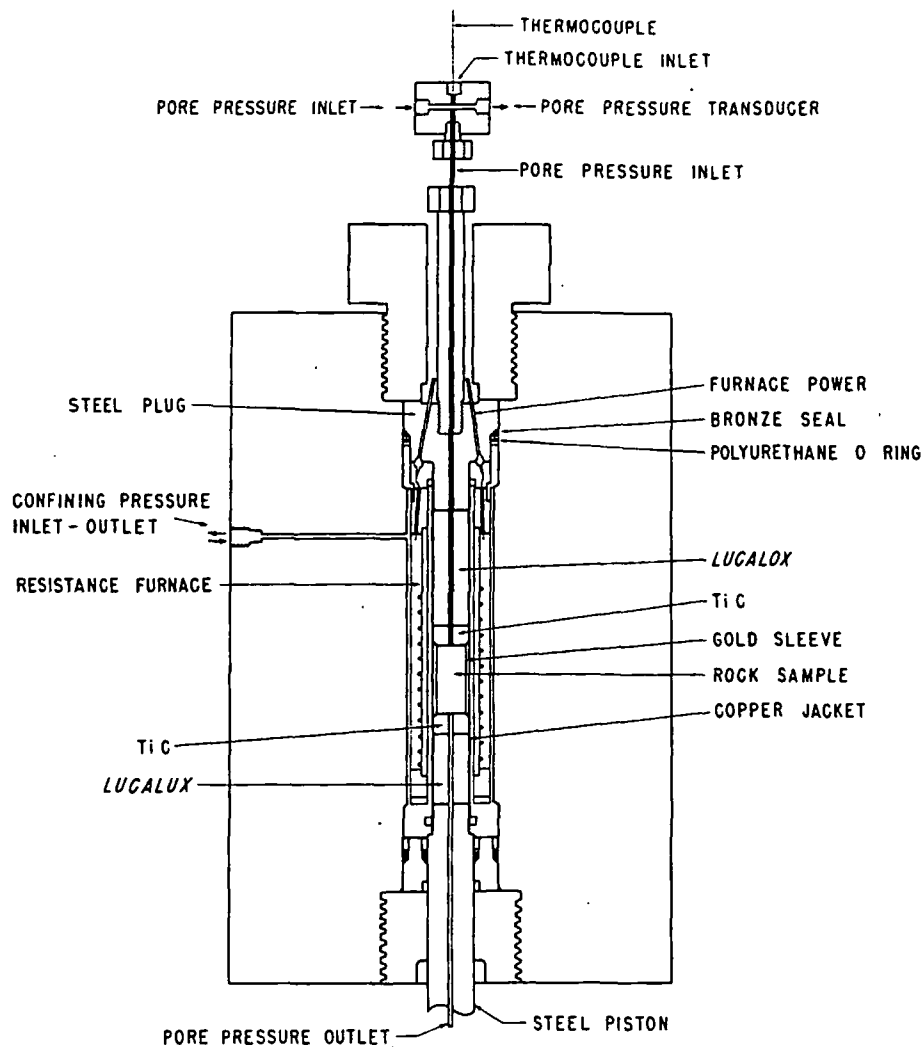
THERMOCOUPLE

THERMOCOUPLE INLET

PORE PRESSURE INLET ——

PORE PRESSURE TRANSDUCER

PORE PRESSURE INLET

STEEL PLUG

FURNACE POWER

BRONZE SEAL

POLYURETHANE O RING

CONFINING PRESSURE INLET - OUTLET

LUCALOX

RESISTANCE FURNACE

Ti C

GOLD SLEEVE

ROCK SAMPLE

COPPER JACKET

Ti C

LUCALUX

PORE PRESSURE OUTLET

STEEL PISTON

Fig. 1. Sample arrangement used in this study.

permeability that we calculated using (1) is exactly an upper limit for the permeability in the blocked regions of the samples. Because of the limited number of parameters that could be measured in these experiments this is the best estimate that could be made of the true local permeability. The outstanding result is not the precise value of the permeability but is rather the fact that permeabilities decrease significantly with time.

EXPERIMENTAL RESULTS

For the six samples run at 100°C (Figure 2), each curve is marked with the value of the differential stress to which the individual sample was subjected. For this set of tests, there was a wide spread in the mass flow rate. Those samples that were run under higher differential stress tended to have higher flow rates during the first day. However, this tendency is not solidly established, since lines for different stress levels cross, and the sample run at a 500-bar differential stress does not fit the trend for higher differential stress to produce a greater flow rate.

The seven tests run at 200°C (Figure 3) exhibited behavior similar to that of the 100°C tests in terms of having high initial flow rates which decreased rapidly during the first ½ day of testing and more slowly thereafter. The applied differential stress did not have a regular effect on the flow rate at 200°C, although for part of the time the tests under higher differential

stress did exhibit lower flow rates than those under lower stress. Two of the samples, one at 0-bar differential stress and one at 500-bar differential stress, showed temporary increases in flow rate. These increases did not persist, and the final values were near those of the other 200°C samples, in which the flow rate had decreased steadily.

The six tests run at 300°C (Figure 4) had initial flow rates that tended to be lower than those of tests run at 100°C and 200°C. All these tests exhibited a rapid decrease in flow rate during the first ½ day. The changes in flow rate with time observed in these samples were by far the most uniform of any of the groups of tests. The test run at 3500-bar differential stress and 300°C deviated from the uniform behavior of the other samples at 300°C. Its initial flow rate was similar but then decreased more slowly than the others until the point at which it failed in compression and the test was stopped. In this one sample the higher flow rate may result from dilatancy.

The results of the flow rate measurements for the six tests at 400°C (Figure 5) were significantly different from the results for the tests run at 100°-300°C. In addition, the behavior of the different samples within this 400°C group was erratic. In five tests, all measurable flow stopped in less than 2 days. Two of these samples had relatively high flow rates which dropped to zero, no indication being given that this was about to occur.

A single sample continued to have a low flow rate until day 11, when the test was stopped.

In order to investigate further the phenomenon of permeability decrease, one test was conducted by using a sample with a sawcut (Figure 6) at 300°C with a hydrostatic confining pressure of 500 bars. This artificial clean joint plane was made parallel to the long axis of the cylinder. The initial flow rate of about 22 mg/s was similar to the highest flow rates observed with the intact samples. For 2½ days the flow rate varied between 7 and 33 mg/s, large increases occurring abruptly and decreases occurring gradually. After 2½ days the flow rate abruptly decreased from 10 mg/s and did not increase again. The final value at the end of the 6-day test was 0.01 mg/s.

ALTERATION WITHIN SAMPLES

The samples were examined for alteration by the use of the optical microscope, scanning electron microscope (SEM), X ray diffraction, and X ray emission spectroscopy. On the inlet face of many samples, feldspar grains were dissolved at points where the water had best access to the surface. Within the samples, plagioclase, orthoclase, and quartz showed evidence of dissolution. Some of the plagioclase was partially altered to sericite, and albite twin structures were blurred or absent over portions of many plagioclase crystals. Deposits of aluminum silicates (identified by X ray spectroscopy) were observed both

on the faces of the saw-cut sample and within a grain boundary crack in an intact sample. In approximately half of the samples, deposits formed on the outlet end in quantity sufficient (up to 0.2 g) to be collected for X ray diffraction. These deposits contained quartz, orthoclase, plagioclase, sericite, cristobalite, and calcite. Several of the 100°C and 200°C tests yielded amorphous deposits, and the deposit from one test run at 400°C was nearly amorphous (two very small peaks). The cristobalite appeared in deposits from several of the 300°C and 400°C tests. Flow rate decrease did not correlate with the amount of material deposited on the outlet end of the sample.

DISCUSSION

Our study has produced data showing that permeability is clearly time and temperature dependent. There appears to be no comparably traceable flow rate stress dependence.

This lack of clear stress dependence agrees with the conclusion of *Sprunt and Nur* [1976] that the rate of porosity decrease is not related to stress on the rock matrix. The extent of time and temperature dependence was unforeseen.

The high initial flow rate of our samples was in marked contrast to the results of work done with Westerly granite at room temperature [*Brace et al.*, 1968; *Zoback and Byerlee*, 1975]. This initial high permeability at elevated temperatures was probably caused by cracks produced in the samples by
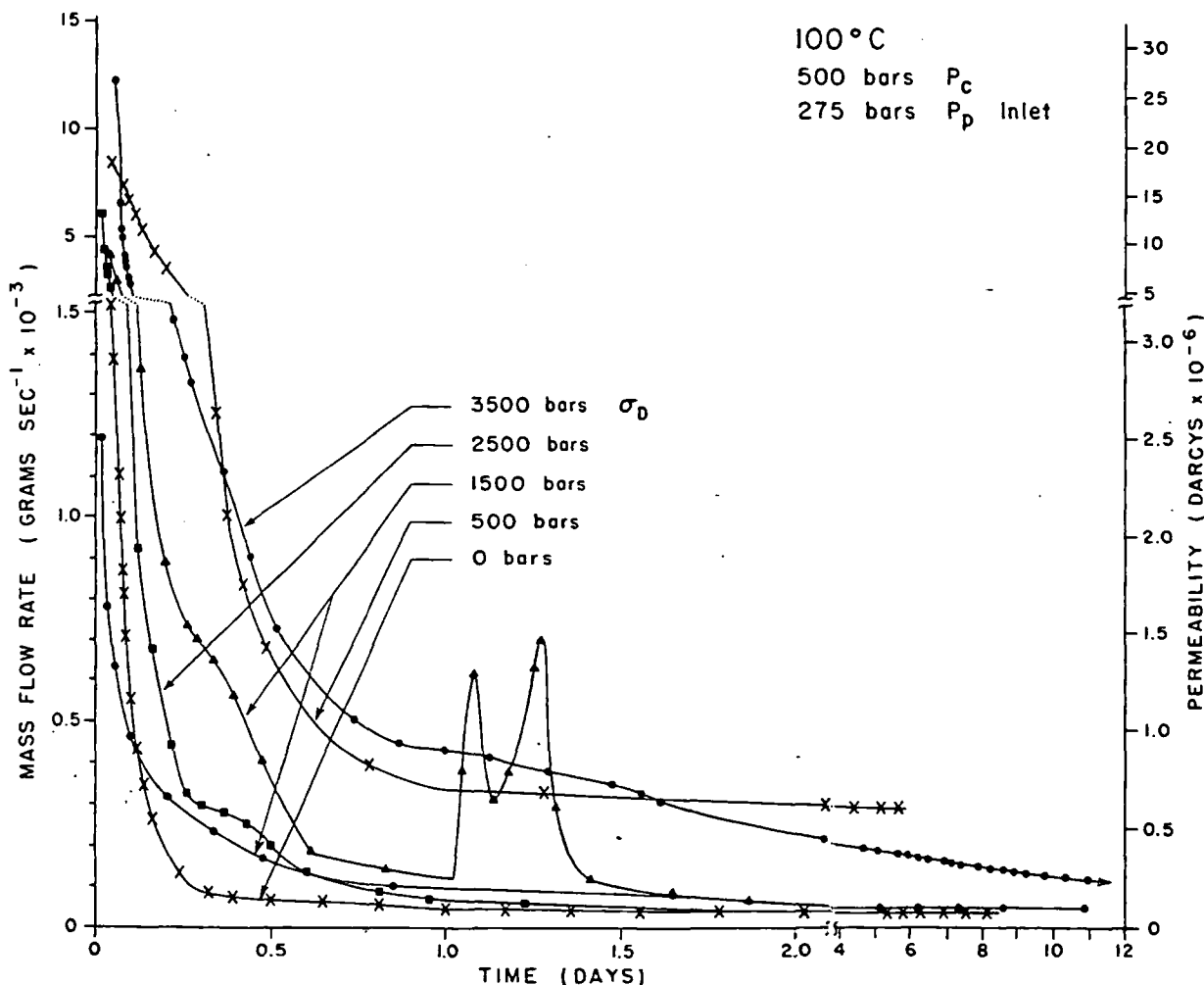

Fig. 2. Flow rates at 100°C plotted as a function of time.
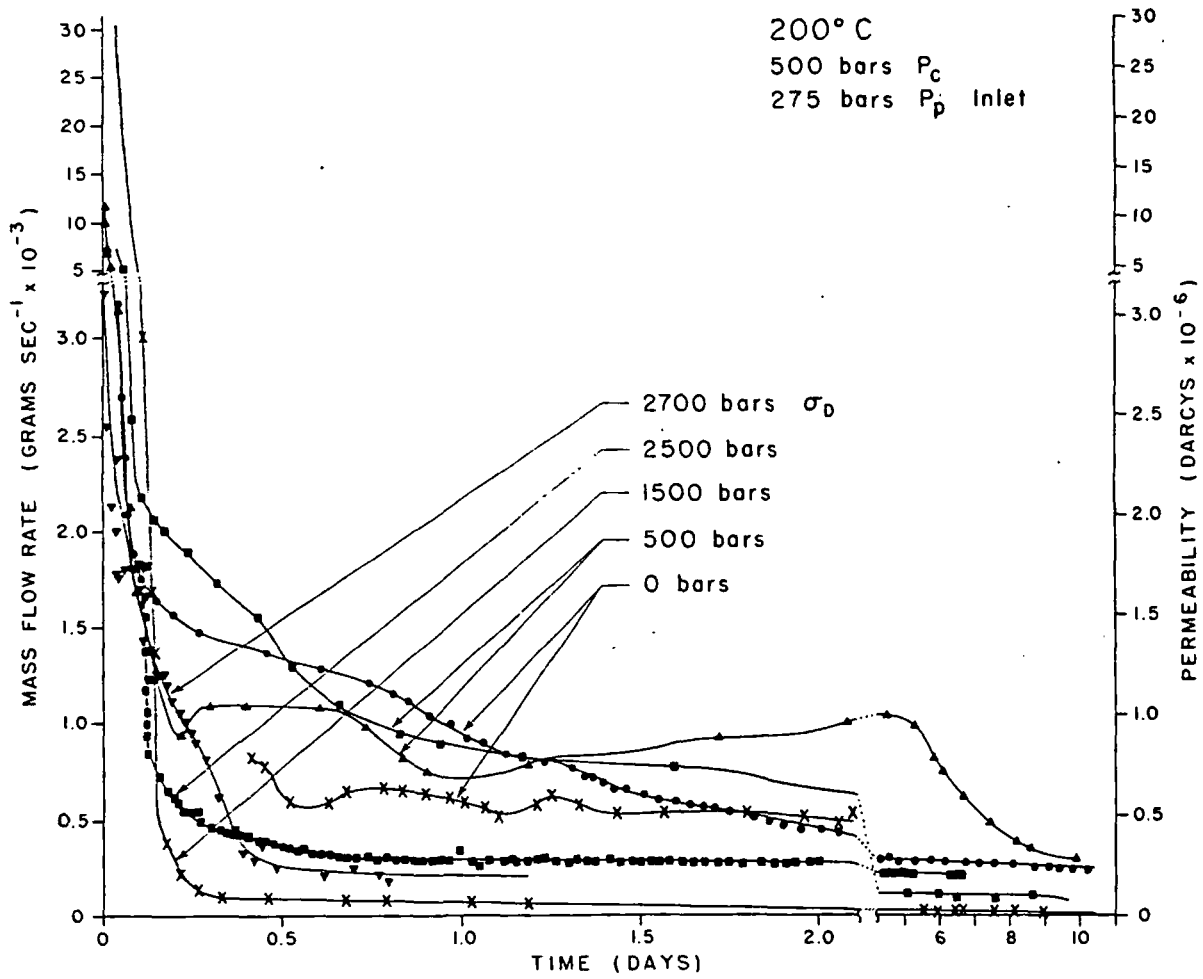
Fig. 3. Flow rates at 200°C plotted as a function of time.

differential thermal expansion of the minerals. This cracking could be detected by monitoring the acoustic emission during heating of the rock samples. A detailed study of this phenomenon was carried out and will be reported on elsewhere.

The dramatic decrease of flow rate with time exhibited by all our tests, without exception, is noteworthy, particularly since the greatest part of the decrease in intact samples occurred quite rapidly.
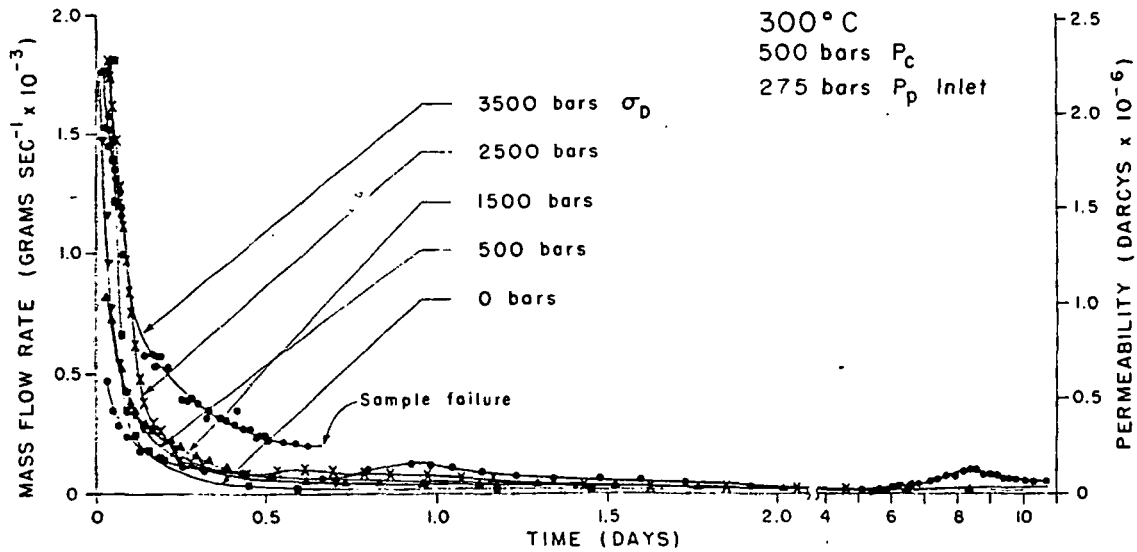

Fig. 4. Flow rates at 300°C plotted as a function of time.
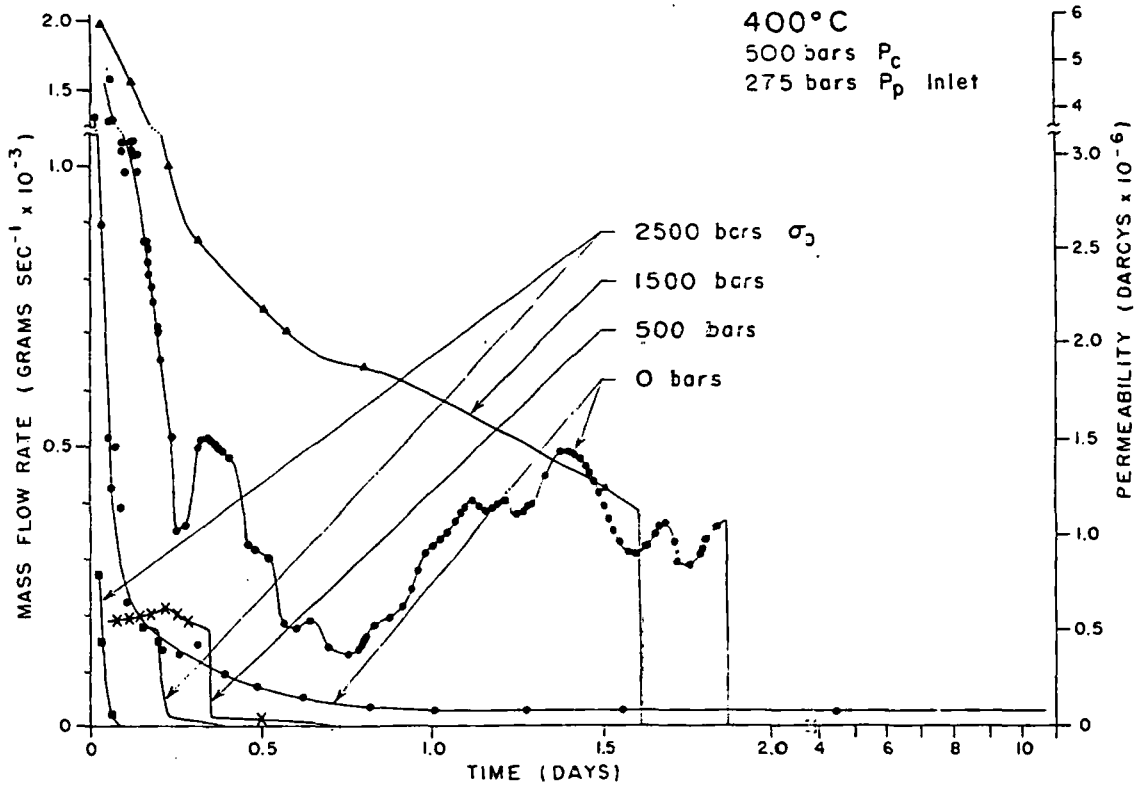
Fig. 5. Flow rates at 400°C plotted as a function of time.

These results may be of particular relevance to the design and operation of artificial geothermal systems. It has been theorized that hydrofracting and then injecting water into a hot batholith will produce a hydrothermal crack system which will remain open and energy productive for an undetermined but economically profitable length of time. However, the extent of mineral alteration and deposition within the crack systems of our samples run at high temperatures indicates that geothermal power developers may want to investigate the nature and extent of mineralogical alteration likely to occur at any chosen site and include it as an important consideration at all stages of planning.
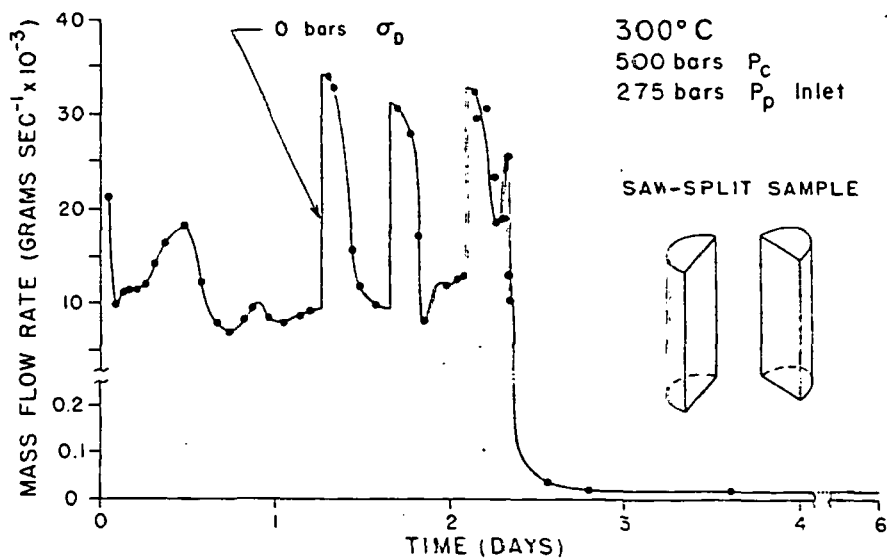

Fig. 6. Flow rate for the saw-cut sample run at 300°C plotted as a function of time.

REFERENCES

Brace, W. F., J. G. Walsh, and W. T. Frangos. Permeability of granite under high pressure, *J. Geophys. Res.*, *73*(6), 2225–2236, 1968.

Keenan, J. H., F. G. Keys, P. G. Hill, and J. G. Moore, *Steam Tables—Thermodynamic Properties of Water Including Vapor, Liquid and Solid Phases*, int. ed., p. 114, John Wiley, New York, 1969.

Kruger, P., Stimulation of geothermal energy resources, *Rep. ERDA-37*, Energy Res. and Develop. Admin., Washington, D. C., 1975.

Smith, M. C., D. W. Brown, and R. A. Pettitt, Los Alamos dry geothermal source demonstration project, *Mini Rev. 75-1*, Los Alamos Sci. Lab., Los Alamos, N. Mex., 1975.

Sprunt, E. S., and A. Nur, Reduction of porosity by pressure solution: Experimental verification, *Geology, 4,* 463–466, 1976.

Todd, T., Effect of cracks on elastic properties of low porosity rocks, Ph.D. thesis, Mass. Inst. of Technol., Cambridge, 1973.

Zoback, M. D., and J. D. Byerlee, The effect of microcrack dilatancy on the permeability of Westerly granite, *J. Geophys. Res., 80,* 752–755, 1975.

PRECIPITATION OF COPPER FROM DILUTE SOLUTIONS:

Where Engineering Study Can Make Important Savings

Recovery of copper from mine waters and dump leaching solutions was long considered as a bonus to the miner and received little engineering study. In recent years, the process of leaching submarginal rock and old workings has been systematized and enlarged. At the Annual Meeting in February, a full session of MBD-EMD was devoted to one phase of the system, the precipitation of copper with iron. The papers from this session are digested herein.

ME DIGEST

UNIVERSITY OF UTAH RESEARCH INSTITUTE EARTH SCIENCE LAB.

The economic recovery of metals from dilute solutions has been the dream of mining engineers for many years. This subject is now receiving greater attention, particularly for copper, in view of the heightened demand for the metal and the tightening supply situation. A Copper Precipitation session, sponsored jointly by EMD Hydrometallurgy Committee and MBD, which took place during the Annual Meeting in March, heard papers on recent research and plant practice.

Although the bulk of research in hydrometallurgy has been carried out in countries other than the United States[1], producers in this country are making important contributions to the heap or dump leaching system. They realize that the processes are essentially simple to install and give high recovery rates at reasonable cost. Jacobi estimated in 1963[2] that the copper mining industry obtained a gross return from scavenging operations —on a worldwide basis—on the order of $20 million annually, subject to the usual deductions for refining and realization charges, overheads, taxes, etc.

Agers, et al.[3] have discussed a liquid ion exchange process for dump liquors involving the use of a reagent. Such a process has shown good results, particularly with a more refined reagent which is effective over a wide pH range. Pressure and high temperature leaching are also being investigated, although in the case of the high temperature techniques the problem in dealing with dilute solutions in large quantities is mainly economic.

Hydrometallurgical practices, which find their origins in 16th-century Germany, are making rapid strides, pushed on by the new technology and the metals requirements of the space age. The session under discussion covered mainly copper precipitation, but it is clear that these practices will be increasingly applied to the recovery of a wide range of metals.

CEMENT COPPER

At the Yerington mine, Weed Heights, Nev., The Anaconda Co. produces each month about 2000 tons of copper as cement copper. **Howard W. Jacky**, Plant Superintendent, who described plant practices and certain experimental procedures, said that the copper is precipitated from copper sulfate solutions made by both tank leaching and dump leaching oxide ore. Since the product is shipped more than 800 miles to the Anaconda, Mont., smelter, a high grade, low moisture precipitate is desirable.

The tank leaching plant treats about 86,000 tons of .59% oxide ore per week. The ore is principally chrysocolla mineralized, and it is leached by a dilute sulfuric acid solution. The mineral in the dump is also primarily chrysocolla and the dump is extremely low in sulfide copper minerals and pyrite. This means that an outside source of sulfuric acid is required since very little solvent is generated in the dump. The balance of the mine's production, some 49,000 tons per week, is handled in the conventional manner of crushing, grinding and concentration by flotation.

The author states that the ideal product is a coarse, granular precipitate which can be obtained by close control over solution purity, strength, flow-rate and distribution. Examination of a fresh, high-grade cement copper nodule has established that it has a sponge-like appearance with a high percentage of open voids. The surface is clean and free of deposited salts and oxidized iron. Color is a uniformly bright copper.

Contamination control, primarily achieved by regulating solvent temperature, acidity and contact period is easier in vat leaching than on the dump. Little increased copper leaching is achieved when solution temperature ascends over 85°F but greater contamination and higher acid consumption result in the 90° to 100° range. During hot weather, solution is circulated over a cooling tower. Above 5 lb of acid makeup per lb of copper leached, contamination by unwanted salts mounts without compensating gains in copper. In the precipitation section, acidity is also controlled to about 4 to 5 gpl acid. Extending contact period of leaching also results in a higher contaminant to copper ratio.

As only minor amounts of sulfide copper ore are present in the Yerington ore to reduce ferric iron during the leach, a high ferric:ferrous iron ratio (5.0:7.2) is produced. The ferric iron is reduced to ferrous iron in the launders when it reacts with the precipitant iron, resulting in increased iron consumption.

The iron precipitant—reclaimed tin cans and scrap tin plate are used at Yerington—must be controlled for type, gage, uniformity and cleanliness. A good source of iron is, therefore, a necessity for the production of high-grade cement copper, reports the author. The ideal charge is iron that is shredded and crumpled to the point where it allows good density in the bedding, without stopping solution flow, creating dead areas or forcing channeling. The metal should be of a configuration that makes it structurally strong until almost completely consumed and uniform gage so that it consumes evenly, leaving a minimum of unused iron, while presenting maximum surface area for the promotion of solution reaction speed. He notes that the highest grade cement copper, assaying well above 90%, was made using war-surplus 50-caliber machine gun clips.

A major problem with stockpiled iron is that it deteriorates through oxidation. Not only is there an iron loss, but precipitate grade declined as much as 4% when the precipitant was changed from fresh iron to iron that had been stockpiled for four years.

Flowsheet of the precipitation plant (Fig. 1) shows six double sections for tank leach liquor precipitation and about two double sections for dump leach liquor precipitation. The remainder of the sections are used for settling basins, scavenging unused iron and stripping solution.

Jacky lists these conditions for the production of high-grade (83% average), low moisture (approximately 15%) cement copper at Yerington: A controlled leach circuit for the production of copper sulfate solution having a low-contaminant-salt: copper ratio; a production solution controlled through the iron launders by using correct acidity, solution strength, flow rate and distribution and a clean, uniform, pure iron precipitant.
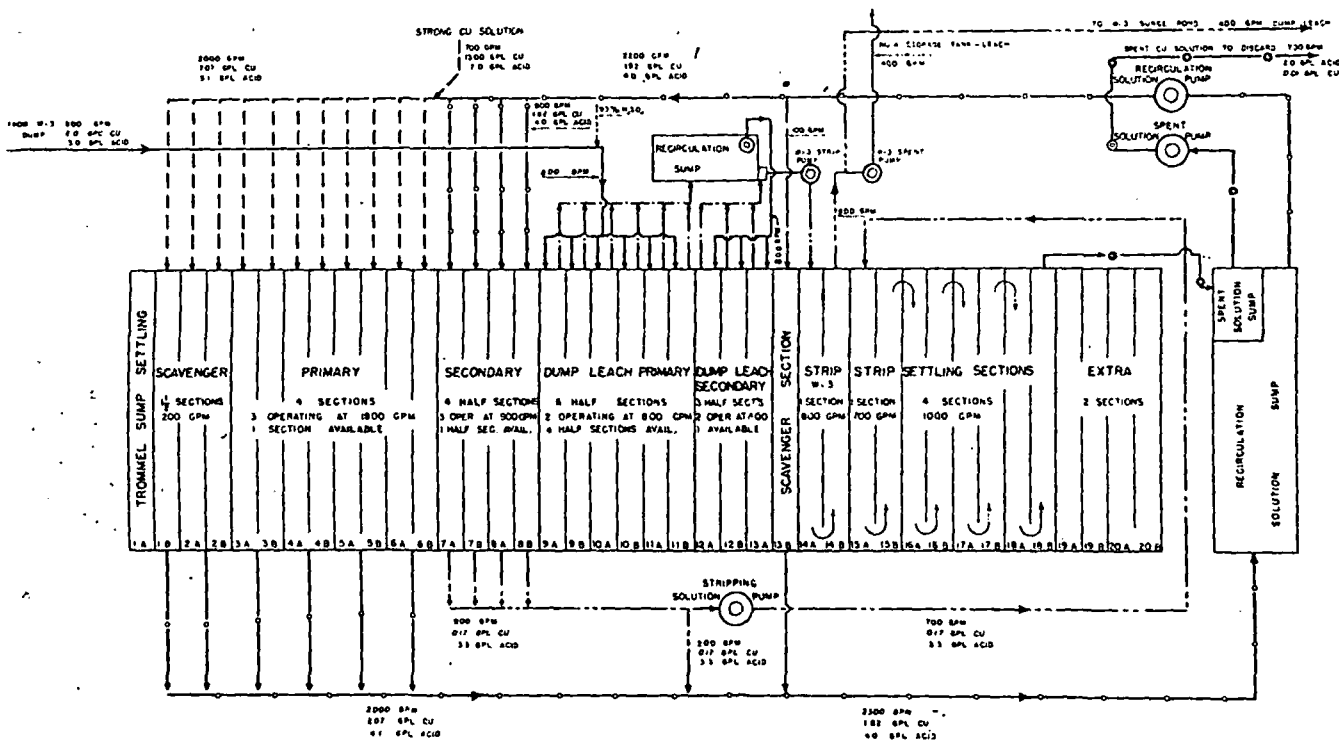
Fig. 1—Flowsheet for Anaconda's cementation plant at Yerington, Nev.

TIN CAN CHARGE AT BUTTE

There is a long history of precipitation of copper from mine waters at Butte but in 1963 dump leaching was added. James K. Ballard, Leach and Precipitation Superintendent, described the mechanized and instrumented system for making cement copper. Considerable experimentation has been undertaken with precipitants.

The present Butte copper precipitation plant became fully operational in November 1949. It uses tin cans as precipitant and is manned by a nine-man crew, total for three shifts. In December 1963, large scale dump leaching was begun using the mine water as leach liquor.

Mine waters of a complex composition are pumped from underground at a rate of 30,000 tpd (5000gpm). They contain: 0.16 gpl Cu, 0.21 gpl ferrous iron, and 0.10 gpl ferric iron at pH level of 2.8. A considerable amount (0.17%) of solids from sand fill is also carried in suspension in the mine waters.

All Butte mine waters are pumped to surface at the High Ore central pumping station. There, a flocculent is added to them and they are flumed to settling ponds. At the flume discharge, sulfuric acid is added in a proportion that will maintain a pH level of 2.1. The acid addition is done automatically.

A pH probe and meter measures the pH level of the water and sends a proportional millivolt signal to a milliamp converter. The converter transmits the signal (current) to a control station at the precipitation plant. There, it is fed into a recorder which continuously records the actual pH. A controller also receives the signal and automatically compares it to the desired pH level. The difference is converted into a proportional signal which actuates a motorized acid control valve.

The solids in suspension in the water are settled from 0.17% (at pond inlet) to 0.0046% (at pond outlet). Water leaving the settling pond is distributed to leach dumps via pipelines.

Off-solutions from the dumps are gathered in a collection basin where they can flow through pipelines to the precipitation plant. Copper recovery at the plant averages 97.7%.

The entire system, from High Ore to the precipitation plant tails, uses gravity flow. All pipeline flows are accurately measured. An orifice in each main pipeline allows a differential pressure cell to measure the pressure across the orifice. The cells are calibrated to be proportional to the square of water flow. The output of the cells is relayed to the control station at the precipitation plant through a signal cable. A square root integrator, upon reception of the signal, totalizes the water volume. A recorder also receives the signal and indicates the flow rate.

A certain amount of soluble impurity salts, iron, calcium, alumina and magnesium exist in pregnant head solutions. As the solution passes through the plant, pH rises due to consumption of excess iron by acid. As the pH rises, the salts hydrolyze and precipitate to become relatively insoluble. Hydrolyzed salts, metallic iron, and cement copper are all flushed into drop tanks by a hydraulic slusher.

According to Ballard, tin cans are efficient both from the standpoint of precipitation and ease of handling. A combination of scrap iron and cans was tried in various sections and individual launders, but cans outperformed such charges as rails and miscellaneous scrap by a considerable margin.

Experiments were carried out with tin plate scrap with indifferent success. Exclusive use of tin plate scrap in any given launder resulted in compaction and prevented solution penetration. Particular difficulty was encountered in flushing cement copper from the lower layers of scrap. Compaction was prevented, it was found, when cans were interspersed throughout the tin plate scrap at a ratio of 10:1.

Sponge iron balls, ¼-in. size, were field-tested at the precipitation plant in a small separate launder set up for test purposes. They were first tested in a normal overflow system, which duplicated plant operation, with unsatisfactory results. No improvement was shown, the author reports, in two other systems which forced pregnant solution through the bedded pellets. In all cases cement copper coated in a thin layer
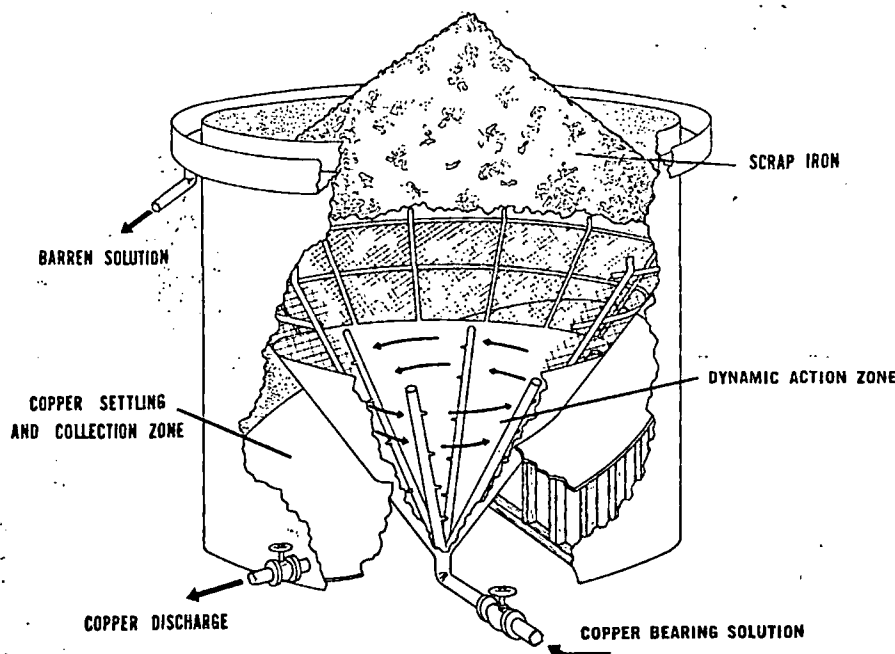
Fig. 2—Diagram of Kennecott's cone-type copper precipitators now being installed at Bingham Canyon.

on the periphery of the pellet and all further precipitation ceased. Penetration of cement copper was very shallow, and it was difficult to flush it free.

Steel lathe cuttings are easily handled, but they are coated with oil which inhibits precipitation. Powdered iron, on the other hand, because of the nature and velocity of solution flow, floated through the launders.

Used baling wire was also tested under operating conditions. Cement copper coated readily on the wire, but exchange of iron for copper was incomplete and the remaining wire disintegrated into short lengths which were flushed down the launder.

Iron pellets were tried in an inverted cone which was force-fed with pregnant solution from below. This system required constant agitation to avoid blinding the entire bed. The tests were performed on a laboratory scale. Results were inconclusive and the method has not been pursued further.

Ballard's conclusion is that the tin can is the best precipitation agent for the Butte operation. Daily consumption of cans is 50 tons. Part of the high can consumption is due to the reduction of ferric iron in solution by metallic iron. Although ½ lb of metallic iron is required to reduce 1 lb of ferric iron, at Butte this is still the most economical means.

KENNECOTT DEVELOPS CONE PRECIPITATORS

Details of Kennecott Copper's cone-type precipitators were described by **H. R. Spedden, E. E. Malouf** and **J. D. Prater,** and published in April's ᴹᴱ.

The prototype precipitation cone used in Kennecott's experimental work consists of a 14-ft diam tank, 24 ft tall, into which is mounted an inverted cone 10 ft high and 10 ft in diameter. The outer 14-ft diam tank contains a 45° sloped false-bottom floor extending from one side of the tank to a bottom side discharge at the opposite side (see Fig. 2). The annular space between the inner cone and the tank is covered by a heavy gage stainless steel screen mounted as a continuation of the cone and anchored to the cone and tank. The cone supports a pressure manifold that consists of six vertical legs with each leg containing a series of nozzles directed inward from the tangent to the cone and upward from the angle of the legs of the manifold. The nozzles are arranged in such a manner as to create a vortex when the copper-

bearing solutions, derived from dump leaching liquors, are pumped through the manifold into the cone. The inner cone and the area of the tank above the stainless steel screens are filled with shredded detinned iron scrap, such as is commonly used in the precipitation of copper.

The pumping of the copper-bearing solutions through the manifold with the nozzles injecting the solutions into the mass of iron has the effect of not only rapidly precipitating copper, but also removing the metallic copper from the iron surface, thereby exposing clean, fresh iron.

The precipitation cone is a continuously operated unit that is self-cleaning, eliminating the need for fire hoses to wash the copper precipitates from the precipitator. The pressure and velocity of the solutions in the lower conical section tend to move the copper precipitates in the same manner as an elutriation column, upward and out of the cone into the reduced velocity zone created by the larger diameter of the holding tank. The copper precipitates settle down through the steel screen and accumulate on the sloped false bottom of the tank. The copper can then be discharged intermittently with the use of a pneumatically operated valve or bled continuously through a small diameter pipe into a thickener or holding basin.

The precipitates so produced are of substantially higher grade than the conventional cement copper produced in a launder-type plant. They typically will analyze 90-95% copper, 0.1-0.2% iron, 0.1-0.2% silica, and 0.1-0.2% alumina, with the balance of the impurity being primarily oxygen.

In addition to the self-cleaning of copper precipitates, the compact cone precipitators lend themselves to automatic control and to lower consumption than is possible with the older launder methods.

Fig. 3—Model of the precipitation plant being built at Bingham Canyon. It will contain 26 cone units.

SOCIETY OF
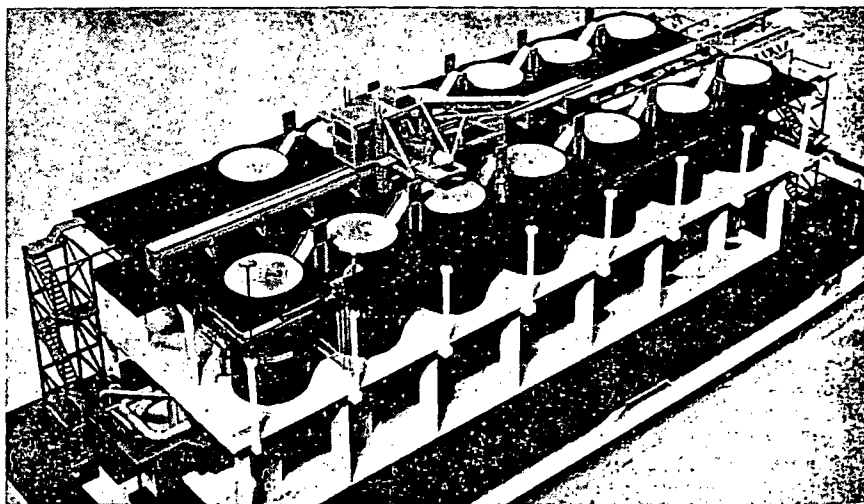
Spedden pointed out that during seven weeks of continuous operation of the experimental cone, copper recovery averaged 89.7% with inclusion of data for periods in which wide fluctuations in the addition of shredded iron was experienced. Sustained periods during optimum operating conditions resulted in copper recoveries exceeding 95% in the single cone.

As a result of this successful experimental work, Kennecott is now constructing a cone precipitator plant (Fig. 3) at Bingham Canyon which will utilize shredded scrap iron. In addition, the company's Chino Mines Division has recently expanded its precipitation plant in New Mexico, and other units are being installed or developed in other western properties of Kennecott.

PARTICULATE IRON AS PRECIPITANT

Spedden[4] has stated that Kennecott's cone-shaped precipitator gives greater operating efficiencies than conventional launder systems for copper precipitation, having the major advantages of automatic control, low iron consumption, and self-cleaning of precipitates. In his paper, A. E. Back, Assistant Research Director, Western Mining Divisions Research Center, Kennecott Copper Corp., writes that his research on copper extraction from dilute solutions centered on the use of particulate (sponge) iron, as distinct from powdered iron used in powder metallurgy. When added to a launder, particulate iron gave incomplete precipitation and inefficient utilization of the iron, but with a prototype cone-shaped precipitator (Fig. 4) recoveries as high as 99% were common.

In a cone precipitation plant, says the author, the copper precipitates are discharged automatically into a filtration system, while in a launder

Fig. 4—Prototype cone precipitator used by A. E. Back in his experiments.


plant the precipitates are washed manually from the launders. Superior iron efficiency resulted in savings of 0.5 to 1.0 lb of iron per lb of copper. Essentially all of the soluble copper was precipitated from the solutions so that a circulating load of dilute copper solution to a leaching system was eliminated.

During the investigation, fourteen different samples of particulate iron from various companies and individuals were evaluated as precipitants. Analyses are shown in the following table.

TABLE I: Typical Analysis of Particulate Iron Samples

Analysis percent		Reduc-tion, percent	Calculated Grade of Copper Precipitates with 0.9 Iron Factor, percent
Fe (Metal)	Fe (Total)		
97.6	99.2	98.4	97.8
96.0	97.1	98.9	96.4
93.8	94.4	99.4	94.4
93.8	96.0	97.7	94.4
93.0	98.0	94.9	93.7
92.0	94.4	97.5	92.8
86.8	90.7	95.7	88.0
86.6	93.0	93.1	87.8
83.6	97.4	85.8	86.6
79.4	87.5	90.6	81.0
65.4	83.4	78.4	67.7
55.2	71.6	77.1	57.8
48.8	64.2	76.0	51.4

The prototype cone now in operation at the Utah Division copper precipitation plant (Fig. 4) is equipped with a variable speed feeder so that the precipitant feed rate can be varied to meet the requirements of the process. The facility is automated so that the progress of the consumption of the available iron can be followed by the decrease in the evolution of hydrogen from the reaction:

$$H_2SO_4 + Fe \ (metal) \rightarrow FeSO_4 + H_2O$$
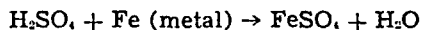
As the hydrogen evolution decreases and comes to a predetermined low value, a system of valves becomes operative which shuts off the incoming solution and opens a discharge valve for approximately 30 sec to remove the precipitate from the lower portion of the cone.

Channeling the hydrogen, or reaction gases, toward the center of the cone into a central exhaust system is essential because particles of copper adhere to the hydrogen bubbles, and, if they are near the overflow of the cone, the particulate copper is transported into the tailings. Thus it is necessary to divert the gas towards the center and allow the bubbles to burst and release the particulate copper to settle back into the bed. It is also necessary to discharge the bed periodically to prevent attrition of the particulate copper.

The author states that operation of the precipitation cone has demonstrated that the decrease in the rate of hydrogen evolution is a sensitive indirect measure of the completeness of the precipitation reaction and can be used for the process control.

A particular advantage of the cone precipitation plant over the launder type is the saving in space. Such a plant, capable of treating 10 million gal of solution per day, would require an area of 10,000 sq ft, whereas a launder plant similar to the one at Bingham Canyon, requires an area approximately 10 times as great.

Operating parameters and engineering data are now being developed, Back reports, for the ultimate installation of a cone precipitation plant utilizing particulate iron as the precipitant to recover some 400,000 lb of copper per day at the Utah Copper Division, as soon as an economic source of particulate iron can be found. Research also is being carried out with copper reverberatory slag as the precipitant which, if successful, would solve the supply problem.

A KINETIC STUDY

The kinetics of copper precipitation on iron of varying purities were observed in experiments carried out by R. M. Nadkarni, C. E. Jelden, K. C. Bowles, H. E. Flanders and M. E. Wadsworth of the Department of Metallurgical Engineering, University of Utah Their paper summarized neatly the state of the art but noted that little had been published on reaction kinetics. Previously published papers, the authors said, differed sharply on whether the rate constant (of the cementation reaction) was a diffusional process at low stirring speeds and a chemical process at higher stirring speeds, or whether the reaction was controlled solely by diffusion, regardless of stirring speed.

The mechanism by which the over-all reaction at a solid-liquid interface can occur is generally considered to go by the following steps: 1) Diffusion of reactants to the surface; 2) adsorption of reactants on the surface; 3) chemical reaction at the surface; 4) desorption of products from the surface; and 5) diffusion of products away from the surface. Any of these steps, say the authors, may be rate controlling.

Experiments were conducted in a three-necked distillation flask of 2000-ml capacity acting as the reaction vessel. A pipet of 10-ml capacity was introduced through one of the side necks, a sample of sheet iron, mounted in a rigid sample holder, through the other. A stirrer was placed in the middle, always at the same depth. The whole assembly was immersed in a constant temperature bath (Fig. 5). Copper was determined by the iodometric method[5] by analyzing 10-ml aliquots of reagent grade cupric sulfate which was used to make up a stock solution containing 10 gm of copper per liter and diluted to various concentrations. Iron was determined by reducing it to the ferrous state with test lead followed by a dichromate titration.[6]
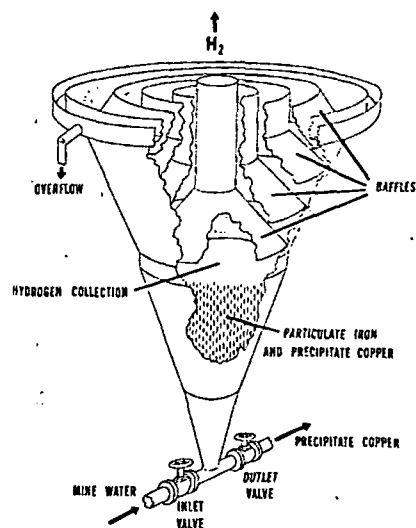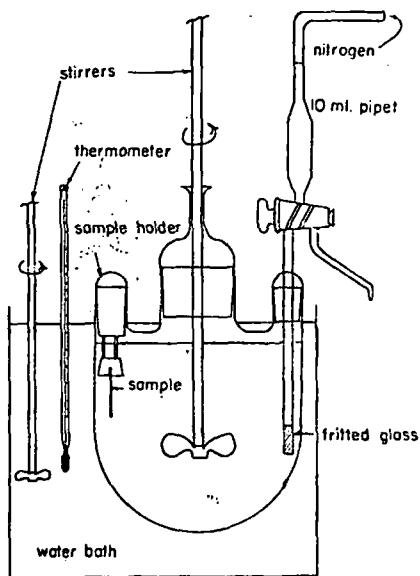
Fig. 5—*Distillation flask and assembly.*

Fig. 6 is a plot of

$$\ln \frac{(Cu^{++})}{(Cu^{++}) \text{ initial}}$$

vs time for different stirring speeds. In this series the precipitated copper deposited on the iron in various degrees of sponginess without peeling off, up to 900 rpm. Around 900 rpm the layers of deposited copper peeled off as bright copper strips with a minimum amount of copper powder being formed. At higher speeds the copper peeled off as a coarse powder, becoming finer at higher and higher stirring speeds. However, even at the higher speeds the solution turbidity was not strong enough to keep the surface of the iron sheet completely free from deposited copper. Instead, precipitated copper clung to the surface as a few scattered islands that peeled off in patches.

The data in Fig. 3 follow the inte-

grated form of the following first-order rate equation:

$$\frac{d}{dt} [Cu^{++}] = - [Cu^{++}] k_o A$$

where

$t =$ time in min
$[Cu^{++}] =$ concentration of copper ions in gpm
$A =$ area in sq. in.
$k_o =$ rate constant $= min^{-1} in.^{-3}$

In the case of high purity iron, the precipitated copper adhered less strongly, and at higher stirring speeds the surface of the pure iron was completely free of the islands described above. In some cases the reaction seemed to follow zero-order kinetics; when the metallic copper deposits adhered to the surface, first-order kinetics were observed.

Tests were carried out with various mesh sizes of cast iron and it was concluded that precipitated copper is more adherent to the iron surface as the impurity content of the iron increases. Large particles of cast iron, high in impurity content, produced adherent copper capable of essentially blocking the cementation reaction.

It was concluded that the rate of precipitation of copper by iron increases with the speed of stirring of the solution and reaches a steady value at high stirring speeds. The authors further concluded that the amount of iron consumed in excess of the stoichiometric amount required for cementation increased with increasing velocity of stirring and with increasing temperature, and that the rate of precipitation of copper was proportional to the area of the reaction interface. It was found that the pH level has a minor effect upon the kinetics of cementation, although iron consumption increased at lower pH.
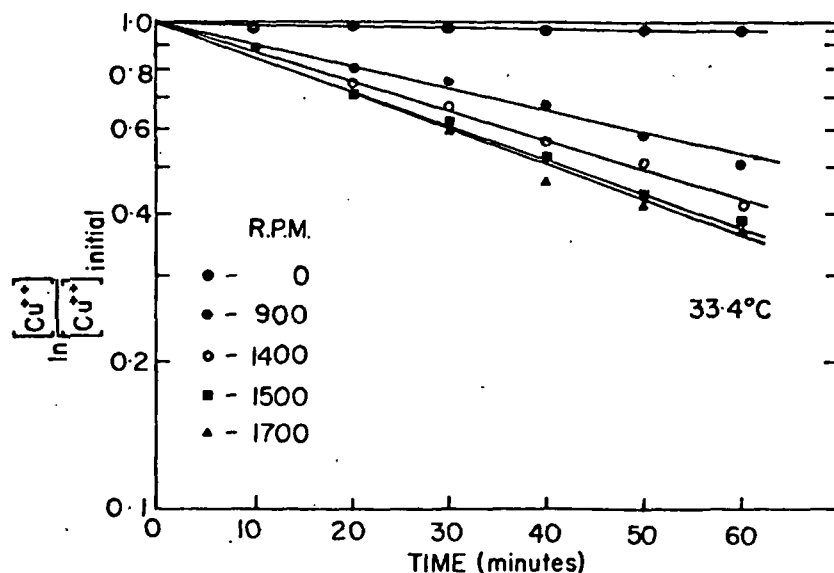
In the final paper of the session, E. A. von Hahn and T. R. Ingraham, both from the Extraction Metallurgy Research Section of the Canadian Department of Mines and Technical Surveys, also reported on the kinetics of cementation. Noting that cementation or displacement reactions occur between aqueous solutions of metal salts and immersed metals according to the general equation:

$$M_1^{n+} + M_2 = M_1 + n/m \, M_2^{n+}$$
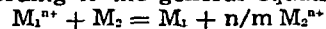
where M_1 is electrochemically the more noble metal, the authors studied the kinetics of the early stages of cementation to obtain an understanding of the reaction mechanism under conditions in which the deposit was sufficiently thin that its inhibiting effect could be disregarded. To achieve this, very dilute solution in M_1^{n+} were used.

Of the many possible cementation reaction systems, the authors used the palladous perchlorate-copper system for their investigation because it was believed to involve simple ion-for-ion exchange. In addition, there are no interfering side reactions, such as the reduction of hydrogen ions, and anion effects are usually absent in perchlorate solutions.

Employing specially prepared electropolished copper cylinders rotated in experimental aqueous perchloric acid solutions having Pd^{II} concentrations from 0.02 to 0.1 mM, it was found that in 0.1M $HClO_4$ solutions, the cemented palladium is dense, adherent, and shiny. The rate data indicated that there are two stages in the deposition. In the initial stage, the rate of cementation is first order with respect to the Pd^{II} concentration. The second stage is much slower. The first stage was shown to be consistent with rate control by the diffusion of Pd^{II} ions to the copper surface, and/or chemical reaction at the surface, and the second stage as consistent with rate control by the diffusion of copper ions from the copper surface through the deposition of cemented palladium from the solution.

In 0.001M $HClO_4$ solutions, only the first stage is evident, and the rate of cementation more rapid than at higher acidities. The deposited material in this case is porous and loose. All of the cemented deposits, according to the authors, were palladium-copper alloys rather than pure palladium. ▨Ξ

References

[1] M. E. Wadsworth and Franklin T. Davis: Foreword. *Unit Process in Hydrometallurgy.* Gordon and Breach, New York, 1964.
[2] J. S. Jacobi: The Recovery of Copper from Dilute Process Streams. *Unit Process in Hydrometallurgy.* Gordon and Breach, New York, 1964.
[3] D. W. Agers, J. E. House, R. R. Swanson and J. L. Drobnick: A New Reagent for Liquid Ion Exchange Recovery of Copper. MINING ENGINEERING, December 1965.
[4] H. R. Spedden: Cone-Type Precipitators for Improved Copper Recovery. MINING ENGINEERING, April 1966.
[5] W. W. Scott: *Standard Methods of Chemical Analysis.* D. Van Nostrand Co., Inc., 1939, p. 371.
[6] W. W. Scott: *ibid.*, p. 471.

Fig. 6—*First order kinetics for the precipitation of copper on 1020 steel at various speeds of revolutions.*

SOCIETY OF

1976 т.17 N6

. SUBJ
MNG
PCH

PRECIPITATION OF COBALT (III) HYDROXIDE FROM CADMIUM SOLUTIONS

UDC 669.253.14

V. I. Bulakhova and E. Ya. Ben'yash

Use of ozone to precipitate cobalt (III) hydroxide makes it possible to implement the process without introducing extraneous ions into the solution; however, the hydroxide produced is finely-dispersed and is not readily filtered.

The structure of a precipitate depends upon the conditions of precipitation. The The degree of supersaturation of the solutions from which the precipitate crystallizes has a decisive effect upon the average size of the crystals.

It became necessary, in connection with developing the technology for cobalt withdrawal by way of the rich cadmium solution in cadmium production to study the conditions of cobalt (III) hydroxide precipitation from these solutions.

The following conditions were set up, to reduce the degree of supersaturation in solid phase formation:

- a reduction in the solution pH, leading to a reduction in the active concentration of hydroxyl ions;

- seeding, reducing the degree of supersaturation by accelerating the formation of the solid phase;

- feeding the initial solution into the suspension obtained by purifying the previous batches, withdrawing a part of the suspension from the reactor (after treatment with ozone) equal to the volume of initial solution to be added to the reactor (the "accumulation method").

Diagram of laboratory ozonizer:
1 - LOV-16 laboratory air drier; 2 - air-flow meter; 3 - LGO-15 laboratory ozone generator; 4 - electric power supply unit; 5 - discharge tube with electric heating to break down ozone; 6 - rheometer; 7 - reactor-disperser; 8 - electric motor; 9 - absorbers for unreacted ozone; 10 - pulp-sampling vessel; 11 - ozone absorbers for determining its concentration; 12 - aspirator; 13 - measuring vessel.

A diagram of the installation used for the studies is shown above. The ozone concentration in the air coming in for ozonizing was 28-30 mg/dm³. The rate of ozonized air feed to the reactor-disperser was kept constant in all the experiments, at 19 dm³/hr. Caustic soda solution was added to neutralize the acid evolving during oxidation. Oxidation was conducted at 50°C, and the pulp heated to 80°C prior to filtration. Cadmium electrolyte containing (in g/dm³) 180 Cd, 40 Zn, and 1 Co was used as the initial solution.

Test results showed the following:

1. Reducing the pH from 4.95 to 1.32 during ozonizing increases the filtration rate by about 14-fold, but in these circumstances the degree of cobalt removal from the solutions drops from 98 to 69%.

2. The introduction, prior to ozonizing, of cobalt (III) hydroxide as a seeding agent at the rate of 1.5 g per dm³ of solution increases filtration rate 2-fold. A further increase in the amount of seeding agent does not alter filtration rates significantly.

3. Using the "accumulation method" yielded cobalt (II) hydroxide which could be filtered 5-6 times better, with 95% cobalt removal from solutions, than that obtained by the former method with the same degree of purification.
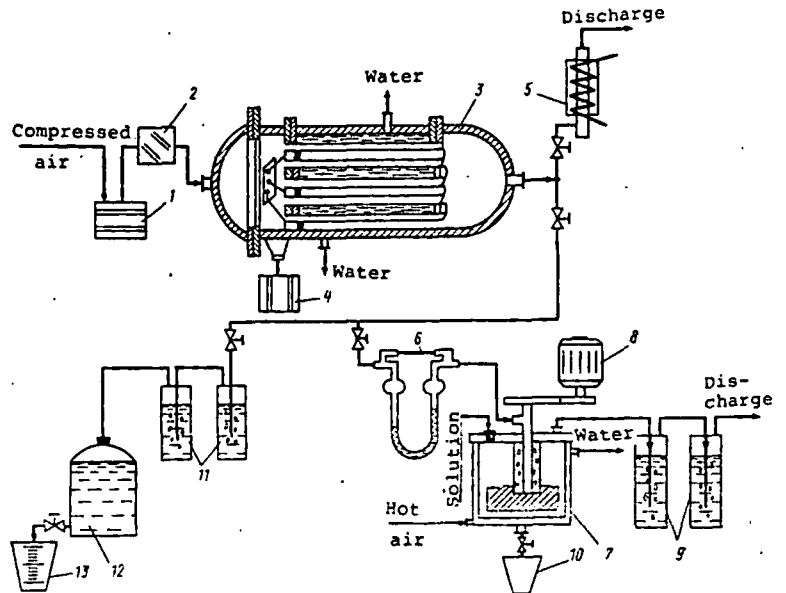
PROJECT PROPOSAL

— PORPHYRY COPPER —
IN SITU RECOVERY BY LEACHING

Submitted By

Interdisciplinary Research Task Force

November 1971

INTERDISCIPLINARY RESEARCH TASK FORCE

Project Proposal: Porphyry Copper - In Situ Recovery by Leaching
                    Following Non-Nuclear Fracturing

Committee: L. W. Gibbs, TCMRC, Chairman
            R. A. Dick, TCMRC
            R. M. Gooding, Div. of Pet. & Nat. Gas, W.O.
            W. R. Hardwick, TMSFO
            W. D. Howell, BERC
            G. A. Johnson, TCMRC
            C. A. Komar, MERC
            W. A. McKinney, SLCMRC
            H. R. Nicholls, DMRC
            W. K. Overbey, MERC
            G. M. Potter, SLCMRC

November 23, 1971
(Rev. December 6, 1971)

FOR OFFICIAL GOVERNMENT USE ONLY

CONTENTS

i

ILLUSTRATIONS - Continued

ii

ILLUSTRATIONS - Continued

INTERDISCIPLINARY RESEARCH TASK FORCE REPORT

PORPHYRY COPPER - IN SITU RECOVERY BY LEACHING
FOLLOWING NON-NUCLEAR FRACTURING

I. Objective and Recommendations

The objective of this report is to outline a specific cooperative
project involving the disciplines of metallurgy research, mining
research, and energy research which could demonstrate the feasibility
of in situ recovery of copper by leaching, following non-nuclear
fracturing of a porphyry copper deposit. The project as herein de-
scribed was selected because it has a reasonably high probability
of success considering the fact that the overall operation represents
a bold new and untried mining concept, and also, because methods and
technology used herein could be modified and adapted for recovery
of other metals, minerals, and fuels; for example, uranium.

We recommend the above cooperative research project be initiated as
soon as possible. We envision a field scale effort costing $2,780,000.
We are of the opinion that the project is justified for the following
reasons:

1. Environmental Considerations - The quantity of land surface
    available to man is virtually fixed. Mineral extraction
    should be so planned as to minimize land spoilage and, in
    fact, aimed at enhancement whenever possible. Impact of
    the minerals industry heretofore has been negative in such
    terms as strip mining, mine water drainage, and smelter
    gases. In situ mining would be very positive in comparative
    environmental effects.

2. Health and Safety - Reduction in injuries and fatalities is
    a primary goal of the Bureau of Mines, and in situ mining
    would tend toward fewer persons exposed to subsurface hazards.

3. Reserves - The "space-ship" concept of the world recognizes
    that reserves of minerals, metals, and fuels are finite.
    They must not be wasted. Exhaustion of known economic deposits
    can be foreseen, and new technology is urgently needed for
    the utilization of lower grade deposits.

4. Balance of Trade and National Security - The United States
    is facing a deficit in world trade. Becoming nationally
    more self-sufficient in mineral raw materials would be of
    help. In the case of copper, expropriation of foreign
    holdings of U.S. based copper companies by foreign countries

1

makes us more dependent on unstable, foreign controlled copper supplies. Utilization of lower grade domestic copper deposits will thus help domestic raw material stability and the balance of payments.

5. Advancement of Present Technology - Much information has been recently generated concerning the in situ leaching or block caving of low-grade porphyry deposits following nuclear fracturing. This project proposes to utilize such data and test the feasibility of non-nuclear fracturing before in situ leaching, as nuclear blasting now seems to be an unacceptable fragmentation alternative.

Briefly, the proposed 3-year project would consist of the selection of a 100- by 100- by 100-ft block of low-grade, less than 0.4 percent, oxide porphyry copper deposit covered by a maximum of 25 ft of overburden. The block would be presplit to isolate it from the surrounding deposit. It would be blasted using non-nuclear explosives and the presplit test block sealed with polymer cement. Leaching and monitoring would follow, after which a post-test evaluation would be made. Details of the proposed project follow.

II. Outline of Proposed Project

A. General Plan of Project

The program, of which the proposed project is a part, has been previously explained in the Interdisciplinary Research Task Force's first report, dated October 18, 1971. The program's thesis was in situ extraction of metals, minerals, and fuels. In addition to the demonstration project to develop technology on the in situ leaching of low-grade porphyry copper deposits following non-nuclear fracturing, in the cited report three other projects were suggested: in situ retorting of oil shales, in situ recovery of heavy petroleum from tar sands, and underground electronic ore sorting (preconcentration) of the deep, low-grade native copper deposits of Upper Michigan. We are not concerned with the latter three items in this report.

The task force has defined five possible research areas for the in situ porphyry leaching project which are basically five options for non-nuclear fracturing of the ore at the selected test site. These fracturing options are:

(1) Conventional chemical explosive fracturing,
(2) hydraulic fracturing (i.e., as practical in the petroleum industry),
(3) combined hydraulic and explosive fracturing (i.e., high density slurries would be exploded in the

2

fractures created by hydrofracturing for added rub-
blizing of the porphyry),

(4) coyote blasting, and
(5) undercut caving.

This report presents the details and related costs involved in
conducting a demonstration site type research project on the
first option using conventional chemical explosive fracturing.
This option was chosen because:

(1) There is very little technical information on the
effect of chemical explosives in deep blasting
(i.e., where there are no free faces to blast to)
and such basic information is needed before en-
gineering type studies can be made on the possible
use of such a fragmentation technique prior to in
situ leaching,

(2) there is substantial industry interest in developing
such information (the task force's preliminary con-
tacts with companies that own the many properties
where such an extraction technique could be appli-
cable has been very encouraging),

(3) the environmental advantages of this kind of a
mining technique are of socio-economic importance,
and

(4) the technology developed in the proposed project
could be applied to deposits other than low-grade
porphyry copper.

Other major advantages of the proposed project independent
of fragmentation methods are:

(1) The development of technology concerning how solution
mining operations can best be monitored for environ-
mental protection and control of the acid leach
solutions,

(2) the conversion of resources to extractable mineral
reserves which would be added to our country's
economic system if in situ leaching following non-
nuclear fracturing could be developed to a point
where it is economically feasible, and

(3) in situ fracturing and leaching is a very safe
mining technique as no men would work underground
in the industrial application.

This research project proposal would utilize men underground
only as research result monitors. They would not be needed
in a commerical in situ extraction operation using chemical
explosives as herein planned.

3

A few comments should be given concerning the other fracturing
alternatives that we rejected for the "first step" of the in
situ fracturing and leaching project. The combined hydraulic
fracturing and slurry blasting technique holds promise as a
possible fracturing technique but should be evaluated as a
"second step" of the project. Coyote blasting or hydraulic
fracturing alone would probably not yield acceptable fractur-
ing results in most formations; thus, evaluation of these
techniques should be delayed until the most applicable methods
are evaluated. Undercut caving would probably yield good frac-
turing results, if properly conducted, but would most likely be
more expensive than one of the simpler "in situ" fracturing
techniques. For deposits deeper than 300 to 400 ft, either the
undercut caving technique or combined hydraulic fracturing
and slurry blasting technique seems likely to offer the best
results.

Long-term extension of the project could include an evaluation
of alternative sealing and solution monitoring techniques,
which is another area in which the mining industry is extremely
interested, or the evaluation of the solvent extraction tech-
nique with regard to the possible elimination of copper
smelting and its related environmental problems and costs.

Details of the proposed in situ porphyry fragmentation and
leaching demonstration project are given below. Figure 1
is a generalized sketch of the demonstration site.

B. Project Detail

1. Pretest Planning (Cost = $100,000)

This part of the proposed project consists of the Bureau
project management personnel that will plan, coordinate and
operate the demonstration project. Most of the $100,000
expenses for this portion of the work will be spent during
the first year of the 3-year project due to the need for
planning and coordination during the initial stages of the
experiment. Once the leaching operation has begun to
function, operating crews will be assigned to the field site.
Their expenses are presented in item 7 below. The pretest
planning cost estimate of $100,000 involves the labor, travel,
and miscellaneous expenses of eight Bureau men, involved at
one-quarter time, for 1 year.

4

4 - SURFACE MONITORING HOLES 90° ON CENTER

117 PRESPLITTING HOLES APPROX. 03° ON CENTER

BORE HOLES FOR BLASTING PATTERNS

Ran 110'

Ran 56'

5 - 6" CORE HOLES

UNDERGROUND DRIFTS

SURFACE MONITORING HOLE

SURFACE MONITORING 2-5 HOLE

~112' D.

SURFACE

UP TO 25' OF OVERBURDEN

SURFACE MONITORING HOLES

PRESPLITT HOLES

105' DEEP TEST "BLOCK"

UNDERGROUND MONITORING HOLES

60°

60°

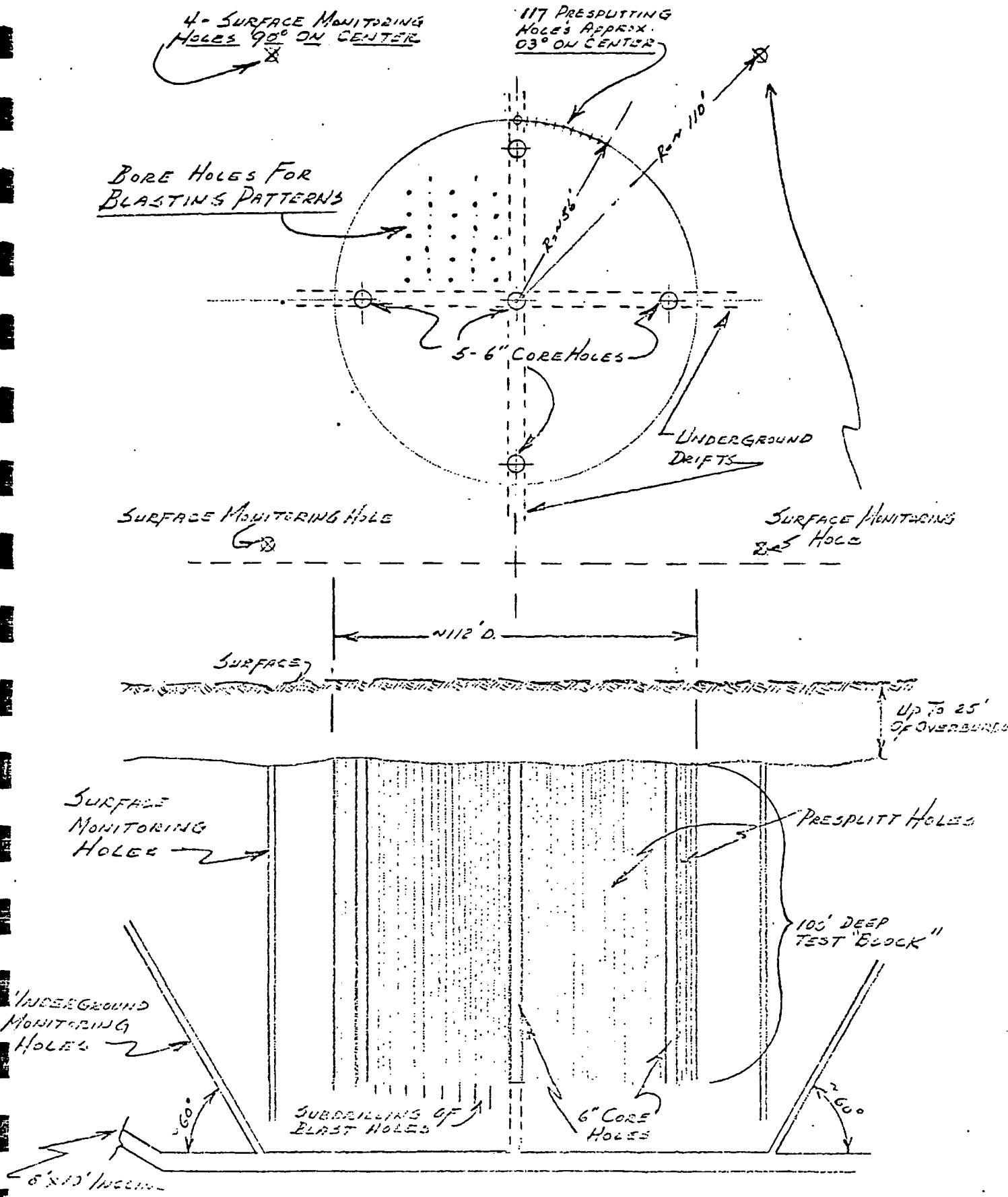SUBDRILLING OF BLAST HOLES

6" CORE HOLES

8'x10' INCLINE

FIG. 1 GENERALIZED SKETCH OF DEMONSTRATION SITE

2. Site Selection, Geological Delineation, and Environmental
   Studies (Cost = $380,000)

The required work and related costs involved in this portion
of the project proposal are dependent on the quantity of
information the property owner has already developed concern-
ing the chosen demonstration site. It is assumed that the ore
block to be used for the test will involve 1,000,000 cu ft of
low-grade (about 4 lb/ton), shallow, oxide porphyry. This is
approximately a 100- by 100- by 100-ft "block." Overburden
is assumed to be no more than 25 ft deep. The tonnage involved
is approximately 80,000 tons. The porphyry will be tested to
make sure it is leachable by acid solutions, if proper frag-
mentation is obtained.

Four technical Bureau personnel are required for the site
selection process. Their time and travel expenses for 6
months of full-time work will be $50,000, and they are in
addition to the project management personnel previously
mentioned. The five, large diameter (6 in core) holes required
for the geological and metallurgical studies will be drilled
in a five spot pattern and will cost $30,000. We recommend
this drilling be contracted out in the interest of expediency
and efficiency. Forty dollars per ft was used in our cost
estimate of drilling, stemming before fracturing, and other
related expenses.

The site fluid flow (reservoir engineering) study will be con-
ducted at a cost of $100,000. This study will involve such
activities as well logging of the five core holes, downhole
photography, and flow testing. The $125,000 cost for the
detailed geological study involves such activities as oriented
core (geological and stress analysis) stress field evaluation,
natural fracture study, and a limited amount of remote sensing
study for possible tectonic influences in the natural fracture
system of the project site. Borehole geological (instrumenta-
tion) study will also be conducted before and after fracturing
to fully understand the geology of the test site.

The environmental effect statement will be an important portion
of our proposed project, and thus, one man will be assigned this
responsibility and given 1 year to turn out first a preliminary
and then a detailed report. This will cost $25,000.

The figure of $50,000 for a possible company lease has been
included in our estimate in recognition of a possible cost.
Most probably, the Bureau could lease the demonstration site
from the owner company for $1.00, returning to the owner the
copper that will be recovered during the test. This should
sufficiently compensate the cooperating company.

5

3. Leachability (Metallurgical) Testing (Cost = $220,000)

The preliminary leachability evaluation that will be conducted
immediately after a site has been chosen is a very important
segment of the proposed project, as a full understanding of
the mineralogy and assay value is needed. This preliminary
work will cost $100,000. Also, the pilot scale testing will be
essential to the design and operation of the leach solution
injection and recovery system. The samples used for the pre-
liminary leachability tests will be a portion of the 6 in core
material (sample acquisition estimated at $20,000). The pilot
scale metallurgical testing will include evaluation of leaching
rates, required acidity of solutions, and possible blocking
of in situ solution passages by precipitated salts and will
cost $100,000.

4. Presplitting (Cost = $70,000)

To insure control over the leach solutions, for operating and
environmental reasons during the test, our test "block" (i.e.,
it may actually be a cylinder of 56 ft radius) will be isolated
from its surroundings. After blasting of the enclosed material,
the presplit fracture will be sealed by grouting. The grout,
a polymerized cement, is resistant to acid solutions. Its "in
place" cost is reported below as a sealing cost.

5. Fracturing (Conventional Chemical Blasting) (Cost = $115,000)

The two-fold objective of the explosive fragmentation portion
of the in situ mining study is 1) to create sufficient per-
meability in the orebody to enable the leaching solution to
enter at given points, pass through the mineralized zone, and
be collected, and 2) to create adequate fragmentation in the
copper-bearing rock to enable the leach solution to contact
a sufficient portion of the copper values, thus assuring a
satisfactory copper recovery. The amount of blasting required
will depend on the degree of permeability and fragmentation
already present in the test area.

Three possible fragmentation systems were considered for ful-
filling the program objectives. The first utilized vertical,
rotary-drilled blastholes, spaced on a staggered grid, drilled
to the base of the zone of intended leaching. The second pos-
sibility was induced hydraulic fracturing augmented by explo-
sive fracturing with liquid slurry explosives to extend the
fractures. The third option involved drifting and cross-
cutting under the orebody and fragmenting the rock with coyote
blasting techniques. Although each technique has certain

6

advantages, the first, utilizing rotary drill holes, was chosen for the initial effort. We feel that the other two techniques may not yield adequate fragmentation to assure a high degree of contact between the solution and the copper values.

In normal bench blasting, each blasthole breaks to a nearby free face. In this blasting program the blastholes will have no free face, other than the original ground surface, to which to break. Our experience with confined cylindrical charges in the absence of a parallel free face is limited. Bureau studies involving totally confined single charges indicate that cracking is developed out to a radius equal to twelve times the charge radius. A heavily cracked region extends out to six charge radii, and the crushed zone to two charge radii. This blasting program will utilize a group of long, cylindrical charges, 9- to 12-1/4-in. in diameter, reaching a depth of over 100 feet. Compared to a single charge, the multiple charges will have the advantage of enhanced blast effects between adjacent charges, and the disadvantage of the 100 feet of overburden to overcome. The net effect of these two factors is not known. The problem cannot be studied at a greatly reduced scale because gross rock structure, large charge diameters, and heavy confinement created by the large overburden depth cannot be accurately scaled down. Thus, in addition to creating the permeability and fragmentation needed for leaching, the blasts will serve as a research tool in an area that has received little study.

Although several tools are available for attempting to quantify the fragmentation attained, the only sure method of determining whether the orebody has been properly broken for in situ mining is to attempt to leach it. We do not know whether uniform, overall rubblization is required for optimum recovery, or whether a coarser fragmentation is sufficient, assuming that the fractures will tend to occur in zones of mineralization, which normally are planes of weakness.

Although logic infers that the finest fragmentation attainable would give the best copper recovery, some persons knowledgeable in the field believe that an excess of fines will cause recementation in the orebody, resulting in a loss of permeability.

Drilling and Blasting Costs

Considered here will be the cost of fragmenting an orebody 100-ft thick and 10,000 sq ft in cross section. Costs cannot be closely estimated without specific data on the target orebody. The following are factors that will affect drilling and blasting costs.

7

Type of contractor. The work could probably be done at a lower cost by a mining company on a piece of ground adjacent to an operating property than by a contractor who would have to set up operations at a site distant from his headquarters. This illustrates the desirability of a cooperative program with a copper producer.

Shape of the orebody. A shallow, tabular orebody will be cheaper to fragment than a deep deposit. An orebody with a large vertical dimension will require a tighter drill pattern and a higher powder factor to obtain the needed swell and permeability for in situ leaching.

Depth of overburden. Each foot of overburden represents unproductive drill footage and resistance to overcome in obtaining orebody swell.

Source of explosives. Involvement of one or more interested powder companies would result in savings in explosives costs.

Rock characteristics. Local geology, the extent of in situ flaws, and the hardness, strength, and density of the rock will affect drilling and blasting costs.

Product size requirements. The degree of fragmentation required for optimum exposure of the copper-bearing minerals to the leaching solution will affect drilling and blasting costs.

Water conditions. The presence of water may adversely affect drilling costs, and severe water conditions will require the use of more expensive, water resistant explosive products.

Proximity to structures. This could require the use of special techniques to control ground and air vibrations and flyrock. Necessary building surveys and insurance would represent a cost that would be charged against the blasting program.

The direct costs of drilling and blasting the experimental block can be described by the equation

$$C_t = \left\{ (T+D+J)(A/S^2)(C_d) \right\} + \left\{ (T+D+J-Y)(A/S^2)(B^2)(G)(.34)(C_e+C_1) \right\}$$

where C_t = total drilling and blasting costs, in dollars
   T = average orebody thickness, in feet
   D = average overburden thickness, in feet
   J = borehole subdrilling depth, in feet
   A = orebody cross-sectional area, in square feet
   S = borehole spacing, in feet
   C_d = borehole drilling cost, in dollars/foot

8

Y = length of stemming, in feet
B = borehole diameter, in inches
G = explosive specific gravity
C_e = cost of explosive, in dollars/pound, and
C_1 = cost of explosive loading and supplies, in dollars/pound.

On the right side of the equation, the first expression repre-
sents drilling costs and the second represents blasting costs.
For drilling and blasting the experimental block, the follow-
ing values have been assumed.

$$T = 100 \text{ ft}$$
$$D = 25 \text{ ft}$$
$$*J = 5 \text{ ft}$$
$$A = 10,000 \text{ sq ft}$$
$$C_d = \$2.50/\text{ft for a 9-in borehole}$$
$$\$3.00/\text{ft for a 12-1/4-in borehole}$$
$$Y = 25 \text{ ft}$$
$$G = 0.85 \text{ for AN-FO}$$
$$1.30 \text{ for slurry}$$
$$C_e = \$.035/\text{lb for AN-FO}$$
$$\$.13/\text{lb for slurry}$$
$$C_1 = \$.03/\text{lb for each product}$$

Table 1 shows drilling and blasting costs for various levels of
effort. Assuming an ore grade of 0.4 percent and 50 percent
recovery, the table values indicate a drilling and blasting cost
range of 5.4 cents to 30.3 cents per pound of copper recovered.

For the program, $100,000 is allocated for drilling and blasting.
This includes an allowance for some reblasting, which may be
necessary. An additional $15,000 is allocated for preliminary
blast design tests.

6. Sealing and Monitoring (Cost = $230,000)

The in-place cost of the polymerized cement used for sealing (as
mentioned above) is $15,000. Monitoring costs for the project
involves drilling four 6-in-diam periphery holes, each 150 ft
deep, around the test area (cost = $10,000). Also 500 ft of
small diameter slant, up holes (cost = $5,000) from underground
drifting (cost = $100,000) will be required. These monitoring
drifts will be beneath all the fractured material and will be
used to control loss of the acid solutions. The electronic
monitoring and analysis equipment used in the project should

---

*The center holes will be slightly deeper than the perimeter holes to
give the bottom of the fractured zone a conical shape. This will
induce the leach solution to drain toward the center.

9

TABLE 1. - Drilling and blasting costs for the test block

Borehole spacing S (ft)	Borehole diameter B (in)	Explosive type	Drilling cost (dollars)	Blasting cost (dollars)	Total cost C_t (dollars)	Powder factor (lb/cu yd)
20	12-1/4	ANFO	9,750	7,400	17,150	3.1
20	9	Slurry	8,125	15,037	23,162	2.5
25	12-1/4	Slurry	6,240	17,829	24,069	3.0
14-2/7	9	ANFO	16,250	7,988	24,238	3.3
10	12-1/4	ANFO	39,000	29,599	68,599	12.3
10	9	Slurry	32,500	60,147	92,647	10.2
12-1/2	12-1/4	Slurry	24,960	71,315	96,275	12.1
7-1/7	9	ANFO	65,000	31,953	96,953	13.3

10

cost $50,000. One man will be given the responsibility of monitoring and analyzing the resultant information. This will cost $50,000. He will probably be the same man that writes the environmental statement during the one year planning and development period required by the project.

7. Solution Injection and Recovery System, and Processing Plant
   (Cost = $1,465,000)

The metallurgical problem when leaching copper orebodies in place comprises (1) injection of a suitable, economical solvent into a fragmented, contained leaching zone, (2) recovery of a copper-bearing pregnant solution, (3) processing the pregnant solution to recover the copper in a marketable form, and (4) recycling the barren leach liquor after regeneration as needed. The accompanying flowsheet (Figure 2) shows a simplified processing plan for a typical leachable copper orebody.

Some important criteria in selecting the leaching solvent are that it be cheap in overall use, readily available, not destroy the permeability of the leaching ore mass through gangue alteration or salt precipitation, readily processed to recover copper, and capable of being recycled. The metallurgical aspects of in-place copper leaching are covered well in the reports "In Situ Recovery of Copper from Sulfide Ore Bodies Following Nuclear Fracturing," by Joe B. Rosenbaum and W. A. McKinney, (presented at the American Nuclear Society Topical Meeting on Engineering with Nuclear Explosive, Las Vegas, Nev., Jan. 14-16, 1970) and "Dissolution of Copper Sulfide Minerals from Fractured Ore Bodies," again by Rosenbaum and McKinney (1970 SME Fall Meeting, St. Louis, Mo., October 21-23), and a number of other reports such as the "Sloop" proposal.

The copper recovery process selected for the in-place leaching project must cheaply and completely remove the copper, regenerate the leach solution for another leach cycle, and not plug the leaching ore mass with salts. The process of using scrap iron to precipitate copper puts up to 2 lb or more iron in the leach solution for each pound of copper recovered. The iron and other salts tend to precipitate in the leaching ore mass as basic sulfates, although a PH of less than about 2.3 helps prevent such precipitation. We may therefore decide to select another process, although more expensive to install, such as solvent extraction, electrowinning, or sulfide precipitation, so as to maintain recycled leach solutions with a minimum of deleterious salts. The costs presented in section IV are, thus, conservative, as are most of the estimates presented. The capital equipment ($150,000) for the injection and recovery system (pumps, piping, etc.) are all acid resistant. The processing plant, as with the injection and recovery system, represents the cost of a "turn key"
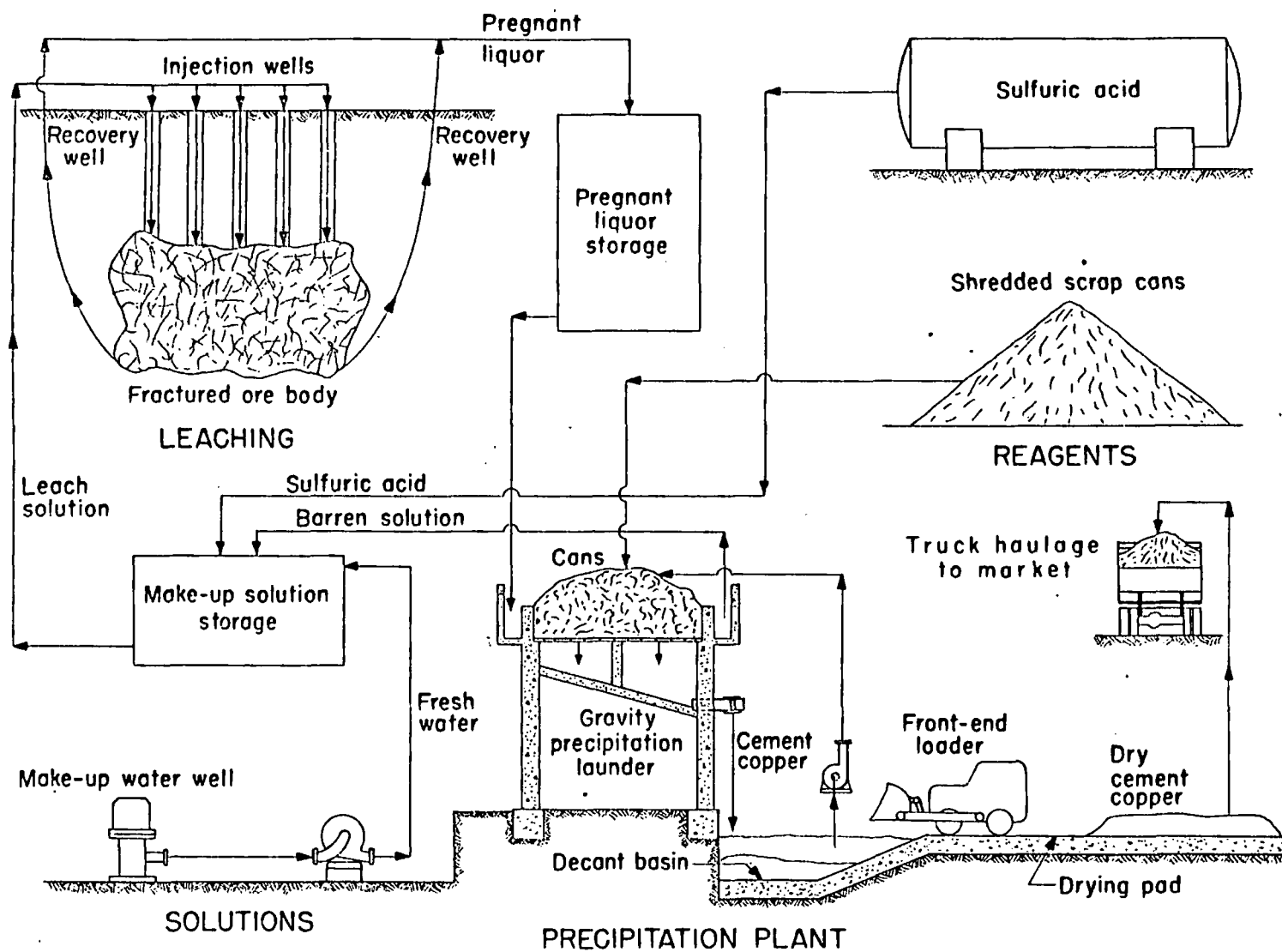
11

FIG. 2.—Generalized Flowsheet For In Situ Leaching and Iron Precipitation to Recover Copper From Non-nuclear Fractured Porphyry Ore.

D-2043-SL

contract ($250,000). The operating cost ($210,000) represents a one shift per day operation (i.e., storage tanks used for solution storage). The cost estimate of the water supply, $50,000, along with the other facilities and utilities could vary from $50,000 to $550,000 depending on the extent of facilities available from the cooperating company. Site preparation, costs such as miscellaneous heavy equipment work, are also reflected in the utilities and facilities cost of $250,000. In addition, $50,000 is needed for working capital.

A major cost of the project, and one that is very controversial, is the cost of the Bureau personnel required on site during the 2-year test run. Most all other operating costs represent contract work, but these 10 BuMines men will add $500,000 to the money required for the 3-year project.

8. Post-Test Evaluation (Cost = $200,000)

The monitoring drifts and incline will be used for access to obtain bulk samples of the test block after the 2-year leaching test. This will cost about $50,000. Releaching and other metallurgical testing ($100,000) will then tell us the success of the conventional chemical blasting fragmentation technique. A written report will be prepared by the project management personnel ($50,000). Other interim reports will be required to describe project progress and possibly the success of some of the more pertinent in situ prophyry leaching procedures such as sealing and monitoring.

C. Project Scheduling

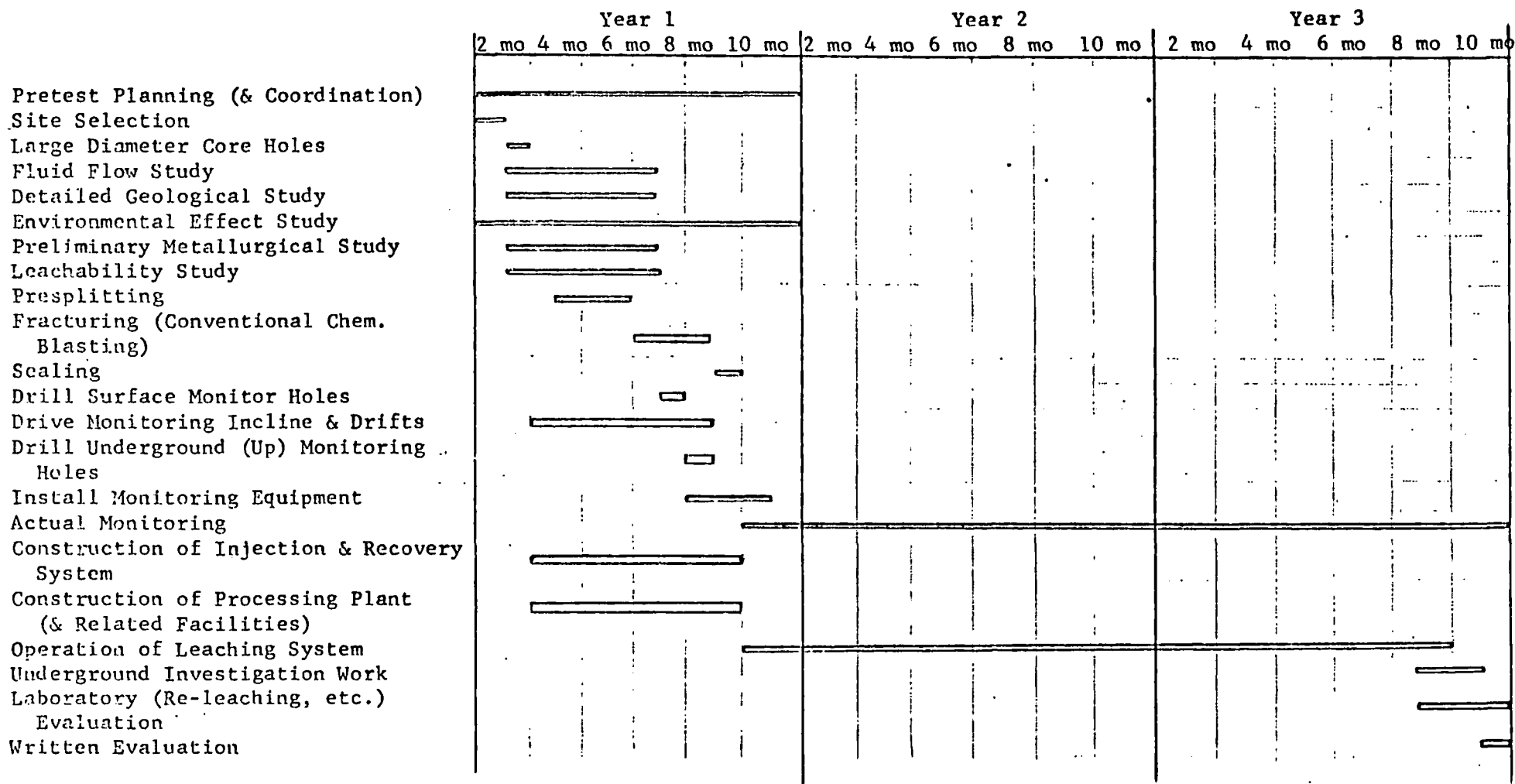Figure 3 depicts the proposed schedule, or timetable, for the in situ porphyry leaching project.

III. Potential Demonstration Sites

A. Selection Criteria

In general, a concise definition of the term "porphyry" copper deposit is impossible. Two characteristics almost universally indicated are:

1. The deposit is of such magnitude and shape that it can be mined advantageously by large-scale, low-per-ton cost methods, either by underground or open pit.

2. The copper minerals are distributed so uniformly through large sections or blocks of the deposit that it is more profitable to mine by "bulk" methods rather than by selective methods.

12

FIGURE 3. - In Situ Porphyry Leaching Project Schedule

	Year 1	Year 2	Year 3
	2 mo 4 mo 6 mo 8 mo 10 mo	2 mo 4 mo 6 mo 8 mo 10 mo	2 mo 4 mo 6 mo 8 mo 10 mo

Pretest Planning (& Coordination)
Site Selection
Large Diameter Core Holes
Fluid Flow Study
Detailed Geological Study
Environmental Effect Study
Preliminary Metallurgical Study
Leachability Study
Presplitting
Fracturing (Conventional Chem. Blasting)
Scaling
Drill Surface Monitor Holes
Drive Monitoring Incline & Drifts
Drill Underground (Up) Monitoring Holes
Install Monitoring Equipment
Actual Monitoring
Construction of Injection & Recovery System
Construction of Processing Plant (& Related Facilities)
Operation of Leaching System
Underground Investigation Work
Laboratory (Re-leaching, etc.) Evaluation
Written Evaluation

Deposits that conform to these characteristics can be further divided as follows:

1. Ore minerals disseminated in intrusive rock: Ore occurs in the apex of a quartz monzonite or quartz diorite intrusive. Generally some ore occurs in fractures of intruded rocks. Copper occurs in minerals chalcopyrite and bornite disseminated as blebs scattered through the rock types, and as discrete grains and veinlets along seams in the rock. The principal products of hydrothermal alteration are sericite and clay. Chlorite and rutile may occur as alteration products of biotite.

2. Ore minerals as filling in brecciated rock: Ore occurs erratically distributed through breccia pipes in masses and bunches. Rock fragments may consist of quartzite, limestone, granite, porphyry and clastic rocks cemented with chalcopyrite, bornite, chalcocite, quartz, and carbonate. Breccia pipe may cut through relatively undisturbed rock and lateral transition from ore to waste may be sharp. Alteration in pipe may be intense with an abundance of sericite and significant amounts of undifferentiated clay minerals.

3. Ore minerals as replacement in intruded rocks: Ore occurs in highly altered rocks that have yielded to chemical reorganization and to metasomatic replacement accompanied by deposition of copper and iron sulfides, sometimes closely associated with intrusive porphyry. Feldspathic rocks, quartz, monzonite porphyry, argillite, and quartzite are altered to show abundant sericite orthoclase, quartz, biotite, and clay. Limey rocks, cherty limestone, pure limestone, and marl are converted to various lime silicite minerals such as tactite which consists chiefly of garnet and hornfels which consist of diopside and calcite. Sulfides, pyrite, and chalcopyrite occur as small grains and thin irregular veinlets in replacement fissures and as pods of massive sulfide.

All three types of deposits may be oxidized with copper values either remaining in place or migrating downward to form a zone of secondary enrichment. This zone may consist of oxidized or sulfide minerals. Some deposits with known oxide ore reserves are as follows:

13

Company	Deposit	Reserves (tons)	Grade (% Cu)
ASARCO	San Xavier	10,800,000	1.00
ASARCO	Sacaton	12,000,000	1.00
Newmont	Vekol	12,600,000	0.53
Newmont	San Manuel	130,000,000	0.70
Anaconda	Twin Buttes	22,000,000	0.60
Anaconda	Helvetia	21,500,000	0.50
Hecla (EPNG)	Lakeshore	207,000,000	0.71
Bagdad	Bagdad	110,000,000	0.40
Ranchers	Bluebird	75,000,000	0.52
Inspiration	Sanchez	39,000,000	0.413
Kennecott	Safford	700,000,000	0.40
Total		1,340,000,000	

Below is a detailed list of the site selection criteria reduced for the proposed project:

1. The porphyry body upon which the test is conducted must contain oxide mineralization at a low grade of about 4 lb of copper per ton. Oxide porphyries will consume more acid during leaching than sulfide deposits, but they are easier to leach and the high use of sulfuric acid has beneficial environmental overtones. As the pollution problems of the Southwest smelters are solved, there will be a need to use up the excess sulfuric acid created when the smelter fumes are cleaned.

2. The oxide porphyry should have no more than 25 ft of overburden and a test "block" of 100 ft by 100 ft by 100 ft (or 100 ft deep and 56 ft in radius) must be able to be separated from its surroundings by presplitting. This presplitting will be used to insure complete control of the leach solutions.

3. Cooperation with the site owner is essential. Economies can be effected in geological studies and in the use of whatever facilities and utilities are present at the demonstration site by agreement with the owner.

B. Description of Possible Demonstration Sites

Table 2 lists a number of possible sites for the proposed in situ porphyry leaching project. The sites are presented in order of desirability according to the information presently available to the task force.

14

TABLE 2. - <u>Potential deposits for in situ leaching field test with known</u>
<u>oxide ore reserves probably having submarginal ore at fringes</u>

Name of deposit	Prior-ity*	Location	Company	Physical descrip. (length, width, depth, tonnage)	Geology and mineralogy, Cu content	Remarks (Prior activity, mine workings, permeability
Lakeshore	A	30 mi. S. of Casa Grande, Arizona near Gu Komelik on Papago Indian reservation.	Hecla Mining Co.	207×10^6 tons oxide ore overlying 300×10^6 tons sulfide ore.	Chrysocolla in quartzite 0.7% Cu, 55% acid soluble.	Co. is presently sinking 2 inclined shafts 7,500 ft in length to a high grade tactite zone containing 1.7% Cu in form of sulfide. Later plans are to strip oxide ore near surface by open pit mining to expose the large reserves of low grade sulfide. Water should be available now for a field test.
Sanchez (formerly United Nuclear).	A	Graham County about 7 mi. N.E. of Safford, Ariz.	Inspiration Consolidated Copper Co.	39×10^6 tons oxide ore near surface 100 to 150 x 10^6 tons. Down to 1,000-ft depth (lower grade).	Chrysocolla 0.4% Cu.	Co. operated small heap leaching pilot plant (5,000-ton heap). Had some problems with jarosite coating 1/2-in material on heap. Water wells probably in and site close to Safford.
Safford	A	9 mi. N.E. of Safford, Ariz.	Kennecott Copper Corp. (Have expressed interest in project.)	700×10^6 tons oxide ore. Most of oxide ore beneath 500 to 1,300 ft of barren overburden.	Chrysocolla and brochantite 0.4% Cu.	Considered for project Sloop. See E&M J. Nov. 1967, pp. 116-122. No water yet. Would have to choose ore near surface for field test.

*Priority: A-Most desirable, according to information now available.
    B-Not as desirable, according to information now available.
    C-Applicable, but least desirable, according to information now available.

TABLE 2. - Potential deposits for in situ leaching field test with known
oxide ore reserves probably having submarginal ore at fringes - Continued

Name of deposit	Prior-ity*	Location	Company	Physical descrip. (length, width, depth, tonnage)	Geology and mineralogy, Cu content	Remarks (Prior activity, mine workings, permeability
San Xavier	A	15 mi. S.W. of Tucson near ASARCO Mission mine.	ASARCO	10.8×10^6 tons oxide ore near surface.	Chrysocolla 1% Cu.	Co. planned to mine by open pit and leach in 4,000 TPD vat leaching operation. Having difficulty reaching agreement with Papago Indians. Close to Mission mine with available water and labor for company assistance. Close to major population center.
Sacaton	B	N. of Casa Grande, Ariz.	ASARCO	12×10^6 tons near surface oxide ore.	Chrysocolla 1% Cu.	Co. plans to mine & process by vat leaching as at San Xavier.
Vekol Hills	B	About 25 mi. S.W. of Casa Grande, Ariz.	Newmont (Contact Bob Fulton in N.Y. for details).	12.6×10^6 tons oxide ore near surface over-lying 103×10^6 tons sulfide ore containing 0.56% Cu.	Chrysocolla 0.53% Cu.	Co. does not plan to develop deposit at present because they feel sulfide ore is marginal because of antici-pated surcharge for smelting of sulfide concentrates. Isolated deposit; probably no water yet.

*Priority: A-Most desirable, according to information now available.
          B-Not as desirable, according to information now available.
          C-Applicable, but least desirable, according to information now available.

TABLE 2. - Potential deposits for in situ leaching field test with known
oxide ore reserves probably having submarginal ore at fringes - Continued

Name of deposit	Prior- ity*	Location	Company	Physical descrip. (length, width, depth, tonnage)	Geology and mineralogy, Cu content	Remarks (Prior activity, mine workings, permeability
American Eagle	B	Copper Creek district 11 mi. E. of Mammoth, Ariz.	Newmont	Unknown reserves pipe-like structure 60-ft diam. on sur- face oxide ore over- lying deep sulfide deposit.	Quartz-sericite rock 0.5 to 0.8% Cu.	Similar to Old Reliable, Prince, & Globe deposits in same area.
Posten Butte	B	N.E. of Florence, Ariz.	Continental Oil Co.	250 x 10^6 tons oxide ore overlying 250 x 10^6 tons sulfide ore. (These estimates based on few drill holes)	Chrysocolla 0.5 Cu high solubility in acid in lab tests.	Co. plans to develop similar to lakeshore operation. Problem with Gila River bed going through center of deposit.
Bluebird	B	5 mi. W. of Miami, Ariz.	Ranchers explo- ration and de- velopment.	75 x 10^6 tons oxide ore near surface.	Chrysocolla malachite and azurite 0.52% Cu.	Co. presently mining by ripping and scraping, leaching in heaps and re- covering Cu by solvent extraction electrowinning. Ore could be easily frac- tured but might encounter some leaching problems with plugging by clay material.

*Priority: A-Most desirable, according to information now available.
B-Not as desirable, according to information now available..
C-Applicable, but least desirable, according to information now available.

TABLE 2. - Potential deposits for in situ leaching field test with known
oxide ore reserves probably having submarginal ore at fringes - Continued

Name of deposit	Prior-ity*	Location	Company	Physical descrip. (length, width, depth, tonnage)	Geology and mineralogy, Cu content	Remarks (Prior activity, mine workings, permeability
Bagdad	B	Bagdad, Ariz.	Bagdad Copper Corp.	110 x 10^6 tons oxide ore near surface overlying 200 x 10^6 tons sulfide ore.	Chrysocolla 0.45% Cu.	Co. has announced plans for expansion and intends to strip oxide ore which will be leached in heaps.
Twin Buttes	C	30 mi. S. of Tucson, Ariz.	Anaconda	22 x 10^6 tons oxide ore overlying sul-fide deposit.	Chrysocolla in high lime rock 0.6% Cu.	Co. presently stripping this material to expose sulfide ore and stockpiling the high acid consuming oxide ore. Could have problems in plugging of a fractured deposit as lime rock breaks down on leaching.
Helvetia	C	25 mi. S of Tucson, Ariz. in Santa Rita mountains across valley from Twin Buttes.	Anaconda	21.5 x 10^6 tons oxide ore over-lying sulfide ore body.	Chrysocolla and some malachite in high lime gangue. 0.5% Cu.	Property not being developed yet. Would have same prob-lem in treating oxide ore as at Twin Buttes.

*Priority: A-Most desirable, according to information now available.
B-Not as desirable, according to information now available.
C-Applicable, but least desirable, according to information now available.

TABLE 2. - Potential deposits for in situ leaching field test with known
oxide ore reserves probably having submarginal ore at fringes - Continued

Name of deposit	Prior-ity*	Location	Company	Physical descrip. (length, width, depth, tonnage)	Geology and mineralogy, Cu content	Remarks (Prior activity, mine workings, permeability
San Manuel	C	San Manuel, Ariz. 45 mi. N.E. of Tucson.	Magma Copper (Newmont)	130×10^6 tons oxide capping over deep sulfide deposit.	Chrysocolla 0.7% Cu. About 70% acid soluble.	Co. presently mining sulfide ore by block caving. Oxide capping has caved and eventually will be treated by in situ leaching as at Miami copper.

*Priority: A-Most desirable, according to information now available.
        B-Not as desirable, according to information now available.
        C-Applicable, but least desirable, according to information now available.

IV. Project Cost Estimate

In Situ Porphyry Copper Leaching with Non-Nuclear Fracturing

1. Pretest Planning.. $ 100,000

2. Site Selection, Geological Delineation and Environmental Studies
   a. Technical Manpower (BuMines men)........................... 50,000
   b. Large Diameter Core Holes (6 in diam)...................... 30,000
   c. Site Fluid Flow (reservoir engineering) Study.............. 100,000
   d. Detailed Geological Study, Including Fracture and Borehole
      Analysis.. 125,000
   e. Environmental Effect Statement............................ 25,000
   f. (Possible) Company Lease.................................. 50,000

3. Leachability (Metallurgical) Testing
   a. Sample Acquisition.. 20,000
   b. Preliminary Metallurgical Testing......................... 100,000
   c. Pilot Scale Leachability Evaluation....................... 100,000

4. Presplitting
   a. Engineering and Design.................................... 20,000
   b. Drilling and Blasting..................................... 50,000

5. Fracturing (Conventional Chemical Blasting)
   a. Preblast Engineering...................................... 15,000
   b. Drilling and Blasting (and possible minor reblasting)...... 100,000

6. Sealing and Monitoring
   a. Polymerized Cement (in place)............................. 15,000
   b. Drill Periphery Monitoring Holes.......................... 10,000
   c. Monitoring Incline and Drifts............................. 100,000
   d. Underground Slant (up) Holes.............................. 5,000
   e. Monitoring Equipment...................................... 50,000
   f. Technical (BuMines) Monitoring Manpower Required........... 50,000

7. Solution Injection and Recovery System, and Processing Plant
   a. Cleaning the Recovery Holes (the 6 in explor. holes)....... 5,000
   b. Capital Cost of Injection and Recovery System.............. 150,000
   c. Capital Cost of Processing Plant.......................... 250,000
   d. Operation Cost of Leaching System (2 yrs)................. 210,000
   e. Construction of Water Supply.............................. 50,000
   f. "Other" Facilities and Utilities (very dependent upon
      facilities available).................................... 250,000
   g. Working Capital... 50,000
   h. On Site BuMines Personnel (10 men, 2 yrs)................. 500,000

8. Post-test Evaluation
   a. Underground Investigation Work (Monitoring Development Used) 50,000
   b. Laboratory Evaluation (Re-leaching, etc.)................. 100,000
   c. Written Evaluation.. 50,000

Total $2,780,000

PHYSICAL AND CHEMICAL PROPERTIES OF OMG, A NEW EXTRACTANT FOR COPPER

UDC 669.33: 66,061.5

I. I. Zeger, G. P. Giganov, and E. M. Fedneva

It is essential that the physical and chemical properties of the organic phase and the design of the extractor should ensure the minimum loss of extractant, because expenditure on making good extractant losses is the principal operating cost item in a solvent extraction scheme for copper. The present paper gives the results of studying some of the physical and chemical properties of a new extractant for copper called OMG, which has been synthesized at the D. I. Mendeleev Moscow Chemical Technology Institute and the State Non-Ferrous Metals Research Institute.

The method of synthesizing the extractant and the results of a study of some of its properties were given in [1,2]. It was established that the capacity for copper of a 10% OMG solution in kerosene at an aqueous phase pH of 2.5 was 5 g/liter, which is twice as great as that of Lix-64.

The good solvent-extraction properties of the reagent and the possibility of using it under industrial conditions were confirmed by large-scale laboratory tests on the solvent-extraction technology for processing heap leaching solutions at the Almalyk Mining and Metallurgical Combine [3].

The investigations were carried out with an extractant having the following basic formula:

$$H_{19}C_9 - \left\langle \bigcirc \right\rangle - \underset{\underset{OH}{\overset{\|}{\underset{NOH}{}}}}{C} - C_nH_{2n+1}$$
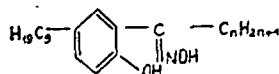
where n = 4-5. Its element composition (5) is 76 C, 10.3 H, and 3.9 N; the refractive index $n_D^{21} = 1.5267$, specific gravity is 0.94 g/cm^3, flash point is 124°C, and purity is 91.3%. The impurities are mostly products of resinification and condensation polymerization of the initial substances and are inactive as regards solvent extraction. Kerosene brand TS-1 was used as the diluent.

It was established that the density of the organic solution increased in proportion from 0.775 to 0.88 g/cm^3 when the OMG concentration rose from 0 to 1.4 M, whereas viscosity rose almost nine times, from 1.25 to 11.2 cSt. The sharp increase in solution viscosity begins at an extractant content > 1 M (~ 40% concentration by volume). This is due to association of the extractant in organic solutions, shown by cryoscopic measurements.

Study of the solubility of OMG in aqueous solutions (Fig. 1) showed that the minimum solubility of 2 mg/liter occurred with an aqueous solution pH of 3-4. Raising and lowering the acidity leads to an increase in solubility. Thus 22 mg/liter of OMG passes into an aqueous solution containing 2 M sulfuric acid.

The increase in solubility at the right-hand end of the curve is due to the formation of alkali metal oximates, which form a second organic phase at pH > 7. The left-hand end of the curve corresponds to formation of extractant-sulfuric acid reaction products which are more soluble in the aqueous medium. Changes in the relationship between the aqueous and organic phases and transition to an aqueous phase containing NaCl + HCl do not affect the solubility of the extractant.

The presence of copper in the range up to 5 g/liter in the systems studies does not alter the nature of the OMG solubility curves.

The investigations showed that losses of extractant caused by dissolution in the aqueous phase at pH 1-3 range from 9.8 to 2.7 mg/liter; this is quite acceptable in the economics of solvent-extraction processing of low-copper solutions, even those from heap leaching. As a rule the copper concentration in them does not exceed 2 g/liter.

The effectiveness of froth separation of the organic phase from the aqueous process solutions (degree of purification up to 70%) in reducing emulsion losses of extractant was confirmed.

Fig. 1. Solubility of OMG in acid solutions (OMG concentration in kerosene 0.3 M). Composition of aqueous phases, M: 1 - 0.18 (H_2SO_4 + Na_2SO_4), O : A = 1 : 1; 2 - 0.18 (H_2SO_4 + Na_2SO_4), O : A = 1 : 10; 3 - 0.18 (HCl + NaCl), O : A = 1 : 1; 4 - 2 (H_2SO_4 + Na_2SO_4), O : A = 1 : 10.

The total capacity of the organic solutions for copper was found by the saturation method. A copper sulfate solution with a concentration of 35 g/liter was used for this purpose, and the total capacity of the organic phase for copper at a given pH was found by bringing it consecutively into contact with fresh batches of solution.
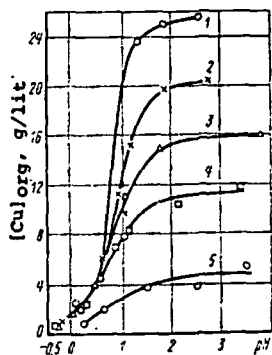
It is apparent from the data given (Fig. 2) that the degree of copper extraction falls sharply as the pH is reduced, in the range of extractant concentrations studied (from 0.2 to 1.4 M). At pH 1 the level is approximately half that at pH 2.5, but remains in the 3-18 g/liter Cu range in the area of concentrations studied.

It can be stated on the basis of the above material that the new extractant for copper (OMG) has a low level of solubility in aqueous solutions and blends well with the diluent, kerosene. The low viscosity of OMG solutions in kerosene ensures rapid phase separation in extraction and reextraction. Thus OMG is not inferior to Lix-64 N in its physical and chemical properties and has double its capacity.

The good extraction, physical, and chemical properties of OMG have made it possible to recommend it as the extractant in pil pilot-plant tests on solvent extraction of copper from heap leaching solutions from unclassified Kal'makyr ores.

Fig. 2. Relationship of capacity of OMG solutions in kerosene for copper to pH of equilibrium aqueous phase. OMG concentration in kerosene, M: 1 – 1.4; 2 – 1.1; 3 – 0.86; 4 – 0.59; 5 – 0.21.

REFERENCES

1. I. I. Zeger, L. V. Kovalenko, V. A. Bykov, et al., Physical Chemistry and Electrochemistry (Moscow Chemical Technology Institute, Issue 71), Moscow, 1972, 129-131.
2. I. I. Zeger, G. P. Giganov, L. V. Kovalenko, et al., Tsvetnaya Metallurgiya (Bull. Inst. Tsvetmetinformatsiya), 1971, No. 19, 27-28.
3. I. I. Zeger, G. P. Giganov, Yu. G. Frolov, et al., Tsvetnaya Metallurgiya (Bull. Inst. Tsvetmetinformatsiya), 1973, No. 17, 20-31.

6) Determining for each project the work required to reach the next decision point and committing the time, money, and human resources required.

7) Insisting on a thorough review at the end of each step, before a decision is made to proceed or not. This involves appraising the future influence of government and regulation on the potential discovery. This includes also abandoning the failing projects without regret and pushing the successful ones with gusto.

Thus, armed with these arrows in his quiver, the exploration manager can project them along the rainbow of success. And, from time to time, his exploration team will assuredly jump for joy and announce, "Yes, we made it; we have made a new ore discovery!"

References

[1]*Business Week*, 1964, "Milestones of Management," Volume I, 23 pp.
[2]*Business Week*, 1966, "Milestones of Management," Volume II, 23 pp.
[3]*Charbonnages de France*, 1978, "Le Charbon En France - Huit Siècles D'Histoire," December 1978, 15 pp.
[4]Cook, Douglas R., 1969, "The Effective Use of Exploration Techniques," Exploration for Mineral Resources, *Circular 101*, New Mexico Bureau of Mines, June 1969, pp. 25-32.
[5]DeLaunay, L., 1908, *La Conquête Minerale*, 389 pp.
[6]Dickerson, Ben F., 1978, "Needed: A New Approach to Exploration Management," *Mining Engineering*, June 1978, pp. 632-636.
[7]Drucker, Peter F., 1964, *Managing for Results*, Harper & Row, 240 pp.
[8]Eisenbeis, H. Richard, 1975, "Managerial Attitudes and Perceived Effectiveness Images of Mining Companies Engaged in Mineral Exploration in North America," Master thesis, Univ. of Arizona, 163 pp.

[9]Emerson, D. W., 1978, "Speculation and Mineral Discovery," *Aust. Soc. Explor. Geophy.*, June 1978, pp. 45-50.
[10]Gardner, John W., 1965, "How to Prevent Organizational Dry Rot," *Harper's Magazine*, August 1965.
[11]Hoffman, Frank O., "The All-Purpose Manager," *Personnel*, January-February 1963, pp. 8-16.
[12]Jay, Anthony, 1968, *Management and Machiavelli*, Holt, Rinehart & Winston.
[13]Joralemon, Ira, 1973, *Copper*, Howell - North Books, 408 pp.
[14]Lespine, J., "Reflexions sur la Recherche Minière,"*Annales des Mines*, November 1972, pp. 37-50.
[15]Millenbruch, D. G., "An Early Appraisal Approach to Exploration Projects," *Mining Congress Journal*, March 1978, pp. 21-23.
[16]Miller, Leo J., "Corporations, Ore Discovery and the Geologist,"*Econ. Geol.*, Vol. 71, No. 4, July 1976.
[17]Mitcham, Thomas W., "Emphasis," *Econ. Geol.*, Vol. 62, No. 3, 1967, pp. 421-425.
[18]Parsons, A. B., 1933, *The Porphyry Coppers*, AIME Volume.
[19]Practical Management Associates, 1971, "Morale: A 4-Dimensional Phenomenon," (Tape Cassette).
[20]Read, Waldemer P., 1962, *Great Issues Concerning Freedom*, Univ. of Utah Press, 138 pp.
[21]Regan, M. D., "Management of Exploration in the Metals Mining Industry," Master Thesis, MIT, June 1971, 137 pp.
[22]Rickard, T. A., 1932, *A History of American Mining*, McGraw Hill Book Co., 419 pp.
[23]Rostad, Ora, "Exploration Philosophy - Top to Bottom," *Mining Engineering*, January 1970, pp. 26-28.
[24]Shepard, Herbert, Lecture on management and defeated R&D organizations at AIME meeting, St. Louis, 1961.
[25]Snow, Geoffrey, "Metals Exploration - Past & Present," March 14, 1976, 8 pp. (mimeographed).
[26]Townsend, Robert, 1970, *Up the Organization - How to Stop the Corporation from Stifling People and Strangling Profits*, Knopf, 202 pp.

Precipitating and Drying Cement Copper at Kennecott's Bingham Canyon Facility

W. Joseph Schlitt, Bruce P. Ream, Lawrence J. Haug, and William D. Southard

Abstract—The operation of Kennecott's Bingham Canyon copper precipitation plant, one of the world's largest, is described. This description includes a brief historical review of precipitation at Bingham and the general layout and operation of the present cone cementation facility. Current practices are based on results of studies undertaken to define improvements needed in each unit operation. These improvements were required to meet changing plant conditions and were implemented primarily within the constraints of the existing facilities. Specific unit operations included were the cone precipitators, the cone discharge thickener, the cone effluent settling basins, and the plate and frame filter presses. As a result of these improvements, loss of precipitated copper decreased and the degree of precipitation increased, raising copper recovery by 9 t/d. At the same time, iron consumption was reduced by 22.5 t/d. Problems in drying the cement copper were also overcome so that a product containing 12 - 15% moisture could be consistently delivered for smelting.

All four authors are employed by Kennecott Copper Corp., Salt Lake City, Utah 84147. **W. Joseph Schlitt**, Member SME, is manager of the Hydrometallurgy Department, Metal Mining Division Research Center; **Bruce P. Ream** is mine planning engineer at the Utah Copper Division; **Lawrence J. Haug** is precipitate plant general foreman at the Utah Copper Division; and **William D. Southard** is manager of engineering services at the Utah Copper Division.

Introduction

Between 1963 and 1967, following several years of research on improved design, Kennecott's Utah Copper Division undertook a major expansion of the dump leaching and copper cementation operation at its Bingham Canyon mine near Salt Lake City, Utah. In the expansion the straight-line launder plant was replaced with two modules each with 13 cone precipitators for copper recovery, and the cement copper decant cells and drying slabs were abandoned in favor of plate and frame filter presses for dewatering the precipitates. Included in the expansion was a 43-m diameter settling basin designed to recover any fine particulate copper entrained in cone effluent and to clarify barren solution being returned to the dumps. Later, a second parallel unit was added. Also installed were a 23-m diameter cone discharge thickener to provide a uniform filter press feed and a conveyor belt-traveling tripper system for charging shredded scrap iron to the cones. The new facility was designed to handle 180 t/d of precipitate copper. In conjunction with this expansion the capacity of the leach water pumping system was increased from 37.8 m^3/min to 150 m^3/min (later 190 m^3/min).

Patents were granted on a number of innovative features of the new plant.[1] Descriptions of the plant and particularly the cone precipitators have also been published.[2,3] However, operating practices at the Bingham facility have not been described since the plant went online. The current practices reflect recent improvements derived from a development program intended to upgrade operating efficiencies and to reduce unit costs, primarily within constraints of the existing facilities. The program overcame the impact of gradually declining copper concentration in the pregnant leach solution and rectified some minor problems inherent in the original plant design.

In arriving at the present mode of operation, each major unit process in the plant (see Fig. 1) was subjected to an in-depth analysis using either available plant process control assays or a separate detailed monitoring program. These efforts identified performance characteristics in four major plant areas. The results of these studies provided the basis for adjusting cone cycle times to improve the degree of copper precipitation, for using flocculants to improve copper settling, for increasing copper recovery from decant and effluent streams, and for enhancing dewatering of the cement copper product.

Cone Precipitators

When the studies began, the copper in the cones was discharged once every 8 hr, one module being discharged at the beginning of each shift and the other in the middle of the shift.
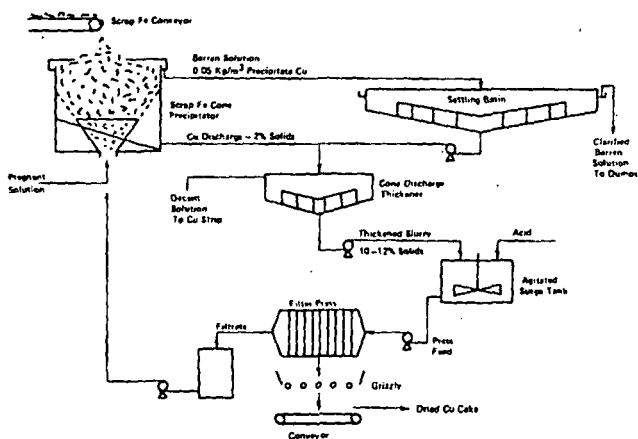

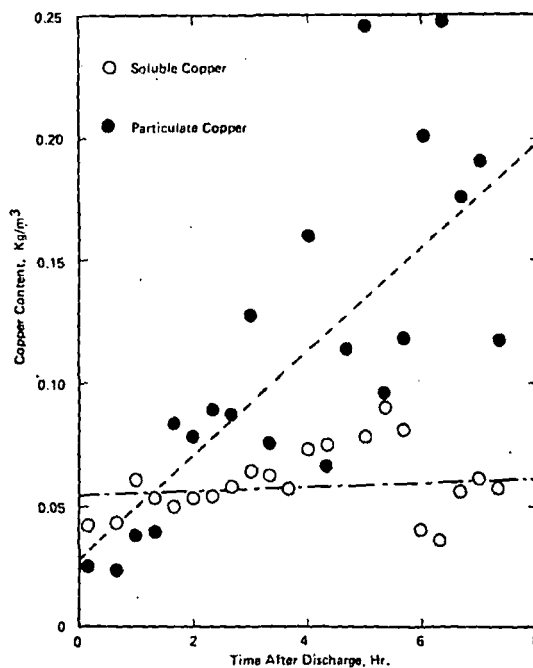Fig. 1—Sequence of unit operations in Precipitation Plant.

Fig. 2—Typical increase in copper losses from cones as a function of time after cone discharge.

Timewise, 30 - 40 min were needed to discharge each cone on line in the module, and 50 - 60 min were reserved at the end of the 240-min cycle to decant the thickener down to the point where the volume of slurry coming from the other module could be easily accommodated. This left 140 - 160 min for copper settling in the thickener under quiescent conditions.

While this operating practice was fine for the cone discharge thickener, copper losses from the cones themselves increased at the rate of about 0.0085 kg/m^3/h, becoming very high toward the end of the 8-hr cycle. As shown in Fig. 2, most of this loss was caused by increased carryover of precipitated copper in the cone effluent. This phenomenon was related to the buildup of copper in the cones and to the gradual formation of channels in the iron bed. Higher flows short circuiting through these channels reduced the degree of precipitation and increased the level of precipitated copper reporting in the cone effluent.

The solution to the problem was clearly to discharge the cones more often in order to avoid the channeling. This was borne out by preliminary tests which showed that a switch from an 8-hr to a 4-hr cone discharge cycle would retain an additional 3.8 t/d of copper in the cones. Before the 4-hr discharge could be adopted, however, a bottleneck in the batch thickener operation had to be overcome. In the 4-hr cycle, 60 - 80 min would be needed for cone discharge and 100 - 120 min would be needed to decant the greater volume of clarified solution. This left only 40 - 80 min for settling copper from the increased volume of cone discharge slurry. To avoid the high decant losses from unsettled copper, flocculants were evaluated as a way of improving settling rates. A nonionic, long-chain liquid polymer proved to be effective at a final dosage of about 5 mL/m^3. This flocculant is now mixed and diluted automatically, and is sprayed into the thin copper slurry (2% solids) before it enters the thickener. As shown in Fig. 3, maximum settling was achieved in 20 min at a depth of 1.2 m and in 50 min at a depth of 4.3 m, the lower limit to which the thickener is decanted.

On the basis of these tests, both the 4-hr cone flush cycle and flocculant addition to the cone discharge slurry were initiated simultaneously. Once these changes were made, the improvements in plant performance were somewhat greater than expected. The net overall increase in plant recovery was 3 t/d of
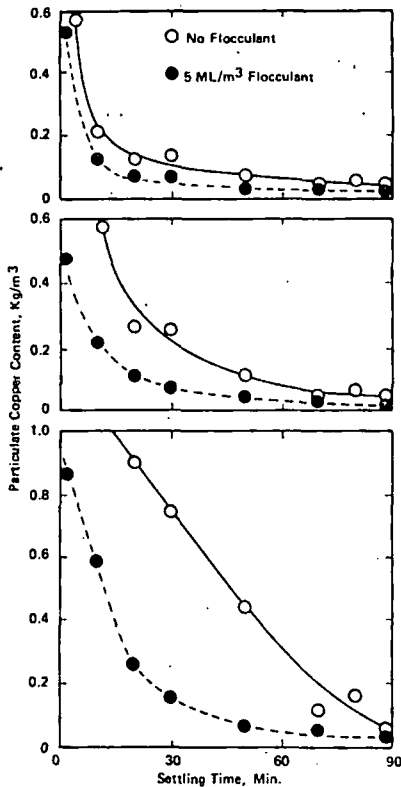
Fig. 3—Effect of flocculant on the settling rate of particulate copper at various depths in the cone discharge thickener.

copper. This was derived from a 1% increase in the degree of copper precipitation and a 6% increase in retention of precipitated copper in the cones. This latter improvement was particularly significant since only about 60% of the suspended precipitate copper in cone effluent was recovered in the settling basins.

The improvements in recovery were due to two factors. The first was the reduced incidence of channeling so that solution flowed uniformly through the bed of iron. The second was the decrease in the amount of copper accumulating in the cones. The more uniform flow also provided an unexpected dividend in the form of lower iron consumption. About 0.07 kg less iron was dissolved per kilogram of copper precipitated. This was due to elimination of stagnant zones away from the channels where solutions continued to dissolve iron without precipitating additional copper. When the improved retention of copper was also taken into account, the overall iron factor based on scrap purchases was reduced by about 0.2 kg of iron per 1 kg of copper actually recovered.

Cone Discharge Thickener

In spite of the enhanced settling rates achieved with flocculant addition, significant copper losses continued to occur when the cone discharge thickener was decanted directly to the two settling basins. One source of loss was the still suspended particulate copper which ranged between 0.08 and 0.10 kg/m³. This was higher than expected on the basis of settling data and indicated that some copper was being resuspended by the decant operation itself. Since much of this copper was very fine and slow to settle, only about 30% appeared to be recovered in the basins. In addition, the settling basins did not recover any of the soluble copper. This averaged about 0.15 - 0.17 kg/m³ (about three times that in the normal effluent), since much of

the water discharged to the thickener from the cones was not completely stripped of copper.

The first alternative treatment method tried was recirculation of decant water to the cones. This proved to be ineffective since the high trash content of the decant water rapidly plugged the solution manifolds in the cones. Therefore, the two center cells in the old launder plant were renovated to treat the decant solution, other small miscellaneous streams, and surface drainage or runoff from the canyon. The upper 145 m in each cell were left open to provide surge capacity and a settling zone for suspended solids. The lower 145 m were charged with iron to strip the soluble copper.

The flow rate for the combined streams fluctuates seasonally but has averaged about 23 m³/min with the feed containing about 0.23 kg/m³ soluble copper, 0.11 kg/m³ particulate copper, 0.14 kg/m³ ferric ion, and only a little acid (pH ≈ 3.2). The settling area and iron bed filtered out virtually all of the contained particulate copper. As indicated in Fig. 4, about 70% of the soluble copper was also recovered. Total copper recovery from the decant solution exceeded recovery in the settling basins by about 1.5 t/d. Furthermore, iron consumption in the stripping operation was quite low, only 1.1 kg iron consumed per 1 kg copper precipated, due to the low ferric ion and acid content of the feed solution.

Cone Effluent Settling Basins

Once performance of the cones and thickener was optimized, an effort was made to improve recovery of the 0.05 kg/m³ of precipitated copper entrained in the cone effluent being fed to the settling basins. Instead of conducting a separate monitoring program, basin performance was assessed by preparing a statistical analysis of daily plant process control assays from a 26-month period. Available plant data included the soluble and particulate copper contents in the basin feeds and effluents as well as the flow rate through each basin. Of these, the flows and copper contents of the feed were taken to be the input or in-
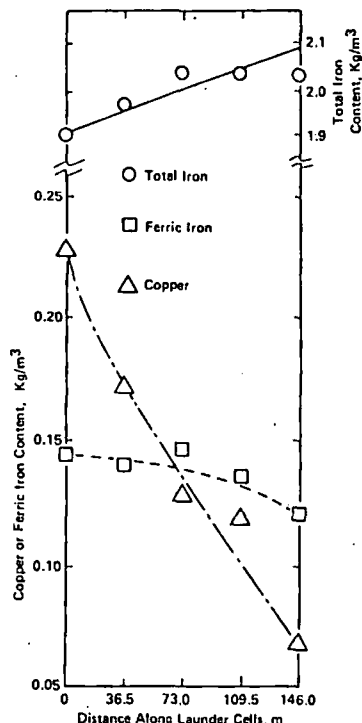

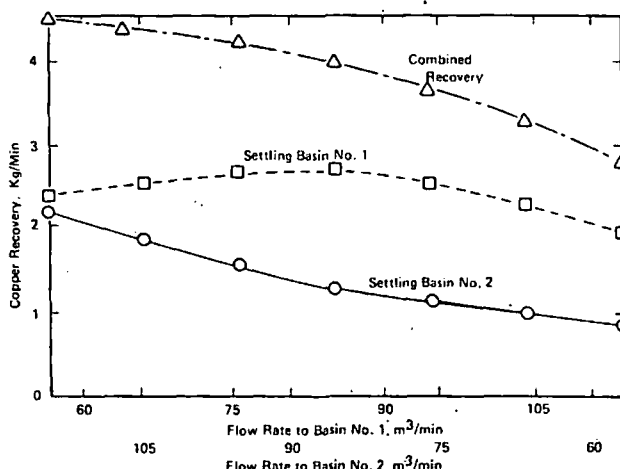Fig. 4—Variation in composition of decant solution during copper stripping in old launder plant.

Fig. 5—Variation in particulate copper recovery in the settling basins as the flow split changes but total flow is fixed at 170 m³/min.

dependent variables. These data also were used to compute various performance indicators for the settling basin, including: Particulate copper solubilized, total particulate loss, total particulate recovery, and percent particulate recovery. The performance indicators, including particulate copper in the basin effluent, were assumed to be the output or dependent variables.

With the large number of variables for each settling basin, multiple linear regression techniques were needed to establish a set of models or mathematical expressions showing which factors influence particulate copper loss and recovery most strongly. Additional techniques were used so that only those independent variables which have a statistically significant impact on loss or recovery were included in the resulting models. For both settling basins, the best indicators of basin performance proved to be the expressions for particulate copper recovery. The models* for each basin are listed below; they account for 96% of the variations observed in particulate recovery during the 26-month period.

Basin No. 1 Particulate copper recovery = 0.084 − 1.069 × 10⁻⁵ × flow rate + 0.843 × particulate copper input

Basin No. 2 Particulate copper recovery = −0.079 + 0.677 × particulate copper input

Unfortunately, methods for optimizing basin performance using these models are limited. The only way this could be done was to optimize the solution flow split between the basins, since total flow is fixed by the volume of pregnant solution coming from the dumps and the particulate copper loading in the basin feed is a function of cone operating efficiency. The optimum flow split can be determined simply by solving the two equations for recovery at different flow splits assuming a normal plant flow rate of 170 m³/min. The result is shown in Fig. 5. Surprisingly, the results indicate that maximum overall recovery is achieved by limiting the flow to Basin No. 1 and not by splitting the flow evenly between the two basins.

This is due to two factors. Although the two center-fed basins are nominally the same, the second unit was actually installed at a later date and utilized an improved feed well design and profile. As a result, No. 2 operates with more uniform radial flow distribution and fewer eddy currents. This probably explains why typical variations in flow rate have a statistically

---

*Expressions for particulate copper recoveries and particulate copper inputs are given in lb/1000 gal and flow rates are given in gal./min, the units currently used in the plant for which the models were developed. SI units can be obtained by appropriate conversion factors.

significant impact on particulate recovery in No. 1, but not No. 2. In addition, the common splitter box only controls the basin flow but does not effectively mix the effluents coming from the two cone modules. For this reason, the particulate loading in the feed to Basin No. 1 is usually about twice that going to No. 2. Thus, limiting flow to No. 1 increases retention time and improves recovery of copper entering this settling basin more than enough to offset losses from No. 2.

For typical particulate copper loadings of 0.035 kg/m³ and 0.060 kg/m³ in the two cone module effluents, the models projected that copper recovery could be increased by 0.6 t/d if an even flow split were changed to send 66 m³/min to Basin No. 1 and 104 m³/min to Basin No. 2. The projected improvement would increase as particulate input increased. However, a higher recovery achieved with a wider flow divergence cannot be inferred from the empirical models since these are really valid only over the range of flows used in their development (55 - 115 m³/min).

After a review of the initial modeling work, plant operators agreed to test the validity of the results by adjusting the settling basin flows to the projected optimum levels. During the first 20 days at this uneven flow split, the average flow to Basin No. 1 was 67 m³/min, and the average flow to Basin No. 2 was 102 m³/min. According to plant process control assays, actual total recovery of particulate copper in both settling basins averaged 5.7 kg/min, or 8230 kg/d. For the same flow split, modeling indicated that total recovery should be 5.4 kg/min, or 7840 kg/d, a difference of only 390 kg/d, or about 4.8%. This close comparison confirmed the validity of the model as a guide for optimizing settling basin operation.

This confirmation also meant that the model could be used to estimate what particulate recovery should have been observed in the 20-day test period if the total flow had been split evenly between the two basins. The resulting estimate was combined recovery of 7300 kg/d. On this basis, use of the projected uneven flow split seems to optimize particulate copper recovery, increasing it by about 0.9 t/d over that obtained with an even split on basin flows.

Precipitate Copper Drying and Handling Facilities

One of the major problems to be overcome as part of the Bingham plant expansion was effectively drying the high tonnage of copper to be produced. In the previous small-scale operations, the cement copper had been washed from the launder cells into quiescent settling basins. Periodically, the standing water was decanted from these and the copper was transferred to drainage pads and then to the smelter. However, the moisture content of the resulting precipitates was high and hard to control, especially in wet or cold weather.

Any suitable alternative drying process had to overcome a number of problems inherent in the nature of cement copper. These include a very fine particle size, typically less than 10 - 20 μm for fresh, as-precipitated material. Furthermore, individual particles are dendritic in nature so that considerable water can be held within each particle as well as between particles. The slurries also have thixotropic tendencies. Partially as a result of these properties, precipitate copper tends to dust excessively at a moisture content below about 8% but becomes sticky and adherent at about 18% moisture, and can be sloppy and free flowing at moisture contents of as little as 25%. Therefore, a number of dewatering processes were evaluated to determine which, if any, could consistently provide a copper product containing a daily average moisture content of 12 to 15%. In addition to plate filter presses, these included: Solid and perforate bowl centrifuges, rotary dryers, cyclone classifiers, spray dryers, vacuum-belt extractors, steam dryers, roll briquetting, rake thickeners, turbo dryers, and various combinations and modifications of these methods.

After the preliminary evaluation, several of these methods were tested in pilot studies. Centrifuges proved to be expensive and difficult to control because of out-of-balance and feed rate control problems. Rotary kilns were unable to consistently meet moisture specifications and would have required expensive air scrubbing equipment. Vacuum-belt extractors available in the early 1960's also did not reduce the moisture content of the precipitate to specified dryness. On the other hand, spray dryers produced a dusty product containing only about 5% moisture. Other methods and combinations of methods were tested but all proved to be less satisfactory than plate filter presses.

Based on the results of tests conducted by Bechtel Corp. at Bingham in 1965, the decision was made to install three Shriver ALP automatic filter presses. Each press had seventeen 1220 mm × 1220 mm × 50 mm chambers with a total of 42 m² of filtering area and 1.1 m³ of cake volume. Each recessed plate was covered with a ∼500 μm stainless steel wire cloth filter medium. The plates were forced together using a hydraulic ram and a teflon impregnated asbestos gasket was used as a seal between each plate. Problems with incomplete chamber filling, pressure equalization between adjacent plates, and gasket failures led to the development of a successful recessed plate and frame filter combination patented by Kennecott.[1] This involved modification of ram length and removal of six filter plates. Between each of the remaining plates a 1200 mm × 1220 mm × 50 mm hollow spacer frame was added, giving a 100-mm-thick cake. These frames were constructed of carbon steel and then rubber coated. Maintenance costs, however, eventually forced the change to the current design of stainless steel spacer frames with "O" ring gaskets. After modification, each press had a capacity of about 2.5 t of contained copper at a precipitate grade of 86 - 90% copper and a moisture content of 12 - 15%.

The equipment specifications and operation of the filter presses and ancillary facilities has been detailed elsewhere.[4] Briefly, the sequence of drying operations begins with the cone discharge thickener. Underflow copper slurry from this unit feeds an agitated surge tank which has the capacity to store material for about 2 hr of press operation. The sole function of the tank is to provide a relatively constant press feed averaging 10 - 12% solids, even though thickener underflow varies from 3 - 30% solids, depending on time after cone discharge.

Under normal conditions, the filter presses are automatically synchronized so that one press is being filled while a second press is being air blown and a third is being unloaded or waiting to be filled again. During filling, the presses are top fed at an average rate of 0.75 m³/min until the press feed pressure reaches the range of 275 - 310 kPa. At this point, there is a 5- to 10-min delay before slurry feeding is discontinued. The length of the feed cycle varies from 15 - 30 min, depending on feed rate and slurry density. During feeding, filtrate passes through the stainless cloth and is fed by gravity to a holding tank via two internal channels. Filtrate is normally recycled to the cones. However, after completing the feed cycle, filtrate is used to flush copper from the feed lines in preparation for the two-stage air blow. The first stage is a low-pressure air blow designed to remove the bulk of the filtrate solution from the precipitate copper cake. After 3 - 5 min, a high-pressure (550 - 620 kPa) air blow is started. This air blow, which lasts from 15 - 20 min, drives out additional water, primarily by evaporation, since the cake is heated by oxidation of the copper. This may raise cake temperatures to more than 90° C, although the average is lower.

Following the air blow, the press automatically opens and the precipitate cake is manually discharged through a grizzly hopper onto a conveyor belt. The copper is then transferred to a storage building where it can be stockpiled or loaded directly into rail cars for shipment to the smelter. When the last compartment in the filter press is emptied, the hydraulic ram automatically closes the press and it is ready for a new cycle.

In spite of the mechanical press improvements and apparent-

ly consistent dewatering procedures, process upsets — particularly high moisture contents — still occurred from time to time. This caused moisture-related operating problems at the smelter. In an effort to gain better control over the drying operation, a monitoring program was undertaken to identify process paramaters which affect drying. Parameters included the level to which the press feed was acidified (a patented process[1]), the percent solids in the feed, the maximum press temperature, and the amount of acid-insoluble material (insol) in the copper. The effect of general material handling after filtration was also examined.

The first portion of the monitoring program was designed primarily to determine the effect of sulfuric acid additions and percent solids on the moisture content of the filter cake. A total of 61 press cycles was sampled over a one-month period. The degree of feed acidification was controlled at four discrete pH levels — 0.5, 1.5, 2.5, and 3.5 (background — no acidification). Percent solids was not intentionally controlled, and varied from 5 - 19%; filter cake moisture ranged from 10.9 - 20.6%, as measured immediately upon discharge from the presses in a vacuum drying oven.

Data were treated using stepwise linear regression techniques, and the results show that the relationships between cake moisture and both percent solids and pH have a high level of statistical significance (greater than 95%). As shown in Figs. 6 and 7, the moisture content drops 1.24 percentage points for
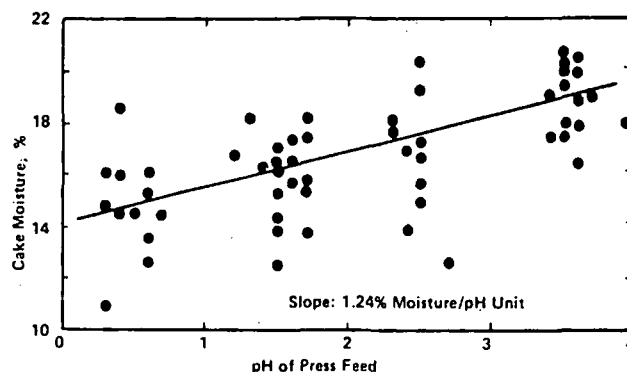

Fig. 6—Relationship between pH of filter press feed and moisture content of as-produced precipitate copper filter cake.
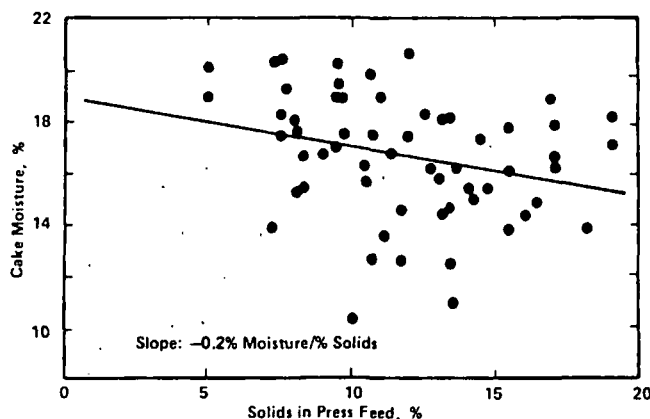

Fig. 7—Relationship between percent solids in filter press feed and moisture content of as-produced precipitate copper filter cake.

| pH Level | Acid Required, Tons/Shift | Average Moisture, Wt % | | | Average Maximum Press Temp °C | Average Solids In Feed, Wt %[1] | Average Soluble Cu In Filtrate, kg/m³ |
		Filter Cake	Rail Car at P-Plant	Rail Car at Smelter			
3.5	None	21.9	12.7	11.7	56	12.7	0.17
1.5	2.75	16.6	10.6	·	71	9.7	0.74
1.0	8.75	17.8	11.8	·	60	9.5	0.92

$$[1] \text{ % solids} = \frac{\left[\dfrac{W_s \cdot V_s \cdot \varrho_f}{(1 - \varrho_f/\varrho_{cu})}\right] 100}{W_s}$$

where W_s = wt slurry sample, V_s = volume slurry sample, ϱ_f = density of solution and ϱ_{cu} = Cu density, all in internally consistent units

each unit decrease in pH, and drops 0.2 percentage points for each percent increase in feed density. However, further analysis of the data showed that the pH effect is so overriding that the observed variation in percent solids has no significant effect on the moisture content.

In the second part of the study, 37 shifts of operation over a two-month period were monitored in detail. Three pH levels were included in this portion of the study, 3.5, 1.5 and 1.0. In addition to press feed acidity and total acid requirements, the following parameters were monitored: The percent solids in the press feed, the soluble copper content in the filtrate, the grade and composition of the precipitate copper, the maximum press temperature, and the percent insol in the copper. These data are summarized in Table 1.

As in the first portion of the study, the five monitored variables were treated statistically using stepwise linear regression. In this analysis, filter cake moisture content was taken to be the dependent variable and all other parameters, either alone or in combination as cross products, were assumed to be independent variables. The results show that only the relationships between moisture content and temperature or pH related terms are statistically significant (95% confidence level). The effects of feed pH and maximum press temperature also proved to be mathematically independent, since cross-product correlations were lower than those for pH and temperature alone. Therefore, the best estimate of moisture in the precipitate filter cake as it drops from the presses is expressed as:

$$\text{% } H_2O \text{ in Cu} = 29.7 - 0.22\,T + 1.43\,pH$$

where T is the maximum press temperature in degrees Celsius. The standard error in this estimate of percent moisture is 1.95, with 80% of the observed variation in moisture attributable to temperature and pH effects. The remaining 20% moisture variation is scatter due to random error or other variables not included in the equation.

The impact of each operating parameter on the moisture content of the precipitate is discussed below in greater detail.

pH

The second portion of this study shows that moisture in the filtered precipitate copper decreases 1.43 percentage points for each unit decrease in pH over the pH range of 1.0 - 3.5. This agrees closely with the value of 1.24 percentage points observed in the first portion of the study. In both cases, the moisture content of filter press discharge was approximately 16% at pH 1.5.

Acidification appears to have both chemical and physical roles in enhancing copper drying. Chemical data listed in Table 2 show that the sulfur content of the copper increases with acidification. This would be expected, since sulfates remaining in the filter cake as water evaporates should increase as more

sulfuric acid is added to the feed. However, the assay data show a greater increase in oxygen content than is accounted for on the basis of higher sulfate loading alone. This suggests that acid catalyzes the reaction

$$2\,Cu + 1/2\,O_2 \rightarrow Cu_2O$$
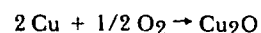
Since this reaction is strongly exothermic, the greater heat generated may be one cause of higher press temperatures and better drying associated with acidification. Sulfation of copper or of copper oxide would also supply heat; however, there is no evidence that sulfation occurs, since the increase in water soluble sulfur or sulfate in the precipitate is less than that expected from higher acid loading alone.

Acid also appears to aid drying by causing the formation of a relatively porous filter cake and by reducing the buildup of inert material on the screens. The result is a more uniform air flow through the filter cake. Evidence for this is found in the increased number of compressor cycles during each press cycle. This increase indicates lower back pressure in the presses with acid addition. The greater number of compressor cycles also means that a greater volume of air moves through the cake. This promotes drying since it provides more complete removal of water. The greater volume of air may even promote the copper oxidation reaction itself.

Acid requirements to enhance drying proved to be low. Only about 2.75 t of sulfuric acid per operating shift were required to maintain pH of 1.5 in the press feed slurry, equivalent to 67 kg of acid per tonne copper. Most of the acid is actually used to overcome the buffering capacity of the mine water. This buffering is high at Bingham so that about 15 kg of acid/m³ of solution are needed just to acidify the mine water to pH 1.5. Also, due to buffering effects, acid requirements are a nonlinear function of final pH and almost 50 kg of acid/m³ are needed to reach a pH of 1.0. This is equivalent to 8.75 t/shift, or 215 kg of acid per tonne copper.

Temperature

As indicated by the analysis, maximum press temperature over the range of 43 - 82°C correlates closely with filter cake moisture. Quantitatively, moisture decreases 2.2 percentage points per 10°C increase in temperature. The relationship clearly provides plant operators with a quick indication of good drying; however, the study did not determine conclusively whether the high temperature is a cause of good drying or merely an effect of other factors which promote drying. As noted above, the temperature may simply reflect the amount of heat being generated through oxidation of the copper. This, in turn, is probably enhanced by uniform air flows and catalytic effects due to acid addition.

| | Assays, Wt % | | | | | | | | |
	Cu	Insol	O	Fe	Sn	Pb	S	Mg	Al
pH 3.5									
As-produced	90.6	0.62	4.95	1.77	0.28	0.20	0.33	0.21	0.28
Water-leached	92.8	0.64	4.18	1.43	0.29	0.24	0.02	0.02	0.40
pH 1.5									
As-produced	91.2	0.77	5.14	1.29	0.25	0.22	0.37	0.18	0.23
Water-leached	93.3	0.88	4.06	0.63	0.26	0.21	0.02	0.02	0.23
pH 1.0									
As-produced	89.5	1.18	6.30	1.01	·	0.22	0.47	0.18	0.39
Water-leached	92.2	1.27	5.10	0.53	·	0.22	0.02	0.03	0.29

Acid insoluble content

The content of acid insoluble material in the copper (insol) only varied from 0.5 - 1.4%. This spread was insufficient to establish statistically significant correlations. However, a sudden jump in insol at the end of the study was apparently responsible for the increase in cake moisture when the pH of the press feed was lowered from 1.5 to 1.0. Insol plugs the filter cake and press screens, creating a high back pressure so that subsequent air blows are less effective. In extreme cases even the flow of copper slurry to the press cavity may be restricted.

Percent solids

In the second part of the study there was not a significant correlation between pulp density or percent solids in the feed and moisture content. In the first part of the study, these two parameters had shown a correlation, but the effect was insignificant relative to pH. These findings were based on percent solids ranging from 7.0 - 15.6% per shift. This does not mean that low percent solids, for example 1 - 2%, would not adversely affect the moisture level in the copper cake.

Effects of acidification other than moisture control

The addition of acid has a minimal effect on precipitate grade as shown in Table 2. Acidification causes a slight increase in sulfur and oxygen levels and a decrease in the iron content. The latter decrease is undoubtedly due to acid-enhanced dissolution of iron or iron oxides, while the former increases are caused simply by higher sulfate loading. The decrease in iron was greater than the increase in oxygen and sulfur raising precipitate grade slightly. The data on water-leached material also show that about 90% of the sulfur and magnesium and a lesser amount of iron and oxygen are water soluble, probably all as sulfates.

Copper losses caused by dissolution of precipitates do increase when acid is added. The soluble copper content in the filtrate rose by 0.57 kg/m^3 when acidifying to pH 1.5. The associated copper loss would be 0.2 t/d for a press filtrate flow of 0.4 m^3/min and a two-shift-per-day operation. The increase in the soluble copper content of the filtrate was even higher, 0.75 kg/m^3, when the press feed was acidified to a pH of 1.0.

During the study there was no indication of a need for increased filter press maintenance because of acidification. In fact, acid addition may reduce the buildup of inert material on the press screens so that less frequent cleaning is required. The only problem encountered was the acid mist released when the filter presses were opened. This was much more noxious at pH 1.0 than at 1.5 and could pose a safety hazard, particularly at the lower pH. Handling concentrated sulfuric acid also entails some risk and requires special safety precautions.

Impact of other factors on the filter press operation

In addition to filter press operation per se, material handling procedures proved to be an important factor in achieving good drying. As indicated by data in Table 1, the warm precipitate copper continues to dry from the time it drops from the filter presses at least until it reaches the smelter. During the study the average moisture content of the copper decreased by 35% while being held for 3 - 4 days before shipment from the precipitation plant. Based on less data, an additional average moisture reduction of 20% took place from the time the cars were loaded at Bingham until they were sampled at the smelter. Clearly, when operating constraints permit copper to be held for several days of additional drying prior to shipment, a significant reduction in moisture can be achieved without acid addition. For example, average car moistures at Bingham for April, May, and June 1975 were 13.2%, 12.9%, and 12.3%, respectively. All were within the desired range of moistures without routine use of acid.

Summary

Efforts to optimize precipitation plant performance to meet gradually changing conditions and to overcome problems in the original plant design proved to be successful. The program reduced plant tail losses by about 0.035 kg/m^3, equivalent to 9 t/d in increased copper recovery. As a result, the plant is now operating at over 90% recovery. Higher recovery would be possible by putting more cones on line and reducing the flow rate per cone. However, the incremental iron consumption needed to achieve a few percent more recovery becomes prohibitive because of the chemistry of the Bingham leach solution.[3] While recovery increased, iron consumption has been reduced by about 0.3 kg iron per 1 kg copper actually recovered. This is equivalent to saving about 22.5 t/d of iron. As a result, reported overall iron consumption has dropped from just over 3 kg to less than 2.8 kg iron per 1 kg copper.

Development work spanning more than 10 years has shown that a modified plate and frame filter press is quite effective for dewatering cement copper. Drying is enhanced by air blowing to oxidize a portion of the copper and to generate heat within the cake itself. Since the hot cake continues to dry after discharge, simply holding copper at the plant for a few days will assure delivery of a product containing the desired moisture level of 12 - 15% at the smelter. When insol levels exceed 1% or when the copper must be shipped immediately, the press feed can be acidified to an optimum pH of 1.5 with sulfuric acid. This level does not adversely affect press maintenance or precipitate composition but does catalyze the exothermic oxidation of copper and does produce a uniformly porous filter cake which promotes drying. The normal range of percent solids in the feed did not affect drying but cake temperature did correlate closely with cake moisture. However, this relationship may be only an effect of good drying, rather than the cause.

References

[1] Precipitation plant patents assigned to Kennecott Copper Corp.:

  (a) US Patent 3,333,953, "Process and Apparatus for the Precipitation of Substances from Solution Using Solid Precipitants," S.R. Zimmerly and E.E. Malouf.

  (b) US Patent 3,540,880, "Process and Apparatus for the Precipitation of Substances from Solution Using Solid Precipitants," H.R. Spedden and E.E. Malouf.

  (c) US Patent 3,567,018, "Method and Apparatus for Filtering Slurries Containing Solid Particles Having Interlocking Tendencies," A.M. Moler.

  (d) US Patent 3,922,167, "Acidification of Precipitate Copper Slurry Prior to Filtration and Drying," A.D. Pernichele and W.D. Southard.

[2] Spedden, H.R., Malouf, E.E., and Prater, J.D., "Cone-Type Precipitators for Improved Copper Recovery," *Mining Engineering*, April 1966, pp.57-62.

[3] Schlitt, W.J., and Richards, K.J., "Chemical Aspects of Copper Cementation," *Solution Mining Symposium*, AIME, 1974, pp. 401-421.

[4] Schlitt, W.J., Ream, B.P., and Southard, W.D., "Dewatering Precipitate Copper in Plate and Frame Filter Presses," presented at 106th AIME Annual Meeting, Atlanta, Ga., March 6-10, 1977, SME Preprint 77B100.

A Comparison of Geochemical Exploration Techniques in the Carolina Slate Belt

P. Geoffrey Feiss and Paul C. Ragland

The Piedmont province of the southern Appalachians is the focus of interest for many exploration geologists. In the past, only those deposits with significant surface exposure were exploited. Thus, few deposits have been found and relatively little exploration has been conducted in recent years. Modern geochemical and geophysical techniques can alleviate this problem of concentrating on exposed ore bodies by allowing us to "look through" the soil and saprolite to detect the presence of significant mineralization at depth. This paper will attempt to evaluate the feasibility and effectiveness of several geochemical exploration techniques in the Piedmont province of Cabarrus and Stanly counties, N.C.

The area chosen for study is shown in Fig. 1, lying almost wholly within the Mt. Pleasant quadrangle, N.C. The area is on the eastern boundary between the Charlotte belt, a zone of plutonic and intermediate grade metamorphic rocks, and the Carolina Slate belt, a series of complexly interbedded volcanic and sedimentary rocks of predominantly low metamorphic grade. The area is considered to be an early Paleozoic active, continental margin.[1] As is typical of most of the piedmont, outcrop is sparse. Figure 2 is a sketch map of the general geology of the area under study, showing the Charlotte belt rocks in the northwestern quadrant and slate belt rocks to the east. Within the area are a number of old mines and prospects, the most famous of which are the Furniss and Phoenix mines in Cabarrus County. All are reported to have contained Au and Cu. Ag and Pb were reported from some. A summary of the deposits is given in Table 1.

Data used in this study are from three Master's theses completed at the University of North Carolina at Chapel Hill.[3,5,6] In separate studies, well waters,[5] B-zone soils,[3] and vein and float quartz[6] from the area were sampled and analyzed. Each study concluded separately that geochemical anomalies in the vicinity of the ores justify use of that specific sampling technique in a geochemical exploration program. However, no comparative study of the methods has been made. It is our intention

to a) determine statistically which pathfinder elements are most effective for locating significant anomalies, b) develop multivariate functions using all the analytical data to enhance the predictive power of the analyses, and c) evaluate which type of sampling is most efficient for locating anomalies associated with relatively small ore bodies at depth in the Piedmont.

Parenthetically, stream and stream sediment analysis may be less effective in the North Carolina Piedmont due to the effects of culture on the chemistry of stream waters and sediments. Furthermore, it has been suggested that the heavy precipitation in this area linked with relatively shallow water tables mitigates against significant amounts of heavy metals entering the surface drainage from buried ore bodies.[7]

Table 2 shows the analytical procedures used and the elements analyzed in each of the studies. The underlined elements were determined on a nonstatistical, subjective basis to the best pathfinder elements.

The studies suggest that Cu and Zn should be effective pathfinders for base metal sulfide deposits buried beneath a deep soil cover in the Piedmont. The Zn anomaly corroborates previous soil geochemical surveys.[7] A reasonable next step is to utilize multivariate statistics to increase the probability of these sampling modes identifying significant anomalies. In this study discriminant function analysis is utilized. This procedure in-

P. G. Feiss is assistant professor of Geology, Univ. of North Carolina at Chapel Hill, Chapel Hill, NC 27514. **P. C. Ragland** is chairman, Dept. of Geology, Florida State Univ., Tallahassee, Fla. 32306. SME preprint 77L85, AIME Annual Meeting, Atlanta, Ga., March 1977. Manuscript Feb. 10, 1977. Discussion of this paper must be submitted, in duplicate, prior to August 31, 1979. In accordance with the Postal Service Regulations, this material has been assessed a page charge and is considered advertisement for postal purposes.

Acknowledgments

R. J. H.
UNITED STATES GEOLOGICAL SURVEY
   Box 25046
      DENVER FEDERAL CENTER
      DENVER, COLORADO 80225

T. J.
   THAILAND DEPARTMENT OF MINERAL RESOURCES
   RAMA VI ROAD
      BANGKOK 4, THAILAND
      February 14, 1979

REFERENCES

Braitsch, O., 1966, Bromine and rubidium as indicators of environment during sylvite and carnallite deposition of the upper Rhine Valley evaporites, *in* Rau, J. L., ed., Second symposium on salt, v. 1: Cleveland, Ohio, Geol. Soc. Northern Ohio, 1965, p. 293–301.
—— 1971, Salt deposits: their origin and composition: Berlin, Springer-Verlag, 297 p.
Hite, R. J., 1972, Potassium and magnesium in Cretaceous evaporites of northeast Brazil [abs.]: Am. Assoc. Petroleum Geologists Bull., v. 56, p. 627.
—— 1974, Evaporite deposits of the Khorat plateau, northeastern Thailand, *in* Coogan, A. H., ed., Fourth symposium on salt, v. 1: Houston, Texas, Geol. Soc. Northern Texas, 1973, p. 135–146.
Holser, W. T., 1966, Bromide geochemistry of salt rocks, *in* Rau, J. H., ed., Second symposium on salt, v. 1: Cleveland, Ohio, Geol. Soc. Northern Ohio, 1965, p. 248–275.
Javanaphet, J. C., 1969, Geologic map of Thailand, scale 1:1,000,000, and accompanying text on the geology of Thailand: Thailand Department of Mineral Resources.
Kinsman, D. J. J., 1976, Evaporites: Relative humidity control of primary mineral facies: Jour. Sed. Petrology, v. 46, p. 273–279.
Raup, O. B., 1966, Bromine distribution in some halite rocks of the Paradox Member, of the Hermosa Formation, in Utah, *in* Rau, J. L., ed., Second symposium on salt, v. 1: Cleveland, Ohio, Geol. Soc. Northern Ohio, 1965, p. 236–247.

nodules ranging from 0.1 to 10 mm in diameter. The later variety is more common in the sylvite deposits. Where boracite is present there is a general absence of anhydrite, suggesting replacement by boracite. Because boracite is water insoluble, it should be expected to concentrate as a residue where potash has been dissolved; thus, it will probably be found in greater abundance in the sylvite deposits than in carnallite.

In the L-1 core hole (Table 2), the interval between 97.25 and 99.11 m averages about 3.7 weight percent boracite. Although the data are not now available, it is expected that the boracite content of other Khorat sylvite deposits should have a similar boracite content. With this much present, plus the fact that boracite is water insoluble, it is reasonable to assume that the boracite could be recovered as a byproduct of potash mining and add considerably to the overall economic value of these deposits.

The Geochemistry of the Khorat Sea

In 1969, the senior author investigated the Cretaceous evaporites of Brazil and came away in a state of utter amazement after seeing the incredible deposits of tachyhydrite. To see deposits of similar size and age on yet another continent (Asia) a few years later was an even more unbelievable experience. Considering the combined volume of tachyhydrite that is now known in these deposits, it is clear that $CaCl_2$ was a major constituent in the Cretaceous evaporite seas. Less direct evidence of $CaCl_2$ involvement in evaporite brine chemistry has come from meagre data on the composition of brine inclusions in halite rock and from connate brines associated with evaporites.

The evaporite deposits of the Maha Sarakham Formation do not contain the correct proportion of minerals expected from the evaporation of sea water. Carbonate minerals are nearly absent, there is a great excess of halite relative to gypsum or anhydrite, and there are no magnesium sulfate minerals. A Khorat sea that could produce tachyhydrite deposits is compatible with a lack of magnesium sulfate minerals, because the necessary concentration of Ca^{+2} should have kept the brine purged of SO_4^{-2} due to the reaction, $Ca_{(aq)}^{+2} + SO_{4(aq)}^{-2} \rightarrow CaSO_{4(c)}$. This reaction explains why there are are no magnesium sulfate minerals present; but then it still must be explained why there is not much more $CaSO_4$. The simplest explanation for the missing $CaSO_4$ may be that it was deposited somewhere near the marine connection with the evaporite basin. The missing carbonate facies may also be located in a similar position. There is some evidence that the anhydrite beds increase in number and thickness

along the western margin of the Khorat and Sakon Nakhon Basins and may indicate that the marine accessway was somewhere to the west of these areas. If the influx came from the west, then the possibility of a connection between the Khorat sea and the Tethys sea is suggestive. Such a connection might have been several thousand kilometers in length and, by virtue of this great length, there should have been a high degree of concentration by the time the influx reached the distal end (Khorat sea) of the system. Seemingly, such a strong concentrative system should be a prerequisite to tachyhydrite deposition, because the salt is so highly soluble and hygroscopic. Furthermore, at the distal end of the system, deposition of evaporite salts should have been influenced by a continental climate (low humidity) rather than a marine climate (high humidity). This problem of deposition of highly soluble and hygroscopic evaporite minerals under the climatic conditions imposed by a sea coast has been addressed by Kinsman (1976). A similarly lengthy marine connection created by the opening of the South Atlantic has been cited as the principle reason that extensive deposits of tachyhydrite were able to form in Brazil, Gabon, and Congo (Hite, 1972). The mineralogical similarities (large volumes of tachyhydrite, carnallite, sylvite, and borate minerals) between the Khorat and Brazilian-African deposits plus their similar age might suggest that the chemistry of the Cretaceous ocean was somehow different from that of the modern ocean; however, it seems more likely that the duplication was simply the result of similar circulatory systems.

Summary

The deposits of the Khorat Plateau have the potential of becoming an important source of potash for Southeast Asia. Although carnallite is the principal mineral in these deposits, there are several core holes that penetrated high-grade sylvite. These sylvite bodies have an unknown geometry and areal extent, but they seem to be related to localities where the thick primary carnallite facies has been subjected to leaching. Hundreds of such localities are probably present on the Khorat Plateau. Finding them, plus the defining of their size, shape, and the geologic controls governing their origin, presents a real problem—one that must be solved if the true economic value of these deposits is to be determined. Should the sylvite deposits prove uneconomic, there are always the enormous carnallite deposits. Although carnallite is not a favored ore for the potash industry, the facts that the deposits are very thick and at shallow depths may balance some of the less desirable features of this ore.
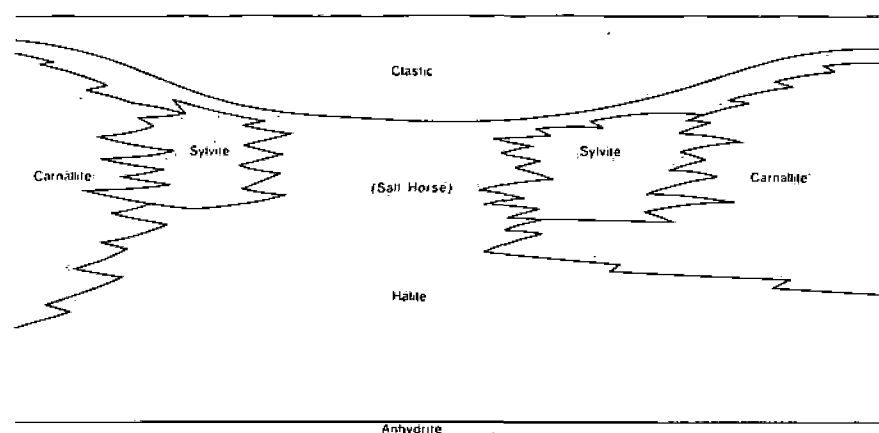
FIG. 9. Diagram showing an interpretation of the relationship of Khorat Plateau sylvite
deposits to areas of barren halite ("salt horses"). The scale of the diagram is hypothetical.

of the carnallite show bromine values of 3,100 to 3,400 ppm, which is in the range of primary carnallite concentration (Braitsch, 1971, table 28). From these data, we conclude that the carnallite is a primary deposit. Initially, the carnallite deposit was probably a thick continuous layer over much of the Khorat and Sakon Nakhon Basins. Drilling has shown that this layer now has holes in it. In these holes, where the Lower Salt is completely barren of potash, the halite shows the type of bromine distribution seen in Figure 7. The conclusion drawn from this is that undersaturated solutions completely leached the carnallite and subsequently redeposited halite with a low bromine content. As long as the solutions involved remained greatly undersaturated in $MgCl_2$, they would have completely removed the carnallite. However, it is well known that any solution in contact with carnallite quickly becomes saturated, or nearly so, in $MgCl_2$. Where this occurs, the KCl, which was also derived from the carnallite but is less soluble than $MgCl_2$, will salt out, forming sylvite. This important process has been termed incongruent alteration (Braitsch, 1971, p. 118). Considering the great thickness of the Lower Salt carnallite exposed to such a leaching process, it seems likely that areas of complete carnallite removal should also be surrounded by a peripheral zone where incongruent alteration has brought about the formation of sylvite. The hypothetical arrangement of halite-sylvite-carnallite facies resulting from this process is shown in Figure 9. Complete dissolution of carnallite or incongruent alteration results in a volume reduction so that younger beds may be deposited in greater thickness over the site (Fig. 9). Additional evidence that Khorat Plateau sylvite is the product of incongruent alteration of carnallite is seen in the bromine content of the sylvite. The Khorat sylvites average about 450 ppm bromine, which is much too low to be considered a primary precipitate (Braitsch, 1966, p. 296).

The horizontal scale of the facies relationships depicted on Figure 9 is unknown. At Khon Kaen in the Khorat Basin, a thick sylvite facies (core hole K-47, Table 2) grades laterally into barren halite over a distance of about 1.3 km. Drilling has not yet defined the transition of sylvite to a carnallite facies at this locality. Not all the Khorat sylvite deposits occur in the manner suggested in Figure 9. For example, the sylvite facies at Wanorn Niwat (Table 1, core hole K-48) was found in a single core hole at the base of 70.5 m of carnallite and tachyhydrite. The core hole nearest to this location, which is about 5 km east, penetrated 82.3 m of carnallite but no sylvite. An explanation for the position of the sylvite deposit at Wanorn Niwat is that the carnallite was subjected to incongruent alteration early in the primary depositional stage and then conditions of high brine concentration were restored. Additional carnallite was then deposited over the alteration product (sylvite). However, if sufficient drill hole data were available to establish the geometry of the sylvite deposit at this locality, data might show that the altering solutions entered the carnallite deposit some distance from the K-48 core hole, penetrated deeply into the deposit, and then spread out laterally along its base. It is quite possible that vertical variations in permeability of the original deposit could have facilitated lateral movement of the altering solutions at some places, such as the base of the deposit at Wanon Niwat, while hindering it at others.

Boracite

The mineral boracite ($MgClB_7O_{13}$) is present in such quantities in the Khorat Plateau potash deposits that it should be considered a potential source of borate. In some of the potash cores, it comprises about 95 percent of the water-insoluble fraction. The mineral occurs in two forms that include pale yellow tetrahedrons up to 3 mm in diameter disseminated through the carnallite and irregular white grains and

TABLE 1. Thick Deposits of Carnallite on the Khorat Plateau

Core hole no.	Locality: city, village, or district	Interval (m)	Thickness (m)	Accessory minerals
		Sakon Nakhon Basin		
K-1	Udon Thani	89.7–129.1	39.4	
K-2	Nong Khai	466.8–497.6	30.8	tachyhydrite
K-3	Sawang Daen Din	421.0–462.5	41.5	tachyhydrite
K-5	Nong Han	378.9–431.1	62.2	sylvite
K-6	Muang	259.9–336.7	76.8	tachyhydrite
K-8	Sri Chiengmai	88.6–117.0	28.4	
K-43	Phauna Nikhom	292.7–312.8	20.1	
K-44	Sri Chiengmai	143.1–210.7	67.6	sylvite, tachyhydrite
K-46	Sri Chiengmai	182.8–224.9	42.1	tachyhydrite
K-48	Wanorn Niwat	407.3–477.8	70.5	sylvite, tachyhydrite
K-55	Wanorn Niwat	393.3–475.6	82.3	
		Khorat Basin		
K-10	Kalasin	143.2–189.6	46.3	sylvite
K-11	Yasothorn	200.9–223.9	23.0	sylvite
K-14	Muang	182.0–207.3	25.3	tachyhydrite
K-17	Non Sung	217.7–245.4	27.7	sylvite
K-21	Non Sung	263.5–280.3	16.5	tachyhydrite
K-22	Non Sung	132.2–195.6	63.4	tachyhydrite
K-24	Non Sung	212.0–226.4	14.4	tachyhydrite
K-25	Non Sung	192.7–223.4	30.7	tachyhydrite
K-30	Non Sung	116.2–211.0	94.8	tachyhydrite
K-36	Maha Sarakam	345.8–381.3	35.5	tachyhydrite
K-40	Roi-Et	533.3–595.4	62.1	sylvite
K-42	Roi-Et	320.5–370.9	50.4	tachyhydrite
K-53	Khon Kaen	283.6–324.4	30.8	sylvite, tachyhydrite
K-56	Chaiyaphum	214.0–257.9	43.9	sylvite, tachyhydrite
K-59	Khon Kaen	213.9–239.0	25.1	sylvite, tachyhydrite
K-60	Khon Kaen	172.4–225.9	53.5	sylvite, tachyhydrite
K-64	Chaiyaphum	122.2–147.9	25.7	sylvite, tachyhydrite
K-65	Chaiyaphum	227.4–254.6	27.2	tachyhydrite
K-67	Chaiyaphum	209.0–238.6	29.6	tachyhydrite

halite. However, the associated halite is often brilliant sapphire blue and then the two minerals are easily distinguished. Intergrowth of sylvite and halite is characterized by an amoeboidal texture. The water-insoluble content of the sylvite deposits is very low, averaging about 1.5 weight percent, except near the top of the deposit where a few thin intervals average as much as 8.5 weight percent. This insoluble material consists almost entirely of boracite ($Mg_3ClB_7O_{13}$) with only a trace of anhydrite.

The geometry and horizontal extent of the Khorat sylvite deposits are largely unknown because of a low density of drill holes. These parameters are necessary before the true economic value of these deposits can be assessed. Additional drilling could provide the necessary data; however, because the areas involved are so large, exploration expenditures could be exorbitant and still not achieve the desired results. Future exploration efforts could be substantially more effective if the origin of these deposits is considered. One particularly revealing data source concerning the origin is the bromine geochemistry. Bromine profiles of the Lower Salt, where a carnallite deposit is present, are textbook examples of what is expected under conditions of primary deposition. The profiles show that the bro-

mine concentration of the halite increases rapidly upward and reaches over 300 ppm just before the onset of carnallite deposition. Pure samples of some

TABLE 2. Sylvite Deposits on the Khorat Plateau

Core hole no.	Locality: city, village, or district	Interval (m)	Thickness (m)	Percent K_2O[1]
		Sakon Nakhon Basin		
L-1	Vientiane, Laos	98.4–102.7	4.3	34.2
		97.5–105.6	8.1	28.5
		97.5–131.0	33.5	25.0 (est.)
K-44	Sri Chiengmai	134.4–138.9	4.5	16.3
		140.8–143.2	2.4	14.0
K-48	Wanorn Niwat	477.9–483.8	5.9	40.4
		438.8–488.1	4.3	19.8
		488.1–497.4	9.3	36.7
		Khorat Basin		
K-11	Yasothorn	190.1–193.3	3.2	8.6
K-40	Roi-Et	531.9–533.3	2.4	9.7
K-47	Khon Kaen	133.6–136.7	3.4	24.0
		132.6–141.2	8.6	17.8
K-49	Khon Kaen	137.8–139.2	1.4	9.3
		139.2–145.2	6.0	12.5

[1] K_2O for core hole L-1 determined by atomic absorption by Wayne Mountjoy and I. C. Frost, U. S. Geological Survey, Denver, Colorado. All other analyses determined by the Thailand Department of Mineral Resources, Bangkok, Thailand.
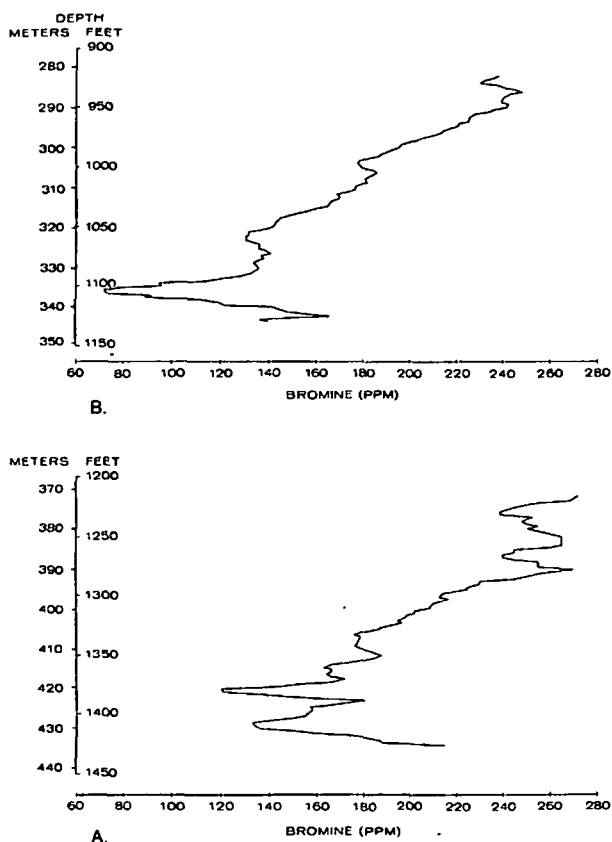
Fig. 8. Bromine distribution through halite of Maha Sarakham Formation, Sakon Nakhon Basin. Halite samples from core hole K-2 at Nong Kai, Thailand. X-ray fluorescence spectrometer analyses were performed by D. Blackburn, U.S. Geological Survey, Denver, Colorado. A. Profile through the Middle Salt. B. Profile through the Upper Salt.

values indicate brine concentration in the range of potash precipitation and suggest that the Middle Salt is a favorable target for potash exploration.

Profiles of the Upper Salt show a pattern of bromine distribution similar to the Middle Salt (Fig. 8B). The basal halite in this bed has a high bromine content (160 ppm) which retreats back to about 70 ppm before beginning a general rapid increase. Again, as in the Middle Salt, the general slope of the profile shows several breaks or periods of brine freshening. The high bromine content of halite at the top of this bed suggests that it may also contain a potash deposit.

Potash Deposits

Since the discovery of potash in 1973 on the Khorat Plateau at Udon Thani, an extensive drilling program by the Department by Mineral Resources has proven that potash underlies about half of the Sakon Nakhon Basin and at least half of the Khorat Basin. The total area underlain by potash may ap-

proach 30,000 km². All the potash found thus far is in the upper third of the Lower Salt. As yet only traces of potash minerals have been found in the Middle Salt and Upper Salt.

The potash deposits of the Khorat Plateau are remarkable in terms of their great' thickness and shallow depth (Table 1). In the Sakon Nakhon Basin, the thickest interval of potash is 82.3 m at Wanorn Niwat (core hole K-55) near the center of the basin. The most shallow occurrence is at a depth of 88.6 m at the village of Sri Chiengmai (core hole K-8) on the northwestern edge of the basin. In the Khorat Basin the maximum known thickness, 94.8 m, is at the village of Non Sung (core hole K-30) in the southwestern part of the basin. The minimum known depth to potash, which is also at Non Sung, is 116.2 m. Although it was previously noted (Fig. 4) that some plastic flow has probably occurred in the lower part of the Lower Salt, the great thickness of potash is the original depositional thickness and not the result of flowage. Local extremes in thickness variation are the result of dissolution after deposition.

The potash deposits include only two potassium minerals, sylvite (KCl) and carnallite (KMgCl₃ · 6H₂O), and the latter is by far the most abundant. Most of the carnallite rock consists of an equigranular mixture of carnallite and halite, although masses of almost pure carnallite are common. In general, the carnallite rock shows little evidence of bedding. Most carnallite is colorless to pale rose and only rarely is the blood-red pigmentation seen that is so common in other deposits. A common constituent of the carnallite deposits is the mineral tachyhydrite (CaMg₂Cl₆ · 12H₂O) (Table 1). Although tachyhydrite generally is in amounts of less than 30 percent of the total carnallite deposit, it locally forms nearly pure layers as much as 16 m thick. The mineral has the same clear honey-colored appearance that is so typical of the Brazilian and African deposits.

The Khorat Plateau sylvite deposits are probably unequaled anywhere in the world in terms of thickness, K₂O content, and shallow depth. The first discovery of sylvite was in a core hole about 15 km north of Vientiane, Laos. In this hole (L-1), the deposit is 33.5 m thick with an average K₂O content of about 25 percent (Table 2). Two select intervals in this deposit, between the depths of 98.4 to 102.7 m and 97.5 to 105.6 m, average 34.2 and 28.5 percent K₂O, respectively. Since the discovery at Vientiane, other impressive sylvite deposits have been found at Wanorn Niwat, about 70 km northwest of Sakon Nakhon and at Khon Kaen in the Khorat Basin. The sylvite of these deposits is typically colorless and locally difficult to distinguish visually from associated
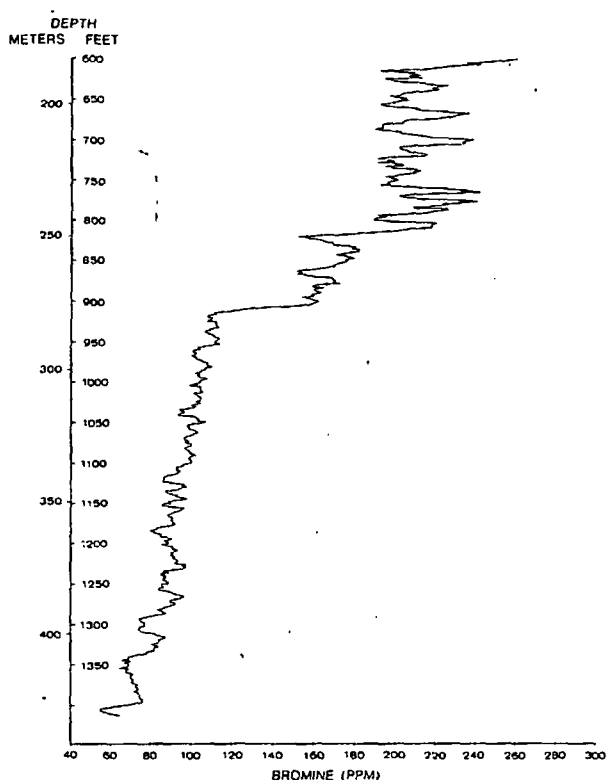
FIG. 6. Bromine distribution through halite of the Lower Salt, Maha Sarakham Formation in the Sakon Nakhon Basin. Halite samples from core hole L-1, near Vientiane, Laos. X-ray fluorescence spectrometer analyses were performed by J. S. Wahlberg, U.S. Geological Survey, Denver, Colorado.

to about 120 ppm through a thickness of about 13 m (Fig. 8A). An initially high bromine content is also characteristic of the basal halite in some of the evaporite cycles of the Paradox Basin (Raup, 1966, figs. 3 and 6). The high bromine values could mean that the basins remained full of brine from the previous cycle of evaporite deposition (Lower Salt). However, as previously stated, there is good evidence that in both the Khorat and Sakon Nakhan Basins the final layer of brine was either completely desiccated or was destroyed during the deposition of the Lower Clastic. Therefore, a more logical explanation of the high bromine content of the basal halites is that they were precipitated from concentrated brines expelled by compaction of the underlying Lower Salt. Considering that the pore water in the upper part of the Lower Salt should be representative of the mother brine from which the great thickness of potash and magnesium salts was deposited, it seems likely that this pore water could have been the highly concentrated source of bromine. Furthermore, nearly all halite beds characterized by basal halite of high bromine content, whether they are on the Khorat Plateau, Paradox Basin, or else-

where, overlie older beds of salts which could have been the source of high bromine pore water.

The bromine profile of the Middle Salt generally shows a very rapid upward increase in bromine. There are, however, numerous breaks in the profile slope which indicate a temporary freshening of the basin brine. These breaks can be correlated over great distances on profiles prepared for this interval from other core holes. These regional correlations allow the determination of how much halite is missing due to dissolution. The maximum bromine value on Figure 8A is about 275 ppm; however, profiles from other core holes show halite at the top of the bed containing as much as 350 ppm bromine. Such high
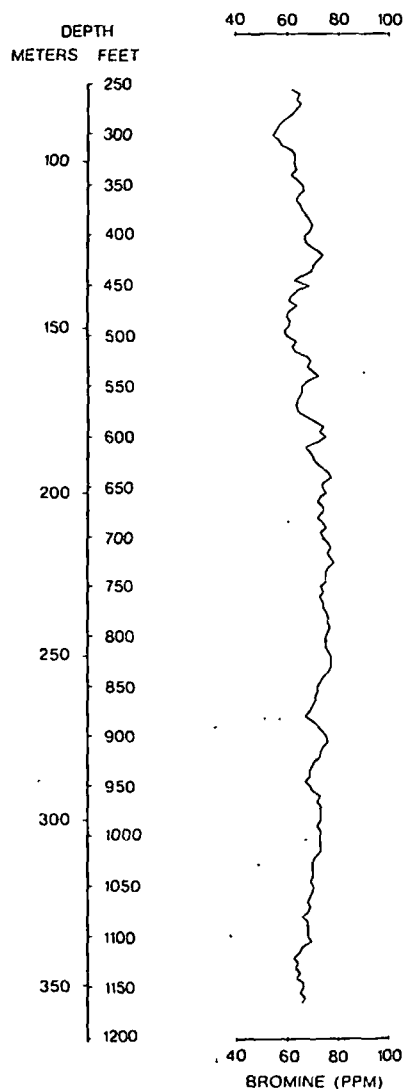
FIG. 7. Bromine distribution through halite of the Lower Salt in the Khorat Basin. Halite samples from core hole K-15 near Khorat, Thailand. X-ray fluorescence spectrometer analyses were performed by H. L. Groves, U.S. Geological Survey, Denver, Colorado.
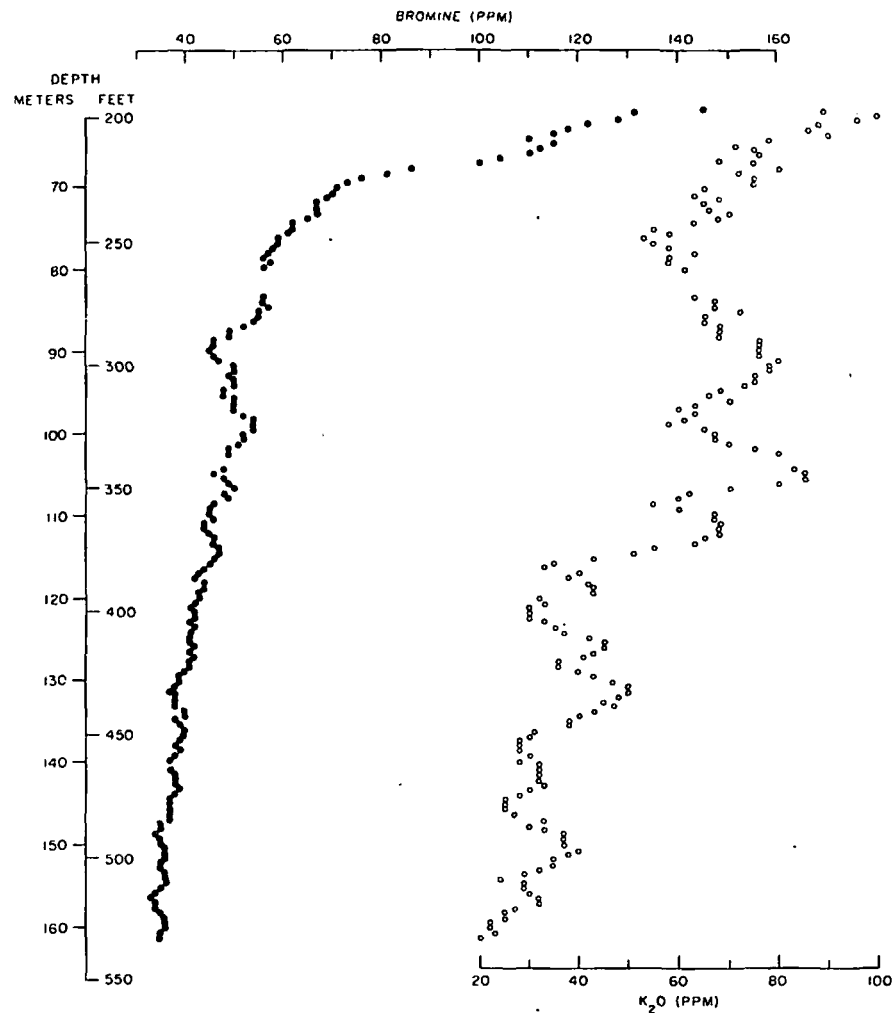
FIG. 5. Bromine and K_2O distribution through halite of the Lower Salt, Maha Sarakham Formation in the Khorat Basin. The core hole is located near Chaiyaphum, Thailand. X-ray fluorescence spectrometer analyses were performed by H. L. Groves, U. S. Geological Survey, Denver, Colorado.

the last halite sample on the profile was not analyzed. The bromine content of the unanalyzed halite would probably have exceeded 300 ppm. A comparison of the two profiles of the Lower Salt shows that the sudden break in the slope on the bromine profile is near 55 ppm in Figure 5 and near 110 ppm on Figure 6. Assuming that this common point on the two profiles is a time-stratigraphic reference, more than 160 m of additional material was deposited at the Vientiane locality. All these factors suggest a salinity gradient between the two locations during the deposition of the Lower Salt.

Several bromine profiles of the Lower Salt in both the Khorat and Sakon Nakhon Basins are drastically different from those in Figures 5 and 6. In these profiles, the bromine content does not increase from the base to the top of the halite bed even though the bed may be as much as 300 m thick (Fig. 7). Halite

from the upper part of these abnormal profiles shows evidence of recrystallization. These relationships suggest that locally the Lower Salt was subjected to leaching by meteoric waters, probably during the deposition of the Lower Clastic, thus causing solution of the original high bromine halite, with attendant recrystallization to low bromine halite.

Bromine geochemistry of the Middle Salt and the Upper Salt

The known bromine distribution in the Middle and Upper Salt is not as complete as that in the Lower Salt, because the younger beds are commonly dissolved. However, enough profiles have been constructed, particularly for the Middle Salt, to establish their bromine signatures.

The basal halite of the Middle Salt starts with a relatively high bromine content (200 ppm) but drops
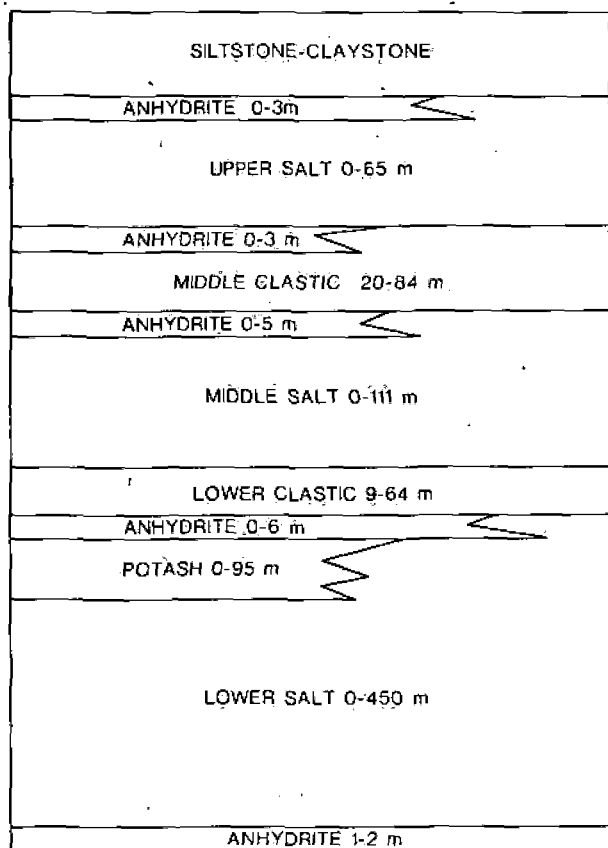
FIG. 3. Informal stratigraphic nomenclature of the Maha Sarakham Formation of Cretaceous age.

Bromine geochemistry of the Lower Salt

The bromine geochemistry of the Lower Salt is known from distribution profiles prepared for about 25 core holes. The first vertical profile of bromine distribution in the Lower Salt was prepared for a core hole drilled on the western edge of the Khorat Basin. This profile (Fig. 5) has a distinctive shape which is also seen in profiles prepared from core holes located deeper in the basin where the halite bed is much thicker. This is also true for bromine profiles from core holes in the Sakon Nakhon Basin (Fig. 6). At the base of the Lower Salt, the bromine content averages about 40 ppm in all core holes. These values are considerably less than the theoretical 75 ppm bromine that is expected in the first crystals of halite precipitated from sea water. They are, however, precisely within the range of bromine values (30–50 ppm) in the basal halites of many other deposits (Holser, 1966, p. 268). As shown in Figure 5, the lower three-fourths of the bromine profile shows a slow but continuous increase in bromine content from the base to the top of the halite bed. Through an interval of nearly 85 m, the bromine content increases by only about 20 ppm. Above this point, the amount of bromine increases rapidly from about 55 ppm to 150 ppm. Another bromine profile of the Lower Salt from a core hole near Vientiane, Laos, shows a similar shape (Fig. 6). This profile does not represent a complete sampling of the Lower Salt, because an additional 52 m of potash overlying
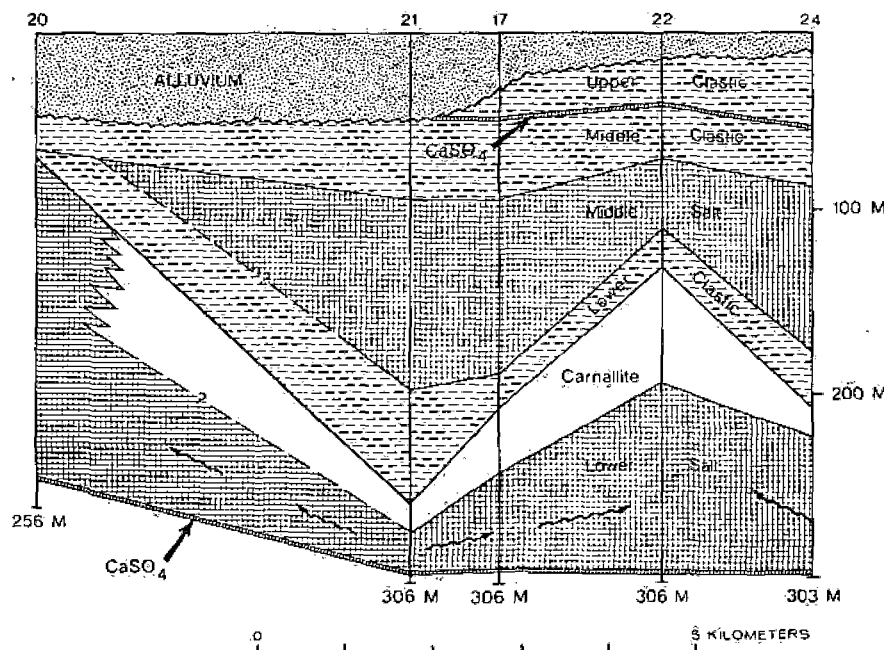
FIG. 4. Cross section through the evaporites and associated clastic rocks of the Maha Sarakham Formation near Khorat, Thailand. The section line trends approximately northeast. Arrows indicate the direction of suspected salt flowage.

depressions on the Lower Salt, the resulting varia-
tions in thickness (9–64 m) created conditions of
differential loading on the Lower Salt. This in turn
caused halite flow to areas of lower pressure (thin
overburden) and the formation of small salt anti-
clines. Once the salt anticlines were established,
they continued to grow because salt transfer from
the adjacent synclines further depressed the site of
initial high-load, thus facilitating greater depositional
accumulation and, in effect, accelerating the whole
process.

4. The salt anticlines continued to grow during
deposition of the Middle Salt, and, as a result, this
unit attained a greater thickness on the anticlinal
flanks. Continued but subdued growth caused gentle
folding of the thin anhydrite bed overlying the Middle
Clastic. Slight additional growth may have con-
tinued through the deposition of the remainder of the
Maha Sarakham Formation; however, drill hole data
are too sparse for verification.

Bromine Geochemistry

Before the Department of Mineral Resources began
a drilling program for potash on the Khorat plateau,
the only data pertaining to the salt deposits in this
area came from about 46 water wells which had
penetrated rock salt and from 5 core holes on the
extreme western edge of the Khorat Basin. Further-
more, no useful geophysical logs were available from
any drill hole. These circumstances presented an
unusual opportunity to use bromine geochemistry to
search for potash deposits. The initial bromine data
suggested that both the Khorat and Sakon Nakhon
Basins probably contained potash deposits (Hite,
1974) and stimulated the Department to undertake
a drilling program which culminated in the discovery
of potash. Since that time, bromine geochemistry
has not only been useful in delineating drilling targets
but has enabled a better understanding of the carnal-
lite-sylvite facies in these deposits.
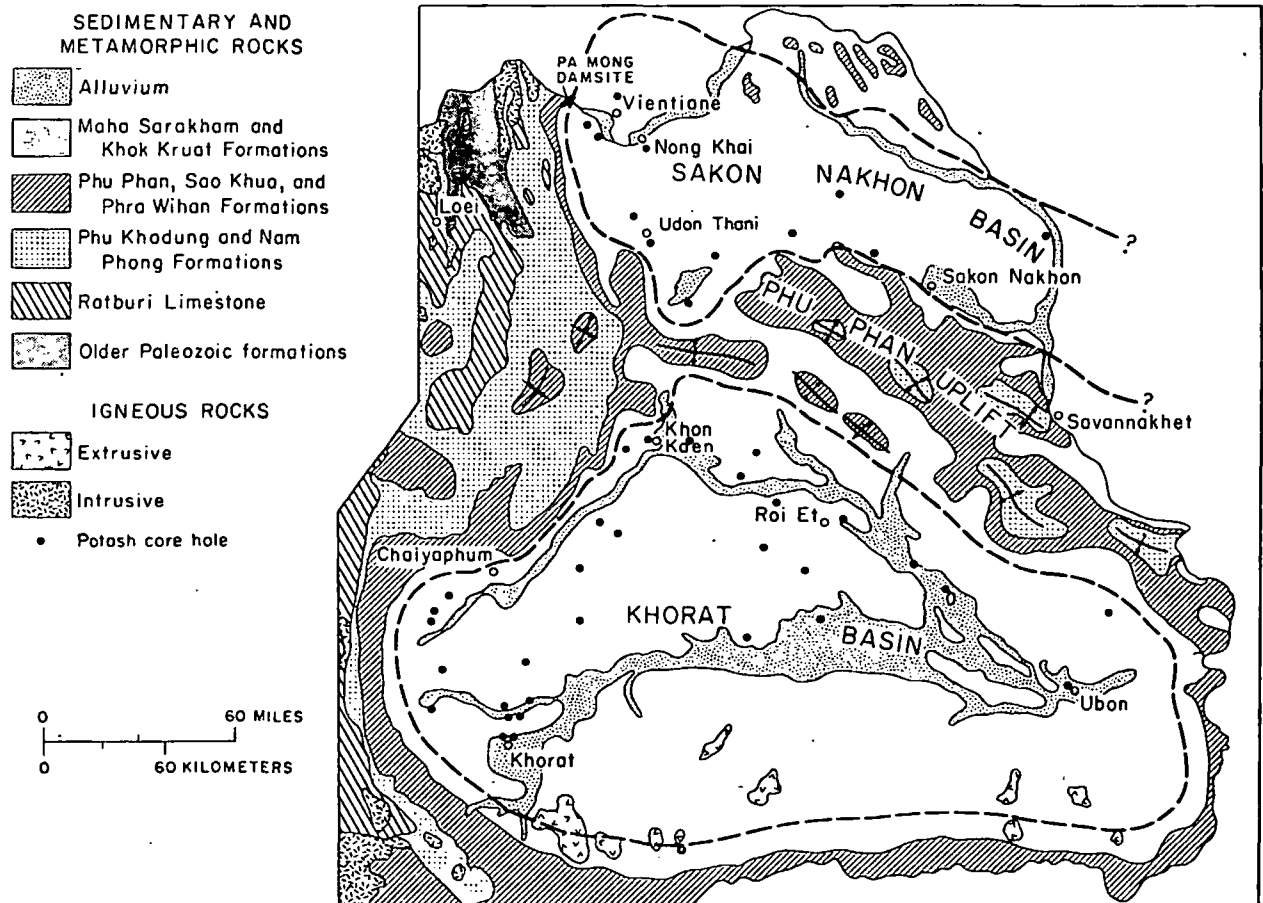
FIG. 2. Geologic map of northeastern Thailand. Where drilling density is high, some of the
core hole locations (black dots) represent more than one hole. Map modified from the
geologic may of Thailand compiled by Jumchet C. Javanaphet (1969).
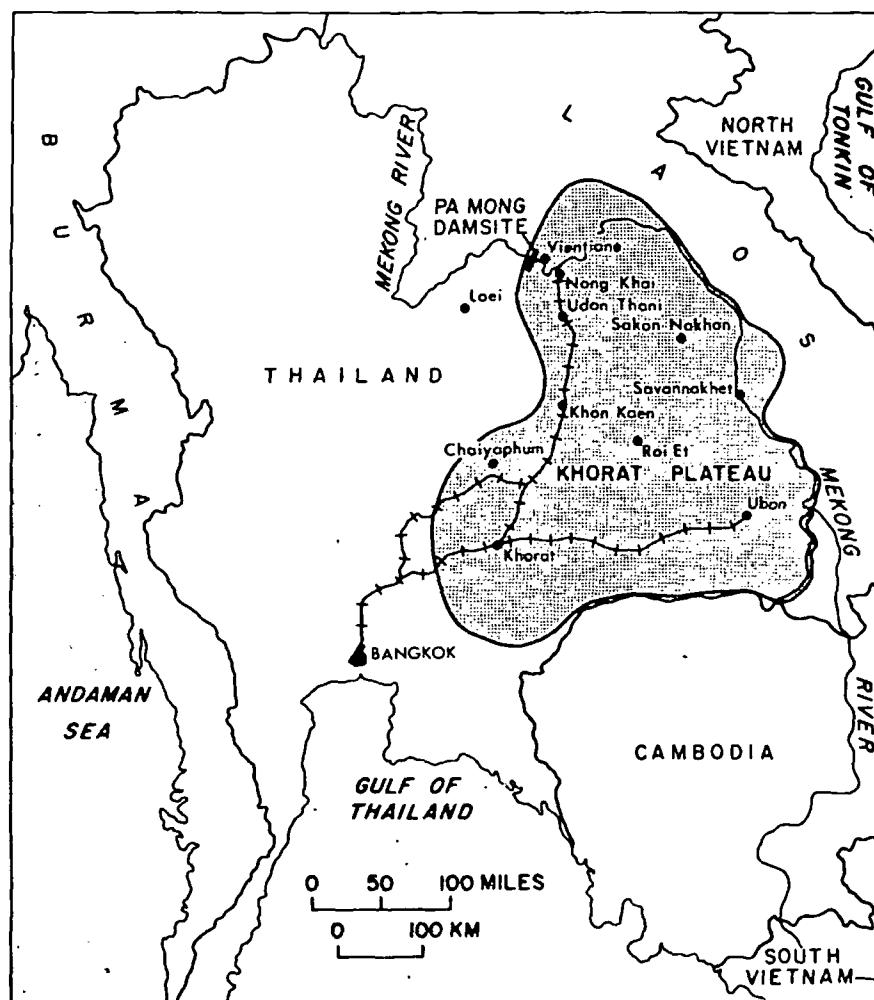
Fig. 1. Index map of the Khorat Plateau. Stippled area shows extent of plateau (Hite, 1974).

separates the Middle Clastic from the uppermost halite bed or Upper Salt. Although the Upper Salt occurs in both basins, it shows an erratic distribution pattern and is absent in many areas because of complete dissolution. No potash minerals have yet been found in this halite bed. Throughout both basins, the Upper Salt is overlain by a sequence of red siltstone and claystone, which contains a few thin units of gypsum or anhydrite in the western part of the Khorat Basin.

The structural geology of the Khorat and Sakon Nakhon Basins is not well known because much of the region has a thick cover of soil and vegetation and too few drill holes have been made. However, in one area near the city of Khorat in the southwest part of the Khorat Basin a cluster of potash exploration core holes has established a local structural style for the Maha Sarakham Formation which may also be characteristic of the entire region. An inter-

pretation of the geology in potash drill holes in this area (Fig. 4) gives a tectonic history for the Maha Sarakham Formation that is summarized as follows:

1. The basal anhydrite of the Maha Sarakham Formation was deposited on a surface of low relief. During or shortly after anhydrite deposition, the basin subsided rapidly to make room for deposition of the thick Lower Salt and to provide restricted conditions necessary to form potash salts. This regional subsidence may have created as much as 50 m of relief on the basal anhydrite.

2. After deposition of the Lower Salt and its associated carnallite, the basin reached a stage of complete desiccation and returned to continental sedimentation. Exposure of the previously deposited highly soluble potash salts brought about local dissolution and development of depressions which were filled by deposition of the Lower Clastic.

3. As the Lower Clastic filled in the dissolution

Potash Deposits of the Khorat Plateau, Thailand and Laos

ROBERT J. HITE AND THAWAT JAPAKASETR

Abstract

Drilling on the Khorat Plateau of northeastern Thailand and central Laos has outlined what may develop into one of the world's largest potash deposits. The potash is in a salt-bearing sequence of Cretaceous age that underlies about 60,000 km² of the plateau. Locally, the deposit is at very shallow depths (90 m), is nearly flat lying, and is as much as 40 m thick. The deposit consists mainly of carnallite, although tachyhydrite and sylvite are also present. High-grade sylvite bodies as much as 34 m thick have been discovered at several localities. The sylvite is apparently the result of leaching of the original carnallite by solutions of unknown origin. In many places the carnallite deposit was completely destroyed, leaving only recrystallized halite. The sylvite bodies seem peripheral to the barren halite, and their size and geometry are not yet known.

Introduction

THE most recent addition to the world's growing list of economically important potash occurrences is found on the Khorat Plateau of Thailand and Laos (Fig. 1). Although this area was known since the 1950s to be underlain by thick deposits of halite, as the result of extensive drilling for potable ground water, it was not until 1973 that potash was discovered by the Thailand Department of Mineral Resources. The discovery hole, located in the city of Udon Thani, intersected a thick and very pure deposit of carnallite. Encouraged by the discovery at Udon Thani, the Department drilled a second location near Nong Kai bordering the Mekong River and also found a thick carnallite deposit. In 1974, United States Agency of International Development drilled a potash test about 15 km north of Vientiane, Laos. This hole intersected a thick deposit of high-grade sylvite. By early 1978, the Department had drilled about 80 core holes for potash, and the results of this drilling suggest that the Khorat Plateau potash may develop into one of the world's largest deposits. Contrary to most potash discoveries, which were a by-product of petroleum exploration, these deposits were found by a direct exploration effort.

Regional Geology

The Khorat Plateau is an area of about 170,000 km² in northeastern Thailand and central Laos. It forms a large blocklike platform between two structurally complex orogenic belts which trend north-south along its east and west boundaries (Fig. 2). The bed rock of the plateau consists of a continental sequence of red beds of Mesozoic age. The Phu Phan uplift or anticlinorium trends east-west across the plateau and divides it into the Khorat Basin on the south and the Sakon Nakhon Basin to the north.

The size, structural configuration, and Mesozoic sedimentary sequence of the plateau are strikingly similar to the Colorado Plateau in the United States.

The potash deposits of the Khorat Plateau are in the Maha Sarakham Formation of Cretaceous age. This formation is present only on the Khorat Plateau. North, in the Sakon Nakhon Basin, the formation extends over an area of about 21,000 km². South, in the Khorat Basin, the formation covers a slightly larger area of about 36,000 km². The maximum thickness of the formation in either basin is unknown, but it could exceed 1,000 m. The Maha Sarakham Formation consists of a continental red-bed sequence of siltstone, sandstone, and shale, which are intercalated with marine evaporites (Fig. 3). The basal unit of the sequence is a thin but persistent anhydrite bed that occurs throughout both the Khorat and Sakon Nakhon Basins. This anhydrite is overlain by the Lower Salt which is the host rock for the potash deposits of the Khorat Plateau. The Lower Salt, which probably represents the thickest continuously deposited halite layer in the world, locally is 450 m thick. For most of the area, the Lower Salt is overlain by the Lower Clastic, which is chiefly a red claystone. In the western third of the Khorat Basin, these two units are separated by an erratically distributed anhydrite bed that attains its greatest thickness (6 m) along the western edge of the basin.

Above the Lower Clastic is another halite unit, referred to as the Middle Salt. This bed is found in both the Khorat and Sakon Nakhon Basins; however, it is missing in many core holes in both basins due to dissolution. Locally, trace amounts of sylvite occur in drill cores from this bed. The Middle Salt is overlain by a red claystone unit, called the Middle Clastic, except along the western margin of the Khorat Basin where a thin anhydrite bed is present. Another thin anhydrite unit in this same area

PHYSICAL EFFECTS IN ROCK UNDER NEGATIVE EFFECTIVE PRESSURES: SOUND SPEEDS AND HYDRAULIC DIFFUSIVITY

T. J. Shankland

Geophysic[
Los Alamos Natic
Los Alamos, Nev

New engineering techniques such as compressed air or pumped hydro energy storage and hot dry rock geothermal energy often use injections of high pressure fluids into rock masses. Especially in the latter case, pore pressure fields may exceed lithologic stress and produce an effectively negative confining pressure. Since physical characteristics of rocks are known to change markedly with confining pressure, measurements of constitutive relations and transport properties under negative effective pressure are needed. We have developed a method for creating negative effective pressure in the laboratory and have measured longitudinal sound speed and gas diffusivity under these conditions.

The pressure field is created inside an annulus of fluid injection holes in a cylindrical sample; fluid flows radially outward down the pore pressure gradient to the sample's exterior. We monitor pore pressure through capillary probes and find the pressure field to be uniform inside the injection ring. With pore fluid pressures to 1.2 MPa we observed decreases in both acoustic velocity and amplitude in an unconfined sample of fine-grained granite. The velocity decrease is about 1.5% per MPa while amplitude decreases by approximately 10% per MPa. By measuring pressure relaxation for stepwise pore pressure increases, we determined increases in gas diffusivity of approximately a factor of three between 0 and -1 MPa effective pressure. Thus, in engineering techniques using high fluid pressures small changes in seismic velocity can indicate large permeability changes.

INTRODUCTION

In this paper we describe sound velocity, attenuation, and permeability measurements on rocks in which the effective pressure has been extended to negative values. Effective pressure P_e is given by

$$P_e = P_c - P_p \qquad (1)$$

where P_c is confining pressure and P_p is pore fluid pressure. This work expands on earlier presentations by Halleck and Shankland (1980). Under most natural conditions and all laboratory situations P_e is positive; yet the condition of zero or negative P_e occurs in some interesting and important circumstances. Natural conditions may include the case of artesian aquifers or injection of magma and volatiles prior to volcanic eruptions; artificial situations include those during hydrofracture in secondary oil recovery or during flow in man-made geothermal systems created by hydrofracture at depth.

Apart from practical considerations, these experiments introduce a new regime for understanding physics of rocks. Do the theories that describe elastic properties as functions of crack density and distribution of pore shapes still apply to rocks under tension? How great are changes of transport properties such as permeability? Are there noticeable changes at the critical region where P_e goes from positive to negative? The present work is a beginning attempt to examine these issues.

EXPERIMENTAL METHODS

We have created negative effective pressure or pore-pressure-induced tension by injecting fluid into an unconfined cylindrical rock specimen of diameter 10.2 cm and thickness 3.87 cm. The rock is Elberton (Georgia) granite.

As shown in Figure 1 the eight equally spaced injection holes are axial and located on a circle of radius 2.54 cm halfway between the center and outside of the cylinder. Epoxy end caps confine the steady-state flow pattern to the radial direction and create a stagnant central region. We monitored pore pressure at three points using capillary tubes connected to pressure transducers; two inside the injection holes at radii 0 and 1.91 cm and 1 outside at radius 3.81 cm. Measured pore pressure in the central region was uniform to 10%. We kept pore pressures below 1.2 MPa to avoid fracturing the specimen.

Compressional velocity was measured in the axial direction using the pulse overlap method (Mattaboni, 1967) at frequencies in a 200-600 KHz range. Acoustic transducers were cemented to the end surfaces inside the central region at a radius of 1.65 cm. Although absolute velocities at zero pressure were reproducible to about 1%, relative measurements within a given pressure run had a standard deviation of 0.2%.

Our procedure consisted of raising injection pressure in stepped increments and monitoring pore pressures. After pore pressure stabilized at each increment, we measured compressional wave velocity.

where a = cylinder radius, here taken as the injection radius. J_o and J_1 are Bessel functions of zero and first degree, and the α_n are roots of $J_o(\alpha_n a) = 0$. Figure 4 shows this theoretical response plotted against dimensionless time variable Dt/a^2; also shown are experimental curves for $P_e(\infty) = 0.9$ MPa at three trial values of D. The best fit to the response at high P_p is $D = 0.015$ cm²/s. The corresponding diffusivity for the step from 0 to 0.1 MPa is 0.005 cm²/s, lower by a factor of three. The poor fit at the beginning is probably due to departures from the assumption of constant β_f. For these experiments the compressibility of the gaseous fluid dominates rock compressibility, and it is therefore responsible for most of the change of D.

VELOCITY VARIATIONS

Figure 5 depicts changes of axial compressional velocity with decreasing and increasing P_e, and Figure 6 shows relative changes in velocity with P_e in a different run. The intercepts $V(0)$ do not agree to within a standard deviation because of the difficulty of matching waveshapes in the pulse overlap method after changes have been made. Within a given pressure run we kept the waveshapes constant and achieved better reproducibility. The pressure coefficients agree well at values of 0.060 ± 0.009 and 0.067 ± 0.008 km s⁻¹ MPa⁻¹ or about $1.6 \pm 0.2\%$ MPa⁻¹. There is an apparent difference of pressure coefficient and of intercept between rising and falling pore pressures. However, velocity is restored to its original value after an overnight wait. In the absence of confining pressure several hours are required for pore fluid to be removed; there may also be a relaxation due to internal friction on crack surfaces.

Figure 5. Measured velocity vs. effective pressure for test 2. Dark circles are velocities measured during pore pressure increase; a least squares fit, $V = 3.967 (\pm.005) + 0.067 (\pm.008) P_e$ (MPa) is shown by the straight line. Open triangles are data taken during pore pressure reduction; velocity returned to near the original value overnight.
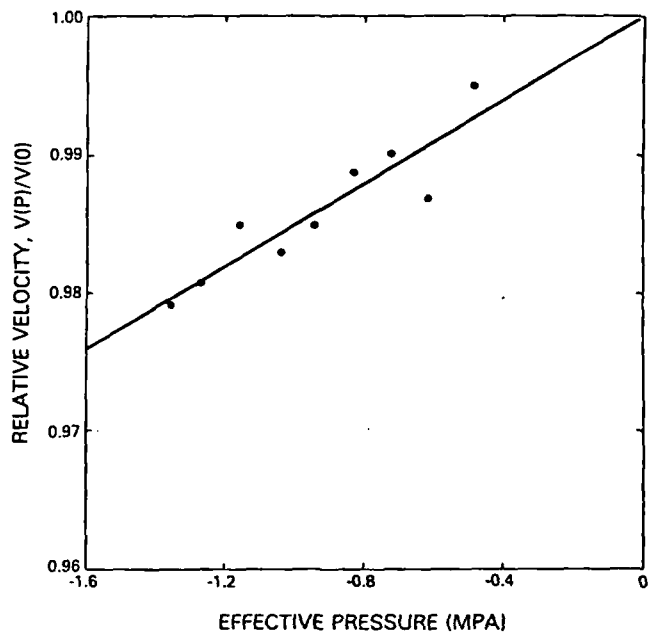

Figure 4. Trial fits of measured relaxation data for test 3. $P(\infty) = 0.8$ MPa. The heavy dashed line is a dimensionless theoretical response for ideal cylindrical geometry. The best match to the theoretical curve is for a diffusivity $D = 0.015$ cm²/S.

Figure 6. Relative velocity change for test 1. All data were taken during pore pressure increase. The best fit line is $V(P)/V(0) = 1.000 (\pm.002) + 0.015 (\pm.002) P_e$ (MPa). The starting velocity was 4.006 km/S.

As yet we have not made these measurements with confining pressure in order to investigate the transition region at $P_e=0$. However, the velocity and its derivative with negative P_e seem to be in the ranges for other granites at positive, low P_e (Birch, 1961; Warren, 1977, 1979). A continuous velocity variation can be expected from theories in which the major velocity variation results from change of crack density (O'Connell and Budiansky, 1977). It is not clear that this should be the case in theories where cracks contain asperities (Gangi, 1978; Walsh and Grosenbaugh, 1979; Walsh, 1981). Brace's (1971) measurements of Young's modulus show a smooth variation through zero stress for the case of uniaxial compression-tension.

DISCUSSION

The man-made geothermal reservoir created in the Los Alamos Hot Dry Rock Project affords an interesting field comparison. Acoustic transmission measurements were made between adjacent boreholes in granite at about 3 km depth. Fehler (1979) calculated that velocity in a frequency range near 10^4 Hz decreased by about 2% on pressurizing the reservoir. More striking were the increases of permeability and static compressibility inferred by Fisher and Tester (1980) on the basis of pumping tests in the reservoir. Thus it appears that in the regime of negative effective pressures very small changes of dynamic elastic moduli can indicate far larger changes in fluid permeability and in static moduli. In order to directly check these effects we are presently conducting experiments in which fluid flow and static moduli are determined directly.

CONCLUSIONS

In this work we report results of rock physics experiments under the novel condition of negative effective pressure. Physical properties measured with rocks in tension have been only rarely reported in the literature (Brace, 1971), yet with increasing use of pumped fluids in geo-engineering practice this regime will see greater study and theoretical development. In our experiments we have measured modest velocity changes with negative effective pressure, 1.5%/MPa, and very large changes, more than a factor of three over 1 MPa range, in hydraulic diffusivity.

ACKNOWLEDGMENTS

REFERENCES

Birch, F., 1960, The velocity of compressional waves in rocks to 10 kb, Part 1, Journal Geophysical Research, 65, pp. 1083-1102.

Brace, W. F., 1971, Micro-mechanics in rock systems, in Structure, Solid Mechanics, and Engineering Design, edited by M. Te'eni, Wiley-Interscience, New York, pp. 187-204.

Carslaw, H. S. and J. C. Jaeger, 1959, Conduction of Heat in Solids, 2nd Ed., Oxford University Press, Oxford.

Fehler, M., 1979, Seismological investigation of the mechanical properties of a hot dry rock geothermal system, Thesis, Massachusetts Institute of Technology, Cambridge, Massachusetts.

Fisher, H. N. and J. W. Tester, 1980, The pressure transient testing of a manmade fractured geothermal reservoir: an examination of fracture versus matrix dominated flow effects, Los Alamos National Laboratory Informal Report LA-8535-MS, Los Alamos, New Mexico.

Gangi, A. F., 1978, Variation of whole and fractured porous rock permeability with confining pressure, International Journal Rock Mechanics Mining Science & Geomechanical Abstr., 15, pp. 249-257.

Halleck, P. M. and T. J. Shankland, 1980, Sound speed measured under negative effective pressure, EOS Trans. AGU, 61, 1102.

Mattaboni, P. and E. Schreiber, 1967, Method of pulse transmission measurements for determining sound velocities, Journal Geophysical Research, 72, pp. 5160-5163.

O'Connell, R. J. and B. Budiansky, 1977, Viscoelastic properties of fluid-saturated cracked solids, Journal Geophysical Research, 82, pp. 5719-5735.

Scheidegger, A. E., 1974, The Physics of Flow Through Porous Media, 3rd Ed., University of Toronto Press, Toronto.

Walsh, J. B., 1981, Effects of pore pressure and confining pressure on fracture permeability, in press.

Walsh, J. B. and M. A. Grosenbaugh, 1979, A new model for analyzing the effect of fractures on compressibility, Journal Geophysical Research, 84, pp. 3532-3536.

Warren, N., 1977, Characterization of modulus-pressure systematics of rocks: dependence on microstructure, in The Earth's Crust, edited by J. G. Heacock, Geophysical Monograph 20, American Geophysical Union, Washington, D.C., pp. 119-148.

Warren, N., 1979, Rock physics characterization of Conway granite from a DOE borehole, Conway, New Hampshire, Los Alamos National Laboratory Informal Report LA-8102-MS, Los Alamos, N.M.

THE PRODUCTION OF ELASTIC WAVES BY EXPLOSION PRESSURES. I. THEORY AND EMPIRICAL FIELD OBSERVATIONS*

JOSEPH A. SHARPE†

ABSTRACT

A solution to the problem of the wave motion produced when a pressure of arbitrary form is applied to the interior surface of a spherical cavity in an ideally elastic medium is derived. This solution is shown to be in qualitative agreement with a number of field observations of the effect of shot-point conditions on the characteristics of reflection seismograph recordings.

INTRODUCTION

Of the three physical processes involved in seismic exploration, namely, the initiation of the seismic waves, their propagation, reflection, refraction, and dispersion, and the recording of some function of the motion of the surface, we possess the least satisfactory understanding of the initiation process. This is in spite of the circumstance that it has been recognized from the very beginnings of reflection exploration that the intensity, quality, and characteristics of seismic records are strongly influenced by conditions at the shot point, and despite the fact that a number of empirical observations concerning the generation of seismic waves have accumulated over a long period of field experience.

These empirical observations, which have become a part of the lore of every field operator, are as follows:[1]

1. A given amount of explosive detonated in a clay or water-saturated sand formation results in a greater amplitude of reflected motion than an equal charge detonated in a dense, rigid formation, such as limestone.

2. If a hole is sprung by an initial large charge in order to form a sizable cavity, later small charges will result in a larger amplitude

of reflected motion than v
ing.

3. The frequency spect
formation in which the ch
zone result in very low f
below the low velocity zor
limestone, result in a much
in, for example, a shale; in
of reflected motion increas

4. The frequency spec
charge size, a larger charge
tion of low frequencies in t

5. The amplitude of re
tity of a high speed explo
greater than that produce
such as black powder, even
that the maximum pressur

That there has been cor
conditions on reflections re
which relate to means of c
order to secure reflection
These patents fall into thre
of the shooting cavity, to in
explosive energy into the g
that formation as the site
to produce correlatable reco
which are intended to impar
is rich in the frequency com
recorded reflection.[5]

As part of a long-range p
investigated the mechanism
sives and the influence on r
point. This investigation has
matical, with the objective
mechanism of the initiation

[1] See McReady. GEOPHYSICS, V, 4, pp. 374, 379–381 (1940) and Beers, VI, 1 (1941), pp. 54–55.

[2] See Nash and Martin, GEOPHY
properties of explosives.

[3] Johnson, U. S. #2,028,286; We
493.

[4] Weatherby, U. S. #2,154,548; I

[5] Scherbatskoy, U. S. #2,156,198

A PLAN FOR DETERMINING
THE FEASIBILITY OF IN SITU
LEACHING OF NATIVE COPPER ORES

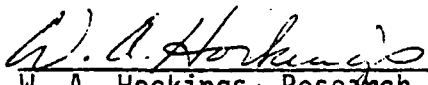Prepared for:

HOMESTAKE COPPER COMPANY
CALUMET, MICHIGAN

By the

INSTITUTE OF MINERAL RESEARCH
MICHIGAN TECHNOLOGICAL UNIVERSITY
HOUGHTON, MICHIGAN

June 14, 1974

W. A. Hockings, Research Fellow   W. L. Freyberger, Director

June 14, 1974

.Mr. O. E. Anderson
Homestake Copper Company
P. O. Box 386
Calumet, Michigan   49913

Dear Mr. Anderson:

    We are pleased to enclose with this letter fifteen (15) copies of a report
entitled "A Plan for Determining the Feasibility of In Situ Leaching of Native
Copper Ores". This report outlines a plan for Homestake Copper Company for
research and development studies on in situ leaching of native copper ores.
The plan presents an orderly and systematic approach to the studies, starting
from small-scale experiments up through the design, construction and operation
of a pilot plant.

    The major features of the plan include gathering information on ore
reserves and their amenability to in situ leaching, developing methods of
preparing ore for leaching, establishing proper environmental control of leach-
ing systems and conducting engineering and economic analyses of leaching
systems. Recommendations for project management and control are presented,
together with a schedule of study and estimated budgets.

    Because of the nature of the research and the unknowns involved at this
time in designing a long range plan, the estimates of time, effort and costs
for the research may not prove to be very accurate. This is particularly true
for estimates of the later stages of the program.

    An important aspect of the plan as presented is that provisions have been
recommended for close control over the program at all times. Such control is
absolutely essential to insure that the research is conducted in the most
efficient manner and that all experiments will be conducted in an acceptable
manner.

    We greatly appreciate the opportunity to have prepared this plan for
Homestake Copper Company and trust you will find the report satisfactory.

                                    Sincerely,

                                    Wilfred L. Freyberger
                                    Director
                                    Institute of Mineral Research

/mjp

Enclosures

TABLE OF CONTENTS

TABLE OF CONTENTS (cont'd)

LIST OF FIGURES

INTRODUCTION

The potential value and advantages of the application of in situ leaching to recovery of copper from native copper ores of the Keweenaw Peninsula have been broadly described in a previous report (Institute of Mineral Research, 1972).. Several alternative methods of conducting such leaching were outlined. At present, this application of in situ leaching is largely in the conceptual stage.

Research toward implementation of the process is being conducted on a limited scale by the Institute of Mineral Research and by the U. S. Bureau of Mines at their Salt Lake City Research Center. This research must be expanded in scope and magnitude to complete process development in a reasonable period of time.

Homestake Copper Company has contracted to have the Institute of Mineral Research prepare for Homestake a plan of research and development with the following broad objectives: to determine the feasibility of in situ leaching as a method of processing native copper ores, to determine the most useful areas of application in the native copper district and to determine which method or methods of leaching offer the greatest promise of successful application. This report describes the plan recommended by IMR to Homestake Copper Company.

General Philosophy of the Plan

Specific goals of the studies included in the plan are as follows: 1) to gather general data concerning deposits in the district to assess the amenability of each toward processing by in situ leaching; 2) to make engineering, environmental and economic evaluations of conceptual in situ leaching systems; 3) to obtain process design information necessary for

development of useful leaching systems; 4) to identify ore deposits for which in situ leaching appears useful and to select leaching systems preferred for those deposits; 5) to select a preferred site (or sites) for location of a pilot-scale operation; and 6) to design, construct and operate one or more pilot-scale in situ leaching systems.

There is no precedence for the application of in situ leaching being considered in this plan. Therefore, accurate prediction at this time of the effort required for any given part of the overall study is not always possible. Fairly large uncertainty factors should be applied to the estimates given in this report for time, effort and money necessary to complete the program. Furthermore, a mechanism is necessary for close assessment of the program at any moment to insure that studies are being directed along proper avenues and that unprofitable research be identified and terminated as early as possible.

A basic assumption inherent in the design of the plan is that there are many deposits of native copper ore potentially suitable for in situ leaching. Furthermore, there are several methods of leaching which potentially may be applied. Present knowledge of the process is inadequate to permit focusing solely on one particular deposit or on one particular method. Indeed, one of the major objectives of the plan is to obtain information on a sufficient variety of ore types and leaching methods so that useful deposits and useful methods, if any, can be rationally identified.

This does not mean that every method must be tested on every ore in the district. This would be an impossible task. Limitations of time and money will require that engineering judgments be made frequently on the basis of information on hand plus general experience, so that emphasis will be placed on deposits and methods which appear the most promising.

Accordingly, the plan has been structured to gather certain forms of information on a broad scale, with a minimum of effort and early in the program, to provide a base for subsequent judgments. Then, as these judgments direct, more detailed information will be gathered on a narrower scale, ultimately focusing on the information needed for design and operation of a specific pilot plant. Obviously, the plan must provide frequent opportunity for making necessary judgments by dividing the effort into a number of discrete blocks, none of which extends overly long in time. Such division will also allow the necessary flexibility to insure that blind alleys are not followed unduly long and that emphasis can be readily shifted to more profitable studies.

Principal Features Requiring Study

Determination of the feasibility of the in situ leaching process involves study of the following major items: 1) Ore Reserves - the parameters of potentially useful ore reserves must be detailed and the amenability of each reserve estimated; 2) Ore Preparation - the ore must be prepared to provide access of leach solutions to the deposit; 3) Leaching and Copper Recovery - the ore must be treated with leach solution to provide for recovery of copper at an economically acceptable rate and copper must be removed from pregnant solutions in the form of a useful product; 4) Environmental* Constraints - the environmental constraints within which the system must operate must be determined, their influences assessed, and provision made to insure proper operation of the system; 5) Engineering and Economic Analyses - total in situ leaching

---

* Throughout this report the terms "environmental", "environment", etc., connote health and safety aspects as well as impact on the physical surroundings.

processes must be designed in concept and analyzed for engineering and economic feasibility; 6) Pilot-Scale Testing - the potential deposits of the district must be surveyed, the best candidate(s) selected and a pilot-scale operation of sufficient scale established to confirm process utility, obtain process design data for scale-up, and identify problems requiring further study.

Project Management

Because of the complexity of the studies required in this program and because of the need to make frequent assessment of progress and judgments pertaining to further work, proper management is essential. For this purpose a Project Manager supported by a Steering Committee is suggested. The Steering Committee should comprise the Research Managers concerned with specific areas of study: Ore Preparation, Leaching and Copper Recovery, Geology and Ore Reserves, Environmental Control, and Economic Analysis - five members in all. The Project Manager may be one of these five, but preferably should be someone removed from the details of any given phase of the study.

Ultimate authority should reside with the Project Manager. He should meet frequently with the Steering Committee. The Project Manager will be responsible to Homestake Copper Company.

An Advisory Committee will also be desirable. This Committee should include members capable of offering advice and assistance in the various phases of the study, plus other interested parties. The Steering Committee should meet with the Advisory Committee at least semi-annually, and should keep the Advisory Committee informed of progress between meetings.

Both the Steering Committee and the Advisory Committee should be formed as soon as possible to establish and maintain proper control of the program.

SCOPE AND PROCEDURES OF RESEARCH

In this section of this report, the scope of study for each of the principal features requiring study is discussed individually to the extent possible at this time. The final section of the report discusses implementation of the program in terms of manpower and funding requirements together with an estimated schedule of work.

Identification and Amenability of Ore Reserves

Early identification of potentially useful ore reserves is imperative. This information is important from several standpoints: 1) Such information will establish the potential scope of application of the process in the district; 2) it will determine whether initial studies may be limited to one ore type, conglomerate or amygdaloid, or whether both must be included from the beginning; 3) the data will be necessary in making preliminary economic assessments of application to a given deposit; 4) the data will be useful in designing conceptual in situ leaching processes for engineering and economic analysis. Whenever possible, samples of ore from potentially useful deposits should be obtained for laboratory examination and amenability testing.

Tabulation of reserves. An initial screening study should be made to classify individual deposits as rapidly as possible according to their potential utility. Those eliminated will require no further immediate attention; for those of interest additional details will be gathered as required. As early as possible the Steering Committee should prepare a list of desired data so that the deposits will be properly evaluated. The desired data will include for example such parameters as size and grade of the deposit, ore type, dimensions, surrounding hydrological conditions, porosity, permeability, and manner of copper occurrence. Obviously, not all of this information can be obtained quantitatively.

However, even best estimates or qualitative descriptions will be useful in evaluating the deposits.

Most of the information pertaining to potential reserves will of necessity come from company files. In addition, laboratory examination and amenability testing will be desirable on as many different ore samples of interest as can readily be obtained.

Laboratory examination of ore samples. Laboratory examination will include basic mineralogical examination, observation of the manner of copper occurrence, measurement of porosity and other measurements or observations as appear significant to assess the potential utility of the ore.

Mineralogical studies will include macro-microscopic examinations. The principal information sought will be to identify major mineral components of the ore, the mineralogical association of the copper, and general observation of the presence of porosity in the rock. An example of the potential utility of such information is that the calcite present in Iroquois ore is closely associated with copper. Since the calcite is likely to fracture very readily on blasting, there is a distinct possibility that with such an ore substantial amounts of copper can be exposed to leaching with a minimum of fracturing of the ore.

The manner of occurrence can be evaluated from mineralogical examinations as well as by estimating copper grain size distributions by means of staged crushing and screening of the ore. It can also be evaluated by means of electronic sorting tests, employing laboratory-scale sorting devices. Such information, particularly in terms of the connectivity of the copper, is significant in estimating the fraction of copper potentially recoverable from the ore. Porosity measurements, as made by established methods, are also of significance in estimating amenability toward in situ leaching.

6

Amenability leaching tests. Amenability testing will consist of a standard leach test conducted on a sample of crushed and sized ore. Exact definition of desirable standard leaching conditions will depend on the results of leaching tests presently underway at IMR with several different ore types and different leaching conditions. However, it is anticipated that strong leach solutions and relatively small ore pieces will be used in order to obtain significant leaching data in a short period of time. Amenability tests will not be conducted to completion. Instead, initial leaching data will be evaluated on the basis of a kinetic model of leaching presently being developed. It is recommended that studies be conducted on a number of "extreme" ore types to estimate the range of leachability of the ores in the district.

Indirect estimation of amenability. At the present time the amenability of an ore to leaching can only be determined by conducting an actual leach test such as those described. The principal disadvantage of this procedure is that it is very slow, particularly for large ore pieces where many months may be required. The desirability of estimating amenability indirectly is apparent.

Present research has suggested indirect estimation of amenability to leaching may be possible, at least in a semi-quantitative manner. Leaching tests at IMR on two conglomerate ores and one amygdaloid ore show direct correlation between leaching results and porosity measurements. This very simple correlation is undoubtedly only part of a more complete and accurate method of indirect evaluation. Further study of relations for the ore types presently under study will serve to identify their potentially useful correlations. The ideas developed in the present study will need confirmation and refinement through similar laboratory measurements and leaching studies made with other ore samples.

7

Therefore, the desired laboratory examination and amenability leaching studies will serve two significant purposes: they will provide necessary information pertaining to the potential application of in situ leaching to particular deposits, and they will serve as a basis for development of a more rapid indirect evaluation of utility of other deposits through ranking of a new ore against a semi-quantitative scale of amenability developed from laboratory studies on a variety of ores.

Ore Preparation

Preparation of the ore in order to provide access of the solution to the copper is probably the most critical operation affecting the feasibility of in situ leaching. There are a number of methods by which an ore deposit might be prepared for leaching and each method must be tested to determine its potential utility. Since the methods are largely dependent on the structural characteristics of the undisturbed ore, much of the testing must be performed underground. The variability between and within ore deposits requires testing a number of ore types and performing replicate tests on each ore type.

The four major methods of ore preparation are: 1) bore-hole leaching; 2) bore-hole fracturing; 3) open fracturing; 4) abandoned mine preparation. Research programs for testing the methods are described below:

Bore-hole leaching. This method of ore preparation is one of the simplest. It consists of drilling holes into the formation and utilizing the natural permeability and porosity of the ore to provide pathways for solution flow from one hole to another. The natural porosity would also provide contact of the solution with the copper. This method of leaching is probably considered to be the least feasible because of the dense appearance of the native

copper ores. However, the ores tested to date show considerably more porosity (about 5%) than one would expect, and if the pores are sufficiently connected then bore-hole leaching may indeed be feasible.

In order to study bore-hole leaching, it will be necessary to measure the amount of rock connected by pores to a bore-hole (pore connectivity) and the permeability between bore-holes. These measurements must be performed on undisturbed underground formations.

The first step in determining pore connectivity will consist of core drilling a hole down the dip of the formation. The length of the hole should be about 30 to 50 feet, and the diameter of the hole should be about 3 inches. The porosity of the core will be measured in the laboratory with a gas pycnometer. The hole will be dried and a packer with an inlet tube will be installed half-way down the hole. The top half of the hole will be sealed with resin, as shown in Figure 1. The purpose of sealing this portion of the hole is to confine the measurements to the bottom half of the hole where the ground is undisturbed. It will also prevent the gas used in the measurements from leaking to the surface.

The hole will then be evacuated and helium gas from a calibrated cylinder will be allowed to expand into the hole and the pores of the surrounding rock. The apparatus is shown schematically in Figure 2. Given the volumes of the cylinder, hole, and inlet tube - V_c, V_h and V_z, and the initial and final pressures - P_1 and P_2, then the pore volume of the rock surrounding the hole can be calculated:

$$V_p = (P_1/P_2-1)V_c - V_h - V_t$$

Since the porosity of the ore, denoted by e, will be known from the measurements on the core, the effective radius of the pore-connected rock can be calculated from:
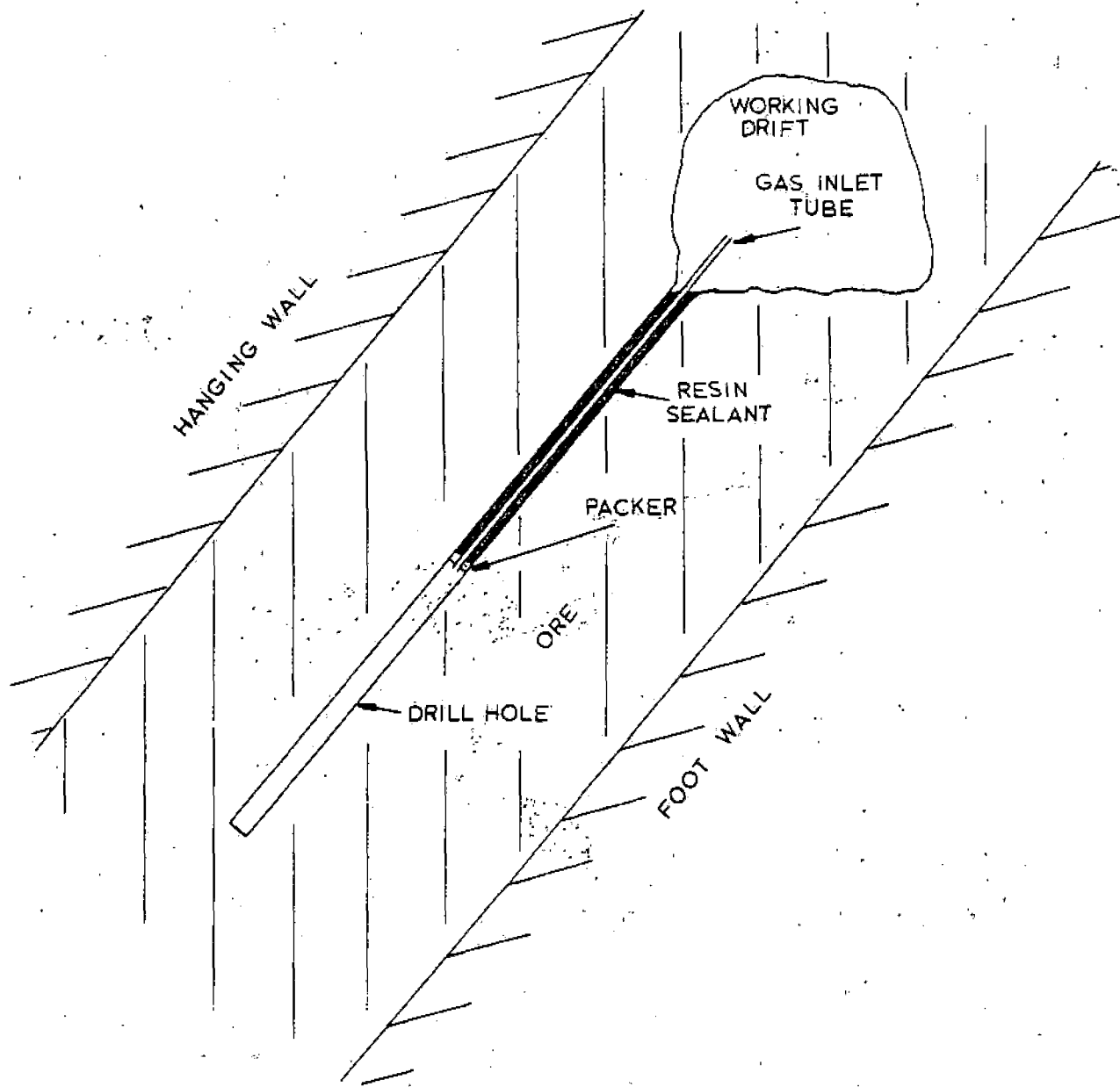
9

Figure 1. Arrangement and Preparation of Drill Hole for Measuring In Situ Porosity
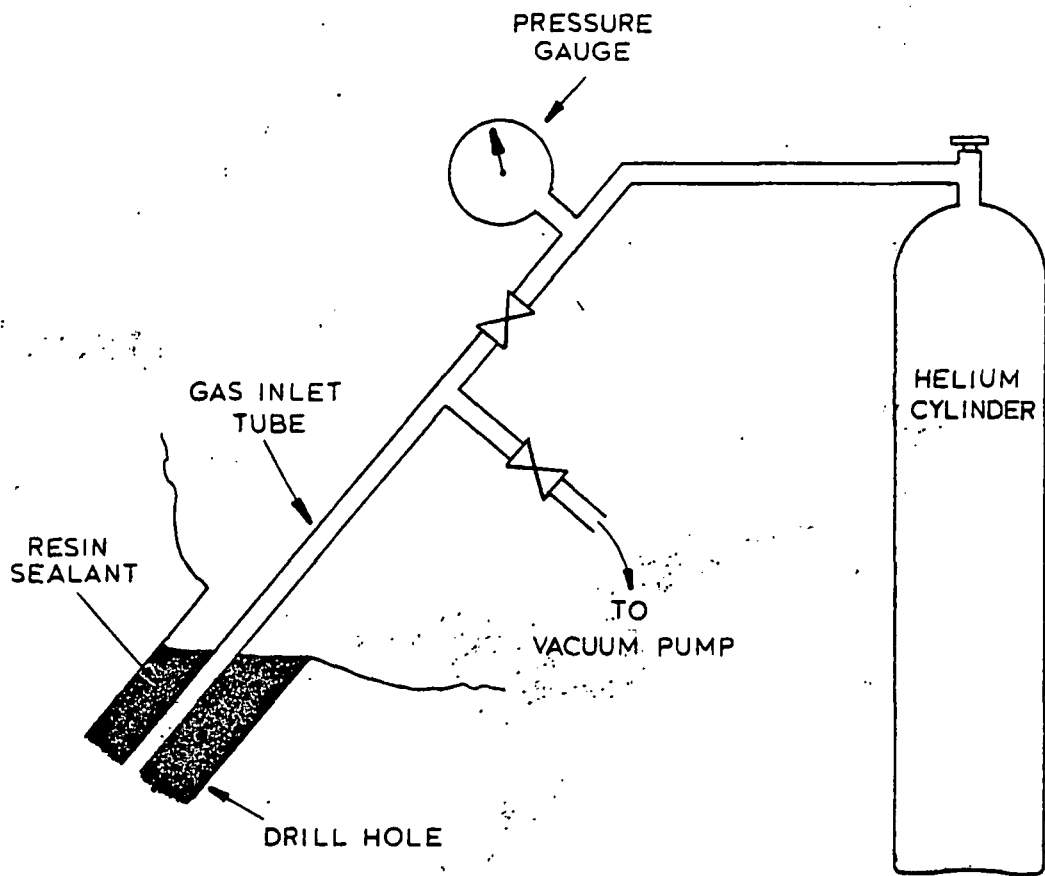
Figure 2. Apparatus for In Situ Porosity Measurements

$$R = \sqrt{r^2 + V_p/\pi eL},$$

where r and L are the radius and length of the hole. R is the average radius of the zone of rock connected by pores to the drill hole. Of course, the actual zone of pore-connected rock will be irregular (compare Figures 3a and 3b).

The above steps should be repeated at one or more locations in the mine to determine the variability of R.

Before proceeding further with the study it will be necessary to determine if R is sufficiently large to warrant further testing. A simple economic criterion would be that the value of the copper in a cylinder of radius R must exceed the cost of drilling the hole.

If this criterion is met then the next step in the study will be to measure the permeability of the ore. Two "permeability" holes will be drilled parallel to the above-described "porosity" hole, and to the same depth, with one hole on each side of the porosity hole. The distances between holes will be 1.5R and 3.0R as shown in Figure 4. By using two holes of differing distances the permeability can be determined as a function of hole spacing.

The holes will be sealed with resin as described above. Helium will then be injected into the porosity hole and the flow rates out of the two permeability holes will be measured at several injection pressures. Permeability will be calculated from the pressure and flow rate data. If the permeability is sufficiently high, water will be substituted for helium and the liquid permeability measured.

These tests should be performed on each of the holes used in the porosity measurements to determine the variability of the ore.

12

(a) ACTUAL PORE-CONNECTED VOLUME

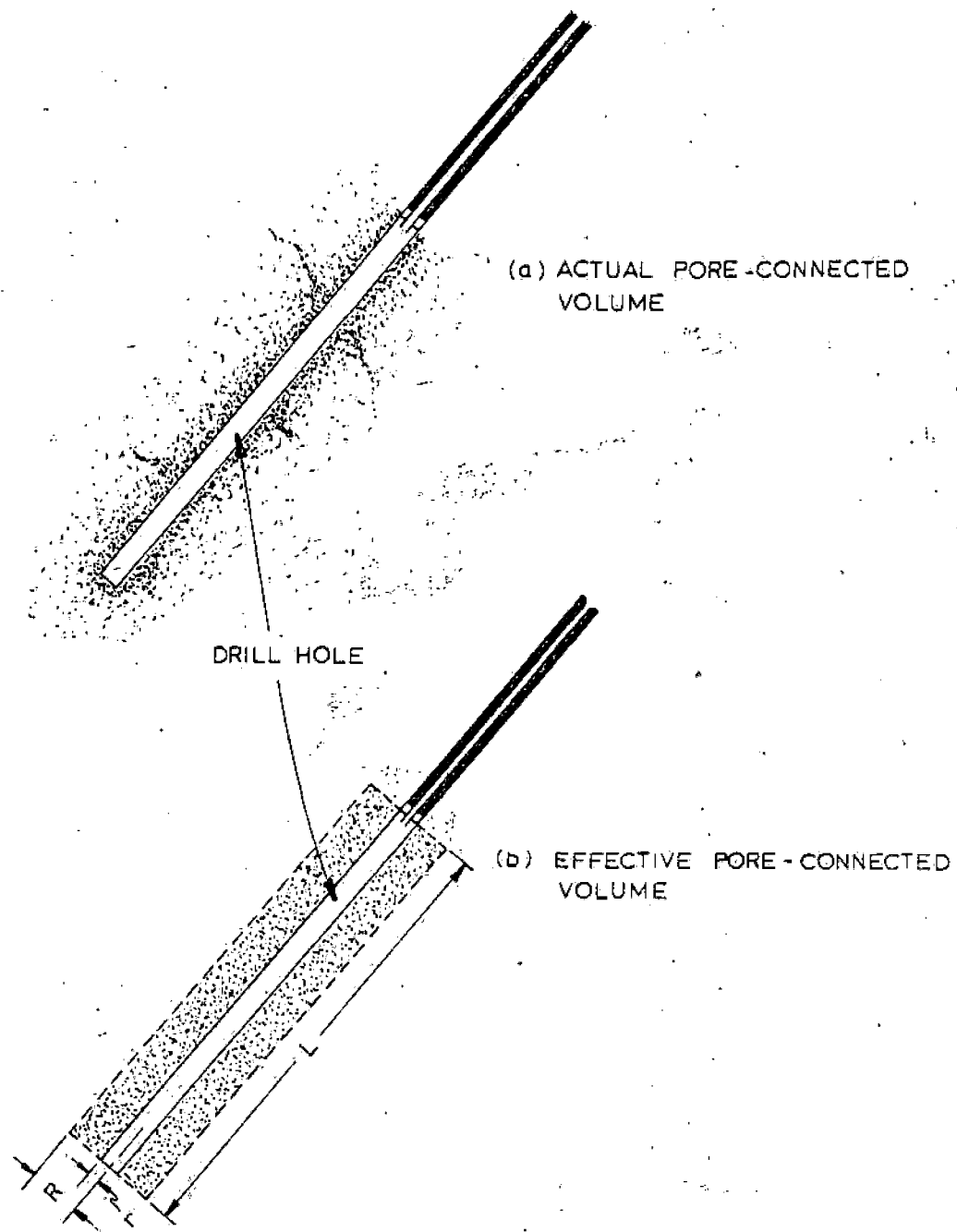(b) EFFECTIVE PORE-CONNECTED VOLUME

DRILL HOLE

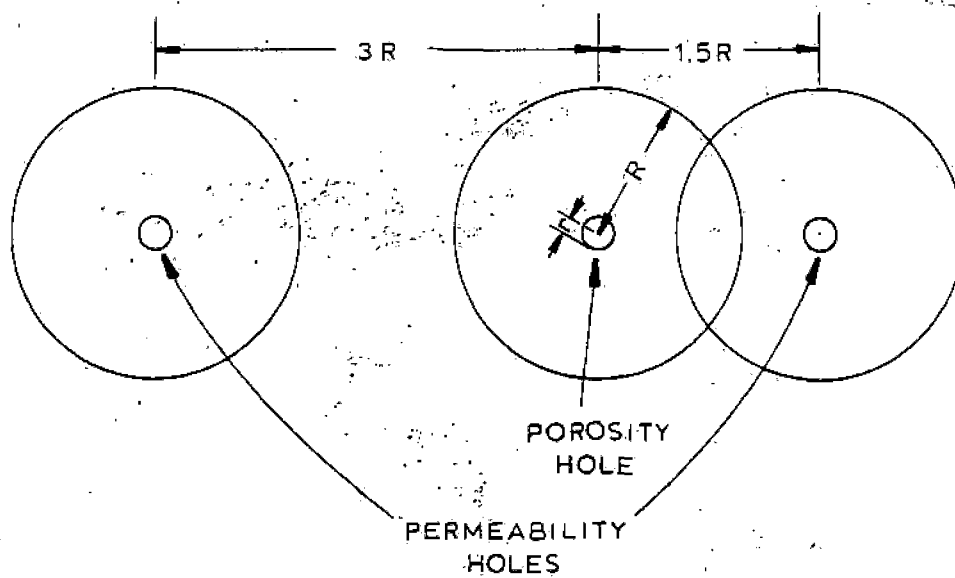Figure 3. Comparison of (a) Actual and (b) Effective Pore-Connected Volume

Figure 4. Arrangement of Permeability Holes with Respect to Porosity Hole

If the results of these tests indicate that the ore is sufficiently porous and permeable, a next desirable step of the study will be to conduct a sub-pilot scale leaching test. This test will have to be carried out on a sizable block of ore in order to ensure that a representative sample of mineralized ore is being used. The block will be prepared for leaching by drilling a number of holes of pattern and spacing determined by the data described above. One half of the holes will be used for solution injection and the other half for solution recovery. Cuttings from the holes will be analyzed and used to estimate the grade of the block of ore.

Solution will be pumped into the injection wells from a solution storage tank and effluent from the recovery wells will flow back into the tank. The solution will be analyzed periodically to determine the amount of copper extracted. The flow rates into and out of the holes will be measured to determine the uniformity of the permeability within the block. If a hole produces an excessively high flow rate (an indication of short-circuiting), the injection line will be throttled to decrease the flow to a reasonable rate.

The test will be continued until the extraction rate decreases to an uneconomically low level. The solution will then be flushed from the block and the block will be mined out, crushed, and analyzed to determine the tailings grade. Chemical analyses and an inventory of the solutions will determine total extraction, reagent consumption, impurity pick-up, and loss of solution out of the block.

Bore-hole fracturing. The objective of this study is to determine the feasibility of preparing ore for in situ leaching by blasting the ore in place (confined blasting). The study will involve measurements of fracture intensity and permeability produced by blasting bore-holes drilled into underground formations.
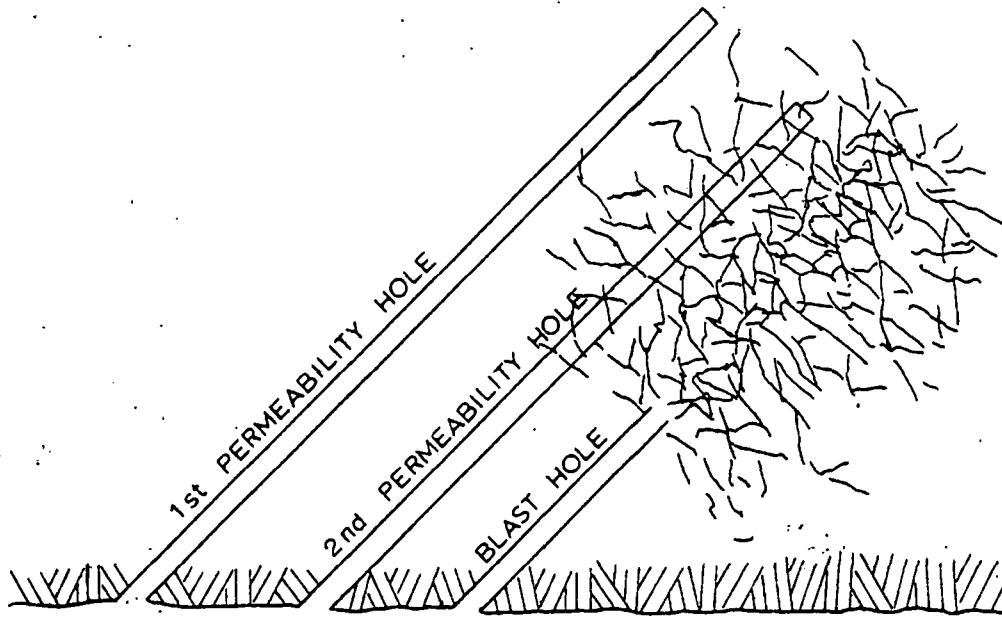
The test work will be performed in stages, starting with single hole blasts and progressing to multiple hole blasts. The principal control variables will be blast hole diameter, type of explosive, hole spacing and ore type. Fracture intensity will be determined from cores obtained by drilling through the blast zones. Permeability will be determined by measuring fluid flow through the blast zones.

a. <u>Single-hole tests</u>. The first stage of the program will consist of blasting tests on single holes. A blast hole will be drilled at 45° to the face with a diamond drill. Core from this hole will be saved for comparison with core obtained after the blast. Only the back of the blast hole will be loaded with explosive and the balance of the hole will be stemmed. The stemmed length will be sufficiently long to prevent the blast zone from breaking out to the face, i.e., to ensure that the blast is completely confined.
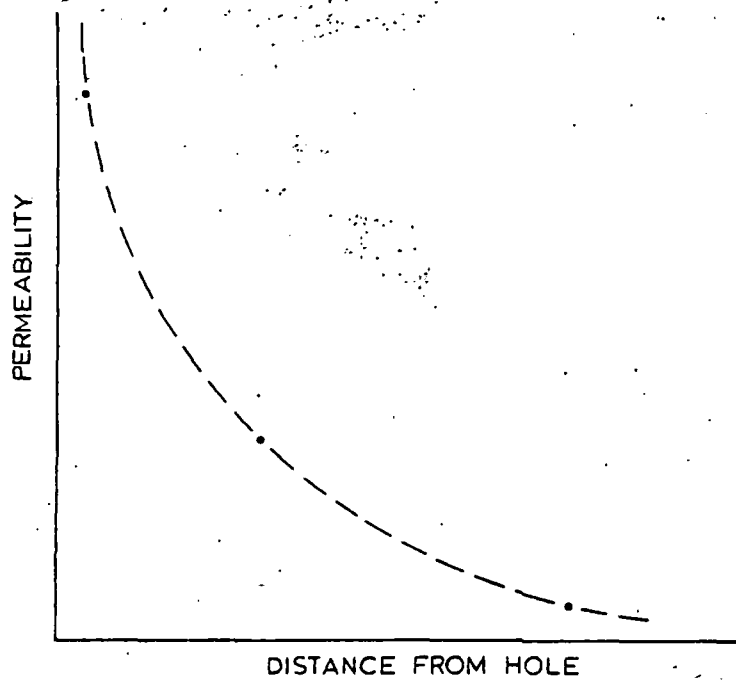
After blasting, a permeability hole (Figure 5) will be drilled parallel to the blast hole. Gas will be injected into this hole and the flow rate into the blast hole (after boring out the stemming) will be measured. If the flow rate (permeability) is too low, a second permeability hole will be drilled closer to the blast hole and the permeability again measured. This procedure will be repeated until a sufficiently high permeability is obtained. The data can be plotted to yield a distance versus permeability curve as shown in Figure 5. The core obtained from these permeability holes will be logged to determine fracture intensity parallel to the blast zone.

After the permeability tests are completed a recovery hole will be drilled through the blast zone at 90° to the blast hole (Figure 6). The core obtained from this hole will be logged to determine the radial fracture intensity distribution as shown in Figure 6. If the fracture intensity cannot be accurately determined because of poor core recovery, the blast zone will be grouted with resin and an additional recovery hole drilled.

16

Figure 5. (a) Arrangement of Blast Hole and Permeability Holes in Single-Hole Confined Blasting Tests.

(b) Expected Relationship between Permeability and Distance from the Blast Hole.

BLAST ZONE

PERMEABILITY HOLES

BLAST HOLE

RECOVERY HOLE

(a.)

FRACTURE INTENSITY - FRACTURES/FT

DISTANCE FROM FACE

(b)

Figure 6.   (a) Arrangement of a Recovery Hole with Respect to the Blast Hole
in Single-Hole Confined Blasting Tests.

(b) Expected Log of Fracture Intensity on Core from the Recovery Hole.

18

Four blast zones will be prepared and tested by the above methods, using two blast hole diameters (e.g., 2 and 4 inches) and two types of explosives (normal and high energy). The test data will be analyzed to determine the most efficient and economical combination of hole size and explosive. An additional test using the best combination will be performed at another location in the mine to determine the variability of the ore.

b. Multiple-hole tests. The data from the above single-hole tests will be used to estimate the blast hole spacing for the first multiple hole test. Three blast holes in a triangular pattern will be used and the holes will be drilled at right angles to the face. As in the single-hole tests, only the back ten feet of the blast holes will be loaded.

After blasting, a permeability-recovery hole will be drilled into the center of the pattern (Figure 7). The core recovered from this hole will be logged for fracture intensity. The permeability between this hole and each of the three blast holes will be measured; in addition, the permeability between each pair of blast holes will be measured. This will provide six measurements from which to determine the average permeability of the blast zone and the uniformity of the permeability within the zone.

The data from this first multiple-hole test will be analyzed to determine if the spacing was too large or too small (Figure 8). A second multiple-hole test will then be performed at a spacing designed to produce a better break. The procedures used will be the same as in the first test. The results of these two multiple-hole tests should provide sufficient data for interpolation and extrapolation over a moderate range of blast hole spacings. If the ore being tested exhibits considerable variability in its fracturing characteristics it may be necessary to perform an additional multiple-hole test to measure this variability.

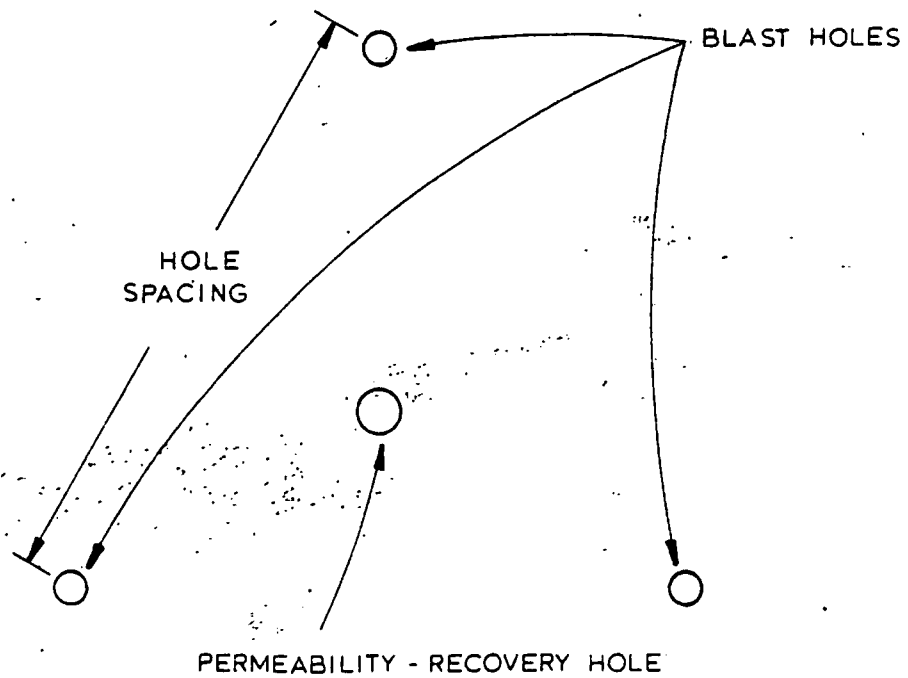Figure 7.   Arrangement of Blast Holes and Permeability-Recovery Hole in a
Multiple-Hole Blasting Test.

(a)
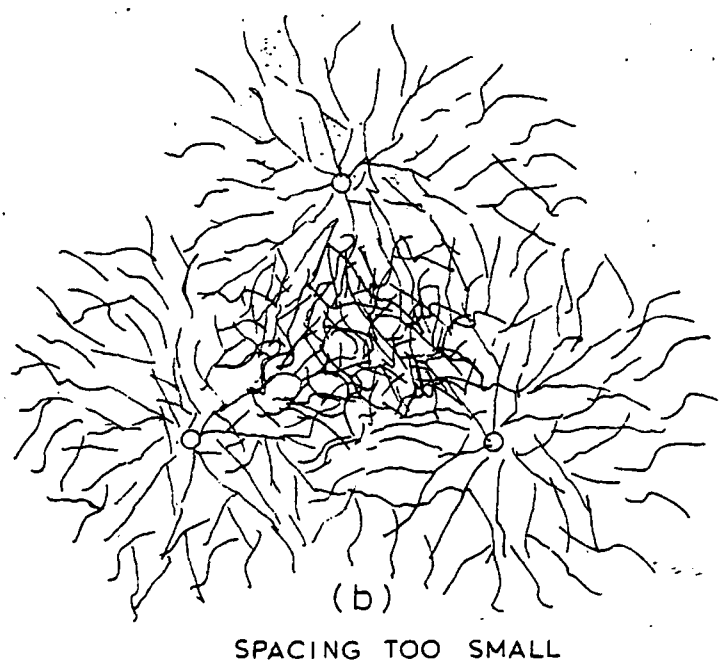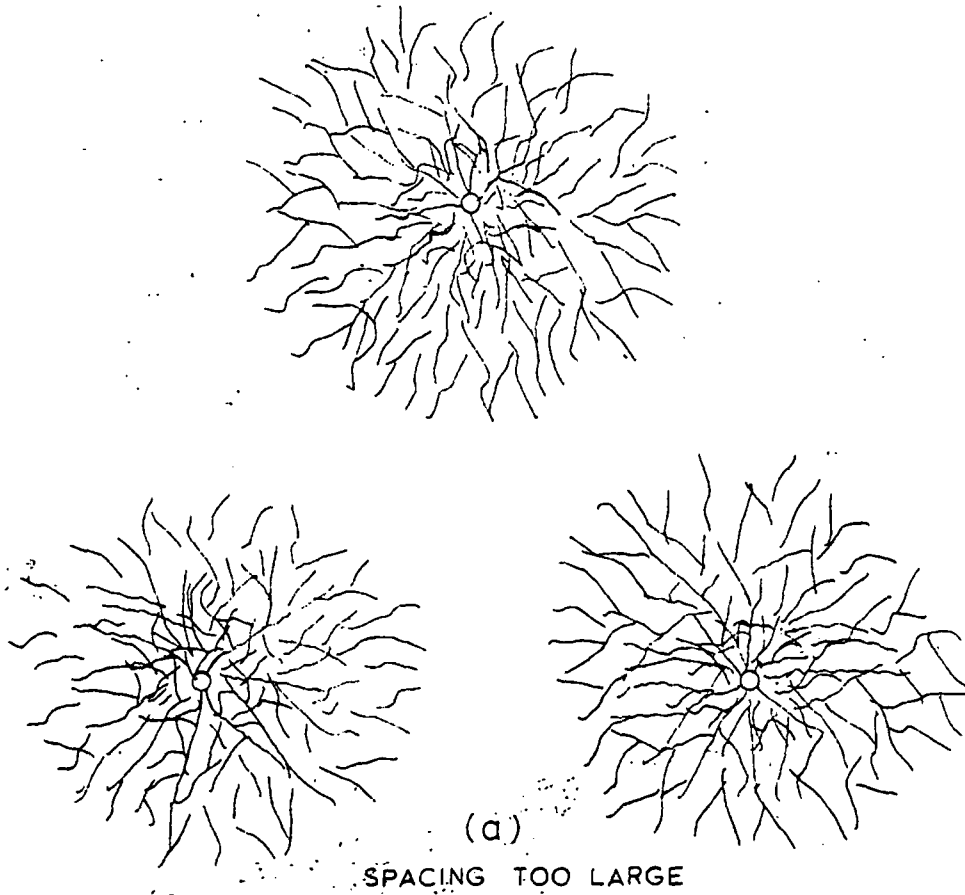SPACING TOO LARGE

(b)
SPACING TOO SMALL

Figure 8. Effect of (a) Excessive Hole Spacing and (b) Insufficient Hole
Spacing in Multiple-Hole Confined Blasting Tests.

The above sequence of single- and multiple-hole tests will have to be performed on each major ore type being considered.

The fracture intensity and permeability data obtained from these tests along with leachability data from laboratory tests will provide the basic information for determining the feasibility of in situ leaching by bore-hole fracturing methods. These data should also be sufficient for designing a sub-pilot scale leaching test. This test would be very similar to the leaching test described earlier in the section on bore-hole leaching. It would consist of drilling a pattern of holes into a mineralized block of ore of sufficient size to be a representative sample; loading the holes and blasting the block; drilling injection wells into the fracture zone; pumping leach solution into the injection wells; collecting and analyzing the effluent solution periodically over a sufficient period of time to determine the rate and extent of copper extraction.

Open fracturing. The term "open fracturing" is used to describe the blasting of rock into prepared underground openings in order to create a column of rubble suitable for underground leaching. The goal of open fracturing is to provide just sufficient dislocation of the fracture surfaces to permit easy percolation of the leach solutions. In contrast to bore-hole fracturing (confined blasting) which produces a zone of fractured ore with minimum induced porosity, open fracturing would produce moderate porosity and a much higher degree of permeability. The objective of this study is to determine the minimum amount of opening needed (expressed as "relief", the percentage of opening volume to rubble volume) and the most efficient blasting method for creating a uniform rubble column having satisfactory leaching characteristics.

Since open fracturing is largely an extension of conventional underground mining methods, the first part of the study will involve an examination of

22

present mining techniques to determine the best approach to the problem. This will be followed by underground fracturing tests. To be meaningful, such tests will have to be conducted on a large scale, and will require considerable time and expense. As only a limited number of tests can be performed it is essential that the most attractive methods be selected for testing and that the tests be carefully planned.

Since the native copper deposits are steeply dipping, the most efficient method of creating rubble would be to break the ore downwards into the prepared opening. This opening would probably be in the form of a drift of suitable cross-section. Drilling and loading of the blast zone could be performed from this drift and from the next drift up the mine; the use of raises may also be advantageous. Since long-hole drilling will probably be used, much of the blasting will be under semi-confined conditions. Therefore the data obtained in the confined-fracturing studies described in the previous section will assist in planning these tests. The first test should probably be performed with insufficient relief so that the problem areas can be identified and corrective changes applied, either in terms of more relief or more blasting. A few additional tests should then provide reasonable data for estimating the feasibility of open fracturing.

Underground leaching experiments on the rubble from these tests will not be required as the results can be estimated sufficiently well from laboratory tests on loose rock.

Abandoned mine leaching. The leaching of abandoned mines is characterized by a number of unique advantages and disadvantages. The foremost advantage is the presence of large quantities of broken rock from the old mining operations. Thus, the costly drilling and blasting steps required in preparing a virgin ore body for leaching are avoided. Moreover, the extensive underground openings in

abandoned mines will probably permit the movement of large volumes of solution with little pressure drop.

The major problems associated with leaching abandoned mines are: the difficulty of gaining access to the old workings because of mine water, caving or subsidence; the large volume of leachant required to flood the old workings; the difficulty of controlling solution flow through the workings; the general lack of information on the grade, size and amount of rubble, particularly in the older mines where records may be incomplete. Thus, the leaching of abandoned mines will be characterized by minimum expense for ore preparation, but large expense for solution inventory and considerable difficulty in controlling and predicting the outcome of the operation.

The study of abandoned mine leaching is complicated because it cannot be readily tested on a small scale. The condition and layout of the mine and the nature of the rubble will vary from one mine to another even and within a single mine, making small-scale testing quite unreliable.

The best approach to determining the feasibility of abandoned mine leaching will be to select a particular abandoned mine as a test case and to perform a detailed feasibility study on it. The mine selected should be moderately small or capable of being compartmentalized so that an actual leaching test of controllable size can be performed if the results of the study are favorable. Because most of the abandoned mines in the district are amygdaloids, the test case should be of this type and the mining methods that were employed should have been conventional. If these criteria can be met the results of the study will be sufficiently general. It is essential that good records of the mine be available. Access to samples of the rubble and to the mine water at depth will be important advantages.

The first part of the study will involve an analysis of the records to derive estimates of the amount, size and grade of the rubble and the volume

24

of the openings. Mine water will be sampled at various depths and its composition, density and temperature determined. If possible, samples of rubble will be obtained and leachability experiments performed.

After these basic data have been obtained, the preparation of the mine for leaching will be investigated. The factors to be considered are whether to dewater the mine or to use the existing mine water for solution make up; whether some dewatering might be required to bring the water level low enough to prevent leakage out of the mine into the environment; the best way of introducing the leachant into the mine, e.g., through existing openings or through wells drilled down to intersect the workings. The strength of the leaching solution will have to be determined; the ratio of extractable copper to the volume of mine openings will set an upper limit on solution strength. Whether the mine can be leached in sections or whether all portions of the mine must be leached simultaneously will be determined and will have an effect on solution strength. The increase in the density of the solution as copper is dissolved will cause movement of the solution and will influence the number and position of the pumping stations for bringing the rich solution to the surface.

After the plan for preparing the mine is established, the rate of copper extraction as a function of time will be estimated. The size of the copper recovery plant and the problem of maintaining a constant feed solution to the plant will be analyzed. The old pumping records of the mine will be used to estimate ground water influx into the mine which will determine how much leach solution must be distilled and discarded.

These and various other factors will be analyzed by the methods described in the sub-section on "Engineering and Economic Analysis" to determine the

25

feasibility of leaching the mine. If the results of the study indicate that such an operation would be profitable, all or a portion of the mine could be leached on an experimental basis.

This study will not only determine the feasibility of leaching the selected test mine but will also provide a general methodology for use in the analysis of other abandoned mines.

Solution Treatment Methods

In the ammonia leaching of native copper, four solution treatment methods are required: 1) solution make up - preparation of the initial solution and replacement of ammonia and carbonate losses; 2) oxidation - conversion of the cuprous ammine to cupric ammine by reaction with air or oxygen; 3) copper recovery - extraction of copper from the pregnant solution and conversion to a marketable form; 4) stripping - removal of the leaching reagents so that water of sufficient purity can be discharged from the process.

The technology for these methods is fairly well understood, and in fact each operation has been demonstrated on a commercial scale. Therefore, only a limited amount of experimental work on these methods will be required. The major emphasis will be on collecting engineering and cost data and on studies as to how the methods can be best applied to the various in situ processes.

Although solution make up and oxidation are generally performed in absorption towers it may be more efficient and require less capital if these operations are carried out underground, using underground chambers and rubble as the absorption tower. If the cuprous ammine can be oxidized underground as soon as it is produced, the maximum driving force for leaching will be obtained.

Some research will be required on the solvent extraction of high concentration solutions. Present practice is to treat fairly dilute solutions,

26

but current studies show that these dilute solutions leach at rather low rates. Although there does not appear to be any fundamental reason why solvent extraction cannot be applied to concentrated selections, it must be tested experimentally for unforeseen problems.

In addition to solvent extraction, a number of other processes for recovering copper from ammonia solutions are possible. They include distillation, direct electrowinning from ammoniacal solutions, gaseous reduction and chemical precipitation. Even though solvent extraction will likely be the preferred process, each of the alternative processes should be studied to determine its possible applicability. Extensive studies will not be required; most of the processes can be evaluated with existing technical and cost data. In some cases laboratory tests will be required to obtain some of the necessary information.

A particularly critical step is the stripping process. Large volumes of solution might be involved and the liminations on reagent levels in the discharge water might be very low. Since there is a possibility that conventional steam distillation will not produce an acceptable effluent, a polishing process such as ion exchange might have to be applied after distillation. A suitable alternative in some cases might be to pump the distillation effluents to the bottom of neighboring abandoned mines.

Environmental Control

Introduction of leaching reagents into the environment is a potential problem associated with in situ leaching. Reagent loss may occur in three ways: 1) by escape of solutions from the mine into the water table and then into lakes, streams or wells; 2) by disposal of spent solutions or leaching by-products; or 3) by evaporation of ammonia into the atmosphere. These might be termed "external" environmental problems.

27

In addition to the external environmental problems there are potential "internal" environmental problems. They are: 1) leakage of ground water into the in situ operation; 2) production of flammable or explosive gas mixtures (NH_3-O_2) within the mine; 3) difficulties in performing underground development and maintenance in the presence of toxic levels of ammonia and either high or low concentrations of oxygen.

The external and internal problems are not independent. For example, leakage of water into the mine requires that an equal volume of solution be discarded if dilution is to be avoided. The cost of removing contaminants from the discard solution to an acceptably low level may be prohibitive. Similarly, ventilation of the underground areas undergoing development may result in nuisance levels of ammonia in the atmosphere.

The magnitude of the environmental problems will depend on three general factors: 1) the characteristics of the ore deposit and its surroundings; 2) the type of in situ process being employed; 3) the statutory regulations governing permissible levels of discharges and safe working conditions.

The first factor is highly dependent on the deposit being considered. Its evaluation will require collection of data concerning the deposit. These data will include pumping records, water analyses, general topography, land ownership, habitation and hydrology of the surrounding area, and the possible steps which might be used to isolate the deposit from the environment. Since only a limited number of deposits can be studied, the best approach would be to select one or two deposits for detailed evaluations. In this manner the more significant factors would be identified and the general procedures for evaluating other deposits would be developed.

Study of the second factor will involve identification of the major environmental problems associated with each of the four general in situ

methods. This will be followed by studies of the monitoring and control procedures which might be applicable to each case.

The third factor will require collection of federal (EPA, OSHA) and state regulations affecting discharges and working conditions. This study will also include collection of data pertaining to environmentally-related properties of the in situ solutions and atmospheres (NH_3 vapor pressure, solution and gas densities, explosive limits, etc.).

Engineering and Economic Analyses

Objectives. Engineering and economic analyses will be directed toward two principal objectives: 1) to guide experimental work into the most useful avenues and 2) to evaluate conceptual in situ leaching systems. These analyses will be conducted in a stepwise fashion, starting from the simplest basis possible. Each step will provide a "go-no go" answer, and subsequent steps involving more sophisticated design and analyses will be taken only when all previous steps have given favorable results.

At various times, depending on specific objectives, analyses will be concerned with overall in situ leaching processes or with individual components of such a system.

Scope. The analyses will generally follow a sequence such as: 1) describe, or design, the process of interest; 2) establish the engineering feasibility to be sure that the process can be operated physically to produce the desired results, making necessary modification in the original design to insure engineering acceptability; 3) evaluate the economic acceptance of the process as finally designed.

For any given system (or part thereof), this analytical procedure may be repeated, if necessary, at increasing levels of detail and sophistication of process design, assuming that previous analyses have yielded favorable results.

That is, it may often prove desirable to design a process first in an oversimplified manner, examining only the obviously key parts of the process. Design and analysis will then proceed through more detailed stages to some desired end point.

It should be emphasized that the analytical procedure can be stopped at any point should either engineering or economic analysis indicate unacceptable performance of the conceptual leaching system. Should such a result appear, a decision will be necessary to choose between the alternatives of abandoning the design completely or attempting to modify it as to make it acceptable.

Analyses as a guide to research and development. The analyses will serve to guide experimentation in two ways. Engineering or economic analysis of a part of the process may indicate that even under the best conceptual conditions, that part will not be acceptable. An example of such analysis has been given in the discussion of work on bore-hole leaching. From an initial engineering standpoint, the leaching technique is acceptable since drilling holes in rock is readily accomplished. However, simple analysis may show that the maximum dollar value of copper which might be recovered from a hole (or set of holes) would be less than the cost of drilling. Under such conditions there will be no point in conducting the experiments. It is important that in making such simple analyses, which may be subject to large errors due to inaccuracies in making estimates, judgments based on the analyses should tend to be optimistic. As more experimental data concerning a process or one of its parts become available, the errors in analysis will be reduced and judgments should become correspondingly more rigorous.

A second way in which engineering and economic analyses will guide experimentation is through identification of problems in leaching systems. That is, in any given system, analysis may well indicate that only one of two parts of the system as conceived are unacceptable from either engineering or economic

30

considerations. This may indicate that further development studies should be conducted in an effort to overcome the difficulties, and therefore save an otherwise useful leaching system.

Thirdly, the analyses will be useful in identifying the parts of a leaching system which most greatly influence costs and/or engineering results. Thus, research and development can be focused on these parts, rather than on less sensitive parts of the system.

Finally, the analyses will indicate needs for better or more complete empirical data pertaining to a particular leaching system. This information can then be gathered by the most appropriate method.

Procedures. The engineering and economic analyses will be conducted by the most convenient method appropriate to the desired analysis. In the initial stages simple hand calculations will probably suffice. As the analyses proceed in development to include more and more details, and produce more accurate results, the calculations and evaluations will require more sophisticated techniques. The ultimate development will almost certainly require use of computer models as a matter of convenience to allow for efficient and complete analysis.

Since the reliability of a system analysis is only as good as the input data, it will be essential to collect and compile an extensive list of engineering and economic information. These data bases will cover a broad spectrum and will include such items as drilling and blasting costs and performances, reagent costs, ore properties (leachability, porosity, reagent consumption), capital expenditures for a solution treatment plant, scale-up factors, kinetic data, fuel and power costs, etc. These data will be obtained from a variety of sources including the technical literature, studies currently underway, studies to be performed in the program, equipment manufacturers, etc. In some

cases only estimates will be available and in others, only a range of values. One of the valuable features of computerized analysis is that the influence of a range of values can be quickly assessed. Another useful technique for limited data is to perform the analysis in reverse - to input a profitable return and calculate the range of values which will ensure this return.

Information will also be needed on the costs of conventional mining. These benchmark data are required because in situ leaching must not only be profitable but also more profitable than conventional mining methods.

In order to assess the feasibilities of the various in situ processes (or any of their parts) the analyses will be formulated to output both technical and profit-oriented information. Analyses will be flexible with respect to variations in input parameters and will allow for sensitivity analysis of the parameters.

Thus, it will be possible to determine under what conditions a given technology may be implemented and to examine variations in the process. In addition it will be possible to examine the feasibility of a mixed process, employing both conventional mining and in situ methods. The ultimate objective of the analysis will be to define the optimum process for a given ore body. This will be accomplished by using the physical characteristics (dimensions, shape, grade, etc.) of existing and abandoned mines as structural constraints on the models.

As mentioned earlier, these system studies will be used to assist in the experimental phases of the program. Thus, it is important that there be close liaison between the system studies and the other phases of the program.

As a final step in the economic analysis of an acceptable leaching system, detailed pro forma income statements should be prepared. These statements will allow managers to assess most carefully the potential profits(losses) of a

32

system. The statements should be developed for a period of five or more years
and should conform to the accepted accounting procedures of Homestake Mining
Company. Armed with these data, and engineering data, the feasibility of a
complete in situ leaching system can be ultimately established.

Pilot Scale Studies

The results of all research and analysis described previously will
ultimately be focused on the design, construction and operation of one or
more pilot scale test sites. Operation of a pilot site will generally
confirm expectations based on previous studies, will provide more refined
data on which to base engineering and economic evaluation of commercial scale
operations, and will define more accurately those aspects of in situ leaching
operation requiring further study and development.

At this time detailed description of a pilot scale operation is not
possible, because so many paramaters will depend on results to be obtained
in other studies. There is, of course, a possibility that these results will
be so negative that the entire program will be terminated short of pilot
operation. For the moment, this possibility will be excluded from the
discussion.

While exact description of the pilot site is not possible at present,
certain significant factors can be described. Of utmost importance is that
the pilot plant be designed with optimum chance of successful operation. The
pilot operation will undoubtedly be very costly - probably in the range of
$500,000 to $1,500,000. If the pilot plant should fail or give very discour-
aging results, it is very unlikely that additional funds will be available for
a second try.

Therefore, great care must be given to site selection, size of operation, method of ore preparation and leaching and copper recovery. Even more important will be to insure that adequate and fail-safe environmental control is provided.

Preference should be given to a site with potential commercial utility. Other factors influencing site selection will be: 1) similarity to other deposits to obtain information of broadest utility; 2) cost of development and provision of services. It is conceivable that more than one site might be desirable, either in different deposits or at different locations within a single deposit. In any case it will be advantageous if the test site includes the major ore types occurring in the mine.

Very little can be said at this time about preferred scale of operation, methods of ore preparation, leaching or copper recovery. Decisions on each of these aspects must be based on results of studies yet to be accomplished. Premature commitment to any of these could well jeopardize opportunity for successful operation of the pilot plant, which in turn will jeopardize success of the entire program.

One aspect of pilot plant design which should be kept in mind when final design criteria are set is the possibility of producing sufficient copper to defray a substantial part of the costs. However, the pilot plant must be considered first and foremost as an experimental tool, designed to obtain data for scale-up to commercial operation.

The pilot plant should operate at least one year. In addition, considerable lead time will be required to design and construct the plant. Provisions should be made to duplicate all phases of anticipated commercial operation as closely as possible, including production of the final product from the system. Great

thought should be given to obtaining as much information as possible from the pilot plant. This will require designing flexibility into the operation so that more than one mode of operation can be studied. Adequate instrumentation must be provided, not only to obtain operating data, but also to provide for acceptable environmental control. At the conclusion of the test, the leach zone will be mined to evaluate the results of the test.

Because design of the pilot plant will require substantial effort, certain aspects should be commenced as early as possible. In particular, preliminary section of likely sites should be made so that the necessary detailed information about these sites can be gathered. Again, of particular importance will be information pertaining to environmental control.

35

IMPLEMENTATION

In this section of the plan, estimates of the manpower, money, and time required for each phase of the program are presented.

It is assumed that the work will be directed by the five Research Managers described on page 4, using various types of support personnel such as miners, technicians, student assistants, etc. Nearly all of the cost of the program will be made up of the salaries and wages of these people. Equipment costs will be relatively small. It is assumed that underground test sites will be readily accessible and will have adequate services.

A rate of $9/hr is used for the professional personnel and $5/hr for the hourly-rated support personnel. The salary rate for the Project Manager who will be involved on a part-time basis throughout the program is taken as $12/hr. Indirect costs are not presented because these costs cannot be determined without knowing which organizations will be performing the work.

The budget shown on the following pages lists the personnel involved, the man-hours required, the cost and the completion time for each major step of the phases making up the program. In some cases, special assumptions were required as to the extent of the test work; these are noted in the budget. Equipment that will be used in more than one phase is listed only once.

The scheduling of the program is shown graphically in Figure 9. This schedule was derived from the man-hour and completion time data of the budget. The various phases are arranged in a logical sequence and in a manner to minimize the total time and make best use of the personnel. The numbers in the bar graphs are the estimated costs of the itemized studies. At the bottom of Figure 9 the cumulative cost of the program up to pilot plant testing is presented.

PROGRAM BUDGET

IDENTIFICATION AND AMENABILITY OF ORE RESERVES

	Man-hours	Cost
1. Tabulation of Reserves		
Company Geologist	160	1440
Clerical	80	320
Completion time - 2 months		1760
2. Laboratory Examination - assume 12 samples		
a. Sample collection and storage		
Company Geologist	60	540
Miner	80	400
Metallurgist	8	72
Technician	16	80
Supplies and services at 25% of salaries and wages		273
Completion time - 3 weeks		1365
b. Laboratory tests (crushing, screening, analysis, porosity, mineralogical examination, sorting)		
Metallurgist	96	864
Technician	480	2400
Supplies and clerical at 10% of salaries and wages		326
Completion time - 5 weeks		3590
3. Amenability Leaching Tests - assume 18 samples		
Metallurgist	116	1044
Technician	252	1260
Supplies and clerical at 10% of salaries and wages		230
Completion time - 4 months		2534
4. Indirect Estimation of Amenability		
Metallurgist	80	720
Technician	80	400
Computer time and clerical at 20% of salaries and wages		224
Completion time - 1 month		1344

Summary:

	Man-hours	Cost
Company Geologist	220	1980
Metallurgist	300	2700
Miner	80	400
Technician	828	4140
Supplies, services and clerical		1373
Completion time - 9 months		$10,593

ORE PREPARATION

1. Bore-Hole Leaching

Assume two mines being tested, three locations in one mine and two in the other; sub pilot-scale leaching test in one mine.

a. Determination of Pore Connectivity

Five tests each requiring:	Man-hours	Cost
Mining Engr.	30	270
Miner	25	125
Technician	18	90
		485 each

b. Permeability Measurements

Four tests each requiring:		
Mining Engr.	39	351
Miner	45	225
Technician	2	10
		586 each

c. Leaching Test

Mining Engr.	40	360
Metallurgist	77	693
Miner	546	2730
Technician	60	300
		4083

d. Interim Evaluations

Mining Engr.	24	216
Metallurgist	16	144
Economist	40	360
		720

Summary:

Estimate two months to complete pore connectivity and permeability studies; seven months for leaching test.

	Man-hours	Cost
Mining Engr.	370	3330
Metallurgist	93	837
Economist	40	360
Miner	851	4255
Technician	158	790
		9572
Equipment (drill, tanks, pump, controls)		$14,500
Supplies, services and clerical at 15% of salaries and wages		1436
Completion time - 9 months		$25,508

2. Bore-Hole Fracturing

Assume two mines being tested, sub pilot-scale leaching test in one mine.

a. Single-hole tests

Ten tests each requiring:	Man-hours	Cost
Mining Engineer	60	540
Miner	64	320
Technician	17	85
		945

b. Multiple-hole tests

Six tests each requiring:		
Mining Engineer	29	261
Miner	52	260
Technician	4	20
		541

c. Leaching test

Mining Engineer	56	504
Metallurgist	80	720
Miner	562	2810
Technician	60	300
		4334

d. Interim Evaluations

Mining Engineer	24	216
Metallurgist	16	144
Economist	40	360
		720

Summary:

Estimate seven months to complete single- and multiple-hole tests; seven months for leaching test.

	Man-hours	Cost
Mining Engineer	854	7686
Metallurgist	96	864
Economist	40	360
Miner	1514	7570
Technician	254	1270
Equipment (tanks, pump, controls)		$3000
Supplies, services and clerical at 15% of salaries and wages		2662
Completion time - 14 months		$23,412

3. Open Fracturing

Assume two mines being tested, two test blocks in the first and one in the second. Test blocks about 100' x 50'. Services and equipment available. Labor supplied by Homestake.

Estimate 5 months and $25,000 required for each block.

Completion time - 15 months $75,000

4. Abandoned Mine Leaching

Evaulation of one test case.

a. Collection and tabulation of records and water analysis, sample collection.

	Man-hours	Cost
Company Geologist	80	720
Envir. Geologist	40	360
Technician	16	80
Completion time - 1 month		1160

b. Evaluation of Data and Design of Plan

Company Geologist	40	360
Metallurgist	120	1080
Envir. Geologist	20	180
Economist	40	360
Technician	16	80
Completion time - 6 weeks		2060

c. Analysis of Plan

Company Geologist	20	180
Metallurgist	120	1080
Envir. Geologist	20	180
Economist	120	1080
Technician	16	80
Completion time - 6 weeks		2600

Summary:

Company Geologist	140	1260
Metallurgist	240	2160
Envir. Geologist	80	720
Economist	160	1440
Technician	48	240
Clerical at 10%		582
Completion time - 4 months		$6402

43

SOLUTION TREATMENT METHODS

Work will consist largely of engineering and costing, along with a limited amount of test work.

		Man-hours	Cost
1.	**Solution Make-up**		
	Metallurgist	80	720
	Economist	40	360
			1080
2.	**Solution Oxidation**		
	Metallurgist	80	720
	Economist	40	360
			1080
3.	**Copper Recovery**		
a.	Literature search and fundamentals		
	Metallurgist	80	720
b.	Distillation		
	Metallurgist	80	720
	Technician	40	200
c.	Solvent Extraction		
	Metallurgist	80	720
	Technician	80	400
d.	Reduction		
	Metallurgist	40	360
e.	Precipitation		
	Metallurgist	40	360
	Technician	40	200
f.	Electrowinning		
	Metallurgist	80	720
	Technician	80	400
g.	Costing and Economic Evaluation		
	Economist	120	1080
			5880
4.	**Solution Clean-up**		
	Metallurgist	80	720
	Technician	40	200
	Economist	40	360
			1280

Summary:

Estimate that the time required to complete these studies will be twice
the metallurgist's hours.

	Man-hours	Cost
Metallurgist	640	5760
Economist	240	2160
Technician	280	1400
Supplies, equipment and clerical at 15% of salaries and wages.		1398
Completion time - 8 months		$10,718

ENVIRONMENTAL CONTROL

1. Obtain Regulatory Data and Solution Properties

	Man-hours	Cost
Environmental Geologist	80	720
Metallurgist	40	360
Technician	16	80
Clerical at 10% of salaries and wages		116
Completion time - 1 month		1276

2. Characterization of In Situ Methods: Monitering and Control Procedures

Environmental Geologist	120	1080
Mining Engineer	48	432
Metallurgist	48	432
Clerical at 10% of salaries and wages		194
Completion time - 1 month		2138

3. Study of Typical Mines.

Assume two mines to be studied:

a. Collect hydrological data

Company Geologist	80	720
Environmental Geologist	240	2160
Technician	120	600
Clerical at 10% of salaries and wages		348
Completion time - 2 months		3828

b. Data evaluation

Company Geologist	16	144
Environmental Geologist	80	720
Metallurgist	24	216
Mining Engineer	24	216
Clerical at 10% of salaries and wages		130
Completion time - 3 weeks		1426

Summary:	Man-hours	Cost
Environmental Geologist	520	4680
Company Geologist	96	864
Metallurgist	112	1008
Mining Engineer	72	648
Technician	136	680
Clerical		788
Completion time - 5 months		$8,668

ENGINEERING AND ECONOMIC ANALYSIS (INCLUDING PROJECT MANAGEMENT)

1. Preliminary - staffing, planning and scheduling of test work, equipment procurement and facility set-up.

	Man-hours	Cost
Project Manager	80	960
Mining Engineer	80	720
Company Geologist	40	360
Metallurgist	80	720
Envir. Geologist	40	360
Economist	40	360
Clerical at 10% of salaries and wages		348
Completion time - 1 month		3828

2. Initial Data Collection

Economist	120	1080
Mining Engineer	40	360
Metallurgist	40	360
Company Geologist	20	180
Envir. Geologist	20	180
Clerical at 10%		216
Completion time - 1 month		2376

3. Initial System Design and Gross Feasibility Studies

Economist	120	1080
Mining Engineer	60	540
Metallurgist	40	360
Company Geologist	40	360
Technician and clerical at 10%		234
Completion time - 1 month		2574

4. Continuing Analysis and Evaluation

	Man-hours	Cost
	416	4992
Project Manager	2340	21060
Economist	2200	19800
Metallurgist	2080	18720
Mining Engineer	312	2808
Company Geologist	340	3060
Envir. Geologist	2080	10400
Programming Asst.		8084
Technician and clerical at 10%		6000
Computer time		$94,924

Completion time - duration of program up to pilot plant design - about two years.

Summary:

	Man-hours	Cost
	496	5952
Project Manager	2620	23580
Economist	2360	21240
Metallurgist	2260	20340
Mining Engineer	412	3708
Company Geologist	400	3600
Envir. Geologist	2080	10400
Programming Asst.		8882
Technician and clerical		6000
Computer time		$103,702

Completion time - 2 years

PILOT PLANT STUDY AND FINAL ANALYSIS OF THE PROGRAM

The following estimates of requirements for design, construction and operation of a pilot plant must be understood to be very rough at best. At this stage of planning there is no basis for establishing such important parameters as the location and size of the operation, the method of leaching and even the information desired from the study. Therefore, the estimates given must be considered as guidelines only.

1. <u>Design</u>. Pilot plant design will require the efforts of several people to cover such aspects as ore preparation, leaching and copper recovery and environmental control. About 1 to 1.5 man-year of effort expended over six to nine months, might be necessary.

2. <u>Operation</u>. The pilot plant should probably be operated for at least one year to insure that adequate and useful data are obtained to allow for making modifications in the sutdy if necessary, and to be sure that operation of the leaching system does not suffer with time due to unexpected side effects in the system. One or two engineers will almost certainly spend most of their time in supervising the study and the part-time efforts of several other engineers and scientists will be required as assistance is needed. <u>Analysis</u>. Complete analysis of the pilot plant study will require three to six months to complete and will probably require 1 to 1.5 man-years of effort in total. The efforts of all professional people having had major responsibility for the test will be necessary to some extent in making the analysis and preparing the final report.

3. <u>Cost</u>. The total effort of design, construction and operation of the pilot plant, analysis of the results and report preparation will

probably cost between $500,000 and $1,500,000. Depending on the size and type of operation it may be possible to defray a portion of this cost by selling the recovered copper.

A PLAN FOR DETERMINING
THE FEASIBILITY OF IN SITU
LEACHING OF NATIVE COPPER ORES

Prepared for:

HOMESTAKE COPPER COMPANY
CALUMET, MICHIGAN

By the

INSTITUTE OF MINERAL RESEARCH
MICHIGAN TECHNOLOGICAL UNIVERSITY
HOUGHTON, MICHIGAN

June 14, 1974

W. A. Hockings, Research Fellow   _W. L. Freyberger_, Director

June 14, 1974

Mr. O. E. Anderson
Homestake Copper Company
P. O. Box 386
Calumet, Michigan   49913

Dear Mr. Anderson:

We are pleased to enclose with this letter fifteen (15) copies of a report entitled "A Plan for Determining the Feasibility of In Situ Leaching of Native Copper Ores". This report outlines a plan for Homestake Copper Company for research and development studies on in situ leaching of native copper ores. The plan presents an orderly and systematic approach to the studies, starting from small-scale experiments up through the design, construction and operation of a pilot plant.

The major features of the plan include gathering information on ore reserves and their amenability to in situ leaching, developing methods of preparing ore for leaching, establishing proper environmental control of leaching systems and conducting engineering and economic analyses of leaching systems. Recommendations for project management and control are presented, together with a schedule of study and estimated budgets.

Because of the nature of the research and the unknowns involved at this time in designing a long range plan, the estimates of time, effort and costs for the research may not prove to be very accurate. This is particularly true for estimates of the later stages of the program.

An important aspect of the plan as presented is that provisions have been recommended for close control over the program at all times. Such control is absolutely essential to insure that the research is conducted in the most efficient manner and that all experiments will be conducted in an acceptable manner.

We greatly appreciate the opportunity to have prepared this plan for Homestake Copper Company and trust you will find the report satisfactory.

Sincerely,

Wilfred L. Freyberger
Director
Institute of Mineral Research

/mjp

Enclosures

TABLE OF CONTENTS

TABLE OF CONTENTS (cont'd)

LIST OF FIGURES

INTRODUCTION

The potential value and advantages of the application of in situ leaching
to recovery of copper from native copper ores of the Keweenaw Peninsula have
been broadly described in a previous report (Institute of Mineral Research,
1972). Several alternative methods of conducting such leaching were outlined.
At present, this application of in situ leaching is largely in the conceptual
stage.

[handwritten: who is doing this, what results?]

Research toward implementation of the process is being conducted on a
limited scale by the Institute of Mineral Research and by the U. S. Bureau of
Mines at their Salt Lake City Research Center. This research must be expanded
in scope and magnitude to complete process development in a reasonable period
of time.

Homestake Copper Company has contracted to have the Institute of Mineral
Research prepare for Homestake a plan of research and development with the
following broad objectives: to determine the feasibility of in situ leaching
as a method of processing native copper ores, to determine the most useful
areas of application in the native copper district and to determine which
method or methods of leaching offer the greatest promise of successful
application. This report describes the plan recommended by IMR to Homestake
Copper Company.

[handwritten: Do we now have a Contract w/ IMR?]

General Philosophy of the Plan

Specific goals of the studies included in the plan are as follows:
1) to gather general data concerning deposits in the district to assess the
amenability of each toward processing by in situ leaching; 2) to make
engineering, environmental and economic evaluations of conceptual in situ
leaching systems; 3) to obtain process design information necessary for

[handwritten: How many of these steps are completed?]

development of useful leaching systems; 4) to identify ore deposits for which in situ leaching appears useful and to select leaching systems preferred for those deposits; 5) to select a preferred site (or sites) for location of a pilot-scale operation; and 6) to design, construct and operate one or more pilot-scale in situ leaching systems.

There is no precedence for the application of in situ leaching being considered in this plan. Therefore, accurate prediction at this time of the effort required for any given part of the overall study is not always possible. Fairly large uncertainty factors should be applied to the estimates given in this report for time, effort and money necessary to complete the program. Furthermore, a mechanism is necessary for close assessment of the program at any moment to insure that studies are being directed along proper avenues and that unprofitable research be identified and terminated as early as possible.

A basic assumption inherent in the design of the plan is that there are many deposits of native copper ore potentially suitable for in situ leaching. Furthermore, there are several methods of leaching which potentially may be applied. Present knowledge of the process is inadequate to permit focusing solely on one particular deposit or on one particular method. Indeed, one of the major objectives of the plan is to obtain information on a sufficient variety of ore types and leaching methods so that useful deposits and useful methods, if any, can be rationally identified.

This does not mean that every method must be tested on every ore in the district. This would be an impossible task. Limitations of time and money will require that engineering judgments be made frequently on the basis of information on hand plus general experience, so that emphasis will be placed on deposits and methods which appear the most promising.

2

Accordingly, the plan has been structured to gather certain forms of information on a broad scale, with a minimum of effort and early in the program, to provide a base for subsequent judgments. Then, as these judgments direct, more detailed information will be gathered on a narrower scale, ultimately focusing on the information needed for design and operation of a specific pilot plant. Obviously, the plan must provide frequent opportunity for making necessary judgments by dividing the effort into a number of discrete blocks, none of which extends overly long in time. Such division will also allow the necessary flexibility to insure that blind alleys are not followed unduly long and that emphasis can be readily shifted to more profitable studies.

Principal Features Requiring Study

Determination of the feasibility of the in situ leaching process involves study of the following major items: 1) Ore Reserves - the parameters of potentially useful ore reserves must be detailed and the amenability of each reserve estimated; 2) Ore Preparation - the ore must be prepared to provide access of leach solutions to the deposit; 3) Leaching and Copper Recovery - the ore must be treated with leach solution to provide for recovery of copper at an economically acceptable rate and copper must be removed from pregnant solutions in the form of a useful product; 4) Environmental* Constraints - the environmental constraints within which the system must operate must be determined, their influences assessed, and provision made to insure proper operation of the system; 5) Engineering and Economic Analyses - total in situ leaching

---

* Throughout this report the terms "environmental", "environment", etc., connote health and safety aspects as well as impact on the physical surroundings.

3

processes must be designed in concept and analyzed for engineering and economic feasibility; 6) Pilot-Scale Testing - the potential deposits of the district must be surveyed, the best candidate(s) selected and a pilot-scale operation of sufficient scale established to confirm process utility, obtain process design data for scale-up, and identify problems requiring further study.

Project Management

Because of the complexity of the studies required in this program and *Was this* because of the need to make frequent assessment of progress and judgments *ever set* pertaining to further work, proper management is essential. For this purpose *up? It* a Project Manager supported by a Steering Committee is suggested. The Steering *So who are the* Committee should comprise the Research Managers concerned with specific areas *members* of study: Ore Preparation, Leaching and Copper Recovery, Geology and Ore Reserves, Environmental Control, and Economic Analysis - five members in all. The Project Manager may be one of these five, but preferably should be someone removed from the details of any given phase of the study.

Ultimate authority should reside with the Project Manager. He should meet frequently with the Steering Committee. The Project Manager will be responsible to Homestake Copper Company.

An Advisory Committee will also be desirable. This Committee should include members capable of offering advice and assistance in the various phases of the study, plus other interested parties. The Steering Committee should meet with the Advisory Committee at least semi-annually, and should keep the Advisory Committee informed of progress between meetings.

Both the Steering Committee and the Advisory Committee should be formed as soon as possible to establish and maintain proper control of the program.

WbW? Was an advisory Committee ever formed?

4

SCOPE AND PROCEDURES OF RESEARCH

In this section of this report, the scope of study for each of the principal features requiring study is discussed individually to the extent possible at this time. The final section of the report discusses implementation of the program in terms of manpower and funding requirements together with an estimated schedule of work.

Identification and Amenability of Ore Reserves

Early identification of potentially useful ore reserves is imperative. This information is important from several standpoints: 1) Such information will establish the potential scope of application of the process in the district; 2) it will determine whether initial studies may be limited to one ore type, conglomerate or amygdaloid, or whether both must be included from the beginning; 3) the data will be necessary in making preliminary economic assessments of application to a given deposit; 4) the data will be useful in designing conceptual in situ leaching processes for engineering and economic analysis. Whenever possible, samples of ore from potentially useful deposits should be obtained for laboratory examination and amenability testing.

Tabulation of reserves. An initial screening study should be made to classify individual deposits as rapidly as possible according to their potential utility. Those eliminated will require no further immediate attention; for those of interest additional details will be gathered as required. As early as possible the Steering Committee should prepare a list of desired data so that the deposits will be properly evaluated. The desired data will include for example such parameters as size and grade of the deposit, ore type, dimensions, surrounding hydrological conditions, porosity, permeability, and manner of copper occurrence. Obviously, not all of this information can be obtained quantitatively.

However, even best estimates or qualitative descriptions will be useful in evaluating the deposits.

Most of the information pertaining to potential reserves will of necessity come from company files. In addition, laboratory examination and amenability testing will be desirable on as many different ore samples of interest as can readily be obtained.

Laboratory examination of ore samples. Laboratory examination will include basic mineralogical examination, observation of the manner of copper occurrence, measurement of porosity and other measurements or observations as appear significant to assess the potential utility of the ore.

Mineralogical studies will include macro-microscopic examinations. The principal information sought will be to identify major mineral components of the ore, the mineralogical association of the copper, and general observation of the presence of porosity in the rock. An example of the potential utility of such information is that the calcite present in Iroquois ore is closely associated with copper. Since the calcite is likely to fracture very readily on blasting, there is a distinct possibility that with such an ore substantial amounts of copper can be exposed to leaching with a minimum of fracturing of the ore. *or use acid to eat calcite out thus opening up channel ways - might be cheaper than blasting*

The manner of occurrence can be evaluated from mineralogical examinations as well as by estimating copper grain size distributions by means of staged crushing and screening of the ore. It can also be evaluated by means of *B. S. o* electronic sorting tests, employing laboratory-scale sorting devices. Such information, particularly in terms of the connectivity of the copper, is significant in estimating the fraction of copper potentially recoverable from the ore. Porosity measurements, as made by established methods, are also of significance in estimating amenability toward in situ leaching. *How do you determine porosity? This is a most important test!*

6

<u>Amenability leaching tests</u>. Amenability testing will consist of a standard leach test conducted on a sample of crushed and sized ore. <u>Exact definition of desirable standard leaching conditions will depend on the results of leaching tests presently underway at IMR with several different ore types and different leaching conditions</u>. However, it is anticipated that <u>strong leach solutions and relatively small ore pieces will be used</u> in order to obtain significant leaching data in a short period of time. Amenability tests will not be con- ducted to completion. Instead, initial leaching data will be evaluated on the basis of a kinetic model of leaching presently being developed. It is recommend- ed that studies be conducted on a number of "extreme" ore types to estimate the range of leachability of the ores in the district.

[handwritten margin note: what did these tests show?]

[handwritten margin note: I disagree, it will be little like actual circumstances]

<u>Indirect estimation of amenability</u>. At the present time the amenability of an ore to leaching can only be determined by conducting an actual leach test such as those described. The principal disadvantage of this procedure is that it is very slow, particularly for large ore pieces where many months may be required. The desirability of estimating amenability indirectly is apparent.

Present research has suggested indirect estimation of amenability to leaching may be possible, at least in a semi-quantitative manner. Leaching tests at IMR on two conglomerate ores and one amygdaloid ore show direct correlation between leaching results and porosity measurements. This very simple correlation is undoubtedly only part of a more complete and accurate method of indirect evaluation. Further study of relations for the ore types presently under study will serve to identify their potentially useful corre- lations. The ideas developed in the present study will need confirmation and refinement through similar laboratory measurements and leaching studies made with other ore samples.

[handwritten margin note: a better way is to get a gallons/vol. velocity relationship. i.e. vs time - how fast the concentration of the pregnant sol. drops in a given system in a poorly fractured rock]

7

Therefore, the desired laboratory examination and amenability leaching studies will serve two significant purposes: they will provide necessary information pertaining to the potential application of in situ leaching to particular deposits, and they will serve as a basis for development of a more rapid indirect evaluation of utility of other deposits through ranking of a new ore against a semi-quantitative scale of amenability developed from laboratory studies on a variety of ores.

Ore Preparation

Preparation of the ore in order to provide access of the solution to the copper is probably the most critical operation affecting the feasibility of in situ leaching. There are a number of methods by which an ore deposit might be prepared for leaching and each method must be tested to determine its potential utility. Since the methods are largely dependent on the structural characteristics of the undisturbed ore, much of the testing must be performed underground. The variability between and within ore deposits requires testing a number of ore types and performing replicate tests on each ore type.

The four major methods of ore preparation are: 1) bore-hole leaching; 2) bore-hole fracturing; 3) open fracturing; 4) abandoned mine preparation. Research programs for testing the methods are described below:

Bore-hole leaching. This method of ore preparation is one of the simplest. It consists of drilling holes into the formation and utilizing the natural permeability and porosity of the ore to provide pathways for solution flow from one hole to another. The natural porosity would also provide contact of the solution with the copper. This method of leaching is probably considered to be the least feasible because of the dense appearance of the native

8

copper ores. However, the ores tested to date show considerably more porosity (about 5%) than one would expect, and if the pores are sufficiently connected then bore-hole leaching may indeed be feasible.

In order to study bore-hole leaching, it will be necessary to measure the amount of rock connected by pores to a bore-hole (pore connectivity) and the permeability between bore-holes. These measurements must be performed on undisturbed underground formations. How?

The first step in determining pore connectivity will consist of core drilling a hole down the dip of the formation. The length of the hole should be about 30 to 50 feet, and the diameter of the hole should be about 3 inches. The porosity of the core will be measured in the laboratory with a gas pycnometer. The hole will be dried and a packer with an inlet tube will be installed half-way down the hole. The top half of the hole will be sealed with resin, as shown in Figure 1. The purpose of sealing this portion of the hole is to confine the measurements to the bottom half of the hole where the ground is undisturbed. It will also prevent the gas used in the measurements from leaking to the surface.

The hole will then be evacuated and helium gas from a calibrated cylinder will be allowed to expand into the hole and the pores of the surrounding rock. The apparatus is shown schematically in Figure 2. Given the volumes of the cylinder, hole, and inlet tube - V_c, V_h and V_z, and the initial and final pressures - P_1 and P_2, then the pore volume of the rock surrounding the hole can be calculated:

$$V_p = (P_1/P_2 - 1)V_c - V_h - V_t$$

Since the porosity of the ore, denoted by e, will be known from the measurements on the core, the effective radius of the pore-connected rock can be calculated from:
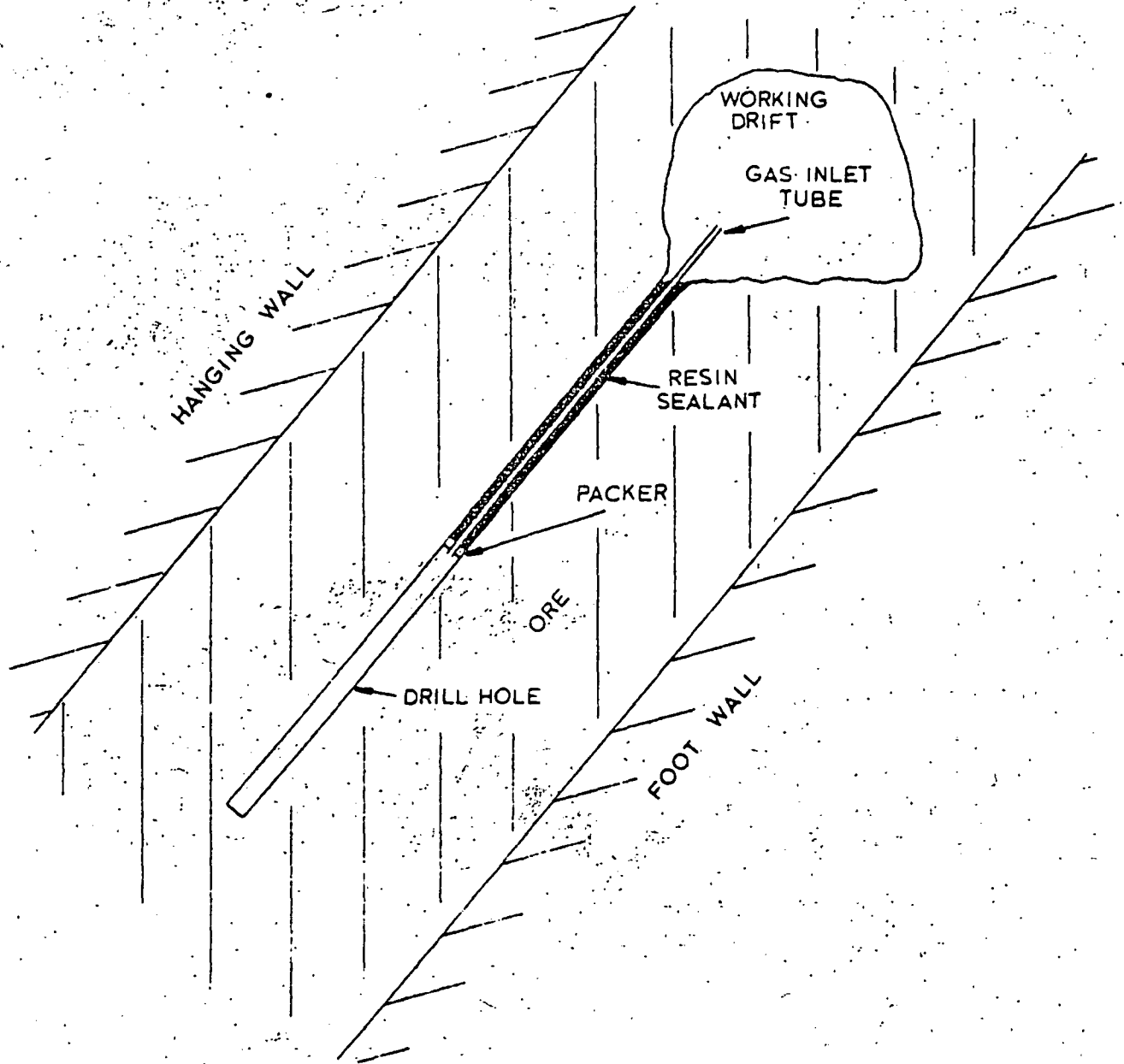
Figure 1.   Arrangement and Preparation of Drill Hole for Measuring In Situ Porosity
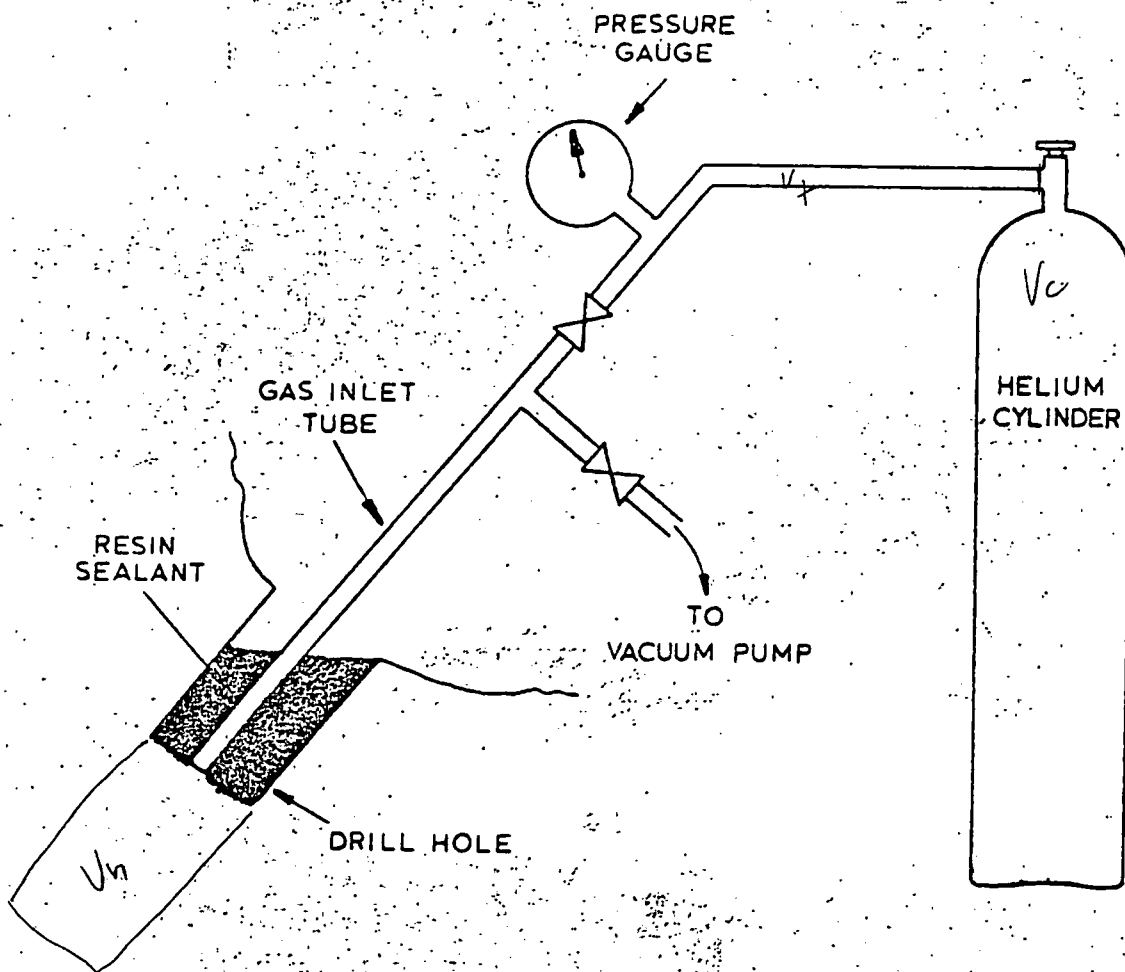
PRESSURE GAUGE

V_x

V_c

HELIUM CYLINDER

GAS INLET TUBE

RESIN SEALANT

TO VACUUM PUMP

V_h

DRILL HOLE

Figure 2.   Apparatus for In Situ Porosity Measurements

$$R = \sqrt{r^2 + V_p/\pi eL},$$

where r and L are the radius and length of the hole. R is the average radius of the zone of rock connected by pores to the drill hole. Of course, the actual zone of pore-connected rock will be irregular (compare Figures 3a and 3b).

The above steps should be repeated at one or more locations in the mine to determine the variability of R. _Should be done in the same area to determine the ability to repeat performance._

Before proceeding further with the study it will be necessary to determine if R is sufficiently large to warrant further testing. A simple economic criterion would be that the value of the copper in a cylinder of radius R must exceed the cost of drilling the hole. _+ pay its share of plant + op. costs_

If this criterion is met then the next step in the study will be to measure the permeability of the ore. Two "permeability" holes will be drilled parallel to the above-described "porosity" hole, and to the same depth, with one hole on each side of the porosity hole. The distances between holes will be 1.5R and 3.0R as shown in Figure 4. By using two holes of differing distances the permeability can be determined as a function of hole spacing.

The holes will be sealed with resin as described above. Helium will then be injected into the porosity hole and the flow rates out of the two permeability holes will be measured at several injection pressures. Permeability will be calculated from the pressure and flow rate data. If the permeability is sufficiently high, water will be substituted for helium and the liquid permeability measured.

These tests should be performed on each of the holes used in the porosity measurements to determine the variability of the ore.
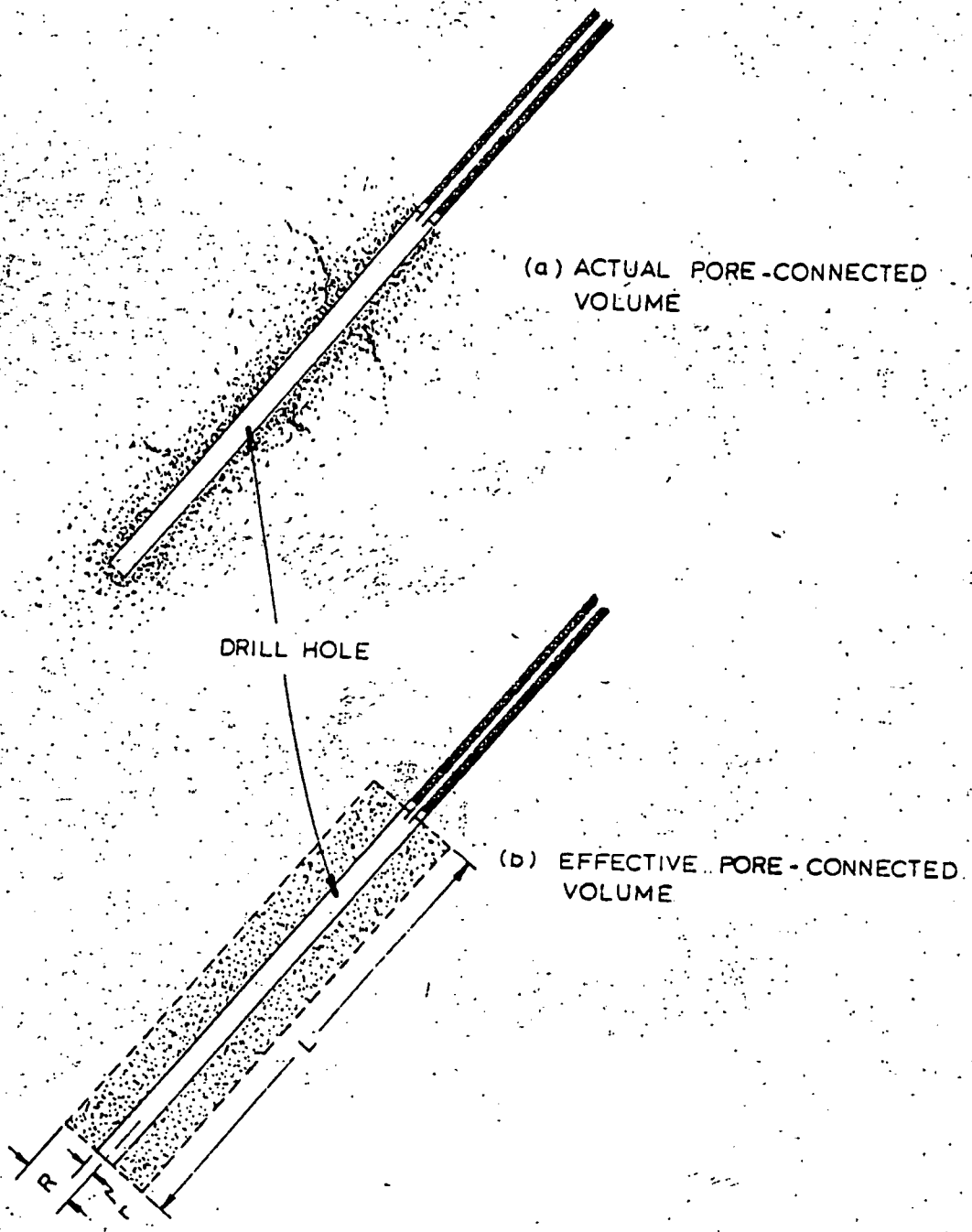
(a) ACTUAL PORE-CONNECTED VOLUME

(b) EFFECTIVE PORE-CONNECTED VOLUME

DRILL HOLE

R

L

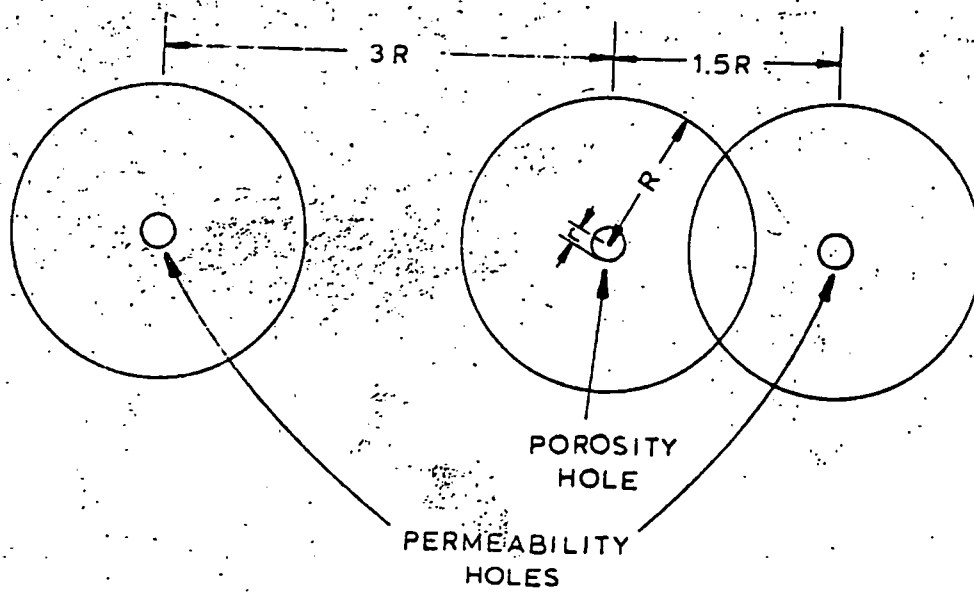Figure 3. Comparison of (a) Actual and (b) Effective Pore-Connected Volume

13

Figure 4. Arrangement of Permeability Holes with Respect to Porosity Hole

If the results of these tests indicate that the ore is sufficiently porous and permeable, a next desirable step of the study will be to conduct a sub-pilot scale leaching test. This test will have to be carried out on a sizable block of ore in order to ensure that a representative sample of mineralized ore is being used. The block will be prepared for leaching by drilling a number of holes of pattern and spacing determined by the data described above. One half of the holes will be used for solution injection and the other half for solution recovery. Cuttings from the holes will be analyzed and used to estimate the grade of the block of ore.

Solution will be pumped into the injection wells from a solution storage tank and effluent from the recovery wells will flow back into the tank. The solution will be analyzed periodically to determine the amount of copper extracted. The flow rates into and out of the holes will be measured to determine the uniformity of the permeability within the block. If a hole produces an excessively high flow rate (an indication of short-circuiting), the injection line will be throttled to decrease the flow to a reasonable rate.

The test will be continued until the extraction rate decreases to an uneconomically low level. The solution will then be flushed from the block and the block will be mined out, crushed, and analyzed to determine the tailings grade. Chemical analyses and an inventory of the solutions will determine total extraction, reagent consumption, impurity pick-up, and loss of solution out of the block.

Bore-hole fracturing. The objective of this study is to determine the feasibility of preparing ore for in situ leaching by blasting the ore in place (confined blasting). The study will involve measurements of fracture intensity and permeability produced by blasting bore-holes drilled into underground formations.

15

The test work will be performed in stages, starting with single hole blasts and progressing to multiple hole blasts. The principal control variables will be blast hole diameter, type of explosive, hole spacing and ore type. Fracture intensity will be determined from cores obtained by drilling through the blast zones. Permeability will be determined by measuring fluid flow through the blast zones.
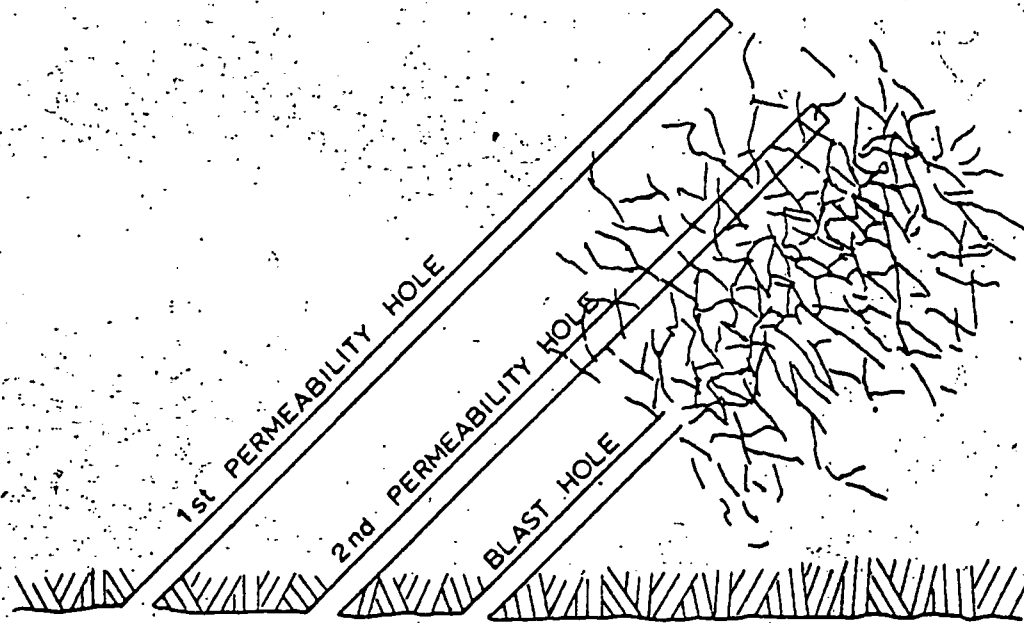
a.   Single-hole tests. The first stage of the program will consist of blasting tests on single holes. A blast hole will be drilled at 45° to the face with a diamond drill. Core from this hole will be saved for comparison with core obtained after the blast. Only the back of the blast hole will be loaded with explosive and the balance of the hole will be stemmed. The stemmed length will be sufficiently long to prevent the blast zone from breaking out to the face, i.e., to ensure that the blast is completely confined.

After blasting, a permeability hole (Figure 5) will be drilled parallel to the blast hole. Gas will be injected into this hole and the flow rate into the blast hole (after boring out the stemming) will be measured. If the flow rate (permeability) is too low, a second permeability hole will be drilled closer to the blast hole and the permeability again measured. This procedure will be repeated until a sufficiently high permeability is obtained. The data can be plotted to yield a distance versus permeability curve as shown in Figure 5. The core obtained from these permeability holes will be logged to determine fracture intensity parallel to the blast zone.
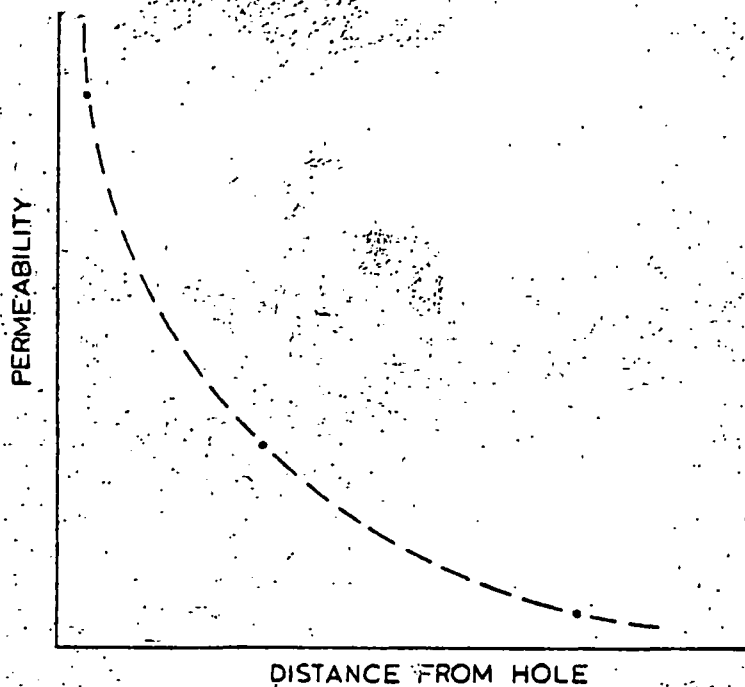
After the permeability tests are completed a recovery hole will be drilled through the blast zone at 90° to the blast hole (Figure 6). The core obtained from this hole will be logged to determine the radial fracture intensity distribution as shown in Figure 6. If the fracture intensity cannot be accurately determined because of poor core recovery, the blast zone will be grouted with resin and an additional recovery hole drilled.
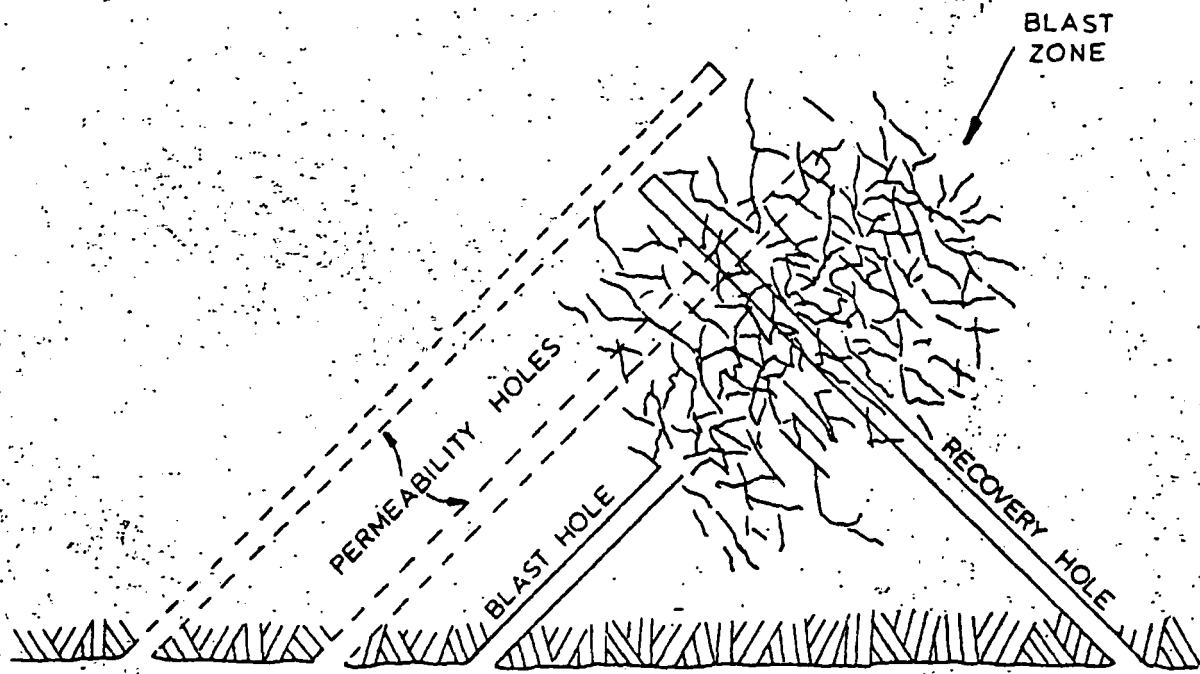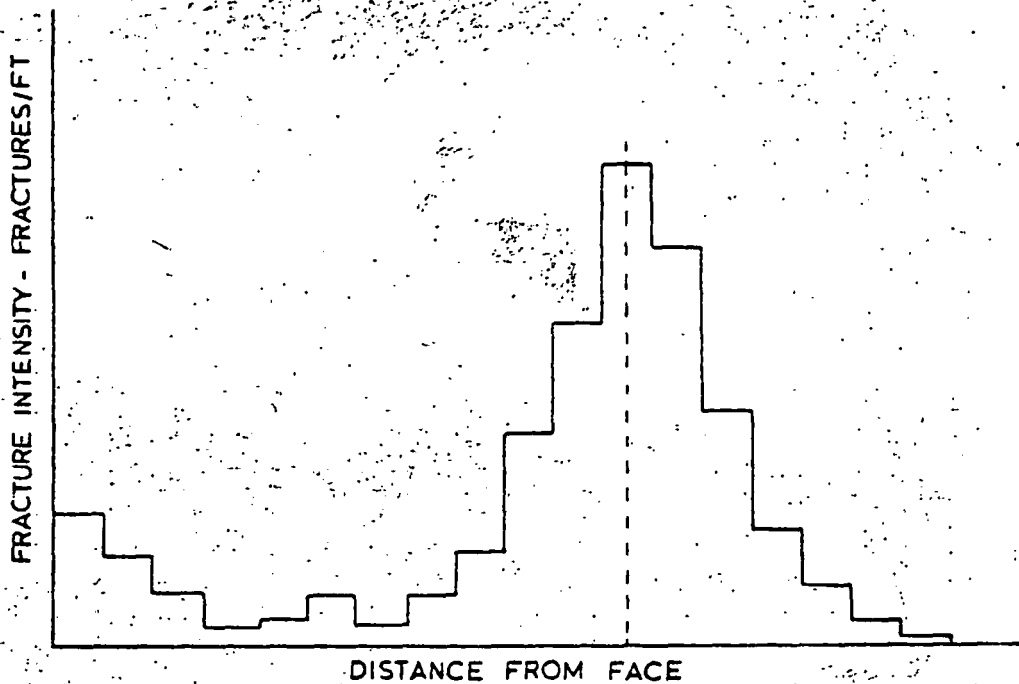
(a)

DISTANCE FROM HOLE

(b)

Figure 5. (a) Arrangement of Blast Hole and Permeability Holes in Single-Hole Confined Blasting Tests.

(b) Expected Relationship between Permeability and Distance from the Blast Hole.

BLAST ZONE

PERMEABILITY HOLES

BLAST HOLE

RECOVERY HOLE

(a)

FRACTURE INTENSITY - FRACTURES/FT

DISTANCE FROM FACE

(b)

Figure 6. (a) Arrangement of a Recovery Hole with Respect to the Blast Hole in Single-Hole Confined Blasting Tests.

(b) Expected Log of Fracture Intensity on Core from the Recovery Hole.

18

Four blast zones will be prepared and tested by the above methods, using two blast hole diameters (e.g., 2 and 4 inches) and two types of explosives (normal and high energy). The test data will be analyzed to determine the most efficient and economical combination of hole size and explosive. An additional test using the best combination will be performed at another location in the mine to determine the variability of the ore.

b. <u>Multiple-hole tests</u>. The data from the above single-hole tests will be used to estimate the blast hole spacing for the first multiple hole test. Three blast holes in a triangular pattern will be used and the holes will be drilled at right angles to the face. As in the single-hole tests, only the back ten feet of the blast holes will be loaded.

After blasting, a permeability-recovery hole will be drilled into the center of the pattern (Figure 7). The core recovered from this hole will be logged for fracture intensity. The permeability between this hole and each of the three blast holes will be measured; in addition, the permeability between each pair of blast holes will be measured. This will provide six measurements from which to determine the average permeability of the blast zone and the uniformity of the permeability within the zone.

The data from this first multiple-hole test will be analyzed to determine if the spacing was too large or too small (Figure 8). A second multiple-hole test will then be performed at a spacing designed to produce a better break. The procedures used will be the same as in the first test. The results of these two multiple-hole tests should provide sufficient data for interpolation and extrapolation over a moderate range of blast hole spacings. If the ore being tested exhibits considerable variability in its fracturing characteristics it may be necessary to perform an additional multiple-hole test to measure this variability.
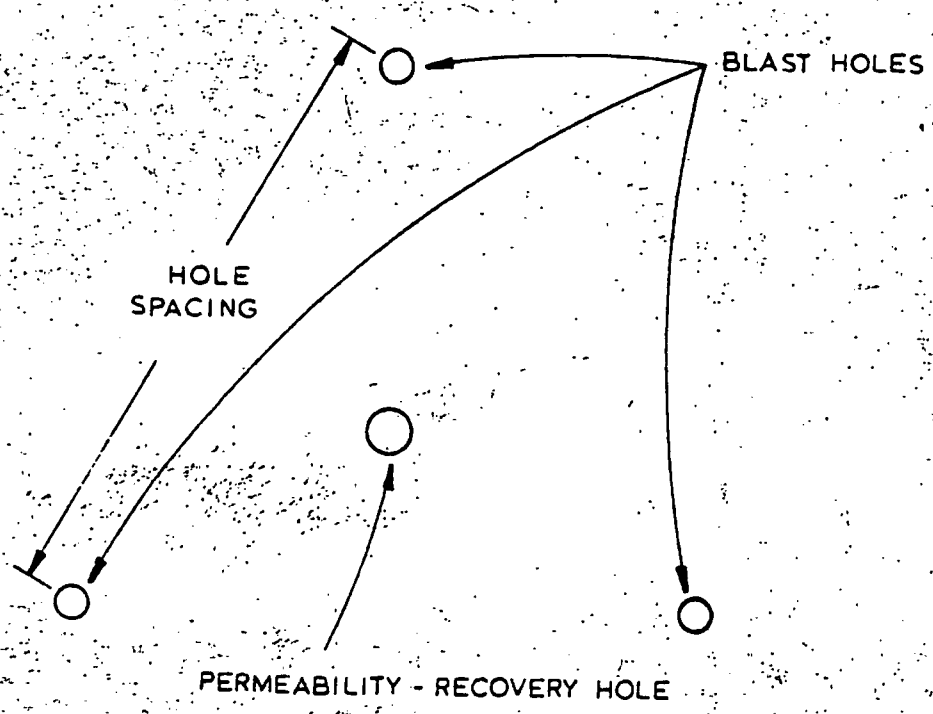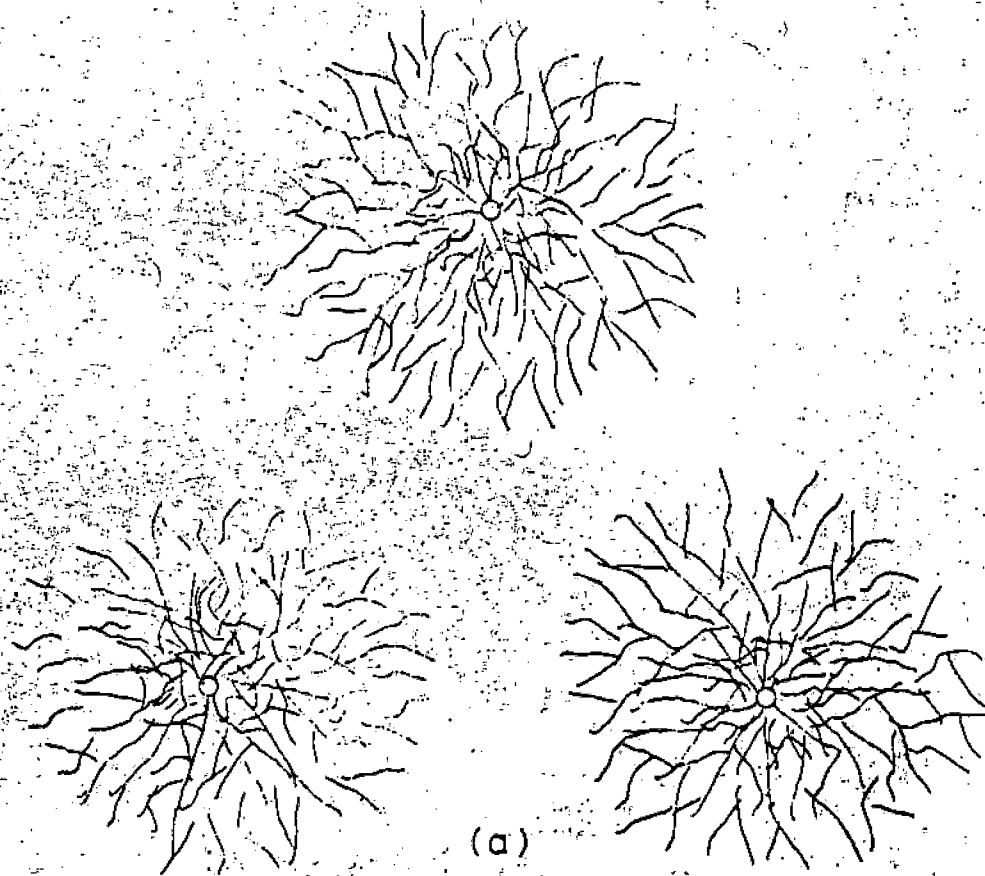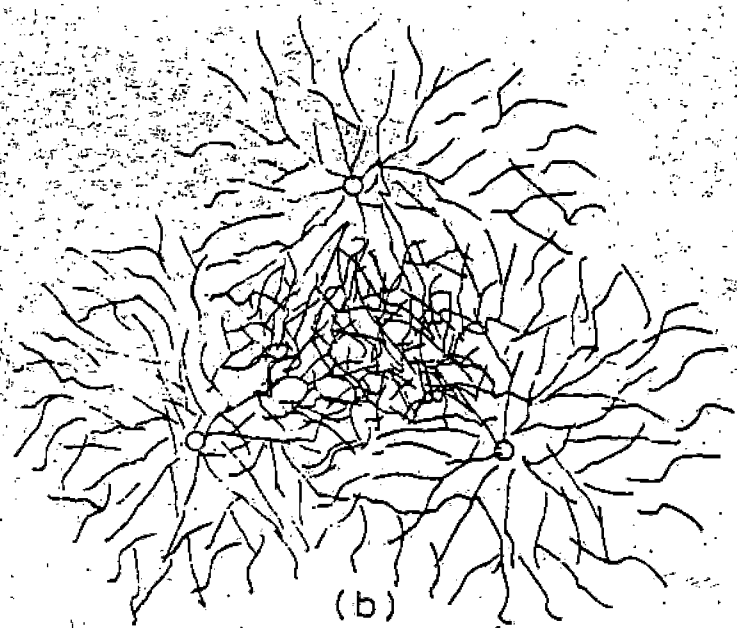
19

Figure 7. Arrangement of Blast Holes and Permeability-Recovery Hole in a
Multiple-Hole Blasting Test.

20

(a)
SPACING TOO LARGE

(b)
SPACING TOO SMALL

Figure 8. Effect of (a) Excessive Hole Spacing and (b) Insufficient Hole Spacing in Multiple-Hole Confined Blasting Tests.

21

The above sequence of single- and multiple-hole tests will have to be performed on each major ore type being considered.

The fracture intensity and permeability data obtained from these tests along with leachability data from laboratory tests will provide the basic information for determining the feasibility of in situ leaching by bore-hole fracturing methods. These data should also be sufficient for designing a sub-pilot scale leaching test. This test would be very similar to the leaching test described earlier in the section on bore-hole leaching. It would consist of drilling a pattern of holes into a mineralized block of ore of sufficient size to be a representative sample; loading the holes and blasting the block; drilling injection wells into the fracture zone; pumping leach solution into the injection wells; collecting and analyzing the effluent solution periodically over a sufficient period of time to determine the rate and extent of copper extraction.

Open fracturing. The term "open fracturing" is used to describe the blasting of rock into prepared underground openings in order to create a column of rubble suitable for underground leaching. The goal of open fracturing is to provide just sufficient dislocation of the fracture surfaces to permit easy percolation of the leach solutions. In contrast to bore-hole fracturing (confined blasting) which produces a zone of fractured ore with minimum induced porosity, open fracturing would produce moderate porosity and a much higher degree of permeability. The objective of this study is to determine the minimum amount of opening needed (expressed as "relief", the percentage of opening volume to rubble volume) and the most efficient blasting method for creating a uniform rubble column having satisfactory leaching characteristics.

Since open fracturing is largely an extension of conventional underground mining methods, the first part of the study will involve an examination of

22

present mining techniques to determine the best approach to the problem. This will be followed by underground fracturing tests. To be meaningful, such tests will have to be conducted on a large scale, and will require considerable time and expense. As only a limited number of tests can be performed it is essential that the most attractive methods be selected for testing and that the tests be carefully planned.

Since the native copper deposits are (steeply) dipping, the most efficient method of creating rubble would be to break the ore downwards into the prepared opening. This opening would probably be in the form of a drift of suitable cross-section. Drilling and loading of the blast zone could be performed from this drift and from the next drift up the mine; the use of raises may also be advantageous. Since long-hole drilling will probably be used, much of the blasting will be under semi-confined conditions. Therefore the data obtained in the confined-fracturing studies described in the previous section will assist in planning these tests. The first test should probably be performed with insufficient relief so that the problem areas can be identified and corrective changes applied, either in terms of more relief or more blasting. A few additional tests should then provide reasonable data for estimating the feasibility of open fracturing.

Underground leaching experiments on the rubble from these tests will not be required as the results can be estimated sufficiently well from laboratory tests on loose rock.

Abandoned mine leaching. The leaching of abandoned mines is characterized by a number of unique advantages and disadvantages. The foremost advantage is the presence of large quantities of broken rock from the old mining operations. Thus, the costly drilling and blasting steps required in preparing a virgin ore body for leaching are avoided. Moreover, the extensive underground openings in

23

abandoned mines will probably permit the movement of large volumes of solution with little pressure drop. *False economy — Surface area has to be the key to high leaching rate.*

The major problems associated with leaching abandoned mines are: the difficulty of gaining access to the old workings because of mine water, caving or subsidence; the large volume of leachant required to flood the old workings; the difficulty of controlling solution flow through the workings; the general lack of information on the grade, size and amount of rubble, particularly in the older mines where records ~~may be~~ *are* incomplete. Thus, the leaching of abandoned mines will be characterized by minimum expense for ore preparation, but large expense for solution inventory and considerable difficulty in controlling and predicting the outcome of the operation.

The study of abandoned mine leaching is complicated because it cannot be *wrong* readily tested on a small scale. The condition and layout of the mine and the nature of the rubble will vary from one mine to another even and within a single mine, making small-scale testing quite unreliable.

The best approach to determining the feasibility of abandoned mine leaching will be to select a particular abandoned mine as a test case and to perform a detailed feasibility study on it. The mine selected should be moderately small or capable of being compartmentalized so that an actual *that's the ticket* leaching test of controllable size can be performed if the results of the study are favorable. Because most of the abandoned mines in the district are amygdaloids, the test case should be of this type and the mining methods that were employed should have been conventional. If these criteria can be met the results of the study will be sufficiently general. It is essential that good records of the mine be available. Access to samples of the rubble and to the mine water at depth will be important advantages.

The first part of the study will involve an analysis of the records to derive estimates of the amount, size and grade of the rubble and the volume

24

of the openings. Mine water will be sampled at various depths and its composition, density and temperature determined. If possible, samples of rubble will be obtained and leachability experiments performed.

After these basic data have been obtained, the preparation of the mine for leaching will be investigated. The factors to be considered are whether to dewater the mine or to use the existing mine water for solution make up; whether some dewatering might be required to bring the water level low enough to prevent leakage out of the mine into the environment; the best way of introducing the leachant into the mine, e.g., through existing openings or through wells drilled down to intersect the workings. The strength of the leaching solution will have to be determined; the ratio of extractable copper to the volume of mine openings will set an upper limit on solution strength. Whether the mine can be leached in sections or whether all portions of the mine must be leached simultaneously will be determined and will have an effect on solution strength. The increase in the density of the solution as copper is dissolved will cause movement of the solution and will influence the number and position of the pumping stations for bringing the rich solution to the surface.

After the plan for preparing the mine is established, the rate of copper extraction as a function of time will be estimated. The size of the copper recovery plant and the problem of maintaining a constant feed solution to the plant will be analyzed. The old pumping records of the mine will be used to estimate ground water influx into the mine which will determine how much leach solution must be distilled and discarded.

These and various other factors will be analyzed by the methods described in the sub-section on "Engineering and Economic Analysis" to determine the

feasibility of leaching the mine. If the results of the study indicate that such an operation would be profitable, all or a portion of the mine could be leached on an experimental basis.

This study will not only determine the feasibility of leaching the selected test mine but will also provide a general methodology for use in the analysis of other abandoned mines.

Solution Treatment Methods

In the ammonia leaching of native copper, four solution treatment methods are required: 1) solution make up - preparation of the initial solution and replacement of ammonia and carbonate losses; 2) oxidation - conversion of the cuprous ammine to cupric ammine by reaction with air or oxygen; 3) copper recovery - extraction of copper from the pregnant solution and conversion to a marketable form; 4) stripping - removal of the leaching reagents so that water of sufficient purity can be discharged from the process.

The technology for these methods is fairly well understood, and in fact each operation has been demonstrated on a commercial scale. Therefore, only a limited amount of experimental work on these methods will be required. The major emphasis will be on collecting engineering and cost data and on studies as to how the methods can be best applied to the various in situ processes.

Although solution make up and oxidation are generally performed in absorption towers it may be more efficient and require less capital if these operations are carried out underground, using underground chambers and rubble as the absorption tower. If the cuprous ammine can be oxidized underground as soon as it is produced, the maximum driving force for leaching will be obtained.

Some research will be required on the solvent extraction of high concentration solutions. Present practice is to treat fairly dilute solutions,

but current studies show that these dilute solutions leach at rather low rates. Although there does not appear to be any fundamental reason why solvent extraction cannot be applied to concentrated selections, it must be tested experimentally for unforeseen problems.

In addition to solvent extraction, a number of other processes for recovering copper from ammonia solutions are possible. They include distillation, direct electrowinning from ammoniacal solutions, gaseous reduction and chemical precipitation. Even though solvent extraction will likely be the preferred process, each of the alternative processes should be studied to determine its possible applicability. Extensive studies will not be required; most of the processes can be evaluated with existing technical and cost data. In some cases laboratory tests will be required to obtain some of the necessary information.

A particularly critical step is the stripping process. Large volumes of solution might be involved and the liminations on reagent levels in the discharge water might be very low. Since there is a possibility that conventional steam distillation will not produce an acceptable effluent, a polishing process such as ion exchange might have to be applied after distillation. A suitable alternative in some cases might be to pump the distillation effluents to the bottom of neighboring abandoned mines.

Environmental Control

Introduction of leaching reagents into the environment is a potential problem associated with in situ leaching. Reagent loss may occur in three ways: 1) by escape of solutions from the mine into the water table and then into lakes, streams or wells; 2) by disposal of spent solutions or leaching by-products; or 3) by evaporation of ammonia into the atmosphere. These might be termed "external" environmental problems.

27

In addition to the external environmental problems there are potential "internal" environmental problems. They are: 1) leakage of ground water into the in situ operation; 2) production of flammable or explosive gas mixtures (NH_3-O_2) within the mine; 3) difficulties in performing underground development and maintenance in the presence of toxic levels of ammonia and either high or low concentrations of oxygen. *Good point*

The external and internal problems are not independent. For example, leakage of water into the mine requires that an equal volume of solution be discarded if dilution is to be avoided. The cost of removing contaminants from the discard solution to an acceptably low level may be prohibitive. Similarly, ventilation of the underground areas undergoing development may result in nuisance levels of ammonia in the atmosphere.

The magnitude of the environmental problems will depend on three general factors: 1) the characteristics of the ore deposit and its surroundings; 2) the type of in situ process being employed; 3) the statutory regulations governing permissible levels of discharges and safe working conditions.

The first factor is highly dependent on the deposit being considered. Its evaluation will require collection of data concerning the deposit. These data will include pumping records, water analyses, general topography, land ownership, habitation and hydrology of the surrounding area, and the possible steps which might be used to isolate the deposit from the environment. Since only a limited number of deposits can be studied, the best approach would be to select one or two deposits for detailed evaluations. In this manner the more significant factors would be identified and the general procedures for evaluating other deposits would be developed.

Study of the second factor will involve identification of the major environmental problems associated with each of the four general in situ

28

methods. This will be followed by studies of the monitoring and control procedures which might be applicable to each case.

The third factor will require collection of federal (EPA, OSHA) and state regulations affecting discharges and working conditions. This study will also include collection of data pertaining to environmentally-related properties of the in situ solutions and atmospheres (NH_3 vapor pressure, solution and gas densities, explosive limits, etc.).

Engineering and Economic Analyses

Objectives. Engineering and economic analyses will be directed toward two principal objectives: 1) to guide experimental work into the most useful avenues and 2) to evaluate conceptual in situ leaching systems. These analyses will be conducted in a stepwise fashion, starting from the simplest basis possible. Each step will provide a "go-no go" answer, and subsequent steps involving more sophisticated design and analyses will be taken only when all previous steps have given favorable results.

At various times, depending on specific objectives, analyses will be concerned with overall in situ leaching processes or with individual components of such a system.

Scope. The analyses will generally follow a sequence such as: 1) describe, or design, the process of interest; 2) establish the engineering feasibility to be sure that the process can be operated physically to produce the desired results, making necessary modification in the original design to insure engineering acceptability; 3) evaluate the economic acceptance of the process as finally designed.

For any given system (or part thereof), this analytical procedure may be repeated, if necessary, at increasing levels of detail and sophistication of process design, assuming that previous analyses have yielded favorable results.

That is, it may often prove desirable to design a process first in an oversimpli-
fied manner, examining only the obviously key parts of the process. Design and
analysis will then proceed through more detailed stages to some desired end point.

It should be emphasized that the analytical procedure can be stopped at any
point should either engineering or economic analysis indicate unacceptable
performance of the conceptual leaching system. Should such a result appear, a
decision will be necessary to choose between the alternatives of abandoning the
design completely or attempting to modify it as to make it acceptable.

Analyses as a guide to research and development. The analyses will serve
to guide experimentation in two ways. Engineering or economic analysis of a
part of the process may indicate that even under the best conceptual conditions,
that part will not be acceptable. An example of such analysis has been given
in the discussion of work on bore-hole leaching. From an initial engineering
standpoint, the leaching technique is acceptable since drilling holes in rock
is readily accomplished. However, simple analysis may show that the maximum
dollar value of copper which might be recovered from a hole (or set of holes)
would be less than the cost of drilling. Under such conditions there will be
no point in conducting the experiments. It is important that in making such
simple analyses, which may be subject to large errors due to inaccuracies in
making estimates, judgments based on the analyses should tend to be optimistic.
As more experimental data concerning a process or one of its parts become
available, the errors in analysis will be reduced and judgments should become
correspondingly more rigorous.

A second way in which engineering and economic analyses will guide experi-
mentation is through identification of problems in leaching systems. That is,
in any given system, analysis may well indicate that only one of two parts of
the system as conceived are unacceptable from either engineering or economic

30

considerations. This may indicate that further development studies should be conducted in an effort to overcome the difficulties, and therefore save an otherwise useful leaching system.

Thirdly, the analyses will be useful in identifying the parts of a leaching system which most greatly influence costs and/or engineering results. Thus, research and development can be focused on these parts, rather than on less sensitive parts of the system.

Finally, the analyses will indicate needs for better or more complete empirical data pertaining to a particular leaching system. This information can then be gathered by the most appropriate method.

Procedures. The engineering and economic analyses will be conducted by the most convenient method appropriate to the desired analysis. In the initial stages simple hand calculations will probably suffice. As the analyses proceed in development to include more and more details, and produce more accurate results, the calculations and evaluations will require more sophisticated techniques. The ultimate development will almost certainly require use of computer models as a matter of convenience to allow for efficient and complete analysis.

Since the reliability of a system analysis is only as good as the input data, it will be essential to collect and compile an extensive list of engineering and economic information. These data bases will cover a broad spectrum and will include such items as drilling and blasting costs and performances, reagent costs, ore properties (leachability, porosity, reagent consumption), capital expenditures for a solution-treatment plant, scale-up factors, kinetic data, fuel and power costs, etc. These data will be obtained from a variety of sources including the technical literature, studies currently underway, studies to be performed in the program, equipment manufacturers, etc. In some

31

cases only estimates will be available and in others, only a range of values. One of the valuable features of computerized analysis is that the influence of a range of values can be quickly assessed. Another useful technique for limited data is to perform the analysis in reverse - to input a profitable return and calculate the range of values which will ensure this return.

Information will also be needed on the costs of conventional mining. These benchmark data are required because in situ leaching must not only be profitable but also more profitable than conventional mining methods.

In order to assess the feasibilities of the various in situ processes (or any of their parts) the analyses will be formulated to output both technical and profit-oriented information. Analyses will be flexible with respect to variations in input parameters and will allow for sensitivity analysis of the parameters.

Thus, it will be possible to determine under what conditions a given technology may be implemented and to examine variations in the process. In addition it will be possible to examine the feasibility of a mixed process, employing both conventional mining and in situ methods. The ultimate objective of the analysis will be to define the optimum process for a given ore body. This will be accomplished by using the physical characteristics (dimensions, shape, grade, etc.) of existing and abandoned mines as structural constraints on the models.

As mentioned earlier, these system studies will be used to assist in the experimental phases of the program. Thus, it is important that there be close liaison between the system studies and the other phases of the program.

As a final step in the economic analysis of an acceptable leaching system, detailed pro forma income statements should be prepared. These statements will allow managers to assess most carefully the potential profits(losses) of a

32

system. The statements should be developed for a period of five or more years and should conform to the accepted accounting procedures of Homestake Mining Company. Armed with these data, and engineering data, the feasibility of a complete in situ leaching system can be ultimately established.

Pilot Scale Studies

The results of all research and analysis described previously will ultimately be focused on the design, construction and operation of one or more pilot scale test sites. Operation of a pilot site will generally confirm expectations based on previous studies, will provide more refined data on which to base engineering and economic evaluation of commercial scale operations, and will define more accurately those aspects of in situ leaching operation requiring further study and development.

At this time detailed description of a pilot scale operation is not possible, because so many paramaters will depend on results to be obtained in other studies. There is, of course, a possibility that these results will be so negative that the entire program will be terminated short of pilot operation. For the moment, this possibility will be excluded from the discussion.

While exact description of the pilot site is not possible at present, certain significant factors can be described. Of utmost importance is that the pilot plant be designed with optimum chance of successful operation. The pilot operation will undoubtedly be very costly - probably in the range of $500,000 to $1,500,000. If the pilot plant should fail or give very discouraging results, it is very unlikely that additional funds will be available for a second try.

Therefore, great care must be given to site selection, size of operation, method of ore preparation and leaching and copper recovery. Even more important will be to insure that adequate and fail-safe environmental control is provided.

Preference should be given to a site with potential commercial utility. Other factors influencing site selection will be: 1) similarity to other deposits to obtain information of broadest utility; 2) cost of development and provision of services. It is conceivable that more than one site might be desirable, either in different deposits or at different locations within a single deposit. In any case it will be advantageous if the test site includes the major ore types occurring in the mine.

Very little can be said at this time about preferred scale of operation methods of ore preparation, leaching or copper recovery. Decisions on each of these aspects must be based on results of studies yet to be accomplished. Premature commitment to any of these could well jeopardize opportunity for successful operation of the pilot plant, which in turn will jeopardize success of the entire program.

One aspect of pilot plant design which should be kept in mind when final design criteria are set is the possibility of producing sufficient copper to defray a substantial part of the costs. However, the pilot plant must be considered first and foremost as an experimental tool, designed to obtain data for scale-up to commercial operation.

The pilot plant should operate at least one year. In addition, considerable lead time will be required to design and construct the plant. Provisions should be made to duplicate all phases of anticipated commercial operation as closely as possible, including production of the final product from the system. Great

34

thought should be given to obtaining as much information as possible from the pilot plant. This will require designing flexibility into the operation so that more than one mode of operation can be studied. Adequate instrumentation must be provided, not only to obtain operating data, but also to provide for acceptable environmental control. At the conclusion of the test, the leach zone will be mined to evaluate the results of the test.

Because design of the pilot plant will require substantial effort, certain aspects should be commenced as early as possible. In particular, preliminary section of likely sites should be made so that the necessary detailed information about these sites can be gathered. Again, of particular importance will be information pertaining to environmental control.

IMPLEMENTATION

In this section of the plan, estimates of the manpower, money, and time required for each phase of the program are presented.

It is assumed that the work will be directed by the five Research Managers described on page 4, using various types of support personnel such as miners, technicians, student assistants, etc. Nearly all of the cost of the program will be made up of the salaries and wages of these people. Equipment costs will be relatively small. It is assumed that underground test sites will be readily accessible and will have adequate services.

A rate of $9/hr is used for the professional personnel and $5/hr for the hourly-rated support personnel. The salary rate for the Project Manager who will be involved on a part-time basis throughout the program is taken as $12/hr. Indirect costs are not presented because these costs cannot be determined without knowing which organizations will be performing the work.

The budget shown on the following pages lists the personnel involved, the man-hours required, the cost and the completion time for each major step of the phases making up the program. In some cases, special assumptions were required as to the extent of the test work; these are noted in the budget. Equipment that will be used in more than one phase is listed only once.

The scheduling of the program is shown graphically in Figure 9. This schedule was derived from the man-hour and completion time data of the budget. The various phases are arranged in a logical sequence and in a manner to minimize the total time and make best use of the personnel. The numbers in the bar graphs are the estimated costs of the itemized studies. At the bottom of Figure 9 the cumulative cost of the program up to pilot plant testing is presented.

PROGRAM BUDGET

IDENTIFICATION AND AMENABILITY OF ORE RESERVES

	Man-hours	Cost
1. Tabulation of Reserves		
Company Geologist	160	1440
Clerical	80	320
Completion time - 2 months		1760
2. Laboratory Examination - assume 12 samples		
a. Sample collection and storage		
Company Geologist	60	540
Miner	80	400
Metallurgist	8	72
Technician	16	80
Supplies and services at 25% of salaries and wages		273
Completion time - 3 weeks		1365
b. Laboratory tests (crushing, screening, analysis, porosity, mineralogical examination, sorting)		
Metallurgist	96	864
Technician	480	2400
Supplies and clerical at 10% of salaries and wages		326
Completion time - 5 weeks		3590
3. Amenability Leaching Tests - assume 18 samples		
Metallurgist	116	1044
Technician	252	1260
Supplies and clerical at 10% of salaries and wages		230
Completion time - 4 months		2534
4. Indirect Estimation of Amenability		
Metallurgist	80	720
Technician	80	400
Computer time and clerical at 20% of salaries and wages		224
Completion time - 1 month		1344

Summary:

	Man-hours	Cost
Company Geologist	220	1980
Metallurgist	300	2700
Miner	80	400
Technician	828	4140
Supplies, services and clerical		1373
Completion time - 9 months		$10,593

ORE PREPARATION

1. Bore-Hole Leaching

   Assume two mines being tested, three locations in one mine and two in the other; sub pilot-scale leaching test in one mine.

   a. Determination of Pore Connectivity

Five tests each requiring:	Man-hours	Cost
Mining Engr.	30	270
Miner	25	125
Technician	18	90
		485 each

   b. Permeability Measurements

Four tests each requiring:		
Mining Engr.	39	351
Miner	45	225
Technician	2	10
		586 each

   c. Leaching Test

Mining Engr.	40	360
Metallurgist	77	693
Miner	546	2730
Technician	60	300
		4083

   d. Interim Evaluations

Mining Engr.	24	216
Metallurgist	16	144
Economist	40	360
		720

Summary:

Estimate two months to complete pore connectivity and permeability studies; seven months for leaching test.

	Man-hours	Co
Mining Engr.	370	33
Metallurgist	93	8.
Economist	40	36
Miner	851	425.
Technician	158	790

Equipment (drill, tanks, pump, controls) 9572

Supplies, services and clerical at 15% of salaries and wages $14,500

Completion time - 9 months

1436

$25,508

2. Bore-Hole Fracturing

Assume two mines being tested, sub pilot-scale leaching test in one mine.

a. Single-hole tests

Ten tests each requiring:	Man-hours	Cost
Mining Engineer	60	540
Miner	64	320
Technician	17	85
		945

b. Multiple-hole tests

Six tests each requiring:		
Mining Engineer	29	261
Miner	52	260
Technician	4	20
		541

c. Leaching test

Mining Engineer	56	504
Metallurgist	80	720
Miner	562	2810
Technician	60	300
		4334

d. Interim Evaluations

Mining Engineer	24	216
Metallurgist	16	144
Economist	40	360
		720

Summary:

Estimate seven months to complete single- and multiple-hole tests; seven months for leaching test.

	Man-hours	Cost
Mining Engineer	854	7686
Metallurgist	96	864
Economist	40	360
Miner	1514	7570
Technician	254	1270
Equipment (tanks, pump, controls)		$3000
Supplies, services and clerical at 15% of salaries and wages		2662
Completion time - 14 months		$23,412

3. Open Fracturing

Assume two mines being tested, two test blocks in the first and one in the second. Test blocks about 100' x 50'. Services and equipment available. Labor supplied by Homestake.

Estimate 5 months and $25,000 required for each block.

Completion time - 15 months $75,000

4. Abandoned Mine Leaching

Evaulation of one test case.

a. Collection and tabulation of records and water analysis, sample collection.

	Man-hours	Cost
Company Geologist	80	720
Envir. Geologist	40	360
Technician	16	80
Completion time - 1 month		1160

b. Evaluation of Data and Design of Plan

Company Geologist	40	360
Metallurgist	120	1080
Envir. Geologist	20	180
Economist	40	360
Technician	16	80
Completion time - 6 weeks		2060

c. Analysis of Plan

Company Geologist	20	180
Metallurgist	120	1080
Envir. Geologist	20	180
Economist	120	1080
Technician	16	80
Completion time - 6 weeks		2600

Summary:

Company Geologist	140	1260
Metallurgist	240	2160
Envir. Geologist	80	720
Economist	160	1440
Technician	48	240
Clerical at 10%		582
Completion time - 4 months		$6402

43

SOLUTION TREATMENT METHODS

Work will consist largely of engineering and costing, along with a limited amount of test work.

		Man-hours	Cost
1.	Solution Make-up		
	Metallurgist	80	720
	Economist	40	360
			1080
2.	Solution Oxidation		
	Metallurgist	80	720
	Economist	40	360
			1080
3.	Copper Recovery		
a.	Literature search and fundamentals		
	Metallurgist	80	720
b.	Distillation		
	Metallurgist	80	720
	Technician	40	200
c.	Solvent Extraction		
	Metallurgist	80	720
	Technician	80	400
d.	Reduction		
	Metallurgist	40	360
e.	Precipitation		
	Metallurgist	40	360
	Technician	40	200
f.	Electrowinning		
	Metallurgist	80	720
	Technician	80	400
g.	Costing and Economic Evaluation		
	Economist	120	1080
			5880
4.	Solution Clean-up		
	Metallurgist	80	720
	Technician	40	200
	Economist	40	360
			1280

Summary:

Estimate that the time required to complete these studies will be twice the metallurgist's hours.

	Man-hours	Cost
Metallurgist	640	5760
Economist	240	2160
Technician	280	1400
Supplies, equipment and clerical at 15% of salaries and wages.		1398
Completion time - 8 months		$10,718

ENVIRONMENTAL CONTROL

1. Obtain Regulatory Data and Solution Properties

	Man-hours	Cost
Environmental Geologist	80	720
Metallurgist	40	360
Technician	16	80
Clerical at 10% of salaries and wages		116
Completion time - 1 month		1276

2. Characterization of In Situ Methods: Monitering and Control Procedures

Environmental Geologist	120	1080
Mining Engineer	48	432
Metallurgist	48	432
Clerical at 10% of salaries and wages		194
Completion time - 1 month		2138

3. Study of Typical Mines

   Assume two mines to be studied:

   a. Collect hydrological data

Company Geologist	80	720
Environmental Geologist	240	2160
Technician	120	600
Clerical at 10% of salaries and wages		348
Completion time - 2 months		3828

   b. Data evaluation

Company Geologist	16	144
Environmental Geologist	80	720
Metallurgist	24	216
Mining Engineer	24	216
Clerical at 10% of salaries and wages		130
Completion time - 3 weeks		1426

Summary:

	Man-hours	Cost
Environmental Geologist	520	4680
Company Geologist	96	864
Metallurgist	112	1008
Mining Engineer	72	648
Technician	136	680
Clerical		788
Completion time - 5 months		$8,668

ENGINEERING AND ECONOMIC ANALYSIS (INCLUDING PROJECT MANAGEMENT)

1. Preliminary - staffing, planning and scheduling of test work, equipment procurement and. facility set-up.

	Man-hours	Cost
Project Manager	80	960
Mining Engineer	80	720
Company Geologist	40	360
Metallurgist	80	720
Envir. Geologist	40	360
Economist	40	360
Clerical at 10% of salaries and wages		348
Completion .time - 1 month		3828

2. Initial Data Collection

Economist	120	1080
Mining Engineer	40	360
Metallurgist	40	360
Company Geologist	20	180
Envir. Geologist	20	180
Clerical at 10%		216
Completion time - 1 month		2376

3. Initial System Design and Gross Feasibility Studies

Economist	120	1080
Mining Engineer	60	540
Metallurgist	40	360
Company Geologist	40	360
Technician and clerical at 10%		234
Completion time - 1 month		2574

4. Continuing Analysis and Evaluation

	Man-hours	Cost
Project Manager	416	4992
Economist	2340	21060
Metallurgist	2200	19800
Mining Engineer	2080	18720
Company Geologist	312	2808
Envir. Geologist	340	3060
Programming Asst.	2080	10400
Technician and clerical at 10%		8084
Computer time		6000
Completion time - duration of program up to pilot plant design - about two years.		$94,924

Summary:

	Man-hours	Cost
Project Manager	496	5952
Economist	2620	23580
Metallurgist	2360	21240
Mining Engineer	2260	20340
Company Geologist	412	3708
Envir. Geologist	400	3600
Programming Asst.	2080	10400
Technician and clerical		8882
Computer time		6000
Completion time - 2 years		$103,702

PILOT PLANT STUDY AND FINAL ANALYSIS OF THE PROGRAM

The following estimates of requirements for design, construction and operation of a pilot plant must be understood to be very rough at best. At this stage of planning there is no basis for establishing such important parameters as the location and size of the operation, the method of leaching and even the information desired from the study. Therefore, the estimates given must be considered as guidelines only.

1. _Design_. Pilot plant design will require the efforts of several people to cover such aspects as ore preparation, leaching and copper recovery and environmental control. About 1 to 1.5 man-year of effort expended over six to nine months, might be necessary.

2. _Operation_. The pilot plant should probably be operated for at least one year to insure that adequate and useful data are obtained to allow for making modifications in the sutdy if necessary, and to be sure that operation of the leaching system does not suffer with time due to unexpected side effects in the system. One or two engineers will almost certainly spend most of their time in supervising the study and the part-time efforts of several other engineers and scientists will be required as assistance is needed. _Analysis_. Complete analysis of the pilot plant study will require three to six months to complete and will probably require 1 to 1.5 man-years of effort in total. The efforts of all professional people having had major responsibility for the test will be necessary to some extent in making the analysis and preparing the final report.

3. _Cost_. The total effort of design, construction and operation of the pilot plant, analysis of the results and report preparation will

probably cost between $500,000 and $1,500,000. Depending on the size and type of operation it may be possible to defray a portion of this cost by selling the recovered copper.

FIGURE 9. PROGRAM SCHEDULE AND GRAPH OF EXPENDITURES

MONTHS 0 1 2 3 4 5 6 7 8 9 10 11 12 1 2 3 4 5 6 7 8 9 10 11 12   2 years 3 years 4 years

1 year

IDENTIFICATION & AMENABILITY ($10,593)
    Tabulation — 1760
    Sampling — 1365
    Lab. tests — 3590
    Leaching tests — 2534
    Indirect studies — 1344

ORE PREPARATION ($130,322)
    Bore-hole leaching — 25508
    Blast-hole leaching — 23412
    Open Fracturing — 75000
    Abandoned mine leaching — 6402

SOLUTION TREATMENT ($10,718)
    Copper recovery — 2705
    Solution clean-up — 1472
    Solution oxidation — 4057
    Solution preparation — 1242   1242

ENVIRONMENTAL CONTROL ($8,668)
    Data collection — 1276
    Method characterization — 2138
    Mine study — 5254

ENGRG. & ECONOMIC ANALYSIS ($103,702)
    Preliminary — 3828
    Initial data collection — 2376
    Initial design — 2574
    Continuing analysis — 94924

TOTAL BEFORE PILOT PLANT ($264,003)

PILOT PLANT ($500,000-1,500,000)
    Design & construction
    Operation
    Analysis

CUMULATIVE COST ($1000)

300

200

100

0   1 year   2 years 3 years 4 years

UDC 669.753.7

Kinetics of the cathodic reduction of antimony sulphide anions

V S Shestitko, N P Ermilov and N V Ishchenko (Krasnoyarsk Institute of Nonferrous Metals. Department of the Metallurgy of Light and Rare Metals)

Summary

The kinetics of the reduction of thioantimonite ions were investigated by a single-pulse galvanostatic method. On the potential-time curves after the region corresponding to the charging of the electric double layer the potential was slowly displaced towards the negative side, which indicated that concentration changes were taking place. The kinetics of the reduction of the thioantimonite ions were therefore investigated by analysis of the cathodic chronopotentiograms with a transitional time, recorded without special agitation.

It was established that the slowest stage of the overall process is transport of the complex ions to the electrode surface. The diffusion coefficient of the complex ions was determined ($0.63 \cdot 10^{-6}$ and $0.68 \cdot 10^{-5}$ cm^2/sec for sodium sulphide concentrations of 90 and 110 g/l respectively). The kinetic parameters of the process were determined. The rate constant of the investigated process amounted to $3.02 \cdot 10^{-5}$ cm/sec, and the mean exchange current for current densities of 40.45 and 50 mA/cm^2 amounted to $5.75 \cdot 10^{-2}$ A/cm^2.

*1975 Sov. Non-Fe...
v.3 N1*

UDC 546.16 + 669.054

Passage of fluorine into solution during autoclave-soda leaching of scheelite concentrates

Yu P Fedorov and I A Khar'kovskii (Moscow Institute of Fine Chemical Technology. Department of the Technology of Rare and Trace Elements)

Table 1: Effect of temperature on the concentration of WO_3 and F^- in the solutions from autoclave-soda leaching

First stage				Second stage			
Composition of solution g/dm³			Soda eq.	Composition of solution g/dm³			Temp. °C
F'	WO₃	Na₂CO₃		F'	WO₃	Na₂CO₃	
1.23	31.9	80.6	2.0	0.84	32.7	115.4	150
1.90	38.7	62.5	1.7	0.97	34.1	113.4	150
1.23	31.4	107	2.5	0.97	34.1	112.0	150
2.75	81.3	42.4	2.0	3.61	27.7	101.8	200
3.32	87.1	71.0	2.5	3.80	19.8	106.0	200
2.47	76.1	–	1.7	3.60	33.8	95.4	200
2.65	86.45	40.3	2.0	4.10	1.8	81.7	220
2.40	84.0	42.3	1.7	3.60	3.0	89.0	220
2.85	90.1	54.0	2.5	–	–	–	220

Table 2: Effect of the length of autoclave leaching on the concentration of fluoride and soda in the solution g/dm³

Length h	Soda	Fluorine
0.5	–	3.15
1	54.55	3.80
1.5	49.06	4.06
2	40.60	2.52
4	38.87	2.70

Table 3: Effect of soda concentration on the equilibrium concentration of fluoride in the solution

Concentration of soda g/dm³	Equilibrium concn. of F ions g/dm³
55	7.6
49	6.8
40	5.5
39	5.4
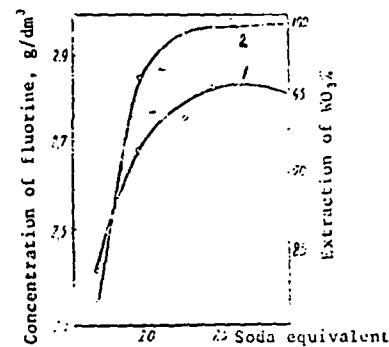
Fig.1 Dependence of the fluorine concentration of the solution (1) and the extraction of WO₃ (2) into the solution on the soda equivalent. Experimental conditions: Weight of intermediate product 80 g; solid-liquid ratio 1:4, 220°C, 2 h.
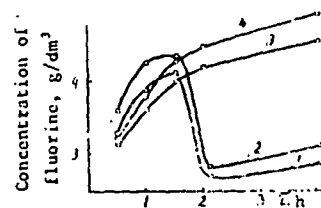
Fig.2 Variation of the fluorine concentration in the solution as a function of the leaching time in the first (1,2) and second (3,4) stages. 1,3 – Soda equivalent = 2; 2,4 – soda equivalent = 2.5. Experimental conditions: Solid-liquid ratio 1:4; 220°C.

Summary

The article gives data from laboratory and industrial investigations of the behaviour of fluorine during autoclave-soda leaching of scheelite products. The concentration of fluorine in the solution during leaching depends on the temperature, the soda equivalent, and the length of the leaching process.

It was established that the fluorine concentration of the solution does not depend on its content in the initial concentrate. To maintain a minimum concentration of fluorine in the solutions it is necessary to realise the leaching process for not less than 2 h with a small excess of soda.

HEAVY NON-FERROUS METALS

THE PRESENT AND FUTURE USES OF SORPTION PROCESSES IN HYDROMETALLURGY[1]

UDC 669.2.053.4:661.183

B. V. Gromov

The large-scale industrial use of methods based upon sorption processes has recently assumed even greater importance in chemical technology for inorganic substances. The high rates of development in atomic technology, the creation of many structural materials, and the effective separation of elements with similar properties are indissolubly linked with advances in sorption and solvent-extraction technology [1].

Sorption and solvent extraction have their own specific advantages:

high selectivity and cleanness of separation;

opportunities for flexible control of selectivity by alteration of pH and oxidation-reduction conditions, complexing, and other methods;

the simplicity and compactness of the process layout;

opportunities for implementing continuous and automated processes.

The significant advance in the utilization of ion exchange for technological purposes dates from the creation (at the end of the thirties) of artificial organic ion-exchange resins. These resins have a remarkable variety of chemical properties, high exchange capacity, and chemical stability in various media; they also maintain favorable rates of ion exchange, especially in the microporous anion-exchange resins. Cation- and anion-exchangers and ampholytes have been created, as well as sorbents which hold the exchange ions and molecules by coordinate bonds. Many of them show a marked capacity for the selective absorption of particular ions.

The uranium industry is now a major field of application of sorption processes [2,3].

The Soviet Union was the first country to make effective use of ion exchange in uranium technology: even in 1948, B. N. Laskorin had suggested that carboxylic resins based upon acrylic and methacrylic acids should be used for the selective extraction of uranium from solutions and pulps containing a large number of salts. Research in this field culminated in 1954 in the industrial adoption of a new continuous filterless method of sorption from thick ore pulps in specially designed apparatus with pneumatic mixing [4,5].

An appreciable reduction in the consumption of chemicals and a simultaneous increase in metal extraction into the ion-exchange resin phase are achieved in the proposed technology by combining the processes of sorption and leaching.

The method permits drastic reductions in the time for processing the ore material and simplifies phase separation. For example, whereas the specific speed of filtration is usually 0.5-1.0 tons/(m^2·hr), in sorption from pulp up to 50-100 tons/hr of ore material can be separated from the resin through 1 m^2 of separating mesh.

The method, which was developed in the USSR [4-8], is suitable for processing pulps containing up to 50-60% solids, including 3-5% of +0.15 mm particles. The volume of sorption apparatus is essentially unlimited, reaching hundreds of cubic meters and having enormous rates of output; this makes it possible to reduce the number of process lines to the minimum. The apparatus used has no moving parts or structures; the process is readily automated and is very stable.

The gold-mining industry is another fairly typical example of the successful adoption of sorption technology in the Soviet Union.

As early as 1915, when N. D. Zelinkskii was studying the sorption properties of activated carbons, an attempt was made to use them for sorption of gold from solutions. Later I. N. Plaksin published a work [9] devoted to the sorption of gold cyanide complexes.

In spite of numerous researches [10], sorption technology for gold using synthetic ion exchangers was not employed in practice abroad right up to 1972. In the hydrometallurgical cyanidation method the solutions have a low gold content and are complex in composition. The researches directed by B. N. Laskorin, I. N. Plaksin, and others which confirmed the basic advantages of sorption technology were therefore of particular importance in its industrial implementation: these advantages are the possibility of eliminating pulp filtration, a substantial increase in gold extraction due to the sorption leaching effect, opportunities for processing leaner raw material, and the consequent expansion of gold ore reserves [11,12].

Application of ion-exchange technology to the most complex auriferous ores is of particular interest; processing these ores by normal methods involves considerable losses of gold, high reagent consumptions, and massive capital investment. An example

[1] Based upon the First All-Union Conference on Hydrometallurgy.

of this is the work on gold extraction from resistant auriferous ore in which the presence of carbonaceous material (a constituent part of carbonaceous argillites) makes it difficult to achieve a sufficiently high level of gold extraction by traditional methods because of the adsorptive capacity of the country rock relative to the gold-cyanide complex: 65% of the gold in the tailings is in the form of metal sorbed by carbonaceous material. Processing such ore became possible only by the sorption leaching of gold with an anion exchanger, added to the pulp at the same time as the cyanide. In the initial leaching period the ion exchanger prevents the sorption of gold by the carbonaceous material, which is much less active than the principal sorbent (the anion exchanger). As a result, extraction of gold from the ore increased by 20% in a number of cases.

Considerable amounts of associated elements pass into solution during cyanidation of auriferous ores; the cyanide solutions therefore contain complex copper, zinc, iron, nickel, etc. cyanides, which are readily sorbed by anion exchangers. The concentration of these elements is many times greater than the gold content, so that serious difficulties arise in organizing the repeated multiple use of ion exchanges in the sorption circuits. The credit for developing reliable methods for the thorough purification of a saturated ion exchanger to remove sorbed non-precious metal impurities belongs to the research workers [13,14].

The results of pilot-plant tests on this technology formed the basis for gold-extraction plant reconstruction projects. The successful adoption of filterless sorption schemes for gold extraction from pulps has increased the extraction of gold and yielded savings of tens of millions of rubles [15].

The sorption process is being successfully linked with new methods for exposing complex sulfide ores (for example, the sorption leaching of auriferous concentrates in autoclaves), replacing pyrometallurgical schemes and schemes involving roasting and cyanidation of the calcine.

Sorption processes play an important part in rare metals technology, particularly in the case of tantalum and columbium. The use of ion exchange in the production of cerium rare earths has increased output by 2-3 times from the same floor area, with a 20-30% reduction in product prime cost [16].

The advances made in the Soviet Union in the industrial adoption of sorption (and solvent-extraction) technology formed the basis for the extensive use of these methods in the national economy.

Up to the present there has been a wide-ranging series of investigations to establish the scientific and technological principles of sorption processes for use in the hydrometallurgy of non-ferrous, rare, and precious metals [16,17].

One indication of developments in this field is the large number of papers on sorption topics read at the First All-Union Conference on Hydrometallurgy in December 1974: there were more than 80 papers from 34 organizations, or almost 45% of the total number.

Papers were read and discussed at the Conference which dealt with research on new aspects of the ionic state of Au, Ni, Co, Cu, Fe, Zn, Mo, and W and a number of rare and rare earth elements in sulfate, sulfate-chloride, chloride, and nitrate solutions. Data were submitted on peculiarities in the behavior of elements which tend to form hydrolyzed ions (Ni, Co, Cu, Fe) and polymerized ions (Mo, W, V). Studies were made of the static, kinetic, and dynamic aspects of ion-exchange processes, as well as the selectivity of sorption extraction and elution for the most varied media with complex salt compositions. A number of works defined the optimum conditions for sorption processes using a wide range of ion-exchange materials of various natures, compositions, structures, and functional groupings. The investigations have made a major contribution to the development of inorganic and physical chemistry.

Papers with a technological bias, describing the production of practically all the non-ferrous, rare, and precious metals, were no less interesting.

In the author's opinion, priority should be given to the application of sorption and solvent extraction to radical improvements in technology and to solving the basic problem of production, not to matters of secondary importance (further extraction of metals by processing various production wastes and dumps). Efforts should be concentrated on the adoption of new processes where they can be most conveniently incorporated into the technology now in use. From this viewpoint the nickel-cobalt industry is among those best-prepared for the adoption of solvent-extraction and sorption processes.

Soviet workers [18] have developed a sorption method for the selective extraction of impurities from nickel electrolyte, based upon the use of complexing ion exchangers selective in relation to the impurity metal (zinc, iron, copper, etc.) with good sorption properties and sufficient mechanical strength. The potential value of ion exchangers with a porous structure in the hydrometallurgy of nickel and cobalt was clearly shown.

A continuous sorption scheme for the removal of zinc from nickel electrolyte was introduced at the Yuzhuralnikel' Combine in 1969-1970. Removal of impurities from electrolyte by sorption is also being adopted at the Noril'sk Combine [19].

Great savings can be obtained by using autoclave-sorption technology in the nickel industry; this has the greatest potential at new enterprises processing copper-nickel sulfide ores [16].

The sorption leaching of nickel and cobalt directly from pulps obtained after autoclave leaching [20, p. 103] creates the conditions for the future implementation of a filterless technology and permits conversion to the hydrometallurgical production of nickel and cobalt with good technical and economic results.

A technical and economic comparison of the ammonia-sorption technology for nickel and cobalt extraction from oxidized nickel ores with electric ore smelting to produce ferronickel has demonstrated the great efficiency of sorption leaching.

A sorption technology has been developed, as a result of research on copper sorption from sulfate and ammonia-carbonate media and the synthesis of AMK, VPK, and VPG ion exchangers specifically for copper, for the extraction of copper from oxidized and mixed copper ores and from heap and underground leaching solutions, for the extraction of copper as a by-product by treatment of copper-bearing products of other non-ferrous metals, and for the extraction of copper from various industrial liquors of complex composition. Provision has been made for various combinations of sorption for copper extraction with hydrometallurgical and concentration processes, ensuring on the whole a significant overall increase in copper extraction from the ore.

Schemes developed in [21-23] have been used for reconstruction projects for concentration plants at the Dzhezkazgan and Almalyk Mining and Metallurgical Combines.

Using sorption technology for processing a blend of oxidized and mixed ores from the Udokansk deposit may appreciably increase the total extraction of copper from the ore into concentrate and cathode copper by comparison with the ordinary concentration scheme.

Sorption extraction of copper from heap leaching solutions delivering a finished product in the form of cathode copper is a simpler task. There are plans to bring in a pilot section for heap leaching of non-rated ores from the Kal'makyr deposit in the immediate future, with a capacity of up to 500 m^3 of leach liquor per day.

The wide variety of plants where copper sorption should be used calls for further comprehensive research on a wide range of sorbents to ensure efficiency in each specific case [20].

Ion-exchange sorption is of potential value for the extraction of molybdenum from molybdenum-bearing ores which are difficult to process by ordinary methods [20, 24-27].

Two enterprises in the Soviet Union have mastered the industrial production of pure molybdenum compounds, using sorption processes in the integrated processing of lean polymetallic ores containing molybdenum.

Sorption should be used in tungsten technology. Up to the present, the hydrometallurgy of tungsten has been based upon chemical processes of selective precipitation involving a large number of cleaning operations which lead to the formation of considerable amounts of recirculating products; the quality of the finished product (tungstic anhydride) often fails to meet present-day requirements. Sorption technology makes it possible to solve these problems at a higher level [28].

The principal factor which has delayed the adoption of sorption processes in tungsten technology has been the lack of high-capacity anion exchangers.

The tungsten sorption schemes, which are being incorporated into the existing technology, have been successfully tested on a pilot-plant scale with various production solutions from the Nal'chik Plant.

Staff from the Ust'-Kamenogorsk Lead-Zinc Combine have reported the results of pilot-plant tests on a method of removing harmful impurities from production solutions (zinc and cadmium electrolytes) by sorption.

A number of research projects submitted to the Conference were devoted to the sorption of rare earth elements, scandium, germanium, rhenium, bismuth, and other metals. Data for implementing the process schemes on an industrial scale were given for most of the developments.

While noting with satisfaction the appreciable advances in the development of scientific and technological studies and in the adoption of sorption, it should be said that they are not being brought into practical use quickly enough. The building of experimental and pilot sorption installations is slow. Quicker adoption of the processes of sorption from pulps which have already been perfected at plants already in operation and at those under construction is desirable.

The Conference noted that there were some difficulties in the adoption of sorption technology due to a shortfall in the production of ion-exchange materials, both in quantity and range. The prices of ion-exchange materials remain high, and this cannot fail to be reflected in the economic results of sorption technology as it is introduced.

On the whole, as has been demonstrated at the Conference, the research and design organizations of the USSR Ministry of Non-Ferrous Metallurgy, the institutes of the Academy of Sciences of the USSR and of the Union Republics, the industrial enterprises, and the higher educational institutions have made considerable advances in recent years in studying the theory of sorption processes and in their industrial adoption.

REFERENCES

1. Soviet Atomic Science and Technology, Moscow, Atomizdat, 1967, 392 pages, illustrated.
2. A. P. Zefirov, B. V. Nevskii, and G. F. Ivanov, Plants Processing Uranium Ores in the Capitalist Countries, Moscow, Gosatomizdat, 1962, 372 pages, illustrated.
3. R. F. Hollis and K. K. MacArthur, in: Nuclear Fuel Chemistry (Papers by foreign scientists at an International Conference on the Wider Use of Atomic Energy), Moscow, Goskhimizdat, 1956, pp. 17-39.
4. Yu. V. Smirnov, Z. I. Efimova, D. I. Skorovarov, et al., Atomnaya Tekhnika za Rubezhom, 1974, No. 10, 8-24.
5. Yu. V. Smirnov, Z. I. Efimova, D. I. Skorovarov, et al., Atomnaya Tekhnika za Rubezhom, 1974, No. 9, 22-26.
6. B. N. Laskorin, in: Separation of Rare Metals with Similar Properties, Moscow, Metallurgizdat, 1962, pp. 11-27.
7. B. N. Laskorin, Atomnaya Energiya, 1960, 9, No. 4, 286-291.
8. B. N. Laskorin, A. P. Zefirov, and D. I. Skorovarov, Atomnaya Energiya, 1960, 8, No. 6, 519-529.
9. I. N. Plaksin, A. I. Sinel'nikova, and A. Yu. Beilin, Dokl. Akad. Nauk SSSR, 1959, 129, No. 6, 1359-1361.
10. S. Seisman and F. Nachod, in: Ion Exchange (edited by K. V. Chmutov), Moscow, IL, 1951, pp. 245-269.
11. B. N. Laskorin, G. I. Sadovnikova, Yu. G. Novikov, et al., Tsvetnye Metally, 1971, No. 6, 76-78.
12. B. N. Laskorin, L. A. Federova, and G. I. Sadovnikova, Dokl. Akad. Nauk SSSR, 1969, 187, No. 4, 810-818.
13. B. N. Laskorin, A. G. Vitkovskaya, E. D. Lebedev, et al., Tsvetnye Metally, 1971, No. 4, 30-34.
14. B. N. Laskorin, A. G. Vitkovskaya, E. D. Lebedev, et al., Tsveynye Metally, 1971, No. 11, 71-75.
15. I. S. Guchetl' and G. M. Lezgintsev, Tsvetnye Metally, 1968, No. 7, 2-5.
16. V. N. Leksin, Tsveynye Metally, 1967, No. 12, 1-6.
17. A. V. Nikolaev and L. M. Gindin, Tsveynye Metally, 1968, No. 4, 32-34.
18. Solvent Extraction and Sorption in the Metallurgy of Nickel, Cobalt, and Copper (A collection edited by E. N. Merkin), Moscow, Tsvetmetinformatsiya, 1970, 182 pages, illustrated.
19. V. L. Konovalov, Tsvetnye Metally, 1974, No. 7, 17-20.
20. Hydrometallurgy 74 (Summaries of papers from the First All-Union Conference on Hydrometallurgy), Moscow, Nauka, 1974, 206 pages.
21. B. N. Laskorin, V. A. Goldobina, N. G. Zhukova, et al., Tsvetnye Metally, 1970, No. 10, 20-22.
22. B. N. Laskorin, V. A. Goldobina, N. G. Zhukova, et al., Tsvetnye Metally, 1970, No. 11, 18-22.
23. B. N. Laskorin, V. A. Goldobina, N. G. Zhukova, et al., in: Ion Exchange and Ion Exchange Resins, Leningrad, Nauka, 1970, pp. 212-217.
24. B. N. Laskorin, A. G. Maurina, and R. A. Sviridova, in: Ion-Exchange Sorbents in Industry, Moscow, Academy of Sciences of the USSR, 1963, pp. 124-131.
25. B. N. Laskorin, A. G. Maurina, N. N. Tokarev, et al., Tsvetnaya Metallurgiya (Bull. Inst. Tsvetmetinformatsiya), 1971, No. 24, 27-30.
26. B. N. Laskorin, V. A. Goldobina, A. G. Maurina, et al., Tsvetnaya Metallurgiya, (Bull. Inst. Tsvetmetinformatsiya), 1972, No. 13, 43-46.
27. A. G. Kholmogorov, S. V. Khryashchev, L. S. Chernikova, et al., Tsvetnye Metally, 1968, No. 11, 73-75.
28. A. G. Kholmogorov, S. V. Khryashchev, L. S. Chernikova, et al., Tsvetnye Metally, 1972, No. 9, 48-51.

7) T N Srivastava et alia: Z. Anorgan. Allgem. Chem. 1970, 379, (1), 82.

8) K A Bol'shakov (editor): Chemistry of rare and trace elements. Vysshaya Shkola, Moscow 1969.

Kinetic characteristics of the reaction of TiCl₃ with metallic titanium in molten sodium chloride

R A Sandler, I I Ivanov and S V Aleksandrovskii (Leningrad Mining Institute)

Summary

The extraction of titanium from wastes during metal-thermic refining to titanium depends on the reaction of TiCl₃ with metallic titanium, and the effectiveness of the purification of the melts from impurities on metallic titanium depends on the rate of establishment of the equilibrium in the melts. The article is devoted to an investigation into the reaction under dynamic conditions.

The dependence of the reaction rate on temperature and on the initial concentration of Ti³⁺ in the melts was investigated, and the apparent activation energy was determined from the results. The high value for the activation energy and the order of the reaction (close to second) showed that the reaction of titanium trichloride with metallic titanium in the sodium chloride medium took place under kinetic control. The results show that realisation of the process under kinetic control increases the reaction rate by approximately 8-10 times. The loss in weight of the compact metallic titanium was increased accordingly by 1.5-2 times, and this in turn intensified the chemical reaction.

Зоот- Nou Ft
1976 т. У N3

UDC 669.21.6

Precipitation of gold from cyanide solutions by metallic iron and some of its compounds

L D Sheveleva, A A Golovin (deceased), T T Tatarinova, M N Tagil'tseva and N G Tyurin
(Urals Polytechnic Institute - Department of the Metallurgy of Noble Metals)

Ores with finely impregnated gold form the bulk of un-yielding gold-containing raw material. Very often the gold in them is associated with iron sulphides. Hydrometallurgical treatment of these ores of their concentration products by cyaniding as a rule gives rise to a series of difficulties associated with increase in the cyanide and oxygen consumption rates, decrease in the dissolution rate of gold, and increased losses with the cyaniding tailings.

According to the results from preliminary tests and also published data[1][3], it could be supposed that the decrease in the gold content of the solution with decrease in the particle size and with increase in the length of agitation of the sulphide products in the cyanide solutions results from precipitation of the dissolved gold by the products from oxidation of iron and its compounds. There are no detailed investigations of the conditions for the precipitation of gold in the literature. The authors made an attempt to investigate certain aspects of the phenomenon.

Precipitation by pyrite. In the first experiments the precipitation of gold from a cyanide solution by a fraction of pure pyrite from the Berezovo deposit with a specific surface area of 0.5m²/g was carried out with agitation at 18-20°C for 10 min. The free cyanide content of the solution was 0.07g/l, the gold content was 69mg/l, the weight of the pyrite sample was 10g, the liquid-solid ratio was 10:1, and the pH of the solution was varied between 3 and 10.5 (fig. 1). It was established that up to 52-58% of the gold is precipitated during treatment of pyrite in acidic solutions (pH 4-4.5), and this is particularly important for the case of acidified cyanide solutions. As found, gold is also precipitated in neutral and alkaline media but to a somewhat lesser degree.

The effect of the surface area of the pyrite (the sample weight) was investigated under the same conditions, where the pH of the solution was kept at 4.5. The results show that with 20g of pyrite (surface area 10m²) up to 65% of the gold is precipitated in 10 min. (fig. 2). In order to establish the degree of precipitation of dissolved gold as a function of the length of contact between the solution and the pyrite, the following series of experiments were set up with 10g samples of pyrite under the same conditions. Under these conditions the process was stabilised after only 10 min. (fig. 3). The variation of the amount of precipitated gold with increase in the concentration of free cyanide in the solution is shown in fig. 4 (pH = 2.7).
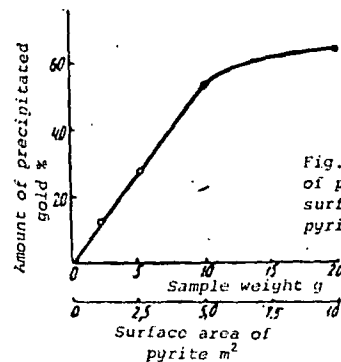

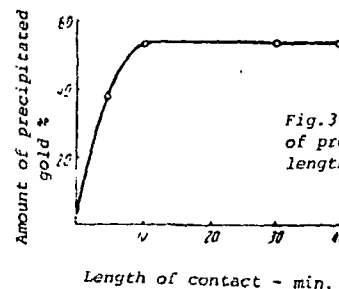Fig.2 Dependence of the amount of precipitated gold on the surface area of the ground pyrite.

Fig.1 Dependence of the amount of precipitated gold on the pH of the medium.

Fig.3 Dependence of the amount of precipitated gold on the length of contact.
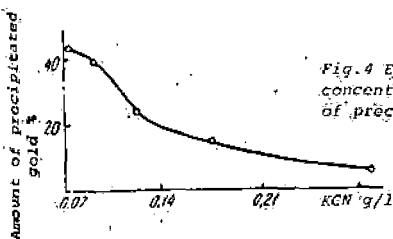
Length of contact - min.

Fig.4 Effect of free cyanide concentration on the amount of precipitated gold.

A series of parallel experiments on the precipitation of gold by floated pyrite concentrate, containing 4.9% of pyrrhotite and ground to 0.044mm were carried out under the following conditions: initial concentration of solution in KCN, 0.011%; NaOH 2.88g/l; weight of concentrate sample 30g; length of contact 3h. Under these conditions 98.2-99.8% of the dissolved gold was precipitated. By prolonged agitation of the samples of flotation pyrite concentrate and the pyrite fraction for 1.5h with strong aeration after precipitation of the gold from them it was possible to transfer 97.3-97.6% of the gold back into solution in the first case and 84% in the second. However, the gold only passes into solution from the pyrite surface at pH = 12-13 even when oxygen is blown through the pulp.

of a fair amount of free cyanide.

In the next series of experiments (table) we used the magnetic fraction isolated from the calcine after the roasting of pyrite concentrate at 500°C, natural magnetite, siderite, and metallic iron. The results show that the magnetic fraction completely precipitates the gold over a wide range of alkalinity in the pulp. Natural siderite and magnetite precipitate the gold with increase of the alkalinity in the solution, while metallic iron precipitates the gold better in a weakly alkaline medium. An excess of alkali passivates the iron. It could be expected that the gold would redissolve from the precipitate on oxidation of the divalent iron. In order to test this we stirred a sample of ferrous hydroxide for 1.5h with strong aeration. In three parallel experiments 87.0-90.0% of the adsorbed gold passed into solution.

Conclusions

1. Compounds of divalent iron precipitate gold from cyanide solutions. The degree of precipitation depends on the conditions under which the process carried out.
2. With intensive agitation and aeration of the pulp in a

Table

Data on precipitation process	Magnetic fraction of calcine		Natural magnetite		Natural siderite		Metallic iron		
Initial cyanide concentration KCN %	0.012	0.012	0.011	0.011	0.011	0.011	0.011	0.011	0.011
Initial alkali concentration NaOH g/l	1.85	3.70	0.012	2.88	0.012	2.88	0.012	1.65	2.92
Amount of precipitant g	25	25	10	30	10	30	10	10	10
Au precipitated %	100.0	100.0	11.4	86.0	19.0	99.0	99.9	51.9	13.0

Precipitation by non-sulphide compounds of iron. To investigate the possibility of precipitation by iron hydroxide we added a freshly prepared ferric hydroxide precipitate to a specific amount of a solution with a known gold content. The contents of the flask were stirred at 18-20°C for 1.5h. At the end of the experiment the gold content of the solution was determined, and the amount of gold in the precipitate was calculated. The initial solution contained 4.88mg of gold, and the solution after the experiment contained 4.87mg of gold, i.e. practically all the gold was found in the solution. The same procedure was used for the precipitation of gold from a cyanide solution with ferrous hydroxide. Different concentrations of potassium cyanide were maintained in three experiments (0.01, 0.03 and 0.054%). Ferrous hydroxide completely precipitates the dissolved gold even in the presence

strongly alkaline medium the precipitated gold passes back into solution.
3. During analysis of the operation of a plant or department which processes sulphide ores, concentrates or the products from their roasting at low and moderate temperatures by cyaniding account should be taken of the fact that part of the lost gold may be due to incomplete transfer of metal absorbed by divalent iron compounds into solution.

References

1) V I Zelenov et alia: Practice in the treatment of gold ores by cyaniding: Moscow 1968, p. 12.
2) I V N Dorr et alia: Cyanidation and concentration of gold and silver ores: New York 1950, 40.

Electrolytic deposition of gold from hydrochlorination pulps

M N Zyranov and N B Bavdik (Irgiredmet)

Summary

A promising method for the isolation of gold from hydrochlorination pulps is electrolysis. The article sets out the results from an investigation into the electrolytic deposition of gold from the pulps from hydrochlorination of gold-containing concentrates after a preliminary investigation of the process in solutions. The effects of the cathode material (titanium, lead, graphite), the length of electrolysis and the current density on the extraction of the gold were investigated.

It was found that gold can be isolated electrolytically from the pulps at lead or graphite cathodes. The process takes place satisfactorily under the following conditions: current density 50-100A/m²; specific cathode surface 10-20m²/m³; particle size of solid phase of pulp -0.15mm. The degree of reduction of gold was 98-99.3%, the approximate current yield was 0.5-1.4%, and the electricity consumption varied between 40 and 170kWh for 1kg of reduced metal.

Permeability of Granite under High Pressure

W. F. BRACE, J. B. WALSH, AND W. T. FRANGOS[1]

Department of Geology and Geophysics, Massachusetts Institute of Technology
Cambridge, Massachusetts 02139

The permeability of Westerly granite was measured as a function of effective pressure to 4 kb. A transient method was used, in which the decay of a small incremental change of pressure was observed; decay characteristics, when combined with dimensions of the sample and compressibility and viscosity of the fluid (water or argon) yielded permeability, k. k of the granite ranged from 350 nd (nanodarcy = 10^{-17} cm^2) at 100-bar pressure to 4 nd at 4000 bars. Based on linear decay characteristics, Darcy's law apparently held even at this lowest value. Both k and electrical resistivity, ρ_r, of Westerly granite vary markedly with pressure, and the two are closely related by $k = C\rho_r^{-1.5\pm0.1}$, where C is a constant. With this relationship, an extrapolated value of k at 10-kb pressure would be about 0.5 nd. This value is roughly equivalent to flow rates involved in solute diffusion but is still a great deal more rapid than volume diffusion. Measured permeability and porosity enable hydraulic radius and, hence, the shape of pore spaces in the granite to be estimated. The shapes (flat slits at low pressure, equidimensional pores at high pressure) are consistent with those deduced from elastic characteristics of the rock. From the strong dependence of k on effective pressure, rocks subject to high pore pressure will probably be relatively permeable.

INTRODUCTION

Many geologic processes depend not only on the properties of solid rock but on characteristics of pore fluids. Of particular significance for mechanical behavior is the relative ease with which fluids can move in and out of a rock. For example, the *Hubbert and Rubey* [1959] theory of overthrusting is based on the existence of pore fluids under high pressure near the base of a fault block; the high pressure is maintained because of the very low permeability of certain layers. A mechanism for deep focus earthquakes is based on the breakdown of hydrous minerals like serpentine [*Raleigh and Paterson*, 1965]. The water given off at high temperature causes embrittlement. The effect, in part, depends on reduction of effective confining pressure, which requires that the rock be permeable to the high pressure pore fluid. In the many applications where the law of effective stress is evoked, permeability of the rock is involved.

Although permeability of sediments and most sedimentary rocks is well known, few data are available for crystalline metamorphic and igneous rocks (Table 1). The problem is that these rocks have very low permeability. The measurements become extremely difficult with conventional techniques. Nevertheless, it would be desirable to have values of permeability of typical crystalline rocks, not only at laboratory conditions but also at pressures and temperatures such as found in the earth.

As a first step, we present here some measurements of permeability for one fairly typical crystalline rock, Westerly granite, as a function of confining pressure. We describe in some detail a technique for measuring permeability under pressures of 4 kb or more and show how changes in permeability are related to changes in electrical resistivity. We suggest a method of obtaining permeability (which is difficult to measure) from resistivity (which is easy to measure), and we use this method to obtain permeability, by extrapolation, from resistivity measurements we have made above 4 kb.

EXPERIMENTAL METHOD

Permeability is usually determined from measurements of flow rate through a sample under a constant pressure gradient. We found it more convenient to use a transient method, that is, to observe the decay of a small step change of pressure imposed at one end of a sample. Pressure and time are more easily measured in a high pressure experiment than

[1] Now at Kennecott Copper Exploration Service, Salt Lake City, Utah.

2225

TABLE 1. Previous Measurements of Permeability[1]

Rock	Permeability, nd	Reference
Shale	1 to 4000	*Gondoun and Scala* [1958]
Fine-grained limestone and dolomite	1 to 50	*Rove* [1939, 1947]
Fine-grained dolomite, Tennessee	80	*Ohle* [1951, p. 907]
Fine-grained limestone, Tennessee	30	*Ohle* [1951, p. 907]
Coarse-grained dolomite, Tennessee	6000	*Ohle* [1951, p. 907]
Granite, Barriefield, Ontario	50	*Ohle* [1951, p. 671]
Granite, Quincy, Mass.	4600	*Ohle* [1951, p. 671]
Diabase, Hudson, N. Y.	0.8	*Ohle* [1951, p. 671]

[1] The unit of permeability is the nanodarcy, abbreviated nd, which equals approximately 10^{-17} cm^2.

flow rate or velocity. We assumed that Darcy's law was valid, and from the decay characteristics of the pressure we calculated the permeability. The validity of Darcy's law could be tested from the decay characteristics as well.

The experimental arrangement is indicated in Figure 1. The sample was a precisely ground right cylinder of Westerly granite [*Brace*, 1965] that was 1.61 cm long and that had a 5.0-cm^2 cross-sectional area. On one side it made contact with a hollow plug of hardened steel that served as a water reservoir; on the other side, with a hollow piston that formed one closure of the pressure vessel. A ½-mm-thick layer of 200-mesh ZrC separated the sample from both plug and piston. The carbide acted as a porous plug even under high pressure and distributed the pore fluid over the entire end surface of the sample. Piston, plug, and sample were enclosed in a 3-mm-thick polyurethane rubber jacket which was clamped with several loops of no. 14 steel wire.

The experimental arrangement is shown schematically in Figure 2. The sample had a reservoir of fluid on either side. Reservoir 1 consisted of the center hole in the piston, as well as the volumes enclosed by tubing, valves, and a pressure transducer which were outside of the pressure vessel. Reservoir 2 comprised the cavity in the steel plug.

During an experiment the sample was jected, through the rubber jacket and steel and piston, to a confining pressure, called P_z. Fluid under pressure filled the two reservoir The fluid pressures, P_1 and P_2, were always nearly equal and less than P_z. The effective

Fig. 1. Experimental arrangement.

 using pressure $\bar{P}$, experienced by the sample, was $P_2 - P_1$, which was always very nearly equal to $P_2 - P_3$.

In a typical experiment, the assembled sample was placed in the pressure vessel and P_Σ applied and held constant. Both reservoirs contained and held under pressure, and, at time t_o (Figure 3), the pressures P_1 and P_3 were equal. At time t_o, P_1 was increased a small amount; ΔP, by adjusting an external valve. The pressures P_1 and P_3 changed as shown in Figure 3, and after some time approached a constant common value, P_f. As shown below, the decay characteristics depend on the permeability, on the dimensions of the sample and reservoirs, and on physical characteristics of the fluid. Certain of these parameters were adjusted in the experiments to give decay times that were convenient. The lowest permeability that could be measured was fixed by the length of time available before changes in pressure due to other causes (temperature changes or leaks) began to predominate. This time was about 30 minutes.

The permeability k of the sample was obtained by comparing the observed decay of pressure in reservoir 1 with the behavior predicted theoretically. As shown in the appendix, one-dimensional transient flow of a compressible
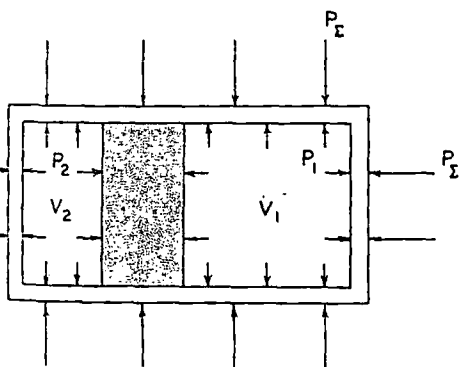

Fig. 2. Experimental arrangement shown schematically. Sample, shown dotted, has fluid reservoirs V_1 and V_2 at either end at very nearly the same pressure. Sample is subjected to an effective confining pressure of $P_\Sigma - P_1 \simeq P_\Sigma - P_3$, which for simplicity is not indicated on the ends of the sample. To measure permeability, P_1 is suddenly changed by a small amount and then the recovery of P_1 with time observed as fluid flows between the two reservoirs; characteristics of this recovery yield permeability of the sample.

Fig. 3. Changes of pressure during an experiment. Typical values of pressure are shown.

fluid through a porous compressible medium is described by (A7):

$$\partial^2 P/\partial x^2 = (\mu\beta/k)$$
$$\cdot \left[\frac{\beta_{eff} - \beta_s}{\beta} + \eta(1 - \beta_s/\beta)\right](\partial P/\partial t)$$

where μ is fluid viscosity, η is porosity, β is fluid compressibility, t is time, P is pressure, and x is distance from the end of the sample. β_{eff} is effective compressibility of the rock as measured for a jacketed sample, and β_s is compressibility of the minerals in the rock.

In the present experiments, β is much greater than either β_{eff} or β_s. For example, in units of 10^{-10} cm^2/dyne, β of water is about 0.42, and β of argon is about 100. At 1-kb effective pressure β_{eff} is about 0.025 for Westerly granite, and β_s is about 0.020 [Brace, 1965]. Accordingly, the term $(\beta_{eff} - \beta_s)/\beta$ will be small. For Westerly granite and for most crystalline rocks, porosity, η, is also small, so that the expression above could be further simplified by setting $\eta = 0$. To check this procedure, an analysis was made for flow through a sample with finite porosity. As shown in the appendix in (A13), porosity in the sample introduces a transient. For porosities of about 0.01 the transient decays to negligible values in a short time (1–10 sec) compared with the course of a typical experiment (300–3000 sec).

We assumed that in our experiment both terms inside the brackets in (A7) are nearly zero, and the expression reduces to

$$\partial^2 P/\partial x^2 = 0 \qquad (1)$$

or

$$\partial P/\partial x = f(t)$$

Thus, the pressure gradient in the sample is constant along its length, although it will vary with time.

A second effect, not included in the analysis leading to (1), arises from the adiabatic changes in temperature caused by suddenly changing P_1. This introduces still another transient, and, to evaluate its characteristics, experiments were done with the rock sample replaced by a glass plug of the same dimensions. The transient due to temperature changes disappeared in 10–20 sec, so that, again, the effect would be negligible. No measurements were made in an experiment until after about 20 sec.

The rock sample in the experiments is equivalent to a resistor in an electric circuit, and the reservoirs behave like capacitors. It is a simple matter to show that the pressure gradient decays exponentially to zero. The pressure P_1 in reservoir 1 is given by the equation

$$(P_1 - P_f) = \Delta P[(V_2/V_1) + V_2]e^{-\alpha t} \quad (2)$$

where

$$\alpha = (kA/\mu\beta L)(1/V_1 + 1/V_2) \quad (3)$$

A is cross-sectional area, L is length of sample, V_1 and V_2 are volumes of reservoirs 1 and 2, P_f is final pressure, and ΔP is the step change of pressure in reservoir at time $= 0$.

The permeability of a sample is found by plotting the pressure decay $(P_1 - P_f)$ on semi-log paper against time; examples are shown in Figure 4. The slope of the resulting line is $-\alpha$. Permeability, k, is found from (3) where it is the only unknown.

It is clear from (3) why ΔP must be small. Both viscosity and compressibility of fluids vary with pressure, and, if P_1 and P_2 were greatly different, these two properties would vary along the sample and (2) would not hold. Also, as it will turn out, permeability varies markedly with effective confining pressure $\bar{P}$, so that it is necessary to maintain $\bar{P}$ nearly constant along the sample. Keeping $\bar{P}$ constant requires that ΔP be no more than a few per cent of P_2 and less than 10% of P_1.

The decay curves in Figure 4 represent one of our most reliable and one of our least reliable runs. Curve 1 represents an almost perfect exponential decay throughout the period of
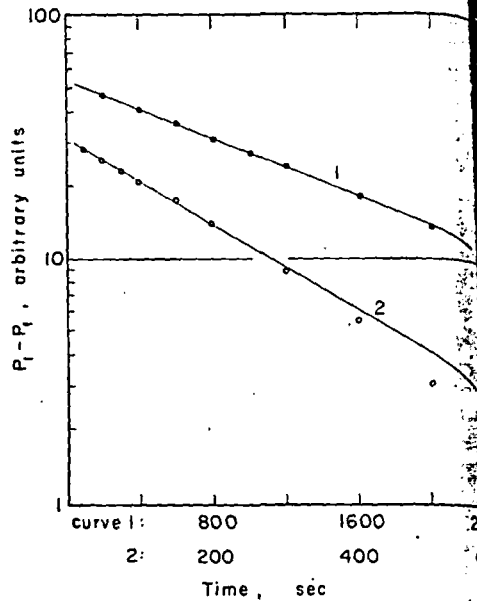

Fig. 4. Sample decay curves.

observation. Curve 2 becomes nonlinear by the time the pulse has decayed about two-thirds of its original value, an effect probably due to temperature variations in the laboratory. Both curves yield α with an acceptable uncertainty.

Measurement of pressure decay in our experiments required some care. First of all, the pressure pulse ΔP was small; initial fluid pressure P_1 was usually about 400 bars, and ΔP about 20 bars (Figure 3). In addition, the pulse decayed only a fraction of ΔP; in a typical setup, $V_2/(V_1 + V_2)$ was about 0.2, so that the decay was only over 3–4 bars of pressure. Clearly, a sensitive pressure transducer was required. We used a GP Pressure Cell (B.L.E. Co.) that had a maximum sensitivity of about 30 μv/bar. As we wished to observe very small increments of pressure at the fairly high pressure level of 400 bars, we used a bucking circuit to cancel the voltage output from the cell corresponding to the 400 bars, and also to the pressure pulse ΔP. The system was, therefore, electrically brought to null at time t_0. As the pulse decayed, the small changes in pressure produced small changes in voltage in the cell which were amplified and recorded. Stability of the bucking circuits, the amplifier (Astrodata model 885) and the pressure transducer power supply (Kepco model ABC) were such that a

NUMERICAL

Data are tabulated in T ⸱:con. Included are total p ⸱:re P_1 at time slightly ⸱:ective pressure $\bar{P}$, which ⸱s noted above, P_1 and ⸱during the run by the an ⸱decay. As this change is ⸱effective pressure during th ⸱:ant and equal to the value ⸱:he run. The uncertainty in ⸱P_1 is 1 bar.

TA⸱

Pressure, bars			
P_2	P_1	$\bar{P}$	ΔP
250	150	100	−20
250	50	200	−20
400	150	250	−20
600	100	500	−18
650	150	500	−20
1000	110	890	−16
1150	150	1000	−20
1150	150	1000	−20
500	410	90	+1⸱
520	400	120	−2
520	400	120	+2
400	175	225	+2
895	365	530	−2
1500	415	1085	+⸱
1500	390	1110	−⸱
2030	410	1620	−⸱
2030	410	1620	+⸱
2500	395	2105	−
4440	390	4050	+

negligible drift sensitivity of better than 0.05 bar per hour could be achieved.

Two fluids were used in the experiments, tap water and commercial grade argon. The several hundred bars of fluid pressure used for both fluids ensured that the flow behavior of the argon would be nearly that of a liquid. As shown by *Klinkenberg* [1941], permeability with gases near atmospheric pressure may be very different from that with liquids, or with gases at pressures such that their mean free path is smaller than the radius of pore spaces. To be sure that gas pressure was high enough, measurements were compared at two pressures.

NUMERICAL DATA

Data are tabulated in Table 2 for water and argon. Included are total pressure P_Σ, fluid pressure P_1 at time slightly greater than t_0, and effective pressure $\bar{P}$, which is equal to $P_\Sigma - P_1$. As noted above, P_1 and therefore $\bar{P}$ change during the run by the amount of the pressure decay. As this change is only a few bars, the effective pressure during the run is assumed constant and equal to the value at the beginning of the run. The uncertainty in P_Σ is 5 bars, and in P_1 is 1 bar.

The size of the pressure step ΔP is found with the BLH cell. The probable error for ΔP is 0.1 bar. The volumes of the reservoirs were known to about 0.1 cm². The uncertainty in time measurement was a few seconds. The error in α, which was the slope of the decay curve in a semilog plot, ranged from 10 to 25%, depending on the slope. The record length is the span of time over which measurements of $P_1 - P_f$ were made.

Compressibilities and viscosities were taken from the literature for the pressures and temperatures of each run. Viscosity and compressibility of argon were taken from *Cook* [1961]. Relative viscosity of water was taken from *Bridgman* [1952], and compressibility from *Clark* [1966]. Absolute viscosity of water at 0°C was assumed to be 1.79×10^{-2} dyne sec/cm². The probable error of viscosity is 1 to 2%; of compressibility, less than 1%. In all of the experiments $(V_1 \div V_2)/V_1 V_2$ was 0.25 cm⁻³, and the ratio of area of sample to length, A/L, was 3.12 cm. The uncertainty in both was less than 1%.

In Table 2, calculated permeability k is expressed for convenience in nanodarcies, abbreviated nd. One nd equals 10^{-9} darcy which approxi-

TABLE 2. Measured Permeability of Westerly Granite

Pressure, bars				Temp., °C	Record, sec	Slope α, 10^{-4} sec⁻¹	Viscosity, 10^{-2} dyne sec/cm²	β 10^{-10} cm²/dyne	k, nd
P_Σ	P_1	$\bar{P}$	ΔP						
						Argon			
250	150	100	−20	25	900	11.2	0.028	66	260 ± 30
250	50	200	−20	28	2400	2.35	0.024	205	148 ± 15
400	150	250	−20	25	1200	6.9	0.028	66	163 ± 20
600	100	500	−18	28	1600	1.54	0.025	102	51 ± 5
650	150	500	−20	22	2000	2.90	0.028	66	69 ± 8
1000	110	890	−16	22	2000	0.92	0.025	94	28 ± 3
1150	150	1000	−20	25	3000	1.83	0.028	66	43 ± 4
1150	150	1000	−20	22	2000	1.28	0.028	66	30 ± 3
						Water			
500	410	90	+10	25	300	29	0.99	0.42	155 ± 20
520	400	120	−20	9	600	30	1.43	0.42	230 ± 25
520	400	120	+20	9	600	30	1.43	0.42	230 ± 25
400	175	225	+20	9	600	17.2	1.43	0.42	132 ± 15
895	365	530	−20	25	900	13.5	0.99	0.42	72 ± 8
1500	415	1085	+20	25	1500	5.0	0.99	0.42	27 ± 3
1500	390	1110	−20	25	1500	5.8	0.99	0.42	31 ± 3
2030	410	1620	−20	9	1500	3.6	1.43	0.42	28 ± 3
2030	410	1620	+20	9	900	2.6	1.43	0.42	20 ± 3
2500	395	2105	−20	25	1800	2.7	0.99	0.42	15 ± 3
4440	390	4050	+20	25	2400	0.75	0.99	0.42	4.2 ± 0.8

mately equals 10^{-17} cm². Permeability is plotted as a function of $\bar{P}$ in Figure 5.

DISCUSSION

Decay characteristics such as shown in Figure 4 test a number of features of the experimental method. They test the applicability of Darcy's law to flow under the present conditions, as well as freedom of the high pressure system from other transients. As it is unlikely that various transients would always cancel one another in an experiment or that nonlinear flow characteristics would become linearized by superposition of random transients, we conclude that our experimental methods and the use of (2) yield reliable values of the permeability. Darcy's law apparently applies here.

The permeabilities obtained for Westerly granite seem reasonable in terms of measurements for other rocks near zero pressure (Table 1). *Ohle* [1951, p. 705] gave the effect of pressure on permeability of a coarse-grained limestone at 40 and 80 bars. His data, shown in Figure 5, suggest a pressure effect not unlike that found here.

The scatter in the measurements of permeability seems to be somewhat larger than the probable errors assigned to the measurements. The scatter may be due to a number of sources. As permeability is dependent on pressure, particularly at low pressure, some scatter may be due to small variation in pressure near the contact with the steel. This may be one more manifestation of *end effects* [*Brace*, 1964].

ht differences in thickness or dist ZrC might produce differences in distribution within the sample, ev in the present situation, the applie hydrostatic.

Small differences in degree of saturation be a source of scatter. It is probable to completely saturate the sam water (for runs with water) or to co ry the sample (for runs with argon the small pressure gradients involved. ces in the vicinity of fluid-gas in ght be sufficiently different in diffe riments to cause scatter in the measu

In any event, the scatter observed permeability is of the same order as in measurements of electrical resis water-saturated granite [*Brace et al.* Presumably, the reasons for the scatter ame.

Differences between permeability with water and with argon are of the sa scatter in values for a single fluid ints near $\bar{P} = 1$ kb in Figure 5). T ear tendency for low pressure argon all below high pressure values, alth an of high and low pressure values more or less randomly about the mea water values. Lacking further detail ctuation, we conclude that perme on and water is the same.

The limit of measurement of per with water near room temperature nanodarcies. This is set by the 30-mi erval available for the experimen sed above. Unfortunately, perme 2 orders of magnitude lower may on, and it would be desirable to e mit of measurement. Extending ght be done either by increasing ailable for measurement or by su ting the parameters in (3). To in me available appears to hold scan cause of the difficulty of controllin high pressure system for long perio the parameters in (3), β and test latitude. The ideal fluid fo nts in the nanodarcy range would β and low μ. An additional req both β and μ be known at the measurement. Search for such an currently under way.

Fig. 5. Permeability k as a function of effective confining pressure $\bar{P}$. Length of short bars indicates probable error for each measurement.

slight differences in thickness or distribution of ZrC might produce differences in detailed stress distribution within the sample, even when, as in the present situation, the applied stress is hydrostatic.

Small differences in degree of saturation might also be a source of scatter. It is probably not possible to completely saturate the sample with water (for runs with water) or to completely dry the sample (for runs with argon). Under the small pressure gradients involved, surface forces in the vicinity of fluid-gas interfaces might be sufficiently different in different experiments to cause scatter in the measurements.

In any event, the scatter observed here for permeability is of the same order as the scatter in measurements of electrical resistivity of water-saturated granite [Brace et al., 1965]. Presumably, the reasons for the scatter are the same.

Differences between permeability measured with water and with argon are of the same order as scatter in values for a single fluid (compare points near $\bar{P} = 1$ kb in Figure 5). There is a clear tendency for low pressure argon values to fall below high pressure values, although the mean of high and low pressure values fluctuates more or less randomly about the mean of the water values. Lacking further details of this situation, we conclude that permeability to argon and water is the same.

The limit of measurement of permeability with water near room temperature is a few nanodarcies. This is set by the 30-minute time interval available for the experiment, as discussed above. Unfortunately, permeabilities 1 to 2 orders of magnitude lower may be common, and it would be desirable to extend the limit of measurement. Extending the limit might be done either by increasing the time available for measurement or by suitably adjusting the parameters in (3). To increase the time available appears to hold scant promise because of the difficulty of controlling leaks in a high pressure system for long periods of time. Of the parameters in (3), β and μ have the greatest latitude. The ideal fluid for measurements in the nanodarcy range would have both low β and low μ. An additional requirement is that both β and μ be known at the conditions of measurement. Search for such an ideal fluid is currently under way.

Relation of permeability to other physical properties. Even with the technique used here, permeability of rocks such as granite is hard to measure under geologically interesting conditions. It would clearly be desirable to find a general relation between permeability and more easily measured properties. One good possibility appears to be electrical resistivity. Conduction in rocks that are saturated with water is due in part to movement of ions. If the water contains a high concentration of ions, ionic conduction predominates [Brace et al., 1965]. Movement of ions through pore fluids is probably influenced by the same parameters that influence permeability, so that we might expect permeability and resistivity of a given rock and given pore fluid to be related in some simple way. To test this possibility, resistivity and permeability of Westerly granite were compared at different pressures. The values of permeability, taken from a smooth curve through the argon and water data points (Figure 5), are given in Table 3 together with resistivities for a saline pore solution at the same pressures from Brace et al. [1965]. The two values are plotted in Figure 6 from which it can be seen that most of the points fall very close to a straight line with slope -1.5 ± 0.1. Additional measurements are needed to tell whether the deviation of the 4-kb point is due to a real change in the situation above this pressure or due simply to the large probable error in the measurement at this pressure.

We now use the relation found above to extrapolate to conditions beyond those of the present experiments. In Figure 6 the line through

TABLE 3. Permeability and Resistivity*
of Westerly Granite

Pressure, bars	Permeability, nd	Resistivity, ohm meters
50	350 ± 40	3.1×10^{5}
100	230 ± 25	4.2×10^{5}
250	118 ± 12	6.5×10^{5}
500	63 ± 7	9.3×10^{5}
1000	35 ± 4	1.4×10^{6}
2000	15.5 ± 3	2.5×10^{6}
4000	4.2 ± 0.8	4.9×10^{6}

* Resistivity from Brace et al. [1965]. Pore water had resistivity of 0.3 ohm meter.
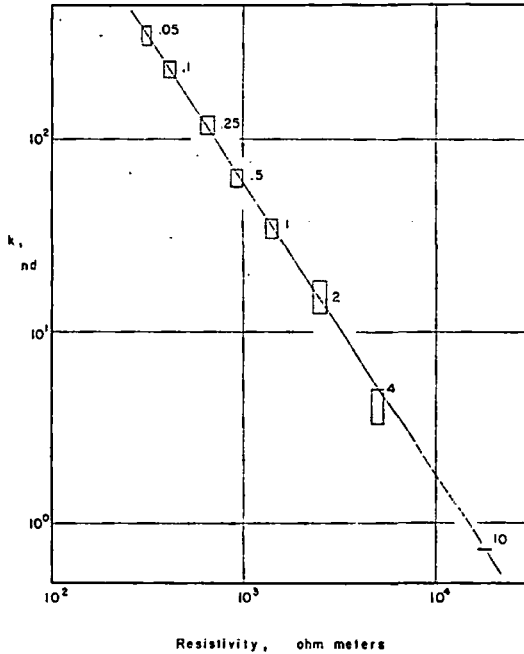
BRACE, WALSH, AND FRANGOS

Fig. 6. Permeability as a function of electrical resistivity. The numbers at each data point give confining pressure in kilobars; the size of the box, the probable errors. Resistivity of the saturating pore fluid was 0.3 ohm meter. The electrical data are from *Brace et al.* [1965].

the data points is extended to resistivities measured to 10 kb. At this pressure extrapolated permeability of Westerly granite would be around 0.5 nd.

Resistivities of a wide variety of crystalline rocks are now available (*Brace et al.* [1965]; Brace and Orange, unpublished results), and it would be highly desirable if these data could be immediately converted to permeabilities. The form of the k versus ρ_e relation may not be the same for all rocks, however. Although, as we show below, the slope of the relation seems to be predictable from theory and may be generally applicable, the intercept could differ from rock to rock. Therefore, we cannot go simply from resistivity of diabase to permeability of diabase using the k versus ρ_e relation for granite. In a rough qualitative way, most crystalline rocks have similar electrical characteristics; all appear, based on resistivity, to be permeable at the highest pressures attained, just as Westerly granite is. Perhaps the k versus ρ_e relation will not differ too greatly from rock to rock. Using

the relation for granite, we find that the low permeabilities indicated for crystalline rock 10 kb would be in the range 10^{-2} to 10^{-3} nd.

Permeability is a measure of the transport material, and it is of interest to compare with those of diffusion. The connection between permeability k and diffusion coefficient D given by

$$k = \mu \beta D$$

where μ is viscosity and β is compressibility. One-nanodarcy permeability to water is roughly equivalent to typical solute diffusion, i.e. diffusion of common salts in water [*Garrels et al.*, 1949], and to surface diffusion in metallic silver [*Brophy et al.*, 1964]. By contrast, volume diffusion in oxides and silicates rarely reaches a rate as high as 10^{-4} nanodarcy; it is typically orders of magnitude lower. Thus, in terms of material transport in rocks under pressure, either solute diffusion or motion of pore fluid is vastly more effective than solid diffusion. Of course, other factors than pressure become important in the earth. High temperature may be of particular significance, even apart from its obvious effect on viscosity of pore fluids and atomic mobility within grains. High temperature will promote plastic flow of minerals, which could ultimately lead to more or less complete closure of the tiny cavities that provide paths for flow of pore fluids. Thus, at high temperature or, in general, under conditions that promote flow or recrystallization, we might expect permeability to become vanishingly small. Presumably such conditions prevail deep in the earth's crust and in the mantle.

High pore pressure and permeability may be related in an interesting way. As pore pressure increases in a rock, effective pressure decreases which in turn leads to increase in permeability (Figure 5). For example, if a rock such as Westerly granite at a depth corresponding to 10-kb total pressure were subjected to a pore pressure close to this, say 9 kb, then permeability would increase by a factor of 100. In general, we might expect regions of high pore pressure to be relatively permeable.

Theoretical relation between permeability and resistivity. A relation as clearcut as that of Figure 6 deserves some sort of theoretical explanation. One approach is through the Kozeny equation, which has been widely applied in the

petroleum industry. Permeability of a medium is related to porosity, specific area of pore spaces, and various geometric characteristics [*Wyllie and Spangler* and *Seidegger*, 1960]. According to the Poiseuille equation,

$$u_e = -(m^2/k_0)(\Delta P/\mu L_e)$$

where u_e is velocity of flow through the viscosity, ΔP is the pressure difference the flow, L_e is the length of pipe, shape factor that can vary between 2 and 3, and m is mean hydraulic radius equivalent to the ratio of volume to pipe. Our porous solid is assumed a network of pipes and openings of shapes with a random pore distribution and *Rose*, 1950], that is, that any plane solid exposes a constant fractional proportional to porosity η. We assume pore space in the solid can be represented angle channel of constant cross-section A, where A is the cross-sectional area normal to the macroscopic flow. According to this idealization the path actually takes, L_e, is longer than the dimensions of the porous solid L. For straight pipes parallel with the flow ($L_e = L$) > 0.

The actual average fluid velocity, porous solid must be greater microscopic approach velocity u, because area available for flow is only η since the actual path length L_e is greater apparent path length L. Thus,

$$u_e = (u/\eta)(L_e/L)$$

We can write Darcy's law as

$$q/A = -(k/\mu)(\Delta P/L) =$$

where k is permeability. If we combine equations, we obtain

$$k = (m^2/k_0)\eta(L/L_e)^2$$

L_e represents a fictitious average path four porous solid. It is impossible directly and is usually evaluated from resistivity. To do this one must assume fluid flow is the same as L_e for reduction in a medium saturated conducting fluid. *Neilson* [1953] has questioned

...oleum industry. Permeability of a porous ...ium is related to porosity, specific surface ...a of pore spaces, and various geometrical ...racteristics [Wyllie and Spangler, 1952; ...deagger, 1960]. According to the well-known ...euille equation,

$$u_e = -(m^2/k_0)(\Delta P/\mu L_e)$$

...re u_e is velocity of flow through the pipe, μ ...viscosity, ΔP is the pressure differential caus... ...the flow, L_e is the length of pipe, k_0 is a ...re factor that can vary between about 2 ...3, and m is mean hydraulic radius, which ...equivalent to the ratio of volume to area of ...pipe. Our porous solid is assumed to contain ...network of pipes and openings of various ...pes with a random pore distribution [Wyllie ...Rose, 1950]; that is, that any plane through ...solid exposes a constant fractional void area ...proportional to porosity η. We assume that the ...re space in the solid can be represented as a ...le channel of constant cross-sectional area ...l, where A is the cross-sectional area of the ...l normal to the macroscopic flow direction. ...ording to this idealization the path the fluid ...ually takes, L_e, is longer than the external ...mensions of the porous solid L. For other than ...raight pipes parallel with the flow direction, $L_e L) > 0$.

The actual average fluid velocity, u_e, within ...porous solid must be greater than the ...roscopic approach velocity u, because the ...area available for flow is only ηA and be...use the actual path length L_e is greater than ...apparent path length L. Thus,

$$u_e = (u/\eta)(L_e/L)$$

We can write Darcy's law as

$$q/A = -(k/\mu)(\Delta P/L) = u$$

...re k is permeability. If we combine these ...ations, we obtain

$$k = (m^2/k_0)\eta(L/L_e)^2 \tag{4}$$

L_e represents a fictitious average path length ...our porous solid. It is impossible to obtain ...ctly and is usually evaluated from electrical ...stivity. To do this one must assume that L_e ...fluid flow is the same as L_e for electrical ...duction in a medium saturated with con...ting fluid. Neilson [1953] has questioned this

assumption on the basis of differences in hydraulic and electrical flow cross sections in a typical channel. On the other hand, the same fluid-filled paths are utilized for both processes [Wyllie and Spangler, 1952], so that, at worst, L_e for the two would differ by a constant factor. Of course, this assumption would be unacceptable if electrical conduction took place through or along surfaces of the solid part of the porous medium. For typical silicate rocks this possibility is eliminated by using highly conductive pore fluids, and in our comparison we give resistivities of Westerly granite saturated with a saline solution.

The electrical resistance of a fluid-saturated porous medium which has a random pore distribution will be the resistance of a single fluid-filled channel of cross-sectional area ηA and length L_e. If ρ_0 is the resistivity of the fluid in the pores and if ρ_e is the resistivity of the fluid-filled medium, then

$$\rho_e(L/A) = \rho_0(L_e/\eta A)$$

and

$$\rho_e/\rho_0 = (L_e/L)\eta^{-1}$$

If we substitute the ratio ρ_e/ρ_0, called *formation factor* in (4) we obtain

$$k = (m^2/k_0)(\rho_0/\rho_e)^2\eta^{-1} \tag{5}$$

In *Brace et al.* [1965] it was found that formation factor of a variety of crystalline rocks bore a strikingly consistent relationship to porosity throughout the porosity range 0.1 to 0.001. The data from the Brace et al. paper together with observations for seven new rocks (to be described in detail separately) are presented in Figure 7. The data points lie very close to the line

$$\sigma_e/\sigma_0 = \rho_0/\rho_e = \eta^r \tag{6}$$

where r is 2.0 ± 0.1. It was shown in the same paper that (6) held not only in this comparison of several rocks but also when porosity of a single rock was changed during hydrostatic compression. As the relationship of formation factor to porosity seems to be general, we will use (6) to eliminate η in (5) and obtain

$$k = (m^2/k_0)(\rho_0/\rho_e)^{2-(1/r)} \tag{7}$$

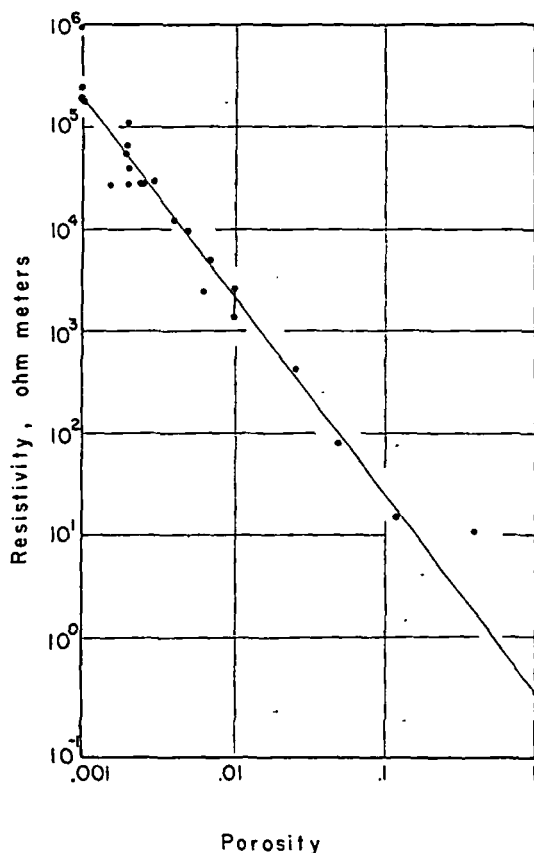With the empirical result that r is about 2, and

Fig. 7. Electrical resistivity at 4 kb as a function of pore porosity. The two points joined by the short vertical bar are two directions in a slate. The point lying well off the curve at about 10^1 ohm meters is for rhyolite tuff.

noting that k_o and ρ_o are constants, we obtain

$$k = C m^2 \rho_s^{-1.5} \quad (8)$$

where $C = $ constant. The quantity m is mean hydraulic radius, which for a tube of constant cross section expresses the shape of the cross section. For example, for a rectangular slit, $m = b/2(1 + b/a)$, where b and a are long and short sides. Comparison of (8) with Figure 6 shows close agreement of observation with the rough theory above. The comparison also suggests that m is constant, which is suprising because pore size and shape in the granite must certainly change with pressure, particularly at low pressure, as shown by measurements of porosity, linear strains, and elastic moduli [*Walsh and Brace*, 1966; *Brace*, 1965]. Perhaps constant m

reflects compensating changes in b and in ratio b/a. In fact, we can use this observation to obtain an estimate of cavity aspect ratio at different pressures.

To calculate m from (7) we use ρ_o of ohm meter and k_o of 2.5 *Wyllie and Spangler* [1952] show that k_o must fall between 2 and With the data in this paper for k, ρ_o and ρ_o is about 10^{-5} cm. In the equation above rectangular slits, the value of b has to be estimated. It is probably of the order of the grain diameter (0.5 mm) at low pressure and perhaps a hundredth of this at 4 kb. The aspect ratio b/a of cavities at 100 bars is 10^2, and at 4 kb about 10. This ratio seems consistent with results of elastic studies of this rock. At low pressure long *cracks* are present [*Brace*, 1965; *Walsh and Brace*, 1966]; an aspect of ratio of 10^3 has been estimated for them on the basis of relation of actual to theoretical compressibility. At high pressure, cracks are believed to close; the remaining cavities are thought to be more equant in shape. Thus, the concepts that are derived from the elastic behavior seem consistent with what may be inferred from flow of pore fluid.

APPENDIX

The rate at which fluid flows in the presence of a pressure gradient $(\partial P/\partial x)$ is related by Darcy's law to the cross-sectional area A, the fluid viscosity μ, and the permeability k.

$$q = -(kA/\mu)(\partial P/\partial x) \quad (A1)$$

The net increase in flow dq across a differential volume element dx in length is $(\partial q/\partial x)\, dx$ or

$$dq = -(kA/\mu)(\partial^2 P/\partial x^2)\, dx \quad (A2)$$

The net storage of fluid in the differential volume is due to compressibility of the fluid and of the solid. The total storage during a time increment dt is

$$(\partial/\partial t)(V_P\, dx/L)\, dt$$
$$+ (V_P\, dx/L)\beta(\partial P/\partial t)\, dt \quad (A3)$$

where V_P is the total pore volume in a sample of length L. The first term in (A3) represents the storage of fluid due to compression of the solid matrix and the second represents storage due to compression of the fluid. The net storage given by (A3) must equal the net volume $dq\, dt$ flowing in. From (A2) and (A3)

$$\partial^2 P/\partial x^2 = (\mu/k)[(\partial V_P/\partial t)(1/AL) + \beta(V_P/AL)(\partial P/\partial t)]$$

$$\partial^2 P/\partial x^2 = (\mu/k)[\partial \eta/\partial t + \beta\eta(\partial P/\partial t)]$$

where the porosity $\eta = V_P/AL$. Here, porosity are due only to changes pressure, so that $\partial \eta/\partial t$ can be uniquely $\partial P/\partial t$ for a specific rock. The change porosity due to an increase in internal dP is

$$d\eta = (-\eta\beta_s\, dP - d\eta_s)$$

where β_s is the compressibility of matrix and $d\eta_s$ is the increase in porosity increase in external pressure. As Walsh [1965]

$$d\eta_s = (\beta_s - \beta_{eff})\, dP$$

where β_{eff} is the effective compressibility rock as measured on jacketed sample (A4), (A5), and (A6), we find

$$\partial^2 P/\partial x^2 = (\mu\beta/k)[(\beta_{eff} - \beta_s)/\beta + \eta(1 - \beta_s/\beta)](\partial P/\partial t)$$

We assume, as described in the text (A7) is very small and that β is much than β_s or β_{eff}, so that the pressure is given by

$$\partial^2 P/\partial x^2 = 0$$

To check this approximation in a simple we assume that all the pore volume is concentrated at the midsection Figure A1. The pressures P_1 at P_2 at reservoir 2, and P_R in the pore related through three differential equations

$$dP_1/dt = -(P_1 - P_R)(\chi V_R/2 V_1)$$
$$dP_2/dt = -(P_2 - P_R)(\chi V_R/2 V_2)$$
$$dP_R/dt = (P_1 + P_2 - 2P_R)(\chi V_R)$$

where

$$\chi = 4k/\beta\mu L^2$$

The initial conditions are that, at

$$P_1 = P_i$$
$$P_R = P_0$$
$$P_2 = P_0$$

and in th
observatio
t ratio b/a

p_0 of $0.$
d Spangler
n 2 and 3
, and ρ_s a
above t_w
to be esti
f the gran
nd perhap
spect rati
d at 4 kb
with result
v pressur
Walsh an
$)^2$ has bee
relation o
r. At high
se; the m
ore equat
re derived
istent with
re fluids.

le presend
related by
rea A, th
y k.

$\partial^2 p/\partial x^2 = (\mu/k)[(\partial \bar{V}_P/\partial t)(1/AL)$
$$+ \beta(V_P/AL)(\partial P/\partial t)]$$

$\partial^2 p/\partial x^2 = (\mu/k)[\partial \eta/\partial t + \beta\eta(\partial P/\partial t)] \quad (A4)$

where the porosity $\eta = V_P/AL$. Here, changes in porosity are due only to changes in fluid pressure, so that $\partial \eta/\partial t$ can be uniquely related to $\partial P/\partial t$ for a specific rock. The change $d\eta$ in porosity due to an increase in internal pressure P is

$$d\eta = (-\eta\beta_s \, dP - d\eta_e) \quad (A5)$$

where β_s is the compressibility of the solid matrix and $d\eta_e$ is the increase in porosity due to an increase in external pressure. As shown by Walsh [1965]

$$d\eta_e = (\beta_s - \beta_{eff}) \, dP \quad (A6)$$

where β_{eff} is the effective compressibility of the rock as measured on jacketed samples. From (A4), (A5), and (A6), we find

$\partial^2 p/\partial x^2 = (\mu\beta/k)[(\beta_{eff} - \beta_s)/\beta$
$$+ \eta(1 - \beta_s/\beta)](\partial P/\partial t) \quad (A7)$$

We assume, as described in the text, that η in (A7) is very small and that β is much greater than β_s or β_{eff}, so that the pressure distribution is given by

$$\partial^2 P/\partial x^2 = 0 \quad (A8)$$

To check this approximation in a simple way, we assume that all the pore volume V_P in the rock is concentrated at the midsection, as shown in Figure A1. The pressures P_1 at reservoir 1, P_2 at reservoir 2, and P_R in the pore space are related through three differential equations

$dP_1/dt = -(P_1 - P_R)(\chi V_R/2V_1)$

$dP_2/dt = -(P_2 - P_R)(\chi V_R/2V_2)$

$dP_R/dt = (P_1 + P_2 - 2P_R)(\chi V_R/2V_P)$

where

$$\chi = 4k/\beta\mu L^2 \quad (A9)$$

The initial conditions are that, at time $= 0$
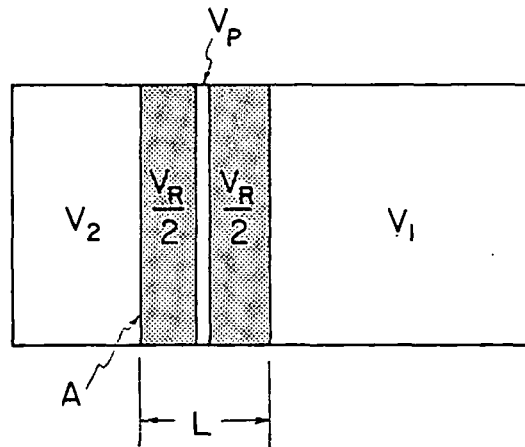
$$P_1 = P_i$$
$$P_R = P_0 \quad (A10)$$
$$P_2 = P_0$$

Fig. A1. The entire pore volume is concentrated at the midsection of the sample.

Taking the Laplace transform of equations A9 with A10, we find

$s\bar{P}_1 - P_i + (\chi V_R/2V_1)$
$$\cdot(\bar{P}_1 - \bar{P}_R) = 0$$
$s\bar{P}_2 - P_0 + (\chi V_R/2V_2)$
$$\cdot(\bar{P}_2 - \bar{P}_R) = 0 \quad (A11)$$
$(\bar{P}_1 + \bar{P}_2 - 2\bar{P}_R)(\chi V_R/2V_P)$
$$- s\bar{P}_R + P_0 = 0$$

Equations A11 are solved simultaneously for $\bar{P}_1$, with the result

$\bar{P}_1[s + \chi V_R(V_1 + V_2)/4V_1V_2][s + \chi V_R/V_P]$
$$= P_i s + (\chi V_R/V_P)$$
$$\cdot[P_i(1 + V_P/2V_2) + P_0 V_P/2V_1]$$
$$+ (1/s)(\chi^2 V_R^2/4V_2V_P)$$
$$\cdot[P_i + P_0(V_P/V_1 + V_2/V_1)] \quad (A12)$$

We now take the inverse transform of (A12) [Churchill, 1958, p. 324] and simplify for $V_P \ll V_1, V_2$, and V_R, with the result

$(P_1 - P_f)/(P_0 - P_f) = V_2 e^{-\alpha t}/(V_1 + V_2)$
$$+ (V_P/4V_1)e^{-\gamma t}$$

where

$\alpha = (k\mu/\beta L^2) V_R(V_1 + V_2)/V_1 V_2$
and

$$\gamma = (k\mu/\beta L^2)4/\eta \qquad (A13)$$

Note that for small V_p, the coefficient and the time constant of the second exponential in (A13) is small, and so the influence of storage in the pore spaces can be neglected in the present calculations.

REFERENCES

Brace, W. F., Brittle fracture of rocks, in *State of Stress in the Earth's Crust,* edited by W. R. Judd, p. 110, American Elsevier, New York, 1964.

Brace, W. F., Some new measurements of linear compressibility of rocks, *J. Geophys. Res., 70,* 391, 1965.

Brace, W. F., A. S. Orange, and T. M. Madden, The effect of pressure on the electrical resistivity of water-saturated crystalline rocks, *J. Geophys. Res., 70,* 5669, 1965.

Bridgman, P. W., *The Physics of High Pressure,* 445 pp., G. Bell and Sons, London, 1952.

Brophy, J. H., R. M. Rose, and J. Wulff, *Thermodynamics of Structure,* 216 pp., John Wiley, New York, 1964.

Churchill, R. V., *Operational Mathematics,* 337 pp., McGraw-Hill, New York, 1958.

Clark, S. P., Jr., *Handbook of Physical Constants,* *Geol. Soc. Am. Mem. 97,* 587 pp., 1966.

Cook, G. A., *Argon, Helium and the Rare Gases,* vol. 1, 277 pp., Interscience, New York, 1961.

Garrels, R. M., R. M. Dreyer, and A. L. Howland, Diffusion of ions through intergranular spaces in water-saturated rocks, *Bull. Geol. Soc. Am., 60,* 1809, 1949.

Gondoun, M., and C. Scala, Streaming potential and the SP log (AIME Tech. Paper 8023), *Petrol. Tech., 10(3),* 170, 1958.

Hubbert, M. K., and W. W. Rubey, Role of fluid pressure in mechanics of overthrust faulting, *Bull. Geol. Soc. Am., 70,* 115, 1959.

Klinkenberg, L. J., The permeability of porous media to liquids and gases, *Am. Petrol. Inst. Drilling Production Pract., 2,* 200, 1942.

Nielson, Ralph F., 'Tortuosity' as related to permeability and resistivity, *Oil Gas J., 83,* Jan., 1953.

Ohle, E. L., The influence of permeability on pore distribution in limestone and dolomite, *Econ. Geol., 45,* 667, 1951.

Raleigh, C. B., and M. S. Paterson, Experimental deformation of serpentine and its tectonic implications, *J. Geophys. Res., 70,* 3965, 1965.

Rove, Olaf, Some physical characteristics of certain limestone ore horizons, Ph.D. thesis, Massachusetts Institute of Technology, 1939.

Rove, Olaf, Some physical characteristics of certain favorable and unfavorable ore horizons, *Econ. Geol., 42,* 57, 1947.

Scheidegger, A. E., *The Physics of Flow through Porous Media,* 313 pp., Macmillan, New York, 1960.

Walsh, J. B., The effect of cracks on the compressibility of rock, *J. Geophys. Res., 70,* 1965.

Walsh, J. B., and W. F. Brace, Elasticity of rock: A review of recent theoretical studies, *Rock Mech. Eng. Geol. 4,* 283, 1966.

Wyllie, M. R., and Walter D. Rose, Some theoretical considerations related to the quantitative evaluation of the physical characteristics of reservoir rock from electric log data, *Petrol. Trans., AIME, 189,* 105, 1950.

Wyllie, M. R., and M. B. Spangler, Application of electrical resistivity measurements to problems of fluid flow in porous media, *Am. Assoc. Petrol. Eng. Bull., 36,* 359, 1952.

(Received November 6, 1967.)

Strength Characteris

EDWARD

Carnegie-Mello

To understand how an extreme fracture mode, and strain energy rock were tested in compression Four groups of specimens were t mens subjected to bakeout and t moderate vacuum, and (4) speci The mode of failure was found and strain energy capacity wer properties were also increased wh All indications are that a stress the lower strength of the specime

INTRODUCTION

The effect of an ultra-high-vacu ment on the fracture strength, fra and strain energy capacity of basa studied. This information was deri understand how an extremely atmosphere will enhance or detra use of rock as a basic material for struction.

The properties of basalt rock ex ultra-high vacuum were determine cially designed vacuum system that for use with a standard mechan machine. Small, cylindrical basalt s subjected to compressive loads at va of vacuum intensity and in air. The deformation behavior was recorded ferent vacuum intensities. The mod was also observed in each test.

To perform these tests, it was certain the nature of the lunar environment. The properties of t ment were based on the data av radar, polarimetric, colorimetric, radio emission investigations of t was also imperative to have an u of material behavior at the mic chemical level because of the sensi of material to the presence of ga A good understanding of certain as fracture mechanics that can be changes in environment is also imp study. All these important factors in detail in this paper.

Permeability of Granite under High Pressure

W. F. BRACE, J. B. WALSH, AND W. T. FRANGOS[1]

*Department of Geology and Geophysics, Massachusetts Institute of Technology
Cambridge, Massachusetts 02139*

The permeability of Westerly granite was measured as a function of effective pressure to 4 kb. A transient method was used, in which the decay of a small incremental change of pressure was observed; decay characteristics, when combined with dimensions of the sample and compressibility and viscosity of the fluid (water or argon) yielded permeability, k. k of the granite ranged from 350 nd (nanodarcy $= 10^{-17}$ cm²) at 100-bar pressure to 4 nd at 4000 bars. Based on linear decay characteristics, Darcy's law apparently held even at this lowest value. Both k and electrical resistivity, ρ_e, of Westerly granite vary markedly with pressure, and the two are closely related by $k = C\rho_e^{-1.5\pm0.1}$, where C is a constant. With this relationship, an extrapolated value of k at 10-kb pressure would be about 0.5 nd. This value is roughly equivalent to flow rates involved in solute diffusion but is still a great deal more rapid than volume diffusion. Measured permeability and porosity enable hydraulic radius and, hence, the shape of pore spaces in the granite to be estimated. The shapes (flat slits at low pressure, equidimensional pores at high pressure) are consistent with those deduced from elastic characteristics of the rock. From the strong dependence of k on effective pressure, rocks subject to high pore pressure will probably be relatively permeable.

INTRODUCTION

Many geologic processes depend not only on the properties of solid rock but on characteristics of pore fluids. Of particular significance for mechanical behavior is the relative ease with which fluids can move in and out of a rock. For example, the *Hubbert and Rubey* [1959] theory of overthrusting is based on the existence of pore fluids under high pressure near the base of a fault block; the high pressure is maintained because of the very low permeability of certain layers. A mechanism for deep focus earthquakes is based on the breakdown of hydrous minerals like serpentine [*Raleigh and Paterson*, 1965]. The water given off at high temperature causes embrittlement. The effect, in part, depends on reduction of effective confining pressure, which requires that the rock be permeable to the high pressure pore fluid. In the many applications where the law of effective stress is evoked, permeability of the rock is involved.

Although permeability of sediments and most sedimentary rocks is well known, few data are available for crystalline metamorphic and igneous rocks (Table 1). The problem is that these rocks have very low permeability. The measure-

ments become extremely difficult with conventional techniques. Nevertheless, it would be desirable to have values of permeability of typical crystalline rocks, not only at laboratory conditions but also at pressures and temperatures such as found in the earth.

As a first step, we present here some measurements of permeability for one fairly typical crystalline rock, Westerly granite, as a function of confining pressure. We describe in some detail a technique for measuring permeability under pressures of 4 kb or more and show how changes in permeability are related to changes in electrical resistivity. We suggest a method of obtaining permeability (which is difficult to measure) from resistivity (which is easy to measure), and we use this method to obtain permeability, by extrapolation, from resistivity measurements we have made above 4 kb.

EXPERIMENTAL METHOD

Permeability is usually determined from measurements of flow rate through a sample under a constant pressure gradient. We found it more convenient to use a transient method, that is, to observe the decay of a small step change of pressure imposed at one end of a sample. Pressure and time are more easily measured in a high pressure experiment than

[1] Now at Kennecott Copper Exploration Service, Salt Lake City, Utah.

TABLE 1.　Previous Measurements of Permeability[1]

Rock	Permeability, nd	Reference
Shale	1 to 4000	*Gondoun and Scala* [1958]
Fine-grained limestone and dolomite	1 to 50	*Rove* [1939, 1947]
Fine-grained dolomite, Tennessee	80	*Ohle* [1951, p. 907]
Fine-grained limestone, Tennessee	30	*Ohle* [1951, p. 907]
Coarse-grained dolomite, Tennessee	6000	*Ohle* [1951, p. 907]
Granite, Barriefield, Ontario	50	*Ohle* [1951, p. 671]
Granite, Quincy, Mass.	4600	*Ohle* [1951, p. 671]
Diabase, Hudson, N. Y.	0.8	*Ohle* [1951, p. 671]

[1] The unit of permeability is the nanodarcy, abbreviated nd, which equals approximately 10^{-17} cm².

flow rate or velocity. We assumed that Darcy's law was valid, and from the decay character-istics of the pressure we calculated the perme-ability. The validity of Darcy's law could be tested from the decay characteristics as well.

The experimental arrangement is indicated in Figure 1. The sample was a precisely ground right cylinder of Westerly granite [*Brace*, 1965] that was 1.61 cm long and that had a 5.0-cm² cross-sectional area. On one side it made con-tact with a hollow plug of hardened steel that served as a water reservoir; on the other side, with a hollow piston that formed one closure of the pressure vessel. A ½-mm-thick layer of 200-mesh ZrC separated the sample from both plug and piston. The carbide acted as a porous plug even under high pressure and distributed the pore fluid over the entire end surface of the sample. Piston, plug, and sample were en-closed in a 3-mm-thick polyurethane rubber jacket which was clamped with several loops of no. 14 steel wire.

The experimental arrangement is shown sche-matically in Figure 2. The sample had a reser-voir of fluid on either side. Reservoir 1 con-sisted of the center hole in the piston, as well as the volumes enclosed by tubing, valves, and a pressure transducer which were outside of the pressure vessel. Reservoir 2 comprised the cav-ity in the steel plug.

During an experiment the sample was su[b]-jected, through the rubber jacket and steel pl[ug] and piston, to a confining pressure, called h[...] P_z. Fluid under pressure filled the two reservo[ir] The fluid pressures, P_1 and P_2, were always v[ery] nearly equal and less than P_z. The effective c[...]
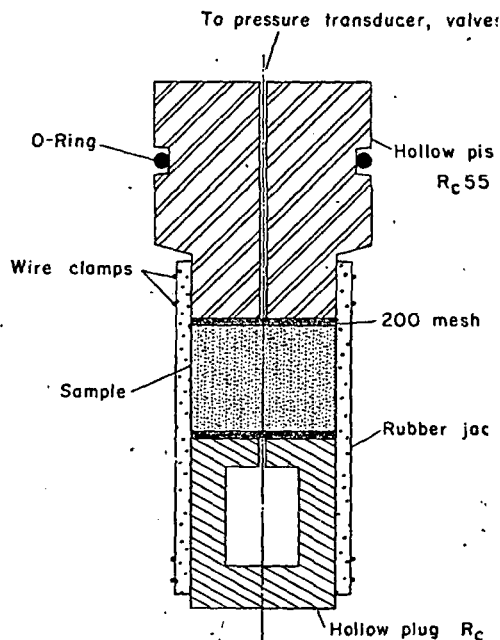

Fig. 1.　Experimental arrangement.

fining pressure $\bar{P}$, experienced by the sample, was $P_z - P_1$, which was always very nearly equal to $P_z - P_2$.

In a typical experiment, the assembled sample was placed in the pressure vessel and P_z applied and held constant. Both reservoirs contained fluid under pressure, and, at time t_0 (Figure 3), the pressures P_1 and P_2 were equal. At time t_0, P_1 was increased a small amount; ΔP, by adjusting an external valve. The pressures P_1 and P_2 changed as shown in Figure 3, and after some time approached a constant common value, P_f. As shown below, the decay characteristics depend on the permeability, on the dimensions of the sample and reservoirs, and on physical characteristics of the fluid. Certain of these parameters were adjusted in the experiments to give decay times that were convenient. The lowest permeability that could be measured was fixed by the length of time available before changes in pressure due to other causes (temperature changes or leaks) began to predominate. This time was about 30 minutes.

The permeability k of the sample was obtained by comparing the observed decay of pressure in reservoir 1 with the behavior predicted theoretically. As shown in the appendix, one-dimensional transient flow of a compressible
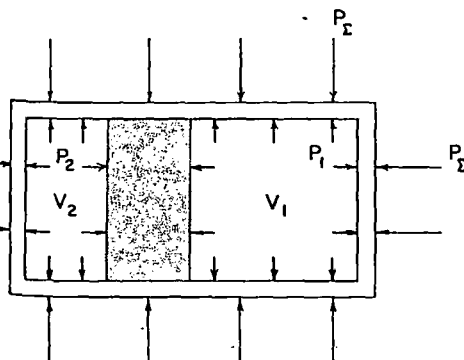

Fig. 2. Experimental arrangement shown schematically. Sample, shown dotted, has fluid reservoirs V_1 and V_2 at either end at very nearly the same pressure. Sample is subjected to an effective confining pressure of $P_z - P_1 \simeq P_z - P_2$, which for simplicity is not indicated on the ends of the sample. To measure permeability, P_1 is suddenly changed by a small amount and then the recovery of P_1 with time observed as fluid flows between the two reservoirs; characteristics of this recovery yield permeability of the sample.
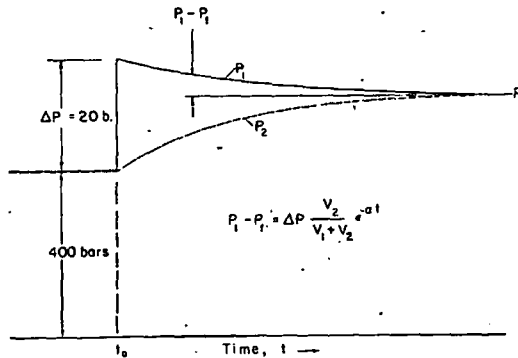

Fig. 3. Changes of pressure during an experiment. Typical values of pressure are shown.

fluid through a porous compressible medium is described by (A7):

$$\partial^2 P/\partial x^2 = (\mu\beta/k)$$
$$\cdot \left[\frac{\beta_{eff} - \beta_s}{\beta} + \eta(1 - \beta_s/\beta)\right](\partial P/\partial t)$$

where μ is fluid viscosity, η is porosity, β is fluid compressibility, t is time, P is pressure, and x is distance from the end of the sample. β_{eff} is effective compressibility of the rock as measured for a jacketed sample, and β_s is compressibility of the minerals in the rock.

In the present experiments, β is much greater than either β_{eff} or β_s. For example, in units of 10^{-10} cm^2/dyne, β of water is about 0.42, and β of argon is about 100. At 1-kb effective pressure β_{eff} is about 0.025 for Westerly granite, and β_s is about 0.020 [Brace, 1965]. Accordingly, the term $(\beta_{eff} - \beta_s)/\beta$ will be small. For Westerly granite and for most crystalline rocks, porosity, η, is also small, so that the expression above could be further simplified by setting $\eta = 0$. To check this procedure, an analysis was made for flow through a sample with finite porosity. As shown in the appendix in (A13), porosity in the sample introduces a transient. For porosities of about 0.01 the transient decays to negligible values in a short time (1–10 sec) compared with the course of a typical experiment (300–3000 sec).

We assumed that in our experiment both terms inside the brackets in (A7) are nearly zero, and the expression reduces to

$$\partial^2 P/\partial x^2 = 0 \qquad (1)$$

or

$$\partial P/\partial x = f(t)$$

Thus, the pressure gradient in the sample is constant along its length, although it will vary with time.

A second effect, not included in the analysis leading to (1), arises from the adiabatic changes in temperature caused by suddenly changing P_1. This introduces still another transient, and, to evaluate its characteristics, experiments were done with the rock sample replaced by a glass plug of the same dimensions. The transient due to temperature changes disappeared in 10–20 sec, so that, again, the effect would be negligible. No measurements were made in an experiment until after about 20 sec.

The rock sample in the experiments is equivalent to a resistor in an electric circuit, and the reservoirs behave like capacitors. It is a simple matter to show that the pressure gradient decays exponentially to zero. The pressure P_1 in reservoir 1 is given by the equation

$$(P_1 - P_f) = \Delta P[(V_2/V_1) + V_2]e^{-\alpha t} \quad (2)$$

where

$$\alpha = (kA/\mu\beta L)(1/V_1 + 1/V_2) \quad (3)$$

A is cross-sectional area, L is length of sample, V_1 and V_2 are volumes of reservoirs 1 and 2, P_f is final pressure, and ΔP is the step change of pressure in reservoir at time $= 0$.

The permeability of a sample is found by plotting the pressure decay $(P_1 - P_f)$ on semi-log paper against time; examples are shown in Figure 4. The slope of the resulting line is $-\alpha$. Permeability, k, is found from (3) where it is the only unknown.

It is clear from (3) why ΔP must be small. Both viscosity and compressibility of fluids vary with pressure, and, if P_1 and P_2 were greatly different, these two properties would vary along the sample and (2) would not hold. Also, as it will turn out, permeability varies markedly with effective confining pressure $\bar{P}$, so that it is necessary to maintain $\bar{P}$ nearly constant along the sample. Keeping $\bar{P}$ constant requires that ΔP be no more than a few per cent of P_2 and less than 10% of P_1.

The decay curves in Figure 4 represent one of our most reliable and one of our least reliable runs. Curve 1 represents an almost perfect exponential decay throughout the period of
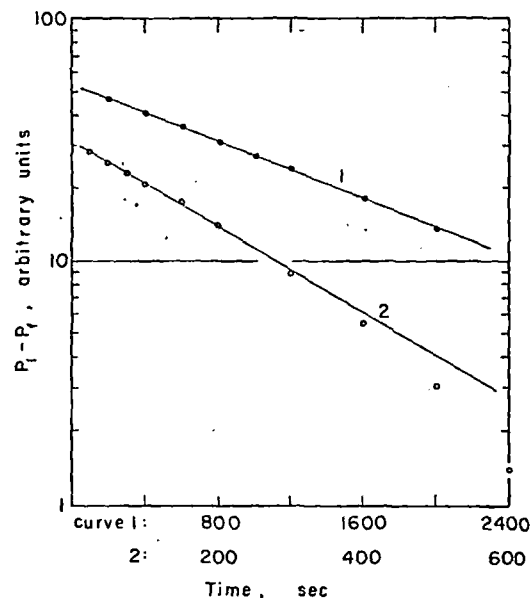

Fig. 4. Sample decay curves.

observation. Curve 2 becomes nonlinear by the time the pulse has decayed about two-thirds of its original value, an effect probably due to temperature variations in the laboratory. Both curves yield α with an acceptable uncertainty.

Measurement of pressure decay in our experiments required some care. First of all, the pressure pulse ΔP was small; initial fluid pressure P_1 was usually about 400 bars, and ΔP about 20 bars (Figure 3). In addition, the pulse decayed only a fraction of ΔP; in a typical setup, $V_2/(V_1 + V_2)$ was about 0.2, so that the decay was only over 3–4 bars of pressure. Clearly, a sensitive pressure transducer was required. We used a GP Pressure Cell (B.L.H. Co.) that had a maximum sensitivity of about 30 μv/bar. As we wished to observe very small increments of pressure at the fairly high pressure level of 400 bars, we used a bucking circuit to cancel the voltage output from the cell corresponding to the 400 bars, and also to the pressure pulse ΔP. The system was, therefore, electrically brought to null at time t_0. As the pulse decayed, the small changes in pressure produced small changes in voltage in the cell, which were amplified and recorded. Stability of the bucking circuits, the amplifier (Astrodata model 885) and the pressure transducer power supply (Kepco model ABC) were such that

ble drift sensitivity of better than 0.05
r hour could be achieved.

fluids were used in the experiments, tap
and commercial grade argon. The several
d bars of fluid pressure used for both
ensured that the flow behavior of the
would be nearly that of a liquid. As

by *Klinkenberg* [1941], permeability
gases near atmospheric pressure may be
different from that with liquids, or with
at pressures such that their mean free
is smaller than the radius of pore spaces.
sure that gas pressure was high enough,
rements were compared at two pressures.

NUMERICAL DATA

ta are tabulated in Table 2 for water and
. Included are total pressure P_{Σ}, fluid pres-
P_1 at time slightly greater than t_0, and
ive pressure $\bar{P}$, which is equal to $P_{\Sigma} - P_1$.
oted above, P_1 and therefore $\bar{P}$ change
g the run by the amount of the pressure
r. As this change is only a few bars, the
ive pressure during the run is assumed con-
and equal to the value at the beginning of
un. The uncertainty in P_{Σ} is 5 bars, and in
1 bar.

The size of the pressure step ΔP is found
with the BLH cell. The probable error for
ΔP is 0.1 bar. The volumes of the reservoirs
were known to about 0.1 cm³. The uncertainty in
time measurement was a few seconds. The er-
ror in α, which was the slope of the decay curve
in a semilog plot, ranged from 10 to 25%,
depending on the slope. The record length is
the span of time over which measurements of
$P_1 - P_f$ were made.

Compressibilities and viscosities were taken
from the literature for the pressures and tem-
peratures of each run. Viscosity and com-
pressibility of argon were taken from *Cook*
[1961]. Relative viscosity of water was taken
from *Bridgman* [1952], and compressibility
from *Clark* [1966]. Absolute viscosity of water
at 0°C was assumed to be 1.79 × 10⁻² dyne
sec/cm². The probable error of viscosity is 1
to 2%; of compressibility, less than 1%. In all
of the experiments $(V_1 + V_2)/V_1 V_2$ was 0.25
cm⁻³, and the ratio of area of sample to length,
A/L, was 3.12 cm. The uncertainty in both was
less than 1%.

In Table 2, calculated permeability k is ex-
pressed for convenience in nanodarcies, abbre-
viated nd. One nd equals 10^{-9} darcy which approxi-

TABLE 2. Measured Permeability of Westerly Granite

Pressure, bars				Temp., °C	Record, sec	Slope α, 10^{-4} sec⁻¹	Viscosity, 10^{-2} dyne sec/cm²	β 10^{-10} cm²/dyne	k, nd
P_{Σ}	P_1	$\bar{P}$	ΔP						
					Argon				
250	150	100	−20	25	900	11.2	0.028	66	260 ± 30
250	50	200	−20	28	2400	2.35	0.024	205	148 ± 15
400	150	250	−20	25	1200	6.9	0.028	66	163 ± 20
600	100	500	−18	28	1600	1.54	0.025	102	51 ± 5
650	150	500	−20	22	2000	2.90	0.028	66	69 ± 8
000	110	890	−16	22	2000	0.92	0.025	94	28 ± 3
150	150	1000	−20	25	3000	1.83	0.028	66	43 ± 4
150	150	1000	−20	22	2000	1.28	0.028	66	30 ± 3
					Water				
500	410	90	+10	25	300	29	0.99	0.42	155 ± 20
520	400	120	−20	9	600	30	1.43	0.42	230 ± 25
520	400	120	+20	9	600	30	1.43	0.42	230 ± 25
400	175	225	+20	9	600	17.2	1.43	0.42	132 ± 15
895	365	530	−20	25	900	13.5	0.99	0.42	72 ± 8
500	415	1085	+20	25	1500	5.0	0.99	0.42	27 ± 3
500	390	1110	−20	25	1500	5.8	0.99	0.42	31 ± 3
2030	410	1620	−20	9	1500	3.6	1.43	0.42	28 ± 3
2030	410	1620	+20	9	900	2.6	1.43	0.42	20 ± 3
2500	395	2105	−20	25	1800	2.7	0.99	0.42	15 ± 3
4440	390	4050	+20	25	2400	0.75	0.99	0.42	4.2 ± 0.8

mately equals 10^{-17} cm². Permeability is plotted as a function of $\bar{P}$ in Figure 5.

DISCUSSION

Decay characteristics such as shown in Figure 4 test a number of features of the experimental method. They test the applicability of Darcy's law to flow under the present conditions, as well as freedom of the high pressure system from other transients. As it is unlikely that various transients would always cancel one another in an experiment or that nonlinear flow characteristics would become linearized by superposition of random transients, we conclude that our experimental methods and the use of (2) yield reliable values of the permeability. Darcy's law apparently applies here.

The permeabilities obtained for Westerly granite seem reasonable in terms of measurements for other rocks near zero pressure (Table 1). *Ohle* [1951, p. 705] gave the effect of pressure on permeability of a coarse-grained limestone at 40 and 80 bars. His data, shown ·in Figure 5, suggest a pressure effect not unlike that found here.

The scatter in the measurements of permeability seems to be somewhat larger than the probable errors assigned to the measurements. The scatter may be due to a number of sources. As permeability is dependent on pressure, particularly at low pressure, some scatter may be due to small variation in pressure near the contact with the steel. This may be one more manifestation of *end effects* [*Brace*, 1964].

Fig. 5. Permeability k as a function of effective confining pressure $\bar{P}$. Length of short bars indicates probable error for each measurement.

Slight differences in thickness or distribution of ZrC might produce differences in detailed stress distribution within the sample, even when, as in the present situation, the applied stress is hydrostatic.

Small differences in degree of saturation might also be a source of scatter. It is probably not possible to completely saturate the sample with water (for runs with water) or to completely dry the sample (for runs with argon). Under the small pressure gradients involved, surface forces in the vicinity of fluid-gas interfaces might be sufficiently different in different experiments to cause scatter in the measurements.

In any event, the scatter observed here for permeability is of the same order as the scatter in measurements of electrical resistivity of water-saturated granite [Brace et al., 1965]. Presumably, the reasons for the scatter are the same.

Differences between permeability measured with water and with argon are of the same order as scatter in values for a single fluid (compare points near $\bar{P} = 1$ kb in Figure 5). There is a clear tendency for low pressure argon values to fall below high pressure values, although the mean of high and low pressure values fluctuates more or less randomly about the mean of the water values. Lacking further details of this fluctuation, we conclude that permeability to argon and water is the same.

The limit of measurement of permeability with water near room temperature is a few nanodarcies. This is set by the 30-minute time interval available for the experiment, as discussed above. Unfortunately, permeabilities 1 to 2 orders of magnitude lower may be common, and it would be desirable to extend the limit of measurement. Extending the limit might be done either by increasing the time available for measurement or by suitably adjusting the parameters in (3). To increase the time available appears to hold scant promise because of the difficulty of controlling leaks in a high pressure system for long periods of time. Of the parameters in (3), β and μ have the greatest latitude. The ideal fluid for measurements in the nanodarcy range would have both low β and low μ. An additional requirement is that both β and μ be known at the conditions of measurement. Search for such an ideal fluid is currently under way.

Relation of permeability to other physical properties. Even with the technique used here, permeability of rocks such as granite is hard to measure under geologically interesting conditions. It would clearly be desirable to find a general relation between permeability and more easily measured properties. One good possibility appears to be electrical resistivity. Conduction in rocks that are saturated with water is due in part to movement of ions. If the water contains a high concentration of ions, ionic conduction predominates [Brace et al., 1965]. Movement of ions through pore fluids is probably influenced by the same parameters that influence permeability, so that we might expect permeability and resistivity of a given rock and given pore fluid to be related in some simple way. To test this possibility, resistivity and permeability of Westerly granite were compared at different pressures. The values of permeability, taken from a smooth curve through the argon and water data points (Figure 5), are given in Table 3 together with resistivities for a saline pore solution at the same pressures from Brace et al. [1965]. The two values are plotted in Figure 6 from which it can be seen that most of the points fall very close to a straight line with slope -1.5 ± 0.1. Additional measurements are needed to tell whether the deviation of the 4-kb point is due to a real change in the situation above this pressure or due simply to the large probable error in the measurement at this pressure.

We now use the relation found above to extrapolate to conditions beyond those of the present experiments. In Figure 6 the line through

TABLE 3. Permeability and Resistivity*
of Westerly Granite

Pressure, bars	Permeability, nd	Resistivity, ohm meters
50	350 ± 40	3.1 × 10²
100	230 ± 25	4.2 × 10²
250	118 ± 12	6.5 × 10²
500	63 ± 7	9.3 × 10²
1000	35 ± 4	1.4 × 10³
2000	15.5 ± 3	2.5 × 10³
4000	4.2 ± 0.8	4.9 × 10³

* Resistivity from *Brace et al.* [1965]. Pore water had resistivity of 0.3 ohm meter.
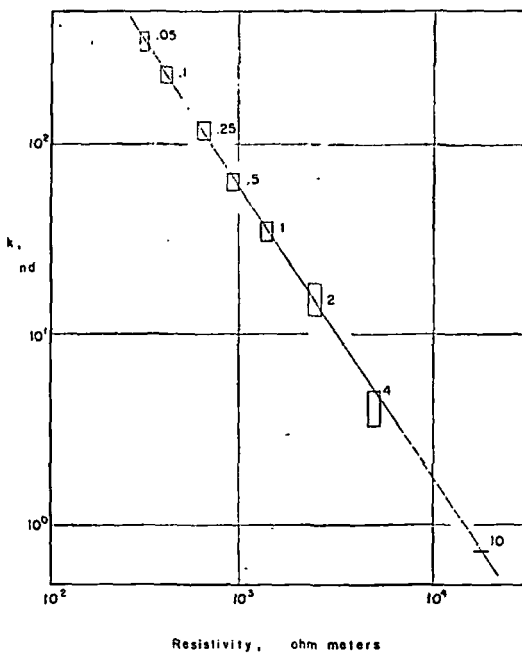
BRACE, WALSH, AND FRANGOS

Fig. 6. Permeability as a function of electrical resistivity. The numbers at each data point give confining pressure in kilobars; the size of the box, the probable errors. Resistivity of the saturating pore fluid was 0.3 ohm meter. The electrical data are from *Brace et al.* [1965].

the data points is extended to resistivities measured to 10 kb. At this pressure extrapolated permeability of Westerly granite would be around 0.5 nd.

Resistivities of a wide variety of crystalline rocks are now available (*Brace et al.* [1965]; Brace and Orange, unpublished results), and it would be highly desirable if these data could be immediately converted to permeabilities. The form of the k versus ρ, relation may not be the same for all rocks, however. Although, as we show below, the slope of the relation seems to be predictable from theory and may be generally applicable, the intercept could differ from rock to rock. Therefore, we cannot go simply from resistivity of diabase to permeability of diabase using the k versus ρ, relation for granite. In a rough qualitative way, most crystalline rocks have similar electrical characteristics; all appear, based on resistivity, to be permeable at the highest pressures attained, just as Westerly granite is. Perhaps the k versus ρ, relation will not differ too greatly from rock to rock. Using

the relation for granite, we find that the lowest permeabilities indicated for crystalline rocks at 10 kb would be in the range 10^{-2} to 10^{-3} nd.

Permeability is a measure of the transport of material, and it is of interest to compare rates with those of diffusion. The connection between permeability k and diffusion coefficient D is given by

$$k = \mu \beta D$$

where μ is viscosity and β is compressibility. One-nanodarcy permeability to water is roughly equivalent to typical solute diffusion, i.e. diffusion of common salts in water [*Garrels et al.*, 1949], and to surface diffusion in metallic silver [*Brophy et al.*, 1964]. By contrast, *volume diffusion* in oxides and silicates rarely reaches a rate as high as 10^{-4} nanodarcy; it is typically orders of magnitude lower. Thus, in terms of material transport in rocks under pressure alone, either solute diffusion or motion of pore fluids is vastly more effective than solid diffusion. Of course, other factors than pressure become important in the earth. High temperature may be of particular significance, even apart from its obvious effect on viscosity of pore fluids and on atomic mobility within grains. High temperature will promote plastic flow of minerals, which could ultimately lead to more or less complete closure of the tiny cavities that provide paths for flow of pore fluids. Thus, at high temperature or, in general, under conditions that promote flow or recrystallization, we might expect permeability to become vanishingly small. Presumably such conditions prevail deep in the earth's crust and in the mantle.

High pore pressure and permeability may be related in an interesting way. As pore pressure increases in a rock, effective pressure decreases, which in turn leads to increase in permeability (Figure 5). For example, if a rock such as Westerly granite at a depth corresponding to 10-kb total pressure were subjected to a pore pressure close to this, say 9 kb, then permeability would increase by a factor of 100. In general, we might expect regions of high pore pressure to be relatively permeable.

Theoretical relation between permeability and resistivity. A relation as clearcut as that in Figure 6 deserves some sort of theoretical explanation. One approach is through the Kozeny equation, which has been widely applied in the

petroleum industry. Permeability of a porous medium is related to porosity, specific surface area of pore spaces, and various geometrical characteristics [*Wyllie and Spangler*, 1952; *Scheidegger*, 1960]. According to the well-known Poiseuille equation,

$$u_e = -(m^2/k_0)(\Delta P/\mu L_e)$$

where u_e is velocity of flow through the pipe, μ is viscosity, ΔP is the pressure differential causing the flow, L_e is the length of pipe, k_0 is a shape factor that can vary between about 2 and 3, and m is mean hydraulic radius, which is equivalent to the ratio of volume to area of the pipe. Our porous solid is assumed to contain a network of pipes and openings of various shapes with a random pore distribution [*Wyllie and Rose*, 1950], that is, that any plane through the solid exposes a constant fractional void area proportional to porosity η. We assume that the pore space in the solid can be represented as a single channel of constant cross-sectional area ηA, where A is the cross-sectional area of the solid normal to the macroscopic flow direction. According to this idealization the path the fluid actually takes, L_e, is longer than the external dimensions of the porous solid L. For other than straight pipes parallel with the flow direction, $(L_e/L) > 0$.

The actual average fluid velocity, u_e, within the porous solid must be greater than the macroscopic approach velocity u, because the free area available for flow is only ηA and because the actual path length L_e is greater than the apparent path length L. Thus,

$$u_e = (u/\eta)(L_e/L)$$

We can write Darcy's law as

$$q/A = -(k/\mu)(\Delta P/L) = u$$

where k is permeability. If we combine these equations, we obtain

$$k = (m^2/k_0)\eta(L/L_e)^2 \qquad (4)$$

L_e represents a fictitious average path length in our porous solid. It is impossible to obtain directly and is usually evaluated from electrical resistivity. To do this one must assume that L_e for fluid flow is the same as L_e for electrical conduction in a medium saturated with conducting fluid. *Neilson* [1953] has questioned this

assumption on the basis of differences in hydraulic and electrical flow cross sections in a typical channel. On the other hand, the same fluid-filled paths are utilized for both processes [*Wyllie and Spangler*, 1952], so that, at worst, L_e for the two would differ by a constant factor. Of course, this assumption would be unacceptable if electrical conduction took place through or along surfaces of the solid part of the porous medium. For typical silicate rocks this possibility is eliminated by using highly conductive pore fluids, and in our comparison we give resistivities of Westerly granite saturated with a saline solution.

The electrical resistance of a fluid-saturated porous medium which has a random pore distribution will be the resistance of a single fluid-filled channel of cross-sectional area ηA and length L_e. If ρ_0 is the resistivity of the fluid in the pores and if ρ_e is the resistivity of the fluid-filled medium, then

$$\rho_e(L/A) = \rho_0(L_e/\eta A)$$

and

$$\rho_e/\rho_0 = (L_e/L)\eta^{-1}$$

If we substitute the ratio ρ_e/ρ_0, called *formation factor* in (4) we obtain

$$k = (m^2/k_0)(\rho_0/\rho_e)^2\eta^{-1} \qquad (5)$$

In *Brace et al.* [1965] it was found that formation factor of a variety of crystalline rocks bore a strikingly consistent relationship to porosity throughout the porosity range 0.1 to 0.001. The data from the Brace et al. paper together with observations for seven new rocks (to be described in detail separately) are presented in Figure 7. The data points lie very close to the line

$$\sigma_e/\sigma_0 = \rho_0/\rho_e = \eta^r \qquad (6)$$

where r is 2.0 $\pm$ 0.1. It was shown in the same paper that (6) held not only in this comparison of several rocks but also when porosity of a single rock was changed during hydrostatic compression. As the relationship of formation factor to porosity seems to be general, we will use (6) to eliminate η in (5) and obtain

$$k = (m^2/k_0)(\rho_0/\rho_e)^{2-(1/r)} \qquad (7)$$

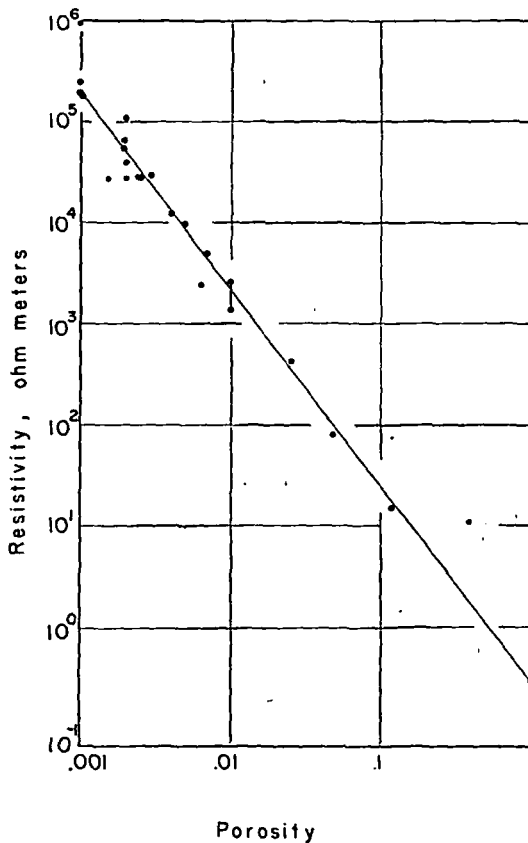With the empirical result that r is about 2, and

Fig. 7. Electrical resistivity at 4 kb as a function of pore porosity. The two points joined by the short vertical bar are two directions in a slate. The point lying well off the curve at about 10^1 ohm meters is for rhyolite tuff.

noting that k_0 and ρ_0 are constants, we obtain

$$k = Cm^2\rho_s^{-1.5} \qquad (8)$$

where $C = $ constant. The quantity m is mean hydraulic radius, which for a tube of constant cross section expresses the shape of the cross section. For example, for a rectangular slit, $m = b/2(1 + b/a)$, where b and a are long and short sides. Comparison of (8) with Figure 6 shows close agreement of observation with the rough theory above. The comparison also suggests that m is constant, which is suprising because pore size and shape in the granite must certainly change with pressure, particularly at low pressure, as shown by measurements of porosity, linear strains, and elastic moduli [Walsh and Brace, 1966; Brace, 1965]. Perhaps constant m

reflects compensating changes in b and in the ratio b/a. In fact, we can use this observation to obtain an estimate of cavity aspect ratio b/a at different pressures.

To calculate m from (7) we use ρ_0 of 0.3 ohm meter and k_0 of 2.5 Wyllie and Spangler [1952] show that k_0 must fall between 2 and 3. With the data in this paper for k, ρ_0 and ρ_s, m is about 10^{-5} cm. In the equation above for rectangular slits, the value of b has to be estimated. It is probably of the order of the grain diameter (0.5 mm) at low pressure and perhaps a hundredth of this at 4 kb. The aspect ratio b/a of cavities at 100 bars is 10^3, and at 4 kb, about 10. This ratio seems consistent with results of elastic studies of this rock. At low pressure, long cracks are present [Brace, 1965; Walsh and Brace, 1966]; an aspect of ratio of 10^3 has been estimated for them on the basis of relation of actual to theoretical compressibility. At high pressure, cracks are believed to close; the remaining cavities are thought to be more equant in shape. Thus, the concepts that are derived from the elastic behavior seem consistent with what may be inferred from flow of pore fluids.

APPENDIX

The rate at which fluid flows in the presence of a pressure gradient $(\partial P/\partial x)$ is related by Darcy's law to the cross-sectional area A, the fluid viscosity μ, and the permeability k.

$$q = -(kA/\mu)(\partial P/\partial x) \qquad (A1)$$

The net increase in flow dq across a differential volume element dx in length is $(\partial q/\partial x)\, dx$ or

$$dq = -(kA/\mu)(\partial^2 P/\partial x^2)\, dx \qquad (A2)$$

The net storage of fluid in the differential volume is due to compressibility of the fluid and of the solid. The total storage during a time increment dt is

$$(\partial/\partial t)(V_P\, dx/L)\, dt$$

$$+ (V_P\, dx/L)\beta(\partial P/\partial t)\, dt \qquad (A3)$$

where V_P is the total pore volume in a sample of length L. The first term in (A3) represents the storage of fluid due to compression of the solid matrix and the second represents storage due to compression of the fluid. The net storage given by (A3) must equal the net volume $-dq$ dt flowing in. From (A2) and (A3)

$\partial^2 P/\partial x^2 = (\mu/k)[(\partial V_P/\partial t)(1/AL)$

$\qquad + \beta(V_P/AL)(\partial P/\partial t)]$

or

$\partial^2 P/\partial x^2 = (\mu/k)[\partial \eta/\partial t + \beta\eta(\partial P/\partial t)]$ (A4)

where the porosity $\eta = V_P/AL$. Here, changes in porosity are due only to changes in fluid pressure, so that $\partial\eta/\partial t$ can be uniquely related to $\partial P/\partial t$ for a specific rock. The change $d\eta$ in porosity due to an increase in internal pressure dP is

$$d\eta = (-\eta\beta_s \, dP - d\eta_e) \qquad (A5)$$

where β_s is the compressibility of the solid matrix and $d\eta_e$ is the increase in porosity due to an increase in external pressure. As shown by *Walsh* [1965]

$$d\eta_e = (\beta_s - \beta_{eff}) \, dP \qquad (A6)$$

where β_{eff} is the effective compressibility of the rock as measured on jacketed samples. From (A4), (A5), and (A6), we find

$\partial^2 P/\partial x^2 = (\mu\beta/k)[(\beta_{eff} - \beta_s)/\beta$

$\qquad + \eta(1 - \beta_s/\beta)](\partial P/\partial t)$ (A7)

We assume, as described in the text, that η in (A7) is very small and that β is much greater than β_s or β_{eff}, so that the pressure distribution is given by

$$\partial^2 P/\partial x^2 = 0 \qquad (A8)$$

To check this approximation in a simple way, we assume that all the pore volume V_P in the rock is concentrated at the midsection, as shown in Figure A1. The pressures P_1 at reservoir 1, P_2 at reservoir 2, and P_R in the pore space are related through three differential equations

$dP_1/dt = -(P_1 - P_R)(\chi V_R/2 V_1)$

$dP_2/dt = -(P_2 - P_R)(\chi V_R/2 V_2)$

$dP_R/dt = (P_1 + P_2 - 2P_R)(\chi V_R/2 V_P)$

where

$$\chi = 4k/\beta\mu L^2 \qquad (A9)$$

The initial conditions are that, at time = 0

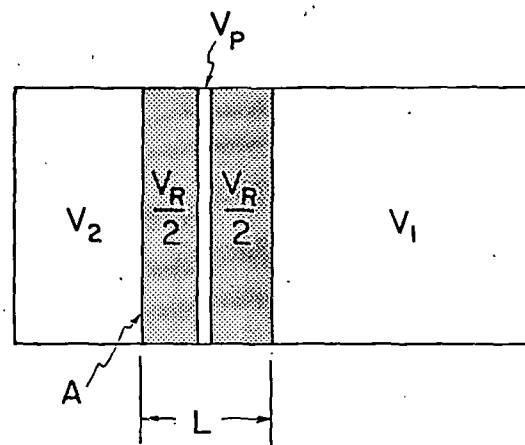$\qquad P_1 = P_i$

$\qquad P_R = P_0$ (A10)

$\qquad P_2 = P_0$

Fig. A1. The entire pore volume is concentrated at the midsection of the sample.

Taking the Laplace transform of equations A9 with A10, we find

$s\bar{P}_1 - P_i + (\chi V_R/2 V_1)$

$\qquad \cdot (\bar{P}_1 - \bar{P}_R) = 0$

$s\bar{P}_2 - P_0 + (\chi V_R/2 V_2)$

$\qquad \cdot (\bar{P}_2 - \bar{P}_R) = 0$ (A11)

$(\bar{P}_1 + \bar{P}_2 - 2\bar{P}_R)(\chi V_R/2 V_P)$

$\qquad - s\bar{P}_R + P_0 = 0$

Equations A11 are solved simultaneously for $\bar{P}_1$, with the result

$\bar{P}_1[s + \chi V_R(V_1 + V_2)/4 V_1 V_2][s + \chi V_R/V_P]$

$= P_i s + (\chi V_R/V_P)$

$\qquad \cdot [P_i(1 + V_P/2 V_2) + P_0 V_P/2 V_1]$

$\qquad + (1/s)(\chi^2 V_R^2/4 V_2 V_P)$

$\qquad \cdot [P_i + P_0(V_P/V_1 + V_2/V_1)]$ (A12)

We now take the inverse transform of (A12) [*Churchill*, 1958, p. 324] and simplify for $V_P \ll V_1$, V_2, and V_R, with the result

$(P_1 - P_f)/(P_0 - P_f) = V_2 e^{-\alpha t}/(V_1 + V_2)$

$\qquad + (V_P/4 V_1)e^{-\gamma t}$

where

$\alpha = (k\mu/\beta L^2) V_R(V_1 + V_2)/V_1 V_2$

and

$$\gamma = (k\mu/\beta L^2)4/\eta \qquad (A13)$$

Note that for small V_P, the coefficient and the time constant of the second exponential in (A13) is small, and so the influence of storage in the pore spaces can be neglected in the present calculations.

REFERENCES

Brace, W. F., Brittle fracture of rocks, in *State of Stress in the Earth's Crust,* edited by W. R. Judd, p. 110, American Elsevier, New York, 1964.

Brace, W. F., Some new measurements of linear compressibility of rocks, *J. Geophys. Res., 70,* 391, 1965.

Brace, W. F., A. S. Orange, and T. M. Madden, The effect of pressure on the electrical resistivity of water-saturated crystalline rocks, *J. Geophys. Res., 70,* 5669, 1965.

Bridgman, P. W., *The Physics of High Pressure,* 445 pp., G. Bell and Sons, London, 1952.

Brophy, J. H., R. M. Rose, and J. Wulff, *Thermodynamics of Structure,* 216 pp., John Wiley, New York, 1964.

Churchill, R. V., *Operational Mathematics,* 337 pp., McGraw-Hill, New York, 1958.

Clark, S. P., Jr., *Handbook of Physical Constants,* Geol. Soc. Am. Mem. *97,* 587 pp., 1966.

Cook, G. A., *Argon, Helium and the Rare Gases,* vol. 1, 277 pp., Interscience, New York, 1961.

Garrels, R. M., R. M. Dreyer, and A. L. Howland, Diffusion of ions through intergranular spaces in water-saturated rocks, *Bull. Geol. Soc. Am., 60,* 1809, 1949.

Gondoun, M., and C. Scala, Streaming potential and the SP log (AIME Tech. Paper 8023), *J. Petrol. Tech., 10*(8), 170, 1958.

Hubbert, M. K., and W. W. Rubey, Role of fluid pressure in mechanics of overthrust faulting, *Bull. Geol. Soc. Am., 70,* 115, 1959.

Klinkenberg, L. J., The permeability of porous media to liquids and gases, *Am. Petrol. Inst. Drilling Production Pract., 2,* 200, 1942.

Nielson, Ralph F., 'Tortuosity' as related to permeability and resistivity, *Oil Gas J.,* 83, Jan. 5, 1953.

Ohle, E. L., The influence of permeability on ore distribution in limestone and dolomite, *Econ. Geol., 46,* 667, 1951.

Raleigh, C. B., and M. S. Paterson, Experimental deformation of serpentine and its tectonic implications, *J. Geophys. Res., 70,* 3965, 1965.

Rove, Olaf, Some physical characteristics of certain limestone ore horizons, Ph.D. thesis, Massachusetts Institute of Technology, 1939.

Rove, Olaf, Some physical characteristics of certain favorable and unfavorable ore horizons, *Econ. Geol., 42,* 57, 1947.

Scheidegger, A. E., *The Physics of Flow through Porous Media,* 313 pp., Macmillan, New York, 1960.

Walsh, J. B., The effect of cracks on the compressibility of rock, *J. Geophys. Res., 70,* 381, 1965.

Walsh, J. B., and W. F. Brace, Elasticity of rock: A review of recent theoretical studies, *Rock Mech. Eng. Geol., 4,* 283, 1966.

Wyllie, M. R., and Walter D. Rose, Some theoretical considerations related to the quantitative evaluation of the physical characteristics of reservoir rock from electric log data, *Petrol. Trans., AIME, 189,* 105, 1950.

Wyllie, M. R., and M. B. Spangler, Application of electrical resistivity measurements to problems of fluid flow in porous media, *Am. Assoc. Petrol. Eng. Bull., 36,* 359, 1952.

Soo·· Non- Fe...

1979 v- 7 NY

Passivation of gold by sulphide ions

: D Sheveleva, I A Kakovskii, S I Efremov, and V A Shchekalkov (Urals Polytechnical Institute)

The passivation of gold in an alkaline cyanide solution can be characterised by the potential corresponding to the transition of the metal from the active to the passive state. During a previous investigation[1]) it was established that the potential corresponding to the beginning of passivation in gold is +0.75V. An argument which confirms the possibility of passivation of gold by its oxygen compounds is the proximity of the thermodynamically calculated potentials of the reactions leading to the formation of Au_2O_3 (+0.67V) and $Au(OH)_3$ (+0.73V) to this value. Metallic gold dissolves in the cyanide solution to form a stable complex of monovalent gold $Au(CN)_2^-$. It was therefore of interest to check the solubility of oxidized compounds of trivalent gold in an alkaline cyanide solution, since the oxidized compounds of copper, mercury and zinc have fairly good solubility in the above-mentioned solvents (2, pp 212-216). In fact, Au_2O_3 and $Au(OH)_3$ obtained in the laboratory according to published data (3, p. 34) dissolved in a cyanide solution. Hedge[4]) solved a similar problem by comparing the behaviour of iron and Fe_2O_3 powder in nitric acid. On the assumption that the layer of the oxide Fe_2O_3 on an iron plate is passivating, the author finally came to the conclusion that the temperature corresponding to the activation of passive iron coincides with the temperature corresponding to appreciable dissolution of Fe_2O_3. It must, however, be remembered that passivating compounds, be they oxides or salts, are surface compounds and are consequently attached to the crystal lattice of the metal. Therefore, both the kinetics of the solution of the surface compounds and the thermodynamic characteristics of these films with thicknesses of one or several crystal lattice cells can differ greatly from the characteristics of the compact oxides (5, p 255). It is indeed oxidized films with such a thickness of gold which were previously discussed in the literature (6, 7, pp 650-652).

A low rate of interaction between the surface oxidized compounds of trivalent gold and the cyanide solution and, their resultant stability are favoured by the formation of a hysteresis loop when the potentiostatic curves for gold in a cyanide solution are recorded in the forward and reverse directions[1]). It is also favoured by the nondependence, established by the same authors, of the anodic current on the concentration of cyanide in the passive state of the metal, whereas a clearly defined effect from the cyanide iron on the magnitude of the current is observed during active dissolution. As known (8, pp 44-62), a consequence of the passivation of gold is a reduction in its dissolution rate in cyanide solutions, revealed by kinetic investigations on a rotating disc.

Apart from oxide films, passivating films also include films of poorly soluble salts and films of adsorbed oxygen or other substances (9, p 253). The secondary formation of films on gold is observed during the treatment of
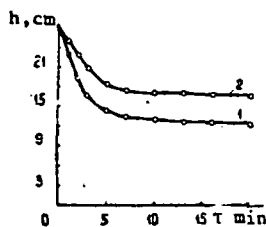
---

ning characteristics of slime from a · with Na_2O_{carb} contents: 1 - Without 1, 2 - 15g/l (1.68), 3 - 25 g/l (1.72); the thickened slime is given in brackets.

Fig. 4

Results from the thickening of ... obtained during leaching of the ... with synthetic solution (2) and ... the solution prepared by leaching ... sinter (1).

1966, (1), 52.

UDC 669.2...

powders alloyed with aluminium

ksandrovskii and B G Vorotinova ent of the Metallurgy of Light and

at titanium powders containing up ... ctly by the joint thermic reduction ... melts with sodium. It was shown that ively as salt base for the titanium-

421

copper and antimony ores. The deleterious effect of antimony films was demonstrated during the cyaniding of a flotation concentrate obtained from the ore of one of the Soviet deposits. However, it is extremely interesting that some of the passivating compounds depassivate the metals under certain conditions (9, p 263).

It is this dual role of the impurities which forms the basis of the change in the kinetics of dissolution of gold in cyanide solutions, i.e., the degree of passivation, with the addition of copper[16]), thallium[11]), and xanthate[12]) ions and also organic substances[13]).

In the present work we studied the effect of sulphide sulphur on the dissolution rate of gold in a cyanide solution. Sulphide ion was not selected for the investigation by chance but as a factor which determines to some degree or other the composition of the pulp during the cyaniding of ores and products which are mineralogically complex and stubborn with respect to the recovery of noble metals. The work was carried out by the rotating disc method.

The preparatory operations and the experimental procedure itself and also the methods for determining the free cyanide and gold were described in detail in the literature[6]). A freshly prepared solution of sodium sulphide with a specific concentration was added to a reaction beaker containing a solution with a known concentration of cyanide and alkali. The concentration of sulphide ion in an aliquot portion was determined[14]) by argentometric titration with potentiometric control. We then began the experiment with the following constant conditions: Temperature of solution 25°C, concentration of protective alkali $2 \cdot 10^{-3}$ mole/l KOH.

The first series included experiments set up in order to determine the effect of the intensity of agitation on the dissolution rate of gold (fig. 1).

The second series was carried out in order to determine the dependence of the dissolution rate on the concentration of cyanide in the solution with constant concentrations of sulphide ion and dissolved oxygen and with a constant intensity of agitation (fig. 2).

The effect of the concentration of sulphide ion was investigated for various concentrations of cyanide and dissolved oxygen (the fourth series of experiments, fig. 3). The fifth series of experiments was carried out with constant concentrations of cyanide ($2.5 \cdot 10^{-3}$ mole/l) and sulphide ion ($1 \cdot 10^{-8}$ mole/l, with a constant intensity of agitation (100 rpm), and with various contents of dissolved oxygen - air and oxygen were blown through the solution. The results are given in the table.

A disc which had been previously treated with a solution of sulphide ion at various concentrations was dissolved with variation in the intensity of agitation during dissolution (experiments of the sixth series, fig. 4).

Other authors[16])[17]) have pointed out the passivation of gold by the ions of

Dissolution conditions	$V \cdot 10^{9}$ r-a·cm^{-2} c^{-1}		
	Concentration of dissolved oxygen mole/l		
	$1.5 \cdot 10^{-6}$	$2.5 \cdot 10^{-4}$	$1.19 \cdot 10^{-3}$
C_{KCN} - $2.5 \cdot 10^{-3}$ mole/l C_S^{2-} - 10^{-4} mole/l n = 100 rpm	0.075	0.1	0.15
C_{KCN} - the same; C_S^{2-} - $1 \cdot 10^{-6}$ mole/l n - the same	0.06	0.13	0.15

sulphide sulphur. However, whereas some [16]) suppose that the effect is due to adsorbed S^{2-} and HS^- ions and surface compounds, others [17]) assert that a film of Au_2S insoluble in the cyanide solution is formed. The character of the interaction probably depends on the conditions of the process. In any case the gold is passivated - the ion of sulphide sulphur greatly retards the dissolution of gold in the cyanide.

The dependence of the dissolution rate on the intensity of agitation is the main criterion of diffusion control (7, p 453). The use of sulphide ion additions makes it possible to follow (fig. 1) how various conditions can alter the kinetics of dissolution of gold in a cyanide solution. A sulphide sulphur concentration of $1 \cdot 10^{-4}$ mole/l brings the gold dissolution process under kinetic control (curves 1 and 2). Account should be taken of the fact that the concentrations of potassium cyanide in the experiments differ by more than an order of magnitude (2.5 and $32.4 \cdot 10^{-3}$ mole/l). The final concentrations of free cyanide are close to the initial value. The possible formation of thiocyanate ion can alter the concentration of the free cyanide by a maximum of 4-5%, and the reduction in the dissolution rate of gold cannot therefore be explained by a reduction in the concentration of free cyanide.

Curves 1 and 5 (fig. 1) differ greatly. First, a reduction in the concentration of S^{2-} in the solution by three orders of magnitude from 10^{-4} to 10^{-7} M makes it possible to dissolve gold in a cyanide solution with the production of considerable maximum rates ($3.75 \cdot 10^{-9}$ g-atom/cm^2·sec). Secondly, sulphide ion in a nelgigible amount keeps the process under diffusion control with disc rotation rates more than twice as high (up to 470-480 rpm) as with dissolution without the sulphide sulphur [cf. curves 5 and 4 from the literature[8])]. Thirdly curve 5 is as it waere a continuation of curve 4, illustrating the transition of the gold dissolution process from purely diffusion control (up to 150-200 rpm)

into a region complicated by passivation by the slowly dissolving oxygen film. This may signify that low concentrations of sulphide ion reduce the formation rate of these surface oxygen compounds on gold, although passivation nevertheless begins with increase in the delivery rate of the reagents to the metal surface, and the dissolution process from this moment agrees with the law of kinetic control (beginning from 480 rpm the dissolution rate does not depend on n).

The role of oxygen here is not yet clear, but it can be stated with certainty that with high agitation rates (more than 740 rpm) the kinetics of the solution are determined only by the concentration of sulphide ion (curves 2 and 3, fig.1)

The retarding action of sulphide sulphur is also demonstrated by the low rate of dissolution of the metal with a significant increase in the concentration of free cyanide in the solution (fig. 2). The stability of the passivating sulphide film is characterised by the fact that when the concentration of potassium cyanide is increased by almost 27 times in comparison with C_{lim} for pure solutions blown with air (8, p 51) the obtained dissolution rate is 2.5 times lower $(0.68 \cdot 10^{-9}$ g-atom/cm$^2 \cdot$ sec). The higher the concentration of sulphide sulphur ion in the solution, the stronger its retarding action (fig.3). With increase in the concentration of dissolved oxygen $(1.19 \cdot 10^{-3}$ mole/l, with oxygen blown through the solution) at sulphide ion concentrations of $10^{-5}, 10^{-4}$, and 10^{-3} mole/l the character of the kinetic curve 1 (fig.3) does not change, contrary to the conviction of some authors that the negative effect of sulphide sulphur can easily be neutralized by increasing the concentration of oxygen in the pulp.

The results from experiments with previous sulphidization of the surface of the gold disc in solutions of sodium sulphide at various concentrations shows that the retarding effect of the sulphide passivating film can be removed by increasing the intensity of agitation (fig.4). There is some increase in the dissolution rate of gold when the concentration of dissolved oxygen in the cyanide solution is increased (table).

Consequently, an excess of sulphide ion in the solution passivates gold more strongly than copper, xanthate, and mercury during cyaniding. At low concentrations even this ion is capable of having some positive effect. To control the negative effect of an excess of sulphide sulphur (more than 10^{-7} mole/l) on the intensity of dissolution of gold in cyanide it is necessary first to oxidize or combine it by analogy with the constant maintenance of the sulphide ion concentration in the noncyanide scheme for selective flotation of copper-zinc ores, where zinc sulphide plays the role of a unique type of buffer[18]). What has been said is of particular interest in the cyaniding of pyrrhotite ores and concentrates.

References

1)   A N Lebedev et alia: Izv. Vuz. Tsvetnaya Metallurgiya 1976, (1), 64.

2)   M D Ivanovskii et alia: Metallurgy of Gold. ONTI 1938.
3)   I N Plaksin: Metallurgy of noble metals. Metallurgizdat, Moscow 1958.
4)   E Hedge: Protective films on metals. Metallurgizdat 1934.
5)   V V Sjorcheletti: Theoretical principles of the corrosion of metals. Khimiya, Leningrad 1973.
6)   I A Kakovskii et alia: Izv. Vuz. Tsvetnaya Metallurgiya 1974, (4), 87.
7)   K J Vetter: Electrochemical kinetics academic Press, New York 1967.
8)   I A Kakovskii et alia: Kinetics of dissolution processes. Khimiya, Moscow 1975.
9)   A N Frumkin et alia: Kinetics of electrode processes. Izd. MGU 1952.
10)   L D Sheveleva et alia: Tsvetnye Metally 1976, (1), 77.
11)   I A Kakovskii et lia: Elektrokhimiya 1975, 2, (9), 1437.
12)   L D Sheveleva et alia: Trudy TsNIGRI, Moscow 1975, (121), 66.
13)   I A Kakovskii et alia: Dokl. Akad. Nauk SSSR 1965, 164, (3), 614.
14)   R N Shchekaleva et alia: Tsvetnye Metally 1974, (12), 58.
15)   M D Ivanovskii: Trudy MITsMiZ, Moscow, (22), 1952.
16)   I N Plaksin et alia: Trudy MITsMiZ, Moscow 1952, (22).
17)   D K A Donyina et alia: Can. Min. J., 1973, 94, (6), 56.
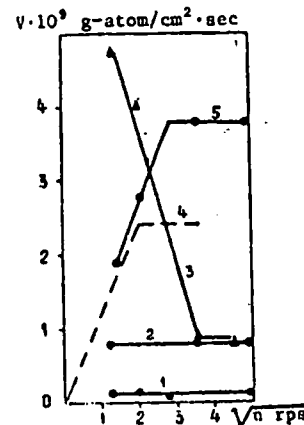18)   R N Shchekaleva et alia: Izv. Guz. Tsvetnaya Metallurgiya 1976, (2), 8.

Fig.1

Dependence of the dissolution rate of gold on the intensity of agitation of the solution (disc rotation rate). C_{KCN}, mole/l: $2.5 \cdot 10^{-3}$ (1,4,5); $32.4 \cdot 10^{-3}$ (2,3). C_{S^2}, mole/l: $1 \cdot 10^{-4}$ (1,2,3), $1 \cdot 10^{-7}$ (5), 0 (4). C_{O_2}, mole/l $2.5 \cdot 10^{-4}$ (1,2,4,5) and $1.19 \cdot 10^{-3}$ (3).
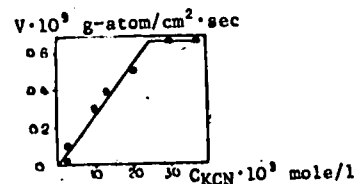

Fig.2

Dependence of the dissolution rate of gold on the cyanide concentration. n = 100 rpm; $C_{O_2(sol)} = 2.5 \cdot 10^{-4}$ mole/l; $C_{S_2} = 1 \cdot 10^{-4}$ mole/l.
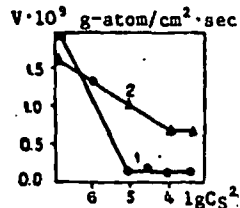
Fig. 3

The effect of the concentration (mole/l) of sulphide ion on the dissolution rate of gold in a cyanide solution with concentration, mole/l: $1 - 2.5 \cdot 10^{-3}$, $2 - 32.4 \cdot 10^{-3}$. $C_{O_2(sol)} = 2.5 \cdot 10^{-4}$ mole/l, $n = 100$ rpm.
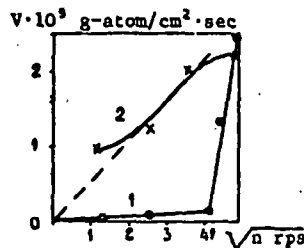

Fig. 4

The effect of the concentration of sulphide during sulphidising on the dissolution rate of gold in cyanide solution. C, mole/l: $1 - C_{S^2}$ $1 \cdot 10^{-2}$, $C_{KCN} = 2.5 \cdot 10^{-3}$, $2 - C_{S_2-} = 5 \cdot 10^{?}$ $C_{KCN} = 2.5 \cdot 10^{-3}$.

UDC 669.223.48:546.33 '273:542.

Recovery of silver from silver-zinc batteries by smelting to borate slag

V N Efimov, I A Sladkova, A M Pogodaev and É E Lukashenko (Krasnoyarsk Institute of Nonferrous Metals - Department of Physical Chemistry and the Theory of Metallurgical Processes)

Spent silver-zinc batteries provide a secondary raw material for the production of silver. The silver in the batteries is present in two forms, i.e., metallic silver and silver oxide Ag_2O. The material of the zinc electrodes consists of zinc and zinc oxide. The silver, zinc, and their oxides represent finely dispersed powders compressed into the form of the electrodes[1].

The moisture content of the electrode materials and the sodium hydroxide content are determined by the amount of electrolyte (an aqueous solution of sodium hydroxide).

Table 1 gives the relative weights of the component parts of STsK-45 batteries used in the present work.

At the present time silver is extracted from spent batteries by smelting to a soda-silicate slag. The high specific consumption rate of fluxes is determined by the impossibility of increasing the zinc oxide content in the soda-silicate slags above 20-25% on account of the appearance of solid phases (SnO, ZnSiO₃); up to 1.2kg of soda and silica is used for 1kg of electrodes.

Table 1: The component parts of the STs

Battery part
Silver electrodes
Zinc electrodes
Polythene envelopes and membranes fro
Plastic body
Silver-plated iron bolts, nuts, and wash
Moisture
Total

The high content of metallic silver in ... due to the incomplete separation of the ... settling of the melt. The degree of pha... difference in the silver-slag melt syste... of the melt, the settling time, and the ... ... by Stokes equation shows that wi... ...osity of $0.5 Ns/m^2$ the limiting size of ... of the bath after 1h is 10^{-1} mm. Finer ... the slag and determine the magnitude ...

The aim of the present investigation ... higher zinc oxide content than in the s... possible considerably to improve the ... from spent batteries. The use of bora... containing zinc oxide (cyanide deposit...

We proposed to use molten borax for ... ...ng of spent silver-zinc batteries. T... analysis of the melting point diagram... oxide and on viscosity measurements ...

The viscosity of the zinc-borate me... viscosimeter designed by S V Shtenge... calibrated against viscous liquids pr... by the previously described method[4]...

Mixtures of ZnO and $Na_2B_4O_7$ were ... grade and borax which had been prev... After thorough mixing in an agate mo... through a quartz tube into an alundu... the crucible was filled as the materi...

Permeability of Granite in a Temperature Gradient

C. Morrow, D. Lockner, D. Moore, and J. Byerlee

U.S. Geological Survey, Menlo Park, California 94025

Changes in permeability of granite were measured as water flowed through samples in a temperature gradient. The experimental conditions simulated those around the 'very deep hole concept' nuclear waste repository. Temperature was maintained between 200° and 310°C, in a borehole of a cylindrical sample. Confining pressures of 30 and 60 MPa, with corresponding pore pressures of 10 and 20 MPa, simulated depths of burial of approximately 1.2 and 2.4 km, respectively. A small pore pressure gradient enabled distilled water to flow from the borehole (high temperature) to the outside of the sample (low temperature). Tests were run for intact samples with initial permeabilities of several hundred nanodarcies and for samples containing throughgoing fractures, with initial permeabilities of about 1 millidarcy. In all cases, permeability decreased between 1 and 2 orders of magnitude at a rate that increased with higher temperatures. At 200°C, permeability dropped by an order of magnitude over a 1-month period, whereas at 310°C, permeability dropped sharply within a few days to 5% of the initial value. The dissolution of quartz and feldspar and redeposition of these minerals within cracks at lower temperature was found to be the major cause of reduction of permeability. If similar processes occurred near a deep hole nuclear waste repository site in granite, then migration of radionuclides away from the site might be suppressed, even if the rock surrounding the waste contained fractures.

INTRODUCTION

Nuclear waste repository schemes, as well as geothermal energy research, have prompted an increasing need to understand the long-term response of geologic environments to fluid flow at elevated temperatures. Fracture systems, as well as thermal and hydraulic gradients, play an important role in the transport of solutions through rock.

The fluid flow properties of crystalline rocks are of particular interest because of their potential use as a nuclear waste repository medium. Their low porosity, low permeability, and high strength are favorable characteristics for the safe containment of nuclear waste.

To date, few studies have investigated flow properties at elevated temperatures. Such information is vital to waste disposal and geothermal studies in assessing the long-term response of these systems. Because of the limited level of understanding of this complex phenomenon we undertook a series of experiments designed to study permeability changes in granite due to the flow of water in the presence of a temperature and pressure gradient. The focus of the study is to observe changes in a setting that simulated a nuclear waste repository; however, the results are equally applicable to problems involved with the extraction of geothermal energy.

Several parameters can affect permeability, including thermal cracking, chemical alterations due to high temperatures, pressure solution, and variable water chemistry. Past permeability studies have touched on these and other topics, and a few studies are mentioned here for their relevance to this investigation.

The effect of stress on granitic rock permeability has been extensively studied by *Brace et al.* [1968], and the transport properties of jointed granite are discussed by *Kranz et al.* [1979], *Pratt et al.* [1977]. *Gale* [1975], and *Iwai* [1976]. It is known that the permeability of jointed rock is several orders of magnitude larger than that of intact rock. Also, permeability is greatly decreased by the closure of joints and cracks from applied stress.

The permeability of crystalline rocks with hydrothermal solutions has been shown both to increase and to decrease with time [*Potter*, 1978; *Tester and Albright*, 1979; *Summers et al.*, 1978]. These results depend largely on the experimental conditions and equilibrium of the system, and clearly different results are desirable depending on the intended application.

Potter [1978] observed both increases and decreases in the permeability of granite as a result of differential thermal expansion and cracking of grains. Permeability minima were dependent on the temperature and pressure environments in which the rocks equilibrated. Cooler temperatures caused contraction and opening of intergranular channelways. Heating above equilibrium caused expansion and crushing of grain boundaries, also producing intergranular channelways and thus higher permeability.

Summers et al. [1978] measured permeability in Westerly granite over several days at temperatures up to 400°C and axial stresses from 0 to 3500 bars. Flow decreased owing to the dissolution of mineral grains and subsequent deposition within grain boundary cracks. The reduction in flow rate did not systematically depend on axial stress.

This progress report is concerned mainly with the effects of temperature-induced geochemical changes on fluid flow through granite under simulated in situ conditions around a borehole in a nuclear waste repository. Future studies will consider other aspects of the problem in more detail.

SAMPLE PREPARATION AND PROCEDURE

Figure 1 shows a schematic view of the sample assembly. Cylindrical samples of Westerly granite, 7.62 cm in diameter and 8.89 cm long with a 1.27-cm borehole, were used in the study. The borehole contained a coiled resistance heater, creating a temperature gradient between the inside and the outside of the rock. Water flowed from the borehole radially out to the edge of the sample. This configuration resembles that of the proposed 'very deep hole' method of nuclear waste isolation, in which canisters would be dropped down deep wells and then plugged with an impermeable material that is compatible with the particular wall rock. Flow away from the borehole in these experiments is of particular interest, as in

THERMOCOUPLE WIRES

PORE PRESSURE INLET

PORE PRESSURE OUTLET

STEEL PLUG

VITON JACKET (3.0 mm)

FUSED SILICA

TEFLON SHIM

SAMPLE

HEATER COIL

TEFLON SHIM

STAINLESS STEEL MESH (0.63 mm)

FUSED SILICA
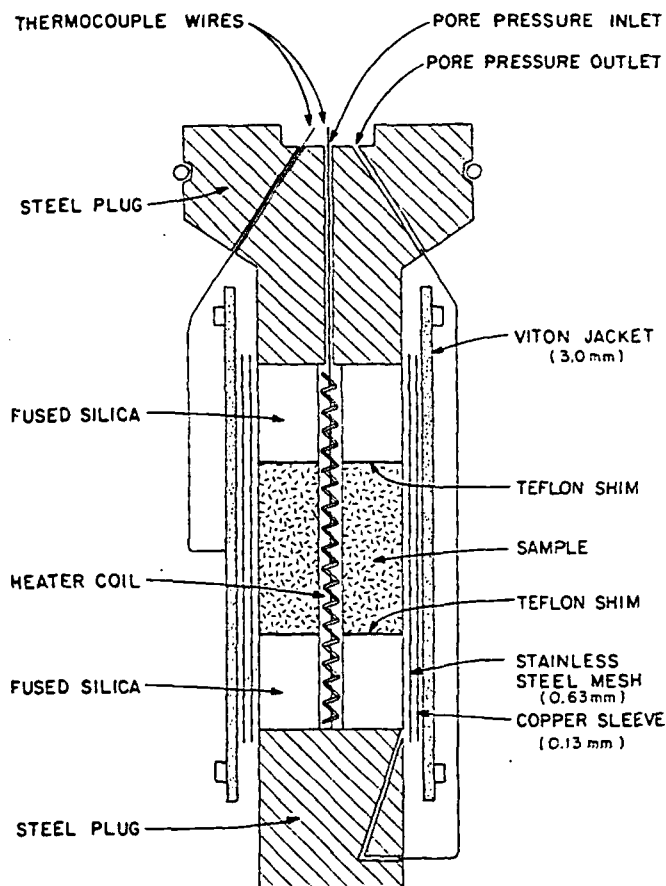
COPPER SLEEVE (0.13 mm)

STEEL PLUG

Fig. 1. Schematic sample assembly.

the natural case, radionuclides could migrate away from the waste via groundwater flow.

All samples were wrapped with a thin sheet of stainless steel mesh to allow drainage of pore fluid from the surface of the sample. The mesh was covered with a 0.013-cm sheet of copper. The entire assembly was jacketed in a 0.30-cm viton sleeve to seal out the confining fluid. The copper jacket ensured that the viton did not press through the steel mesh onto the rock surface and inhibit fluid flow. Teflon shims (Figure 1) prevented water from leaking at the interfaces between the sample, silica cylinders, and steel plugs. The fused silica cylinders at the ends of the sample acted as thermal insulators to help maintain a uniform temperature along the length of the sample. Temperature varied by 2°C between the middle and the ends of the sample. Temperatures in the range of 200°–

310°C were chosen for these experiments on the basis of expected temperatures around a borehold [*Apps et al.*, 1978].

Hydrostatic confining pressure and pore pressure were held constant by a microprocessor control system. Distilled water was used as the pore fluid medium to allow chemical reactions to occur between the solution and the rock and at the same time to introduce no new chemical constituents into the system.

In the natural condition. permeability around a borehole would be strongly dependent on structures developed as a result of tectonic activity. For this reason it is important to study the flow properties of both intact and fractured samples. Thus of the three experiments described in Table 1 the sample for experiment 3 was an intact specimen, whereas the samples for experiments 1 and 2 both contained a single throughgoing fracture. These were made by mechanically expanding the borehole, creating two tension fractures 180° apart along the length of the rock.

The confining and pore pressures of experiments 1 and 2 ($P_{conf} = 600$ bars, $P_{pore} = 200$ bars) represent a depth of burial of approximately 2.4 km, where confining pressure is due to the weight of the overlying rock and pore pressure results from the hydrostatic head. Experiment 3 simulates a depth of about 1.2 km in the earth. The lower confining and pore pressures ($P_{conf} = 300$ bars, $P_{pore} = 100$ bars) were chosen because of the much lower permeability expected from an intact sample. At these pressures, flow rate and differential pore pressure remained in an accurately measurable range throughout the experiment. Current feasibility studies of the very deep hole disposal concept extend to a depth of 10 km [*Roy and White*, 1975; *U.S. Department of Energy*, 1979].

Permeability was determined by either (1) monitoring the differential pore pressure between the center and the outside of the sample while maintaining a constant flow rate (experiment 1 and the first half of experiment 2) or (2) measuring a changing mass flow rate over a constant pore pressure drop (experiment 3 and the last half of experiment 2). Differential pore pressure could be resolved to 0.01 bar and was kept low (5 bars or less) to ensure that flashing to steam was not caused by a sharp pressure gradient; thus pore fluids remained in liquid at all times. The flow condition in experiment 2 was changed midway through the experiment to prevent a large buildup of differential pore pressure.

Permeability is not uniform throughout the sample, owing to the imposed pressure and temperature gradients and nonuniform mineral alteration. Thus reported permeability is an average value over the radius of the sample. However, we are

TABLE 1. Experimental Conditions

	Experiment		
	1	2	3
Sample configuration	split	split	intact
Confining pressure, bars	600	600	300
Pore pressure, bars	200	200	100
Flow condition	constant flow rate	constant flow rate and constant head	constant head
Mass flow rate, g/s			
initial	1.5×10^{-4}	1.5×10^{-4}	2.0×10^{-4}
final	1.5×10^{-4}	2.4×10^{-5}	1.6×10^{-6}
Temperature, °C			
borehole	200	280	310
jacket	95	125	115
Duration of experiment, days	32	6	12

TABLE 2. Flow Rate and Resulting Pressure at Room Temperature

	Mass Flow Rate Q_m, g/s	Differential Pressure, bars
	2.88×10^{-3}	5.8
Flow rate decreased	3.02×10^{-4}	0.6
Flow rate increased	2.88×10^{-3}	6.0

not so much interested in the exact value as in the significant changes in permeability that occur over time.

Permeability for the intact sample was determined assuming that Darcy's law holds. For radial flow,

$$\frac{Q_m}{2\pi l} = \frac{kr}{\nu} \frac{dP}{dr} \qquad (1)$$

or

$$k = \frac{Q_m}{2\pi l \Delta P} \int \nu \frac{dr}{r} \qquad (2)$$

where Q_m is the mass flow rate, l is the length of the sample, k is permeability, r is the radius of the sample, dP/dr is the pressure gradient between the center and the outside of the sample, and ν is the dynamic viscosity of water; ν is a function of temperature and therefore varies with radius in these experiments. This equation is not appropriate for describing flow in the two cracked samples, because flow is not uniformly radial but concentrated along the crack. The parallel plate model analogy to Darcy's law [Gale, 1975] is often used to describe flow in this case. Flow per unit crack length is given by

$$Q = (d^3/12\nu)(dP/dx) \qquad (3)$$

where d is the separation between two parallel plates. To test if the parallel plate model was valid for describing flow through the irregular hydrofracture surface, we tested the proportionality of flow rate to differential pressure at room temperature. When flow rate was increased or decreased by a factor of 10, the pore pressure also changed by the same amount. The results are shown in Table 2. The absolute values of flow rate and pressure are not significant here, only their ratios. Since the flow rate was indeed proportional to differential
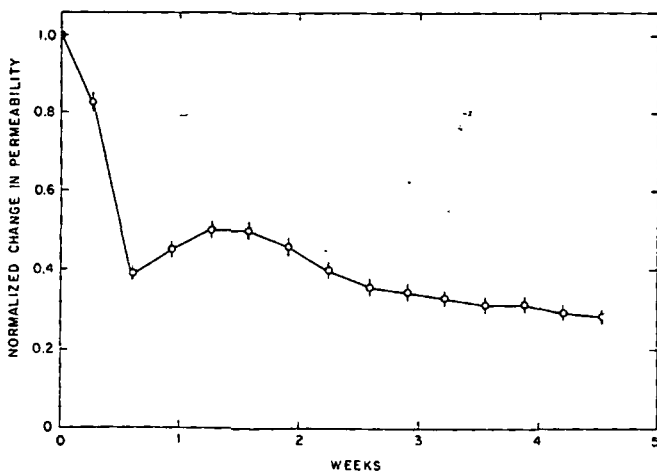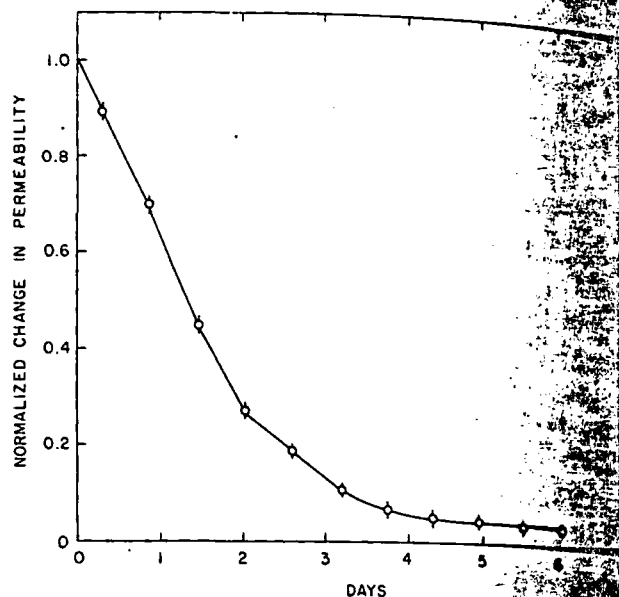

Fig. 3. Normalized change in permeability of experiment sample over a period of 6 days. Sample contained a throughgoing fracture and had a borehole temperature of 280°C.

pressure, then the parallel plate model was applicable to the hydrofractured surface.

Because the separation between plates (crack width d) was not known in these experiments, (3) could not be used directly. Then instead of crack width we substitute a coefficient such that the flow per unit crack length is given by

$$\frac{Q}{l} = \frac{\lambda}{\nu} \frac{dP}{dx} \qquad (4)$$

The constant λ is similar to permeability in that it relates flow in a crack to the pressure gradient. However, λ has units of distance cubed rather than distance squared and therefore is not strictly a crack 'permeability.'

OBSERVATIONS

Permeability was found to decrease with time for all samples. The effect of temperature is pronounced; Figures show the change in permeability with time normalized to the initial permeability. Temperatures refer to the temperature measured at the borehole as given in Table 1.

The cracked specimen at 200°C showed unexplained irregular behavior in the first $1\frac{1}{2}$ weeks (Figure 2) before a smooth trend in permeability was apparent. After 32 days, permeability had decreased to 30% of the initial value and was continuing to decline at a slow rate when the experiment was ended. At 280°C, again with flow through a crack, permeability decreased rapidly within the first 4 days and then continued more slowly thereafter (Figure 3). The intact specimen at 310°C showed similar behavior, although the steep decline in permeability was more rapid, extending over only a 1-day period (Figure 4).

Initial and final values of permeability for the three experiments are given in Table 3. The permeability of the cracked samples in experiments 1 and 2 is shown as λ, as derived above. Based on flow rates of the experiments prior to raising the temperature, the introduction of a crack into an intact sample raised the flow rate by an order of magnitude.

Fig. 2. Normalized change in permeability of experiment 1 sample over a period of 32 days. Sample contained a throughgoing fracture and had a borehole temperature of 200°C.
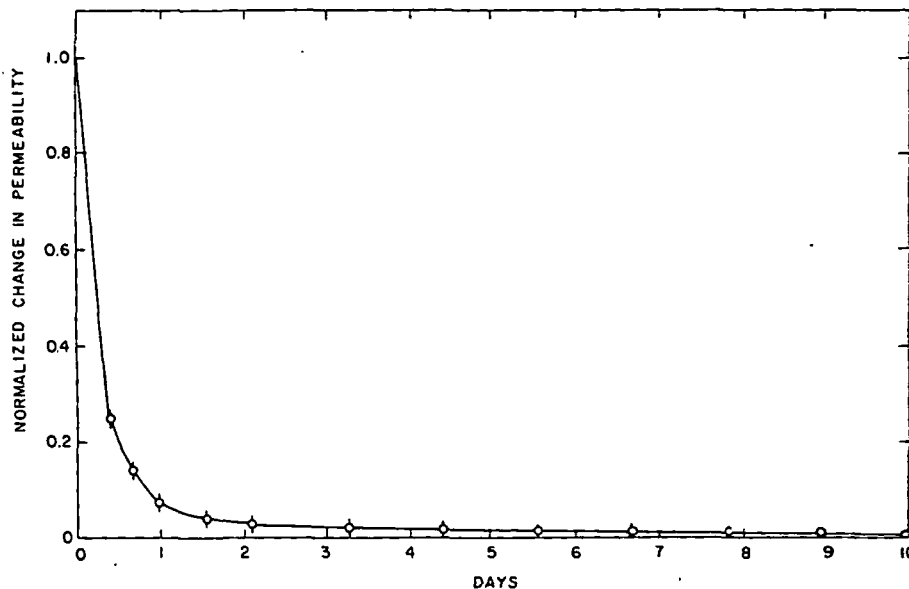
Fig. 4.   Normalized change in permeability of experiment 3 sample over a period of 10 days. Sample was intact, with a borehole temperature of 310°C.

The split faces of the samples in experiments 1 and 2 and a fracture surface of the sample in experiment 3 were examined using the scanning electron microscope (SEM) and attached energy dispersive X ray analyzer. The observations were compared with those of a fresh piece of Westerly granite to determine changes as a result of exposure to temperature and flow. Thin sections were also analyzed to find possible differences in mineralogy between the borehole and the outer side of the rock. These two techniques revealed somewhat different information, because deposition along grain boundaries exposed from fracturing was more easily detected with the SEM and thin sections were more useful in observing alteration within grains.

At a borehole temperature of 200°C, dissolved and redeposited silica was found near the edge of the sample with the SEM. The silica occurred as patchy masses or long, thin fibers on top of quartz grains. Silica fibers were not present in the fresh samples of Westerly granite. Figure 5 shows a typical example of deposition features. Here silica is preferentially precipitated on a quartz grain.

At higher temperatures, similar features were observed near the edge of the sample. In addition to silica, feldspar constituents were present in the deposits. Figure 6 shows calcium-rich fibers on top of a calcium-rich plagioclase. These are probably fiberous zeolites, favored over clay precipitation because of the neutral pH of the pore fluids. Alteration products tended to favor precipitation on grains of similar composition. Note how the fibers have grown down the fresh faces of the albite twins exposed from the artificially produced fracture. Such structures were not present in the fresh samples of Westerly granite.

It was difficult to identify unequivocally dissolution features near the borehole by using the SEM because of the irregular fracture surface and misleading surface structures (lines and pits) present in the fresh samples. In future experiments this difficulty can be overcome by observing etching along saw-split polished faces.

Preliminary thin-section analysis yielded evidence of mineral reaction in one of the samples, the intact granite block of experiment 3. Fresh Westerly granite shows some evidence of natural, probably deuteric alteration that in part consists of the partial alteration of plagioclase by sericite, saussurite, and calcite. Generally, the sericitic alteration is a very fine grained, pale green material that is disseminated in the plagioclase crystals. Saussuritic alteration is also fine grained and poorly crystallized, but some good crystals of epidote/clino-zoisite are observed.

Reaction features produced during experiment 3 consisted of modifications to these natural, preexisting alteration minerals in plagioclase, in an 8- to 10-mm-thick concentric zone extending into the block from the borehole edge. Within this zone the sericitic material was altered to a distinctive bright yellowish-brown, somewhat coarser grained chloritic phyllo-silicate that showed anomalous dark yellowish-green interference colors under the crossed nicols. These yellowish-brown minerals were especially well developed along cleavages and internal fractures of the plagioclase, although small amounts of the phyllosilicate occurred at some grain boundaries. In addition, saussuritic alteration minerals intergrown with the yellowish-brown phyllosilicates may be slightly better crystallized after the experiment on the average than those occurring elsewhere in the sample. With increasing distance

TABLE 3.   Initial and Final Permeabilities

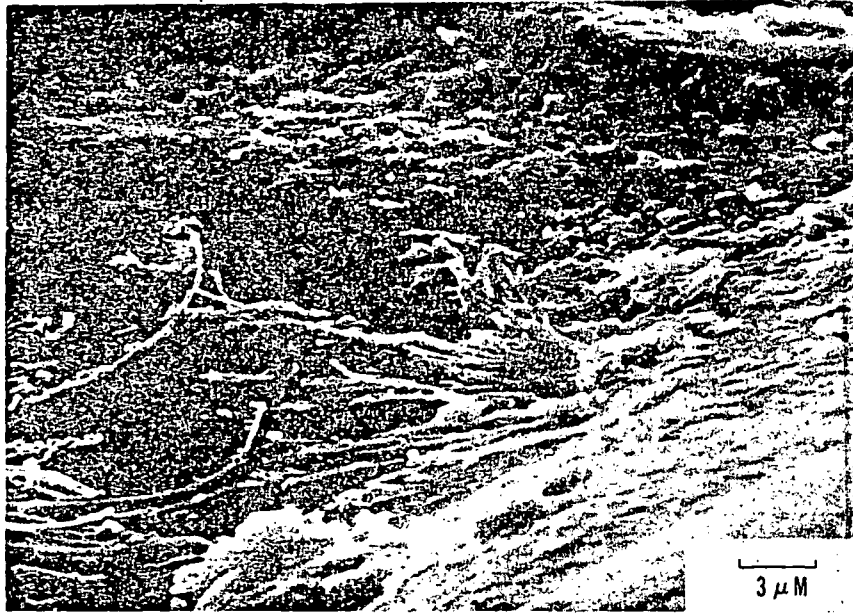|	Experiment	Initial λ, cm^3	Final λ, cm^3	Initial k, darcies	Final k, darcies
Calculated from parallel plate model	1	2.94×10^{-4}	8.18×10^{-5}		
	2	1.72×10^{-5}	6.29×10^{-7}		
Calculated from radial flow model	3			3.00×10^{-7}	2.20×10^{-9}

Fig. 5. SEM photomicrograph of deposition features in experiment 1 sample. Silica from solution has redeposited as fibers on a quartz grain. Magnification is 30,000×.

from the borehole, alteration features became progressively less pronounced and disappeared entirely 10 mm from the borehole edge.

Similar alteration features were not observed in granite in the other two experiments. In these, flow was concentrated within the fracture, and solution/redeposition features at the surface predominated over chemical reactions within the granitic block. In the intact block all flow must occur along grain boundaries and cracks of the rock itself, which may promote reaction of the water with the minerals in the rock. In addition, the experiment with the intact block was conducted using the highest borehole temperature, 310°C, which may have facilitated reaction. The concentration of reaction products near the heat source in the borehole supports this idea. Cal-

cite and the fine-grained and poorly crystallized sericitic and saussuritic minerals are the minerals most likely to show the most alteration given the short duration of these experiments. At the lower maximum temperatures of the other two experiments, mineral reaction rates may have been slowed sufficiently so as not to be detected.

The observed geochemical changes resulting from flow at high temperatures are consistent with other studies of systems at elevated temperatures. It is worthwhile to mention some of these results because they explain in part the observations of this study as well as reactions that may have occurred but were not evident from the analysis techniques used here.

Quartz solubility has been extensively studied; much of this work is summarized by *Holland* [1967]. For temperatures be-
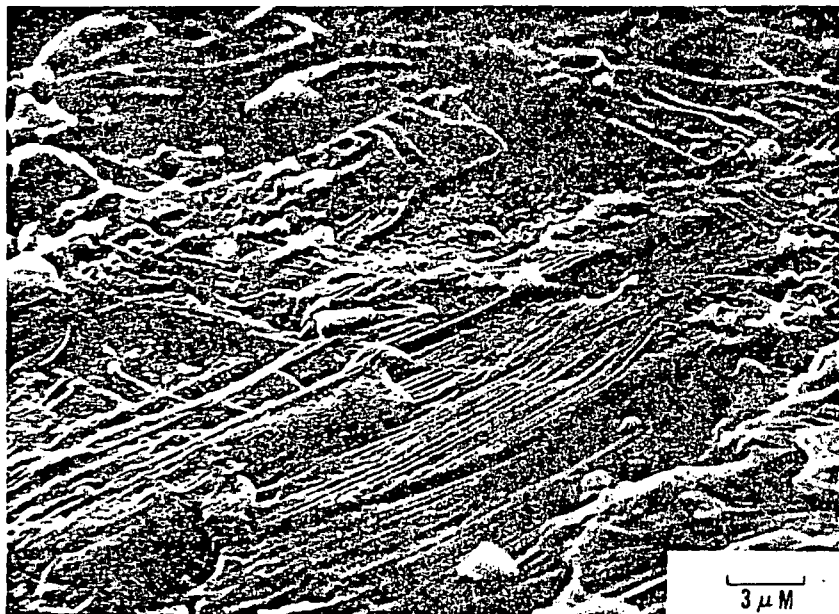

Fig. 6. SEM photomicrograph of fibrous Ca-rich zeolitic deposits on a plagioclase grain of experiment 2 sample. Magnification is 30,000×.

than about 325°C, quartz solubility decreases with decreasing temperature and is extremely low at temperatures less than 1600°C. Thus simple cooling is an important mechanism in precipitating quartz [*Holland,* 1967]. Decreasing pressure at constant temperature also results in a slight decrease in quartz solubility. Dissolution of quartz is essentially independent of pH of the aqueous solution and is also independent of the concentration of dissolved salts in the geologically important range of *P* and *T.* In the pressure range of approximately 250–400 bars, quartz solubility in water for the three temperatures used in these experiments is about 800 ppm at 310°C, about 700 ppm at 280°C, and nearly 300 ppm at 200°C [*Kennedy,* 1950].

Thus it is not surprising that quartz was observed near the edge of the sample (Figure 5). On the basis of the discussion above we infer that a large amount of quartz dissolved near the heater (borehole). As temperature dropped in the direction of flow, the pore fluid became supersaturated with respect to quartz, and quartz was deposited along cracks and channelways, the amount of deposition varying with *T, P,* and the flow rate. Cracks that are clogged by deposition very effectively inhibit fluid flow and thus reduce permeability. Minerals other than quartz behave in a similar manner. For instance, experimental results of a number of workers (see, for example, *Gruner* [1944], *O'Neill* [1948], *Hemley* [1959], *Orville* [1962, 1963], and *Hemley and Jones* [1964]) have shown that variations in *T, P,* pH, and salt concentration of the coexisting fluid phase influence the stability of feldspar minerals. Feldspars remain stable in near-neutral alkaline solutions in the temperature range 250°–400°C and pressures to 100 bars; at least weakly acidic environments are required to permit hydrolytic base leaching of feldspars to produce muscovite or clays [*Gruner,* 1944; *O'Neill,* 1948; *Meyer and Hemley,* 1967].

Morey and Chen [1955] and *Morey and Fournier* [1961] passed a continuous stream of distilled water over powdered samples of albite and microcline in closed vessels. Liquids were collected from the vessels and analyzed, and samples and vessel were examined for the presence of alteration minerals. With increasing temperature and pressure, progressively larger amounts of albite and microcline are dissolved into solution. At the same conditions of reaction, albite has a higher rate of dissolution than does microcline. In addition, *Morey and Fournier* [1961] observed that Na-rich layers of perthitic microcline were preferentially dissolved, leaving behind skeletal crystals of potash feldspar.

Charles [1978] passed distilled water over polished disks of granodiorite at 295°C and 330 bars total pressure for periods of 1–8 months. The disk subjected to 8 months flow of hydrothermal fluid showed 14% weight loss. The reactivity of minerals in the granodiorite was quartz $\gg$ microcline $>$ plagioclase $>$ mafic and accessory minerals. The presence of quartz contributing SiO_2 to solution apparently suppressed the reactivity of the feldspars. Throughout most of the experiment the total concentration of dissolved material in solution was 720 ppm, and the SiO_2 concentration was 680 ppm. The amount of Na in solution was 24 ppm, the K concentration was near 7 ppm, and the Ca concentration was approximately 0.25 ppm. Secondary minerals on the disks included the zeolites philipsite and thomsonite that formed coatings on plagioclase and vermiculite that occurred as prominent black crystals adjacent to mafic minerals. Quench fibers of silica formed on residual quartz grains and on other minerals. Wollastonite and silica precipitated on the experimental apparatus.

It is clear from these examples of feldspar studies that the dissolution and precipitation of feldspars and their breakdown products are significantly more complex than the quartz system. The results of *Charles* [1978] on the reactivity of minerals support our observation that silica precipitation in cracks was dominant over that of feldspar constituents, particularly at lower temperatures. Also, plagioclase feldspars were preferentially altered over orthoclase, as reported by *Morey and Chen* [1955] and *Morey and Fournier* [1961].

DISCUSSION

It has been shown that permeability decreases with time, at a rate that is strongly dependent on temperature. At a borehole temperature of 200°C the permeability gradually decreased to one third of the original value over a period of several weeks. With increased temperature the permeability drop was much sharper, occurring within 4 days at 280°C. For the intact sample at 310°C the major permeability drop occurred within the first day and a half. Final permeability values of the two higher-temperature experiments were about 3 to 5% of the initial values, regardless of the stress applied to the rock mass.

These results agree with those of *Summers et al.* [1978], who found a rapid decrease in permeability with time owing to decreasing solubility of dissolved minerals, and hence deposition and clogging of pores. However, pore water flashing to steam caused by the sharp pore pressure gradient was probably responsible for the marked solubility decrease. The resulting deposition and drop in permeability occurred within the first half day of the experiments, independent of temperatures up to 400°C.

In the experiments reported here, mineral deposition was due mainly to decreasing solubility along the temperature gradient and not to the production of steam through a pressure drop. Differential pore pressure was small, and the fluids remained in the liquid state throughout. Thus the variable rates of decrease of permeability are consistent with the model of a highly temperature dependent system.

Variations of physical factors as well as temperature will affect the time required to achieve a permeability drop. For instance, increased effective stress will tend to close cracks and inhibit flow but at the same time enhance the solubility of minerals in the rock by pressure solution. A decrease in the flow rate will increase the amount of time available for reaction within the rock.

Clearly, several chemical and mechanical parameters can affect permeability. Temperature gradients, as well as groundwater chemistry, in situ stresses, fracture density, and rock mineralogy, must be understood in order to make well-founded decisions on nuclear waste disposal sites.

Our studies demonstrate that the permeability of granite in a temperature gradient decreases with time. This decrease occurs even in samples containing a throughgoing fracture. If the same process occurs in the natural situation, then migration of radionuclides away from a repository in granite may be suppressed, even when the rock surrounding the repository contains preexisting fractures or they are developed at a later time by tectonic activity.

REFERENCES

Apps, J. A., N. G. W. Cook, and P. A. Witherspoon, An appraisal of underground radioactive waste disposal in argillaceous and crystalline rocks: Some geochemical, geomechanical, and hydrogeological

questions, *Rep. LBL-7047*, Lawrence Berkeley Lab., Berkeley, Calif., 1978.

Brace, W. F., J. B. Walsh, and W. T. Frangos, Permeability of granite under high pressure, *J. Geophys. Res.*, *73*(6), 2225, 1968.

Charles, R. W., Experimental geothermal loop, 1, 295°C study, *Informal Rep. LA-7334-MS*, 44 pp., Los Alamos Sci. Lab., Univ. of Calif., Los Alamos, N. M., 1978.

Gale, J. E., A numerical field and laboratory study of flow in rocks with deformable fractures, Ph.D. thesis, 255 pp., Univ. of Calif., Berkeley, 1975.

Gruner, J. W., Hydrothermal alteration of feldspar in acid solution between 300 and 400°C, *Econ. Geol.*, *39*, 578–589, 1944.

Hemley, J. J., Some mineralogical equilibria in the system K_2O-Al_2O_3-SiO_2-H_2O, *Am. J. Sci.*, *257*, 241–270, 1959.

Hemley, J. J., and W. R. Jones, Chemical aspects of hydrothermal alteration with emphasis on hydrogen metasomatism, *Econ. Geol.*, *59*, 538–569, 1964.

Holland, H. D., Gangue minerals in hydrothermal deposits, in *Geochemistry of Hydrothermal Ore Deposits*, edited by H. L. Barnes, chap. 4, pp. 382–436, Holt, Rinehart, and Winston, New York, 1967.

Iwai, K., Fundamental studies of fluid flow through a single fracture, Ph.D. thesis, 208 pp., Univ. of Calif., Berkeley, 1976.

Kennedy, G. C., A portion of the system silica-water, *Econ. Geol.*, *45*, 629–653, 1950.

Kranz, R. L., A. D. Frankel, T. Engelder, and C. H. Scholz, The permeability of whole and jointed Barre granite (abstract), *Int. J. Rock Mech. Min. Sci. Geomech.*, *16*, 225, 1979.

Meyer, C., and J. J. Hemley, Wall rock alteration, in *Geochemistry of Hydrothermal Ore Deposits*, edited by H. L. Barnes, pp. 166–235, Holt, Rinehart, and Winston, New York, 1967.

Morey, G. S., and W. T. Chen, The action of hot water on some feld spars, *Am. Mineral.*, *40*, 996–1000, 1955.

Morey, G. W., and R. O. Fournier, The decomposition of microcline, albite and nepheline in hot water, *Am. Mineral.*, *46*, 688–699, 1961.

O'Neill, T. F., The hydrothermal alteration of feldspar at 250–400°C, *Econ. Geol.*, *43*, 167–180, 1948.

Orville, P. M., Alkali metasomatism and felspars, *Nor. Geol. Tidsskr.*, *42*, 283–316, 1962.

Orville, P. M., Alkali ion exchange between vapor and feldspar phase, *Am. J. Sci.*, *261*, 201–237, 1963.

Potter, J. M., Experimental permeability studies at elevated temperature and pressure of granitic rock, M. S. Thesis, Univ. of N. M., Albuquerque, 1978.

Pratt, H. R., H. S. Swolfs, W. F. Brace, A. D. Black, and J. W. Handin, Elastic transport properties of an in-situ jointed granite (abstract), *Int. J. Rock Mech. Min. Sci. Geomech.*, *14*, 35, 1977.

Roy, D. M., and W. B. White, Borehole plugging by hydrothermal transport—A feasibility report, subcontract 4091, Oak Ridge Nat. Lab., Oak Ridge, Tenn., 1975.

Summers, R., K. Winkler, and J. Byerlee, Permeability changes during the flow of water through Westerly granite at temperatures of 100°–400°C, *J. Geophys. Res.*, *83*(B1), 339–344, 1978.

Tester, J. W., and J. N. Albright (Eds.), Hot dry rock energy extraction field test: 75 days of operation of a prototype reservoir at Fenton Hill, Seg. 2 of ph 1, *Informal Rep. LA-7771-MS*, Los Alamos Sci. Lab., Univ. of Calif., Los Alamos, N. M., April 1979.

U.S. Department of Energy, Draft environmental impact statement, Management of Commercially Generated Radioactive Waste, *Rep. DOE/EIS-0046D*, U.S. Dep. of Energy, Washington, D. C., 1979.

PHOSPHATE

Peter F. Howard

THERE are three types of phosphate rock, namely, sedimentary phosphorites of marine origin, apatite-bearing alkaline igneous complexes, and phosphorites of guano origin. Of these, the sedimentary phosphorites have historically dominated the world production scene. At the same time the igneous complexes have been gaining and the guano-origin deposits diminishing in importance in the last two decades. Table 1 shows those trends and also that three countries, the United States. U. S. S. R., and Morocco, dominate both world production and export of phosphate. In fact three deposits or mining districts are preeminent in this respect and their production capacities have kept abreast of world demand. These deposits are in Florida, U.S.A.; Khibiny, Kola Peninsula, U. S. S. R.; and Morocco. Other important deposits, however, include the Phosphoria Formation and North Carolina. U. S. A.; Kara Tau and European U. S. S. R.; the belt of deposits extending along western Africa through North Africa and the Middle East; the Sinian of Yunnan, China; Christmas, Nauru, and Ocean Islands, South Pacific;

Palabora. South Africa; Lao Kay, Vietnam; and Udaipur. India (Fig. 1).

Large deposits or fields found before 1968 but which are not in production at the present time due to economic, trade, or political considerations are Bou Craa, western Sahara; Georgina Basin, Australia; Sechura, Peru; Sokli, Finland; and the Colombian deposits.

In 1971, after a decade or more of stable prices, the inadequate production of phosphate rock coupled with an increased demand by fertilizer companies who wanted to maintain their inventories led to an explosion of prices. As a result, with support from the United States and other North African producing countries, Morocco increased its price range such that, in the period 1971 to 1975, prices rose exponentially from approximately $11 to $68 f.a.s.[1] per short ton for 75/77 BPL[2]-grade rock; that is, an increase of more than 500 percent. Subsequently, the price softened and by early 1978. after world trade fell

[1] Free alongside ship.
[2] Bone phosphate of lime = percent $P_2O_5 \times 2.18$.

TABLE 1. World Production of Phosphate Rock by Type

	1956 (1)	1966 (1)	1976 (2)
Percent (rounded)			
Sedimentary	80	83	82
Igneous	12	13	16
Guano	8	4	2
Total metric tons	30.4×10^6 (100%)	89.2×10^6 (100%)	106.5×10^6 (100%)

World Production of Phosphate rock by Principal Countries

	1956 (1)	1966 (1)	1976 (2)
Percent			
U.S.A.	47	40	41
U.S.S.R.	11	22	23
Morocco	16	11	14
Total percent	74	73	78

World Export of Phosphate Rock by Principal Countries

	1956 (3)	1966 (3)	1976 (2)
Percent			
Morocco	37	29	35
U. S. A.	19	27	24
U. S. S. R.[1]	8	15	*15
Total percent	64	71	74

[1] Includes an unspecified tonnage of North Vietnam exports.
Sources: (1) U. S. Bureau of Mines, (2) British Sulphur Corporation, and (3) Isma Ltd. and Institute of Geological Sciences.
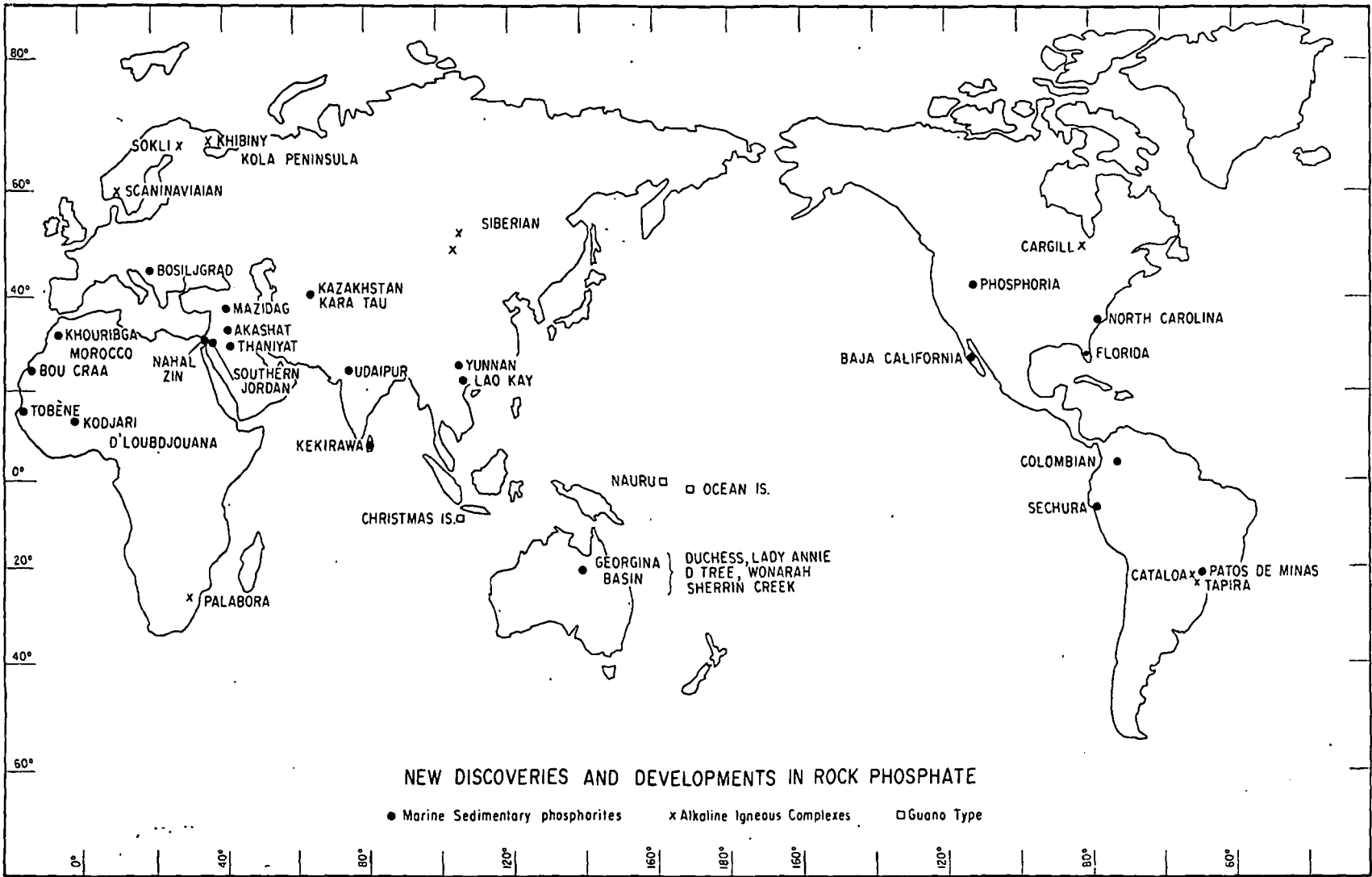
FIG. 1. New discoveries and developments in rock phosphate.

into decline, it stabilized at $39.50. The marked events of 1971 to 1975, however, led to a resurgence of worldwide exploration for phosphate rock by many nations with a view to self-sufficiency. Many known deposits suddenly became economic, and both companies and governments undertook feasibility studies and began development of existing and new deposits at Cargill, Canada; in the Tapira-Cataloa belt of Brazil; Tobène, Senegal; Nahal Zin, Israel; southern Jordan; India; Akashat, Iraq; the Mazidag Mountains, Turkey; Thaniyat, Saudi Arabia; Kodjari and D'Loubdjouana, Upper Volta; Kekirawa, Sri Lanka; Bosiljgrad, Yugoslavia; numerous deposits in Kazakhstan and Siberia; and alkaline igneous carbonatite complexes in Scandinavia (Fig. 1). However, perhaps the most significant discoveries of this period have been the marine phosphorite deposits of Patos de Minas in Minas Gerais, Brazil; the various deposits on Baja California, Mexico; and especially the expansion of the known districts in Florida extending outward from nearly all existing deposits found in the mid 1960s. These southeast U. S. deposits comprise a vast addition to potential low-grade reserves for the future.

In this volume are papers on phosphate deposits not previously described in the literature, namely, Sechura, and Cargill. In addition, European and some U.S.S.R. deposits are reviewed; a synthesis is presented on the geology of the shelf and onshore deposits of South Africa; new views are put forward on the weathering, geochemistry, and origin of deposits in the Georgina Basin; and a detailed analysis is set forth on the sedimentology and origin of the Florida fields. Finally, there is a paper which brings together, in space and time, data on marine phosphorites in terms of paleolatitude, paleooceanic orientation related to plate tectonic theory, and the relationship of phosphorites to other sedimentary types such as iron ores and evaporites.

School of Earth Sciences
  Macquarie University
    North Ryde, N.S.W. 2113, Australia
      October 6, 1978

THE POSSIBILITY OF INTENSIFYING GOLD
DISSOLUTION IN CYANIDE SOLUTIONS

UDC 669.213

L. D. Sheveleva, I. A. Kakovskii, and V. M. Samoilenko

Oxygen is essential in the dissolution of gold in cyanide solutions as a receiver of electrons, but excess oxygen causes passivation of the metal surface and a drastic reduction in speed of dissolution [1]. Passivation has been proved by electrochemical methods [2, 3], and it has been established by electron diffraction that the passivating film consists of trivent gold oxides and hydroxides [4].

In cyanide solutions the normal potential of gold is -0.543 V [4], i.e., the metal becomes somewhat less noble and capable of giving up its electrons to oxygen to form oxidized trivalent gold compounds, because the normal potentials for the corresponding reactions are +0.532 and +0.590 V for Au_2O_3 and $Au(OH)_3$.

It has been found potentiostatically [3] that passivation begins at +0.75 V and the potentials for these reactions, computed to take account of actual reacting constituent concentrations under the conditions prevailing in this experiment are +0.67 and +0.73 V respectively. The results of this experiment accord well with the electron diffraction data [4].

The presence of the oxidized film on the gold surface and the hysteresis loop in forward and reverse plotting of the potentiostatic curves [3, Fig. 2, curves 2 and 3] lead to the conclusions that these surface films are fairly stable, react fairly slowly with cyanide, and screen the metal surface.

As a result of these complications, the speed of gold dissolution in cyanide solutions decreases when the rate of mixing rises and the oxygen concentration in the solution increases (Fig. 1, curves 1 and 2).

When the number of disk revolutions is above 150-200 per min, the process of gold dissolution makes the transition from a diffusion to a kinetic routine (the speed does not depend upon the rate of mixing).

However, a number of results obtained recently indicate gold may dissolve in cyanide solutions according to the principles of diffusion kinetics at higher rates of mixing. Thus if potassium ferricyanide is used as the oxidizing agent instead of oxygen (see Fig. 1, curve 4) oxidized films do not form on the surface of the gold and there is no reduction in the speed of dissolution even at a high rate of mixing [6, p. 62].

It was found possible in our experiments to increase the speed of gold dissolution somewhat by adding carefully washed sand to the solution, due to the abrasive action of the solid grains. The definite beneficial effect of vibratory mixing [7-9] may also be regarded as due to abrasion of the film by ore particles.

A series of investigations [10-12] using activating additions also gives grounds for the view that the passivation of gold in cyanidation can be appreciably reduced and the process intensified by mixing (see Fig. 1, curve 5) and not by increasing the cyanide concentration (see Fig. 1, curve 3), which is less
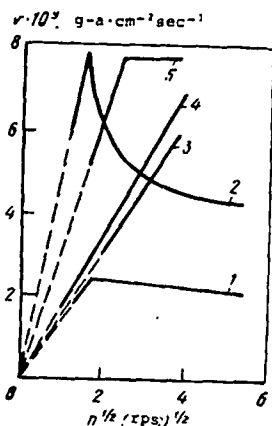

Fig. 1. Relationship of speed of dissolution to mixing rates:
1 - blowing with air [KCN]$4 \cdot 10^{-3}$ moles/lit;
2 - blowing with oxygen [KCN]$1.0 \cdot 10^{-2}$ moles/lit
3 - blowing with air [Ex]$1.5 \cdot 10^{-5}$, [KCN]$3 \cdot 10^{-2}$; 4 - [K$_3$Fe(CN)$_6$]$1.55 \cdot 10^{-3}$, [KCN]$4 \cdot 10^{-3}$ moles/lit; 5 - blowing with air [Tl$^+$]10^{-4}, [KCN]$3.85 \cdot 10^{-3}$. Curves 1 and 2 are taken from [1].
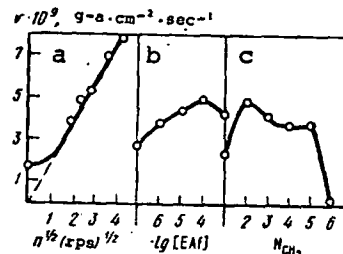

Fig. 2. Effect of the following factors upon speed of gold dissolution in the presence of dithiophosphates with air blown through the solution:
a - disk revolutions ([EAf] 10^{-4}, [KCN]10^{-2} moles/lit;
b - ethyl Aerofloat concentration ([KCN]10^{-2} moles/lit, disk speed 340 rpm);
c - length of Aerofloat hydrocarbon chain: number of alcohol CH$_2$ links ([RAf] 10^{-4}, [KCN]$\cdot 10^{-2}$ moles/lit, disk speed 340 rpm).

economical.

It was shown in this work that dialkyldithiophosphates (Aerofloats) were exceptionally effective additives. A kinetic study carried out at 25°C under conditions analogous to experiments in gold dissolution in the presence of xanthates [12] showed that the process took place under diffusion conditions and at a very high rate of solution mixing (Fig. 2a). The speed of dissolution at 1200 rpm was 8×10^{-9} g.atom/(cm².sec) or 76% of theoretical with full utilization of the oxidizing capacity of oxygen in the above-limit region in terms of cyanide [6, p. 51].

When air is blown through pure cyanide solutions, the maximum speed of dissolutions, the maximum speed of dissolution in them is $2.1-2.4 \times 10^{-9}$ g.atom/(cm².sec), or almost 4 times lower than in the presence of Aerofloat. The optimum Aerofloat concentration in the solution is $\sim 10^{-4}$ moles/liter, but even a tenfold increase reduces the speed of gold dissolution only by 18% (Fig. 2b). It is a particularly interesting fact that an increase in the length of the Aerofloat hydrocarbon chain has comparatively little effect upon the speed of gold dissolution: it is 4.8×10^{-9} g-atom/(cm².sec) for the ethyl homolog and 3.8×10^{-9} g-atom/(cm².sec) for the amyl homolog, i.e., only 1.25 times lower (Fig. 2c).

Since there are indications in the literature that the surfaces of minerals (and metals) coated with a collector are capable of adsorbing frother from solution [13] and this may be accompanied by an increase in the stability of the superficial passivating film on gold, we mounted a series of experiments on gold dissolution in cyanide solutions in the presence of certain frothers. The experimental conditions were: concentrations of alcohols in the normal homologous series 5.5×10^{-4}, ethyl xanthate 10^{-3}, potassium cyanide 3×10^{-2} moles/liter, t = 25°C, n = 430 rpm, blowing with air. It was found that additions of alcohols with a long hydrocarbon chain ranging from 3-10 CH₂ links and also pine oil had no effect whatever upon the speed of gold dissolution: it was $4.6-4.7 \times 10^{-9}$ g-atom/(cm².sec) as in the presence of xanthate but without alcohol additions.

CONCLUSIONS

1. The anodic phase of gold dissolution in cyanide solutions proceeds without kinetic complications; this confirmed by our own work [2, 3] and by the authors of [14], who dissolved gold anodically in deoxygenated cyanide solutions.

2. A reagent has been found which is fairly effective in eliminating passivation of gold by atmospheric oxygen during cyanidation.

3. The process of gold dissolution in cyanide solutions in the presence of Aerofloats is fairly stable.

4. Dithiophosphates are much more effective than xanthates as depassivators for gold: the adverse effect of excess reagent concentration in the solution and of an increased rate of mixing is less apparent [12, Figs. 2 and 3]. It should be noted here that although ethyl dithiophosphate is less active than ethyl xanthate [15, p. 306], nevertheless amyl dithiophosphate has practically the same chemical activity (capacity to resist the action of depressants) as ethyl xanthate but also gives a greater contact angle (degree of water-repellency).

These factors make it possible to recommend dithiophosphates for flotation of gold from ores instead of xanthates, especially if cyanidation of the flotation concentrate is proposed.

REFERENCES

1. I. A. Kakovskii and Yu.B. Kholmanskikh, Izv. Akad. Nauk SSSR, Otdel Tekhn. Nauk, Metallurgiya i Toplivo, 1960, No. 5, 207-218.
2. I. A. Kakovskii and A. N. Lebedev, Izv. Vuzov, Tsvetnaya Metallurgiya, 1970, 13, No. 1, 56-59.
3. A. N. Lebedev, V. V. Gubailovskii, and I. A. Kakovskii, Izv. Vuzov, Tsvetnaya Metallurgiya, 1976, 19, No. 1, 64-67.
4. G. F. Cherkasov, I. A. Kakovskii, and V. D. Pankrashova, Izv. Vuzov, Tsvetnaya Metallurgiya, 1973, 16, No. 4, 51-54.
5. I. A. Kakovskii, in: Proceedings of the Third Mekhanobr Scientific and Technical Meeting, Moscow, Metallurgizdat, 1955, pp. 269-270.
6. I. A. Kakovskii and Yu. M. Potashnikov, Kinetics of Dissolution Processes, Moscow, Metallurgiya, 1975, 224 pages, illustrated.